Transition Metal Catalyzed Alkenylation and Alkylation of Inert C-H Bonds

by

SMRUTI RANJAN MOHANTY

CHEM11201604028

National Institute of Science Education and Research,

Bhubaneswar, Odisha

A thesis submitted to the

Board of Studies in Chemical Sciences

In partial fulfillment of requirements

for the Degree of

DOCTOR OF PHILOSOPHY

of

HOMI BHABHA NATIONAL INSTITUTE

May, 2022

Homi Bhabha National Institute[1]

Recommendations of the Viva Voce Committee

As members of the Viva Voce Committee, we certify that we have read the dissertation prepared by **Smruti Ranjan Mohanty** entitled "**Transition Metal Catalyzed Alkenylation and Alkylation of Inert C-H Bonds**" and recommend that it may be accepted as fulfilling the thesis requirement for the award of Degree of Doctor of Philosophy.

Chairman - Prof. A. Srinivasan Date: 26.08.'22

Guide / Convener - Dr. Ponneri C. Ravikumar Date: 26/08/2022

Examiner – Dr. M. Jeganmohan Date: 26.08.22

Member 1- Dr. C. S. Purohit Date: 26.08.22

Member 2- Dr. S. Peruncheralathan Date: 26.08.22

Member 3- Dr. Shantanu Pal Date: 26/8/22

Final approval and acceptance of this thesis is contingent upon the candidate's submission of the final copies of the thesis to HBNI.

I/We hereby certify that I/we have read this thesis prepared under my/our direction and recommend that it may be accepted as fulfilling the thesis requirement.

Date: 26/8/2022 -/-/2022

Signature

Place: NISER, Bhubaneswar

Guide Dr. P.C. RAVIKUMAR

[1] This page is to be included only for final submission after successful completion of viva voce.

STATEMENT BY AUTHOR

This dissertation has been submitted in partial fulfillment of requirements for an advanced degree at Homi Bhabha National Institute (HBNI) and is deposited in the library to be made available to borrowers under rules of the HBNI.

Brief quotations from this dissertation are allowable without special permission, provided that accurate acknowledgement of source is made. Requests for permission for extended quotation from or reproduction of this manuscript in whole or in part may be granted by the Competent Authority of HBNI when in his or her judgment the proposed use of the material is in the interests of scholarship. In all other instances, however, permission must be obtained from the author.

Smruti Ranjan Mohanty

Smruti Ranjan Mohanty

DECLARATION

I, hereby declare that the investigation presented in the thesis has been carried out by me. The work is original and has not been submitted earlier as a whole or in part for a degree / diploma at this or any other Institution / University.

Smruti Ranjan Mohanty

Smruti Ranjan Mohanty

List of Publications

Published (* pertaining to thesis)

*1) **S. R. Mohanty**; B. V. Pati; S. K. Banjare; G. K. D. Adhikari; P. C. Ravikumar. Redox-Neutral Cobalt(III)-Catalyzed C–H Activation/Annulation of α,β-Unsaturated Oxime Ether with Alkyne: One-Step Access to Multisubstituted Pyridine. *J. Org. Chem.* **2021**, *86*, 1074–1083.

*2) **S. R. Mohanty**; N. Prusty; L. Gupta; P. Biswal; P. C. Ravikumar, Cobalt(III)-Catalyzed C-6 Alkenylation of 2-Pyridones by Using Terminal Alkyne with High Regioselectivity. *J. Org. Chem.* **2021,** *86*, 9444–9454.

*3) **S. R. Mohanty**; N. Prusty; S. K. Banjare; T. Nanda; P. C. Ravikumar, Overcoming the challenges towards selective C(6)-H functionalisation of 2-pyridone with maleimide through Mn(I)-catalyst: Easy access to all-carbon quaternary center. *Org. Lett.* **2022**, *24*, 848–852.

*4) **S. R. Mohanty**; N. Prusty; T. Nanda; S. K. Banjare; P. C. Ravikumar. Pyridone directed selective Ru catalyzed olefination of sp^2(C-H) bond by using acrylate as reacting partner: Creation of drug analogues. *J. Org. Chem.* **2022**, *87*, 6189–6201.

5) N. Prusty; **S. R. Mohanty**; S. K. Banjare; T. Nanda; P. C. Ravikumar, Ni-catalyzed Easy Access to Hetero-polycyclic compound through Chelation assisted Cascade C-H bond activation. *Org. Lett.* **2022**, *24*, 6122-6127.

6) N. Prusty; S. K. Banjare; **S. R. Mohanty**; T. Nanda; K. Yadav; P. C. Ravikumar, Synthesis and Photophysical Study of Heteropolycyclic and Carbazole Motif: Nickel-Catalyzed Chelate-Assisted Cascade C–H Activations/Annulations. *Org. Lett.* **2021**, *23*, 9041–9046.

7) B. V. Pati; P. S. Sagara; A. Ghosh; **S. R. Mohanty**. P. C. Ravikumar, Ruthenium-Catalyzed Cross Dehydrogenative Annulation of N-(7-Azaindole) benzamides with Maleimides: One-Step Access to Highly Functionalized Pyrroloisoquinoline. *J. Org. Chem.* **2021**, *86*, 6551–6565.

8) P. Biswal; S. K. Banjare; B. V. Pati; **S. R. Mohanty**. P. C. Ravikumar, Rhodium-Catalyzed One-Pot Access to N-Polycyclic Aromatic Hydrocarbons from Aryl Ketones through Triple C–H Bond Activations. *J. Org. Chem.* **2021**, *86*, 1108–1117.

9) G. K. D. Adhikari; B. V. Pati; **S. R. Mohanty**; N. Prusty; P. C. Ravikumar, Co(II) Catalyzed C-H/N-H Annulation of Cyclic Alkenes with Benzamides at room temperature: An access to the core skeleton of hexahydrobenzo[c]phenanthridine-type alkaloids. *Asian J. Org. Chem.*, **2022**, **ASAP**.

10) T. Nanda; S. K. Banjare; W. Y. Kong; W. Guo; P. Biswal; L. Gupta; A. Linda; B. V. Pati; **S. R. Mohanty**; D. J. Tantillo; P. C. Ravikumar. Breaking the Monotony: Cobalt and Maleimide as an Entrant to the Olefin-Mediated Ortho C−H Functionalization. *ACS Catal.* **2022**, *12*, 11651−11659.

b. Manuscript Communicated

1) P. Biswal; T. Nanda; N. Prusty; **S. R. Mohanty**; P. C. Ravikumar. Rhodium-Catalyzed Synthesis of 2-Methylindole via C-N bond Cleavage of *N*-allylbenzimidazole.

2) P. Biswal; T. Nanda; S. K. Banjare; S. Prasad; **S. R. Mohanty**; D. J. Tantillo; P. C. Ravikumar. *N*-allylbenzimidazole as a Strategic Surrogate in the Rh-catalyzed Stereoselective Mono-Alkenylation of Aryl sp^2 C-H bonds. **(ChemRxiv, doi: 10.26434/chemrxiv-2021-w1d35)**

c. Book Chapter

1) T. Nanda; **S. R. Mohanty**; P. C. Ravikumar. Recent advances in group XI metal catalyzed C-H bond activation involving Multicomponent cascade reaction, Handbook of C-H functionalization, **Wiley-VCH 2022**. **(Book chapter, accepted)**

Conferences

1. Co(III)-Catalyzed Annulation of α,β-Unsaturated Imine with Alkyne for the Synthesis of Tetrahydroquinoline; **S. R. Mohanty**, B. V. Pati, S. K. Banjare, G. K. D. Adhikari, P. C. Ravikumar; National Conference on Organic Synthesis (N-COS-2020), Organized by PG Department of Chemistry, Berhampur University, Odisha during 02-03 March, 2020. (Poster presentation and, Short oral presentation)
2. Co(III)-Catalyzed C-6 Alkenylation of Pyridones by using Terminal Alkyne with High Regioselectivity; **S. R. Mohanty**, N. Prusty, L. Gupta, P. Biswal, P. C. Ravikumar; 27th CRSI-NSC Kolkata four day symposium (hybrid mode) held on 26th to 29th September, 2021.

Smruti Ranjan Mohanty

Smruti Ranjan Mohanty

Dedicated to

My Family

ACKNOWLEDGEMENTS

First and foremost, I want to express my gratitude to my supervisor for allowing me to pursue my PhD program in his research group. Through the PhD program most excellent experience with sir is the freedom he gave me to think independently and explore myself. His commitments and dedication to research will continue to inspire me. I can't thank you enough for the way he has taken care in all aspect and gave me consistent advice on a daily basis.

For the financial support I thank to DST-Inspire. I am thankful to National Institute of Science Education and Research (NISER) and Department of Atomic Energy (DAE) for providing instrumental facilities.

I would like to thank the members of my doctorate committee Prof. Alagar Srinivasan, Dr. C. S. Purohit, Dr. S. Peruncheralathan and Dr. Shantanu Pal for their useful suggestions.

I sincerely thank to my labmates (Namrata, Pragati, Shyam, Tanmayee, Gopal, Bedvyas, Dr. Rajesh, Dr. Laxman, Dr. Asit, Rohit, Gaji, Lokesh, Pranay, Saista, Ashish, Astha, Lam, Pranav, Lipsa, Nitha, Fastheem, Annapurna, Soumya) for their help.

I would like to thank Bibhuti bhusan palai (Bibhu bhai) for his constant help.

Special thanks to Samser (Sera) and Namrata Di for their constant help and support.

Finally, I wish to express my sincere gratitude to my father - Mr. Surendra kumar mohanty and Mother - Alok Prabha mohanty, my brother - Tapas ranjan mohanty, Satya ranjan mohanty, my sister-in-law - Suchismita mohanty, niece - Tanisha mohanty (Mamunu) for their unconditional love, care, blessing and support. Without their support and love it would not have been possible.

Smruti Ranjan Mohanty

Smruti Ranjan Mohanty

CONTENTS

SYNOPSIS

Thesis has been divided into five chapters.

In chapter 1 contains brief introduction about C-H activation **(Scheme 1)**.

Scheme 1: Transition metal catalyzed inert C-H bond activation

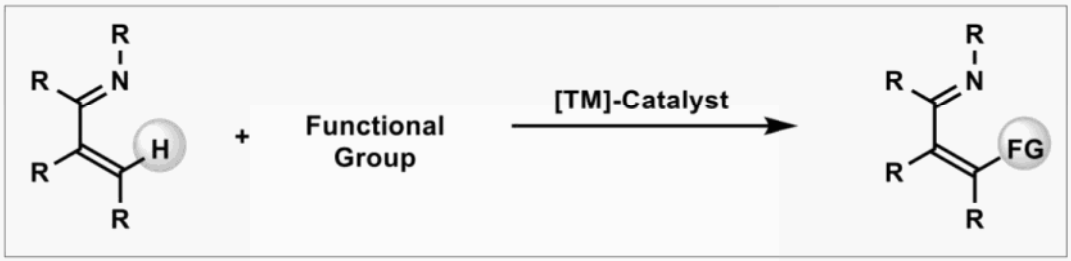

In chapter 2, a redox neutral Co(III)-catalyzed annulation of *α,β*-unsaturated oxime ether with alkyne to synthesize tetrahydroquinoline derivative has been reported (**Scheme 2**). In this protocol N-O bond is acting as a internal oxidant, which avoids the use of heavy metal oxidants. The developed methodology tolerates a variety of functional groups present in substrate and coupling partner. Notably, this transformation has been applied to late-stage modification of complex bioactive molecule dehydropregnenolone. This is the first report of Co(III)-catalyzed annulations of *α,β*-unsaturated oxime ether with alkyne to synthesize multisubstituted pyridine under redox neutral conditions.

Scheme 2: Cobalt catalyzed annulation of α,β-unsaturated imine with alkyne and the proposed catalytic cycle

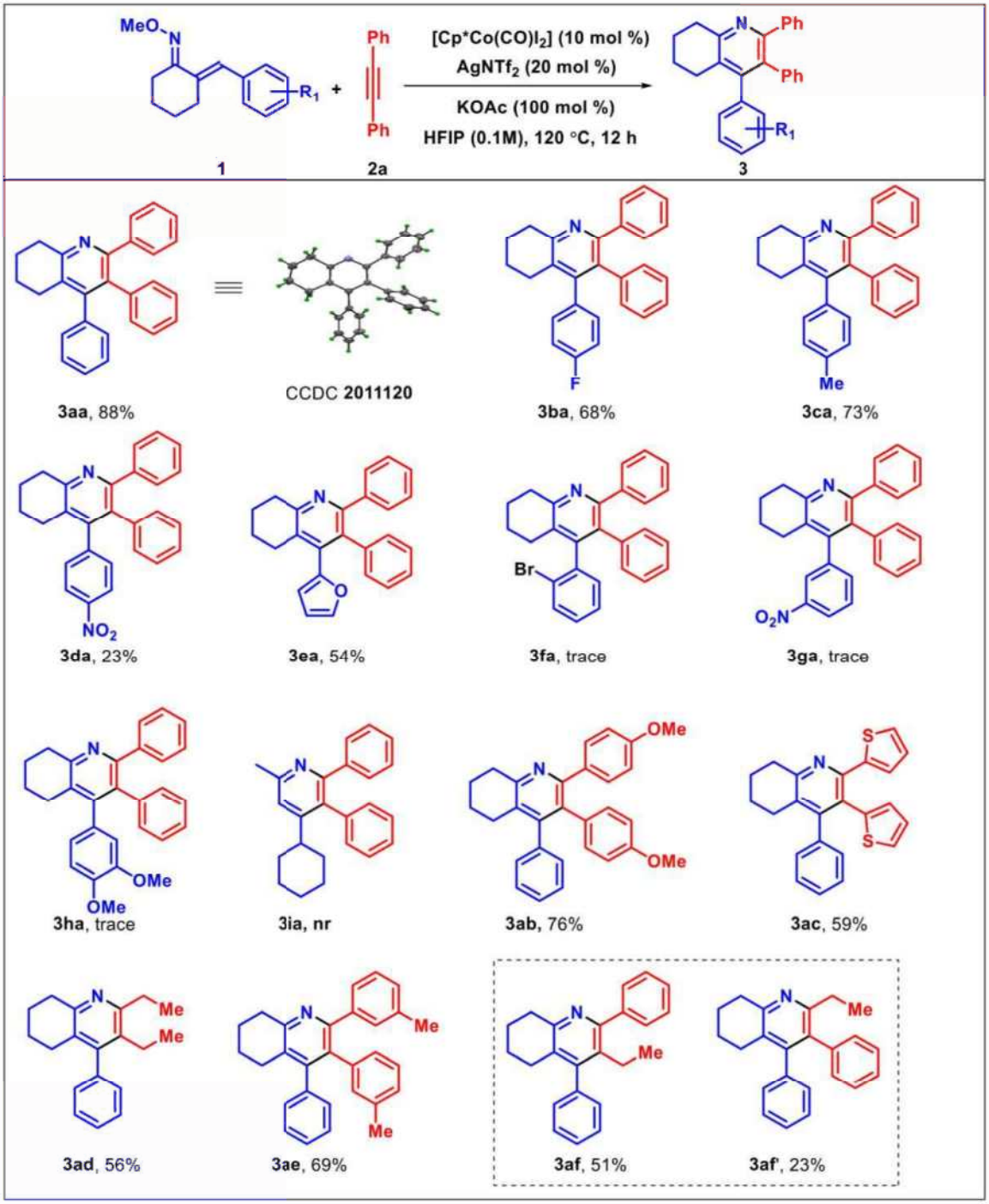

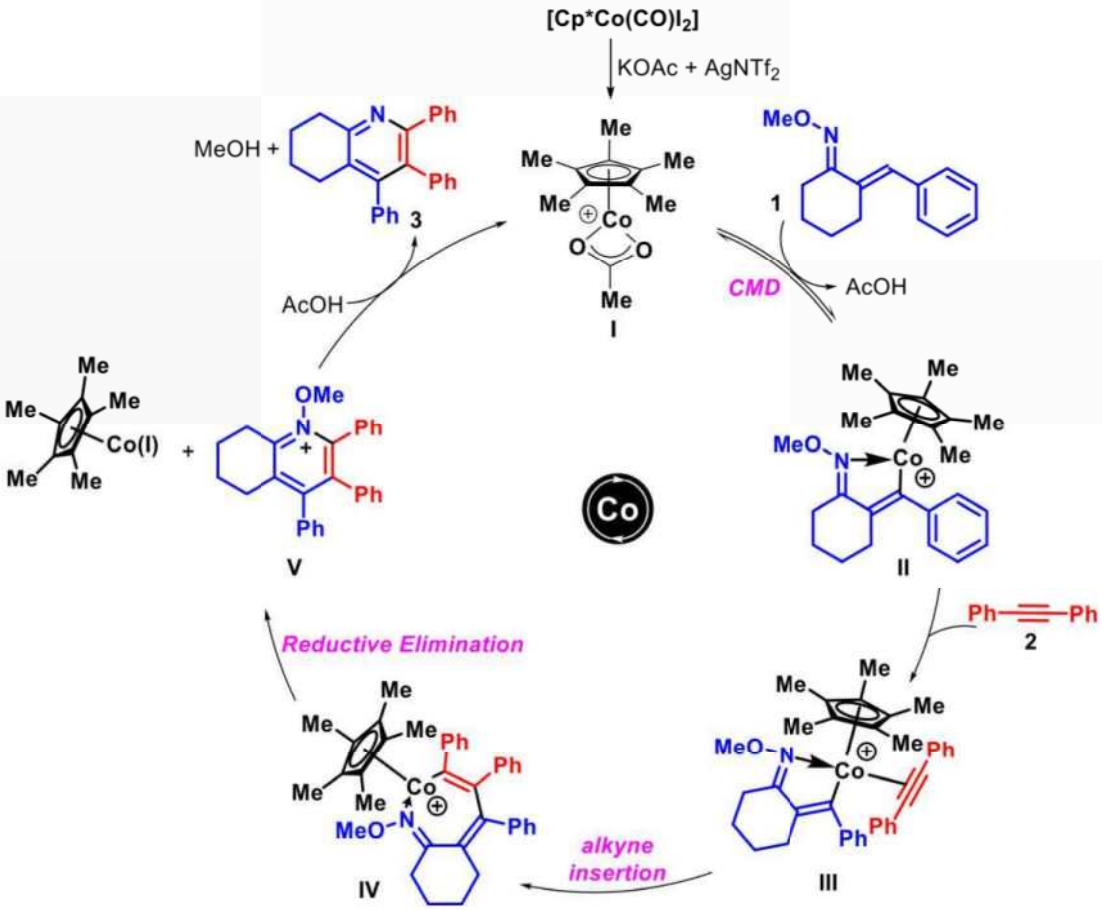

In chapter 3, we have described Co(III)-catalyzed alkenylation of 2-pyridones by using terminal alkyne as reaction partner (**Scheme 3**). We observed alkenylated products with high regioselectivity. The reactions are compatible with a wide range of electronically and sterically biased substrates and coupling partners. It proceeds through cyclometallation followed by alkyne insertion and protodemetalation steps. The formation of five and seven membered cobaltacycle intermediate was also detected through high resolution mass spectrometry. In this work we have shown the first Cp*Co(III)-catalyzed highly regioselective C-6 alkenylation of 2-pyridone with terminal alkynes under mild conditions.

Scheme 3: Cobalt catalyzed C(6)-H alkenylation of 2-pyridones with terminal alkynes and the proposed catalytic cycle

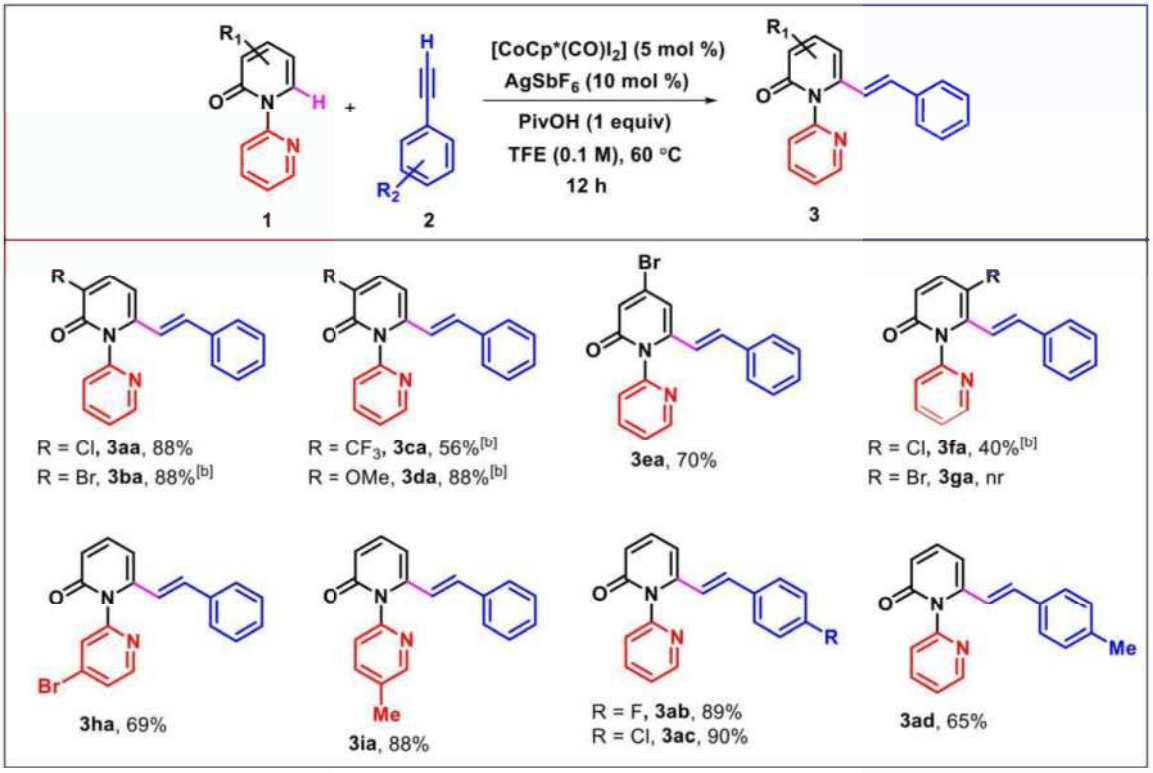

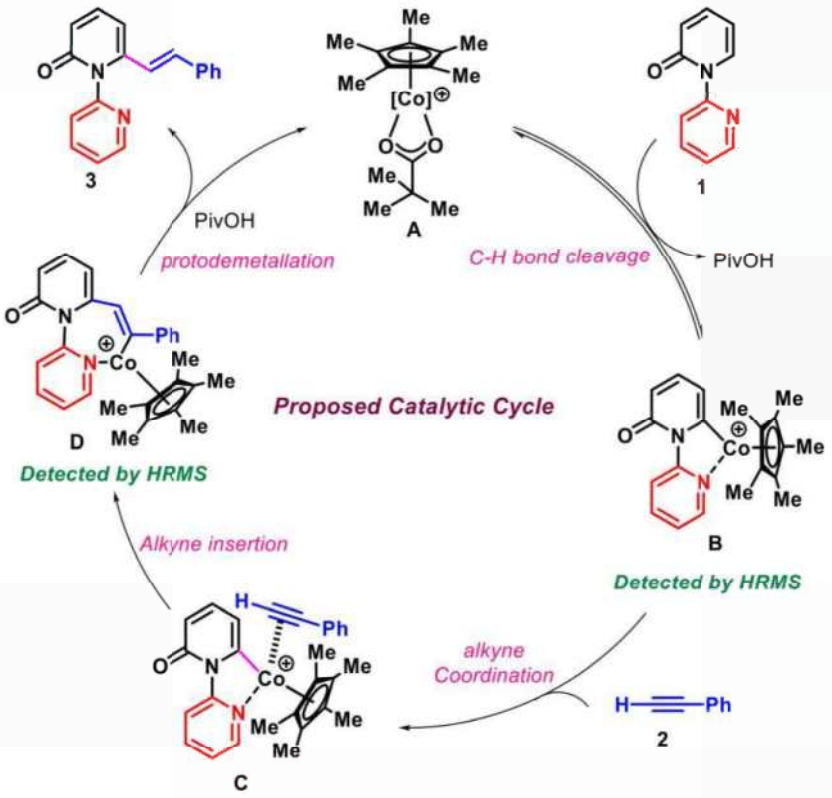

In chapter 4, we have performed the ruthenium-catalyzed regioselective sp^2(C-H) mono-alkenylation of *N*-arylpyridones where the pyridone was utilized as a weakly coordinating directing group (**Scheme 4**). Importantly, the current methodology has been effectively applied to the synthesis` of many drug analogues such as pirfenidone, naproxen, ibuprofen, geraniol, umbelliferone, pregnenolone and estrone. A six-membered ruthenium complex was also identified by high resolution mass spectrometer, which supports our catalytic cycle. This methodology tolerates different functional groups present in the substrate and coupling partner.

Scheme 4: Ru catalyzed selective olefination of *ortho*-C-H bond using acrylates and the proposed catalytic cycle

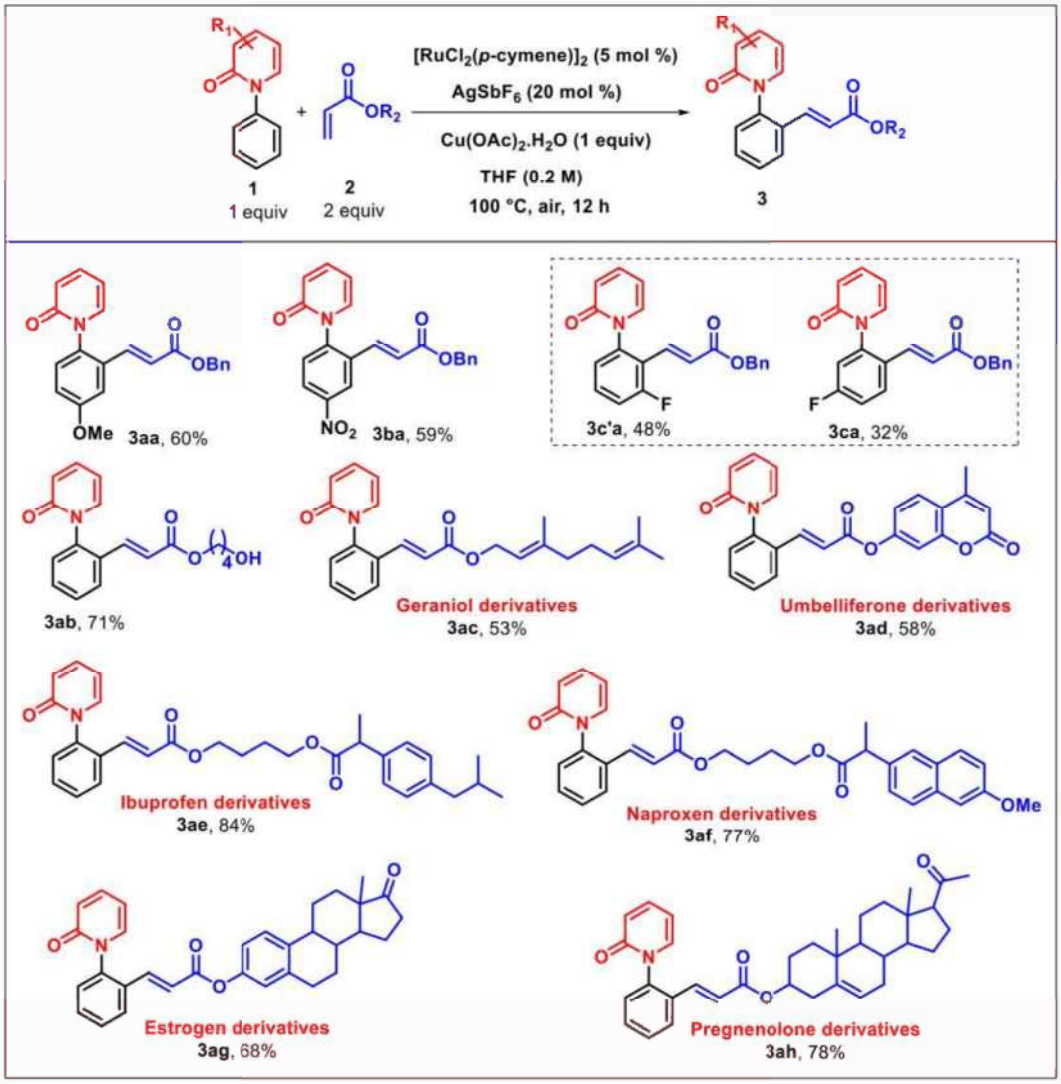

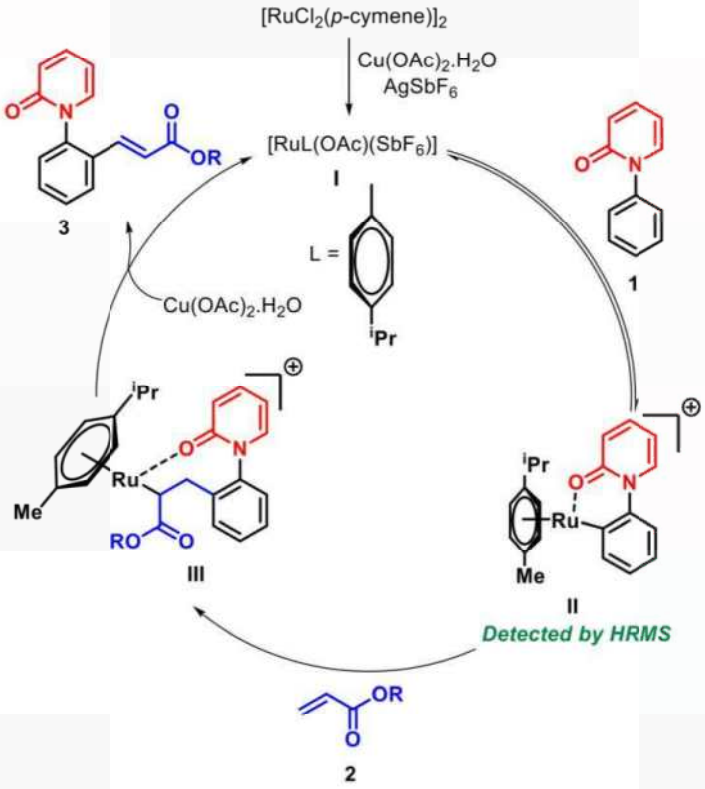

In chapter 5, we have demonstrated that an earth-abundant and inexpensive Mn(I)-catalyzed alkylation of 2-pyridone with maleimide as a alkylating agent (**Scheme 5**). In previous report, reactivity of pyridone with maleimide is known for Diels-Alder products where maleimide acting as a dienophile. This is the first Mn(I)-catalyzed alkylation at C(6) position of 2-pyridones with maleimide, leading to various biologically active succinimide derivatives. This methodology works well with a wide variety of functional groups delivering the alkylated products in moderate to excellent yields. Furthermore, single crystal X-ray and HRMS revealed a five-membered manganacycle intermediate.

we discovered an acetic acid assisted unusual rearrangement through C-N bond cleavage followed by the formation of a new C-C bond as well as an all-carbon quaternary center. However, synthesis of structural units with all carbon quaternary centers has been a challenging task for the synthetic community due to the steric restriction imposed by all carbon quaternary centers.

Scheme 5: Mn catalyzed C(6)-H alkylation of 2-pyridones with maleimides and the proposed catalytic cycle

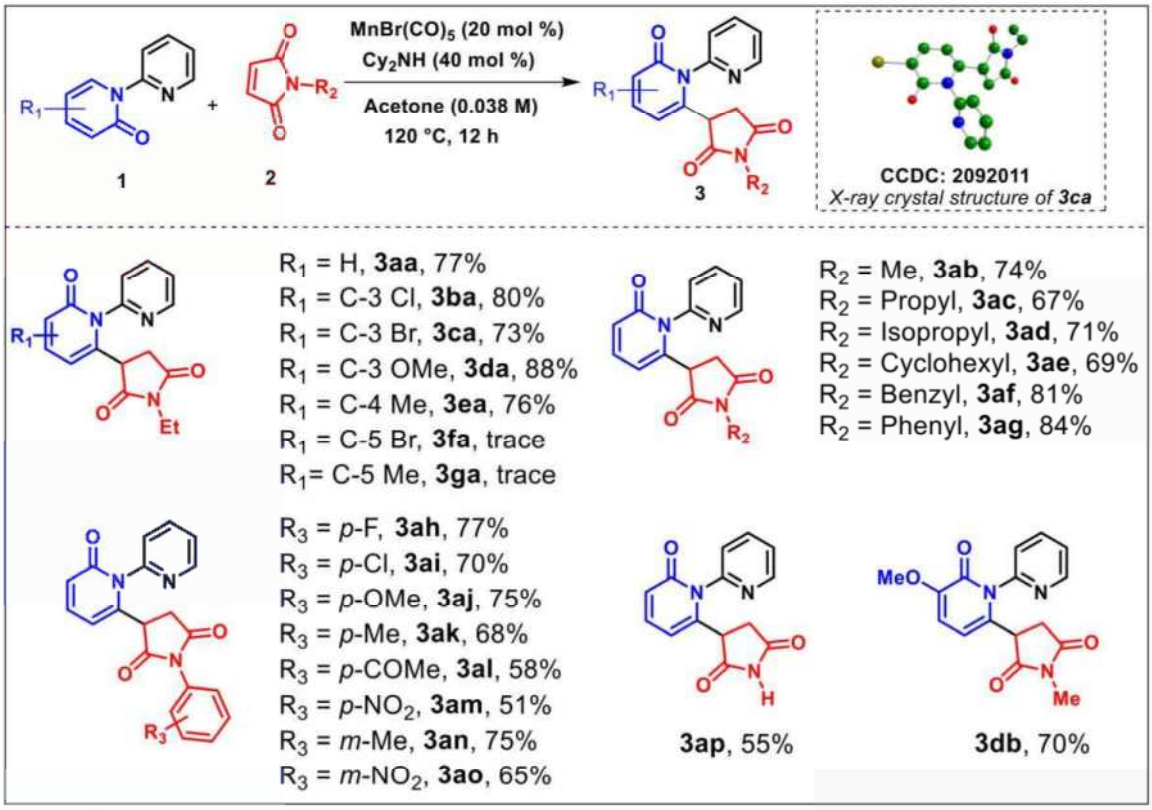

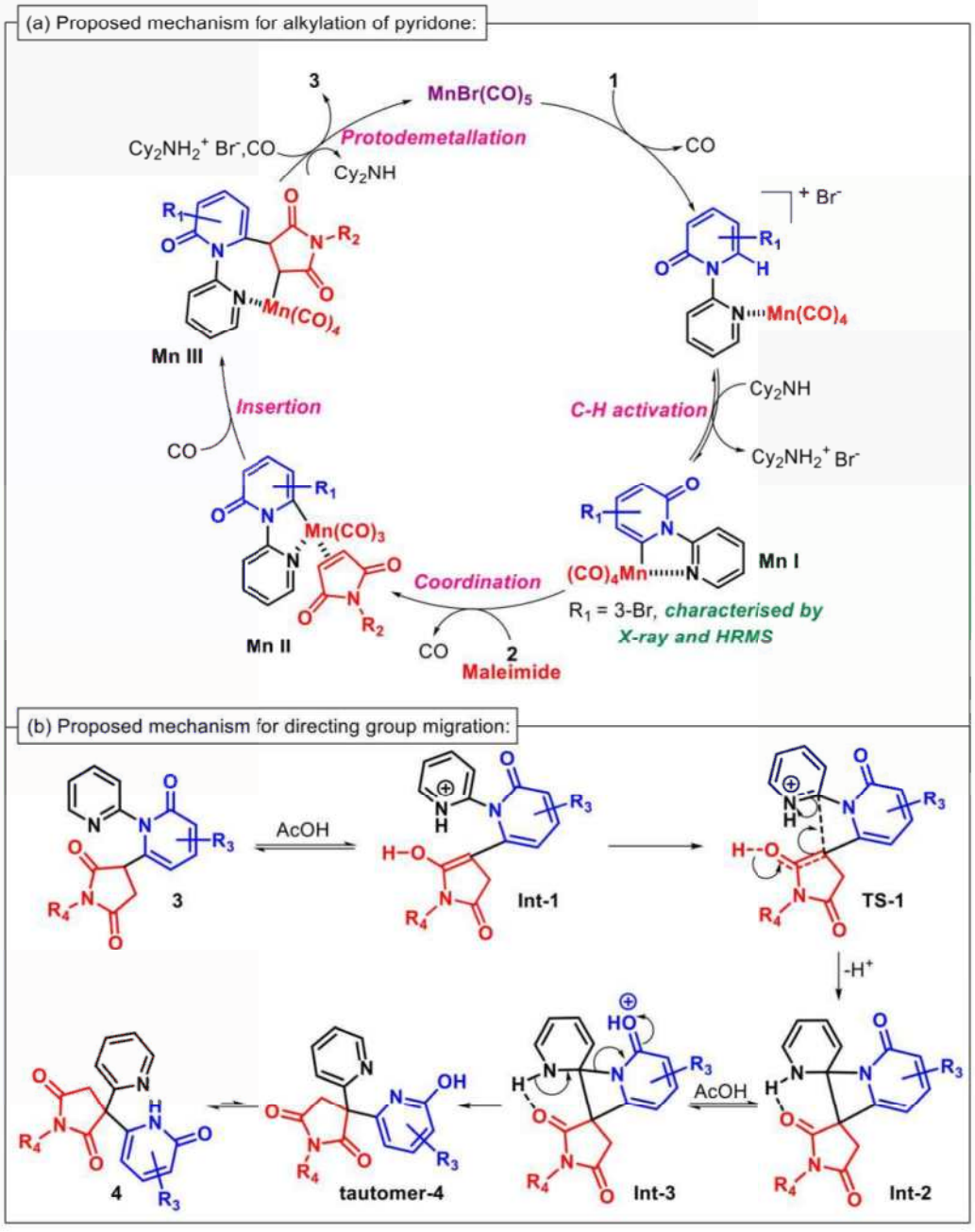
(a) Proposed mechanism for alkylation of pyridone:
3
MnBr(CO)5
1
Cy2NH2+ Br-,CO
Protodemetallation
Cy2NH
CO
+ Br-
Mn III
Insertion
C-H activation
Cy2NH
CO
Cy2NH2+ Br-
Mn(CO)3
Mn I
Coordination
(CO)4Mn
R1 = 3-Br, characterised by
X-ray and HRMS
Mn II
CO
2
Maleimide
(b) Proposed mechanism for directing group migration:
AcOH
3
Int-1
TS-1
-H+
AcOH
4
tautomer-4
Int-3
Int-2

List of figures

List of schemes

List of tables

List of Abbreviations

TM	Transition metal
DG	Directing group
FG	Functional group
NMR	Nuclear magnetic resonance
^{1}H NMR	Proton nuclear magnetic resonance
^{13}C NMR	Carbon nuclear magnetic resonance
HMBC	^{1}H-^{13}C Heteronuclear Multiple Bond Correlation Spectroscopy
MHz	Megahertz
ppm	Parts per million
IR	Infrared
$CHCl_3$	Chloroform
$CDCl_3$	Chloroform-d
HRMS	High resolution mass spectrometry
calcd	Calculated
mg	milligram
mmol	millimole
mp	melting point
mL	milliliter
min.	minute
h	hour
Fig.	Figure
TLC	Thin-layer chromatography

UV	Ultraviolet
DMF	Dimethylformamide
MeCN	Acetonitrile
DCE	1,2-dichloroethane
PhMe	Toluene
THF	Tetrahydrofuran
TFE	Trifluoroethanol
EtOAc	Ethylacetate
DCM	Dichloromethane
MeOH	Methanol
EtOH	Ethanol
HFIP	1,1,1,3,3,3-Hexafluoro isopropanol
$AgSbF_6$	Silver hexafluoroantimonate
$AgNTf_2$	Silver bis(trifluoromethanesulfonyl)imide
AgOTf	Silver trifluoromethanesulfonate
$AgBF_4$	Silver tetrafluoroborate
AcOH	Acetic acid
TFA	Trifluoroacetic acid
PTSA	*p*-Toluenesulfonic acid
1-AdCOOH	1-Adamantanecarboxylic acid
PivOH	Pivalic acid
LiOAc	Lithium acetate
NaOAc	Sodium acetate
KOAc	Potassium acetate

CsOAc	Cesium acetate
AgOAc	Silver acetate
Na_2CO_3	Sodium carbonate
Ag_2CO_3	Silver carbonate
Cy_2NH	Dicyclohexylamine
Et_3N	Triethylamine
DIPEA	*N*, *N*-Diisopropylethylamine
CuO	Copper(II) oxide
$Cu(OAc)_2$	Copper(II) acetate
$Cu(OAc)_2.H_2O$	Copper(II) acetate hydrate
$Pd(OAc)_2$	Palladium(II) acetate
PCy_3	Tricyclohexylphosphine
IMes	1,3-Bis(2,4,6-trimethylphenyl)-1,3-dihydro-2*H*-imidazol-2-ylidene
Ph	Phenyl
^{i}Pr	iso-propyl
^{t}Bu	tert-butyl
KIE	Kinetic Isotope Effect
BIES	Base-assisted intramolecular electrophilic substitution
CMD	Concerted metalation deprotonation
TEMPO	2,2,6,6-Tetramethylpiperidinyloxy
BHT	Butylated Hydroxytoluene
MeOTf	Methyl triflate
$NaBH_4$	Sodium borohydride

Chapter 1

Introduction to Alkenylation/Alkylation of inert C-H bonds

Chapter 1

Introduction to Alkenylation/Alkylation of inert C-H bonds

1.1 INTRODUCTION

C-C bond forms the backbone for all organic molecules, hence C-C bond forming reactions are considered as very important reaction in organic synthesis. Development of efficient C-C bond forming methods continues to be a hot area in synthetic chemistry. Classical C-C bond forming reactions such as Friedel-Crafts reaction and Grignard reactions, C-C bond coupling reactions catalyzed by Transition metals have been considered as highly effective strategies. Since the pioneering work by Heck in 1960, on palladium catalyzed cross-coupling of alkenes with aryl halides, significant research has been dedicated to the evolution of cross-coupling reactions catalyzed by transition metals.[1] Various types of cross coupling (C-C formation) reactions (Stille, Suzuki, Negishi, Kumada, and Hiyama) resulted the crucial techniques for important chemical synthesis (Figure-1.1).[2]

Figure-1.1: Transition metal catalyzed C-C coupling method

Despite the remarkable achievement in metal catalyzed C-C bond formation reactions, these processes mostly require prefunctionalized starting materials and a stoichiometric quantity of base.[3] The necessity of prefunctionalized substrate is an intrinsic disadvantage because of lack of availability of the substrate and additional steps required for the synthesis

of these starting material extra steps are required. Furthermore, the usage of stoichiometric quantity of base results in the formation of unwanted salt as byproduct. As a result, the C-H activation techniques catalyzed by transition metal have attracted synthetic chemists since last two decades (Figure-1.2).[4]

Figure-1.2: Schematic representation of C-H activation

Murahashi group in 1955 developed the first breakthrough for the Co-catalyzed insertion of CO into the inert C-H bond of the imine to form annulated product (Figure-1.3).[5]

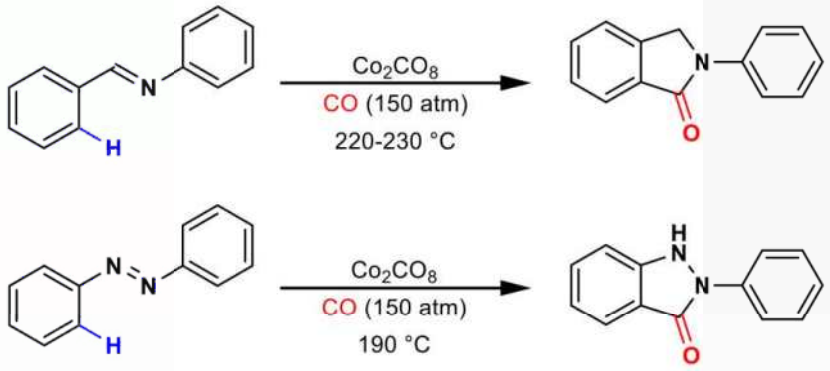

Figure-1.3: Evolution of directing group

When the reaction was first documented, this methodology received less attention. However, as a first example of arene C-H activation, we are now grateful for this extraordinary discovery and for the formation of valuable C-C and C-X bonds, which opened up a new era of C-H activation reaction. Based on the previous findings several research groups explored C-H activation as a method for the formation of C-C bonds.[6]

To date, C-H bond activation area has got huge attention from synthetic community, and they divided the C-H bond activation in to two major categories, such as (a) non-directed C-H bond activation and (b) directed C-H bond activation.

1.2 NON-DIRECTED C-H ACTIVATION

In previous report, mainly heterocycle and carbocycle were used as the substrate for non-directed C-H activation technique.[7]

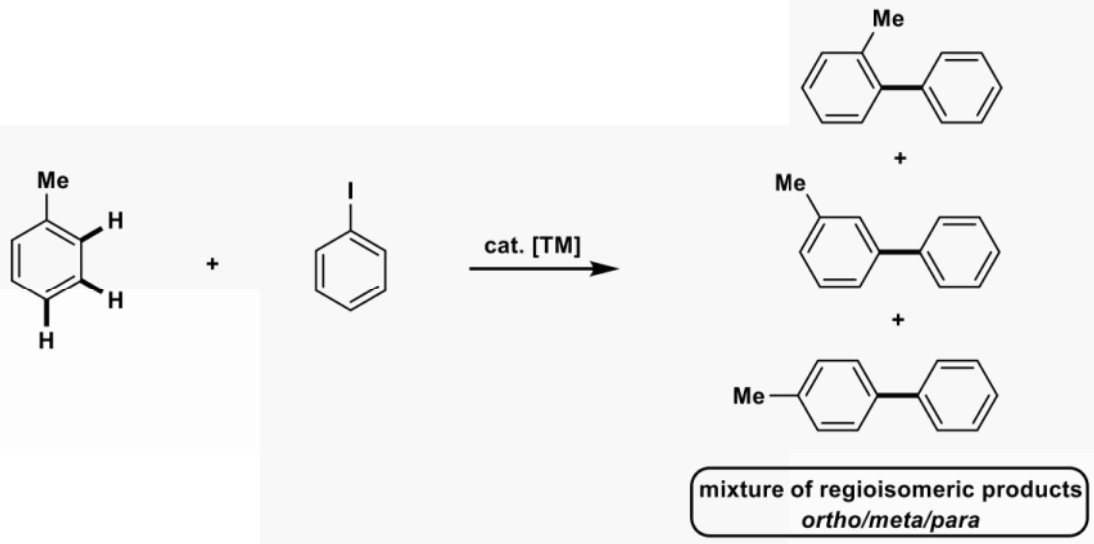

Figure-1.4: Non-directed C-H activation

Despite this, due to the drawbacks associated with nondirected C-H bond activation technique (Figure-1.4), such as low functional group tolerance, lack of site selectivity, unusual reactivity, and high catalyst loading. To overcome these issues the attention has shifted towards directed C-H bond activation technique.

1.3 DIRECTED C-H ACTIVATION

We can resolve the site selectivity issue in the realm of C-H bond activation through chelation of metal catalyst with the directing group, which brings the metal catalyst in close

proximity with the particular C-H bond of the substrate, C-H bond activation will occur with better selectivity (Figure-1.5).

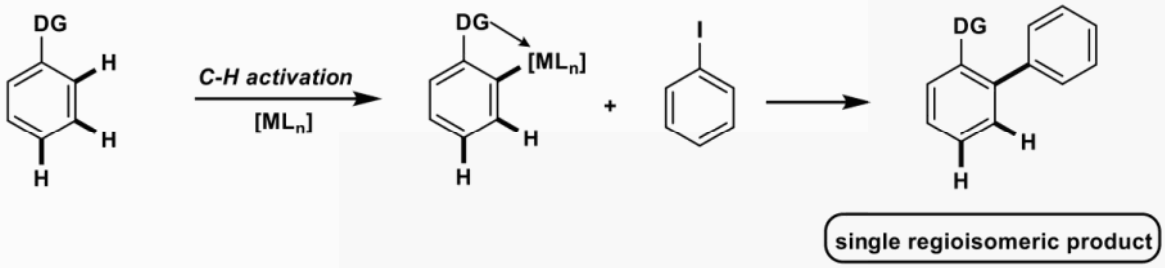

Figure-1.5: Directed C-H activation

In 1993 Murai group developed the methodology for the activation of inert C-H bond of the arene followed by functionalization. They demonstrated the ketone assisted ruthenium catalyzed alkylation of arene by using alkene (Figure-1.6).[8] This breakthrough accelerated the development of metal catalyzed C-H bond activation technique and as a result, a variety of directing groups such as ketones, aldehyde, acids, and esters have been discovered to be useful.[9]

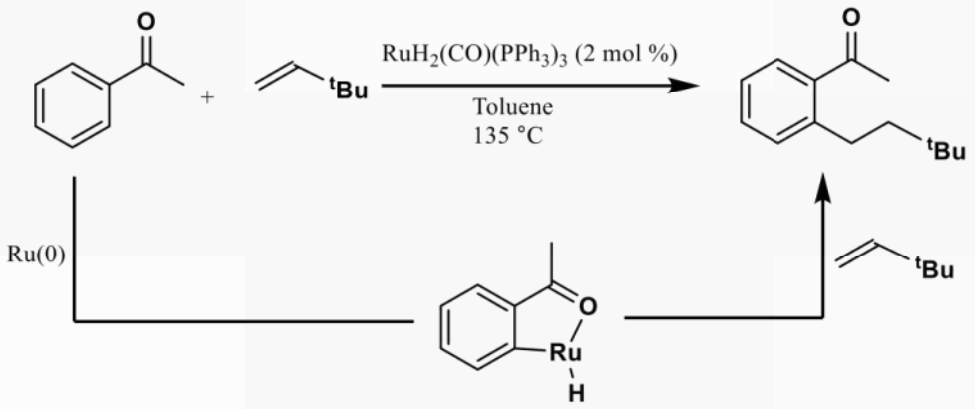

Figure-1.6: Ru catalyzed alkylation of ketone

1.4 TYPES OF DIRECTING GROUP

Based on the nature of directing group it can be classified into four types, which we have discussed below.

(a) Non-removable directing group:

Directing groups that are not removable from the substrate are called non-removable directing group (Figure-1.7).

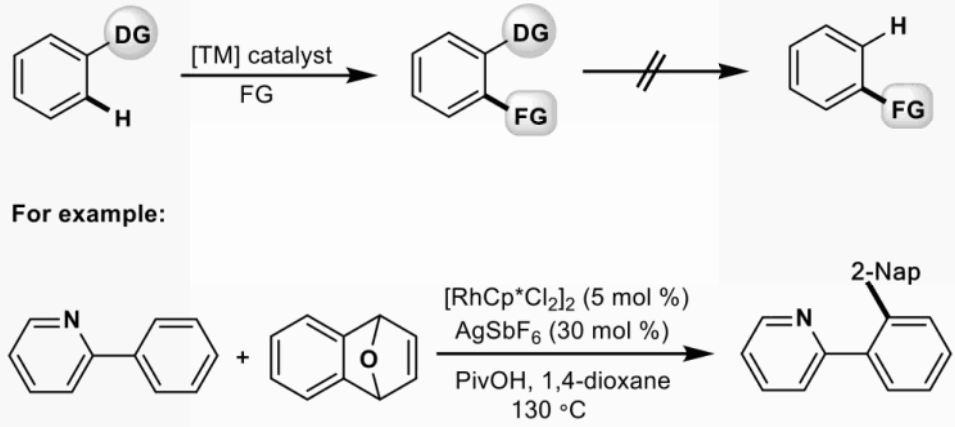

Figure-1.7: Non-removable directing group

It is difficult to remove these directing group from the product after functionalization and the directing group will remain as a part of the product after functionalization.[10] Since these directing groups are not a part of the biological scaffolds, it is a disadvantage to use them.

(b) Removable/Modifiable directing group:

Directing groups that are easy to remove and modify are called as removable/modifiable directing groups (Figure-1.8).[11] However, the major drawback is that removal or modification of the directing group from the product requires extra steps, which is a disadvantage from atom economy point of view. It is industrially less viable.

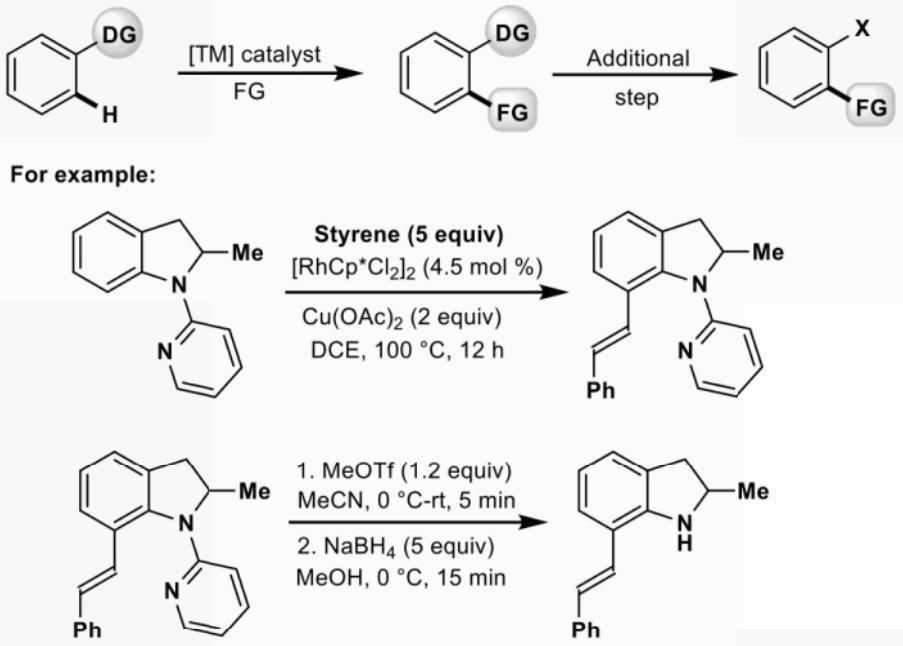

Figure-1.8: Removable/Modifiable directing group

(c) Transient Directing group:

Molecules which transiently attaches itself to the substrate in a reversible manner are called as transient directing groups (Figure-1.9).[12]

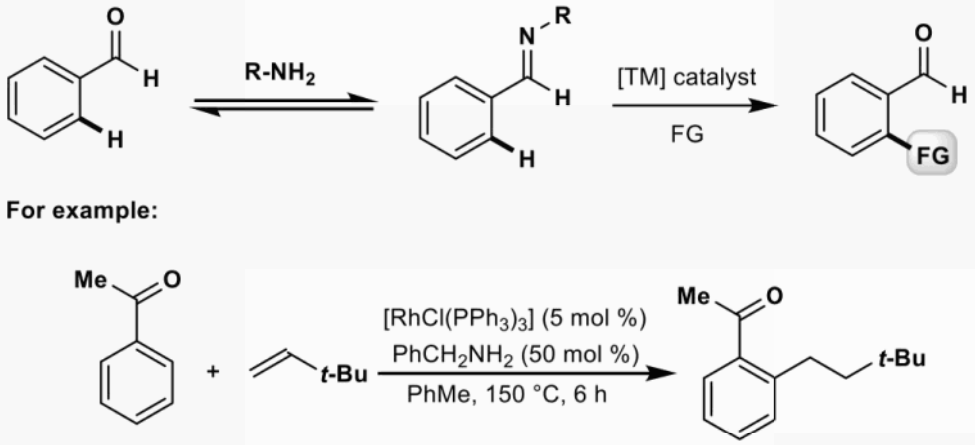

Figure-1.9: Transient Directing group

Although for the development of these directing group significant efforts have been dedicated, the limitations are that substrate need to have some functional groups which is unstable to which transient directing group can reversibly coordinate.[13, 14]

(d) Traceless directing group:

Directing groups that get detached from the substrate during the C-H functionalization step are called as traceless directing groups (Figure-1.10). Difference between traceless directing group and transient directing group is very small. Both transient and traceless directing groups gets removed from the substrate after C-H functionalization. In the case of traceless directing group, it is either inherent with the substrate or need to be attached with the substrate which requires additional step. Whereas transient directing group is attached or detached in one pot.[14c]

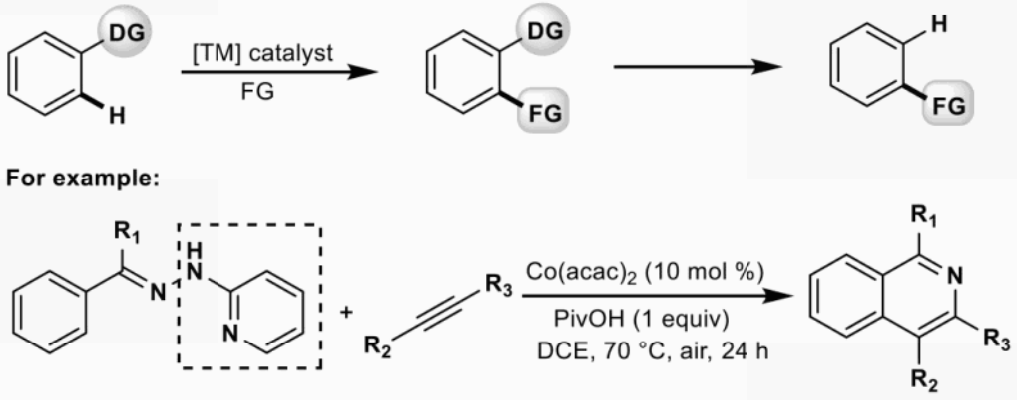

Figure-1.10: Traceless directing group

1.5 DIFFERENT MECHANISM OF C-H ACTIVATION:[15]

To know the elementary pathways involved in the C-H activation step, the mechanism has been studied by a number of research groups. There are few well-known mechanisms among the various mechanisms, such as (a) oxidative addition (OA), (b) electrophilic aromatic substitution (S_EAR), (c) σ-bond metathesis (σ-BM) and (d) concerted metalation deprotonation (CMD). Herein, we will describe each one of them individually.

(a) Oxidative Addition (OA):

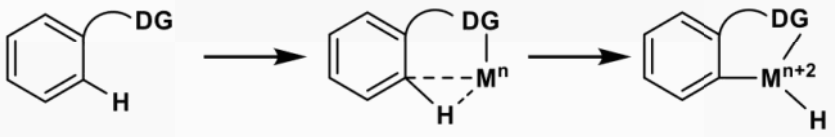

Figure-1.11: Oxidative addition

Oxidative addition process frequently observed with metal catalyst which is electron rich and oxidation state is lower. There will be a strong interaction between the electron rich metal and inert C-H bond of the substrate in a synergistic fashion resulting in the increase of oxidation state of metal by two units. A reactive organometallic species containing M-C bond is generated (Figure-1.11).

(b) Electrophilic Aromatic Substitution (S_EAR):

Transition metal catalyst can behave as a Lewis acid. Similar to the aromatic electrophilic substitution mechanism metals do act as electrophiles especially with electron rich systems and forms reactive M-C bond as shown above.

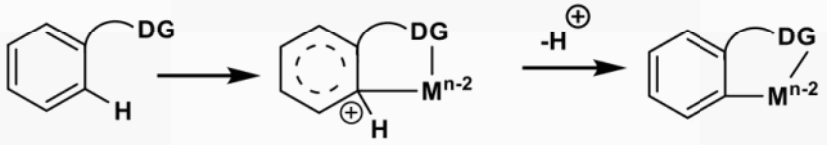

Figure-1.12: Electrophilic aromatic substitution

In this process the oxidation state of metal remains same. It affects the acidity of the neighbouring C-H bond, which can be removed in presence of a base to regain the aromatization (Figure-1.12).

(c) Sigma-bond metathesis:

Sigma bond metathesis is favourable with electron deficient metal centers and metals with higher oxidation state, the bond breaking and bond making occurs in a concerted manner

through a four-membered transition state. In this process oxidation state of the metal remain unchanged (Figure-1.13).

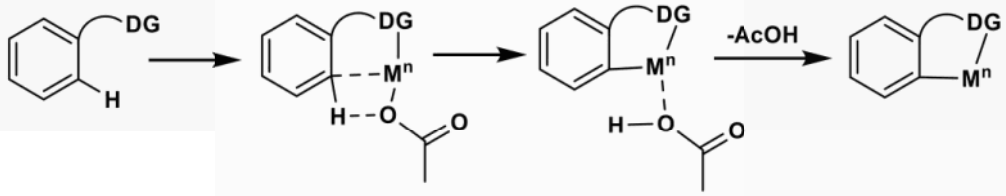

Figure-1.13: Sigma-bond metathesis

(d) Concerted Metalation Deprotonation (CMD):

Directing group promotes the C-H activation of the substrate which is close proximity to the metal center. In this process base will coordinate to the metal catalyst to enhance the deprotonation process and forms the reactive metallacycle (Figure-1.14).

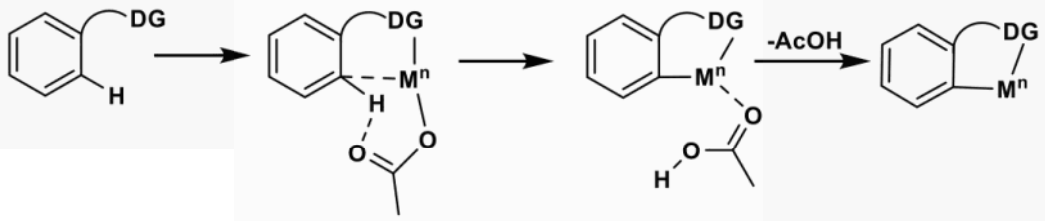

Figure-1.14: Concerted metalation deprotonation

1.6 OVERALL REACTION PROCESSES:

Generally, there are two types of processes involved in C-H activation:

(a) Redox-neutral process:[16]

Major features of redox-neutral process are oxidation state of the metal will remain same throughout the catalytic cycle and no external oxidant required for generating the catalytically active metal catalyst (Figure-1.15).

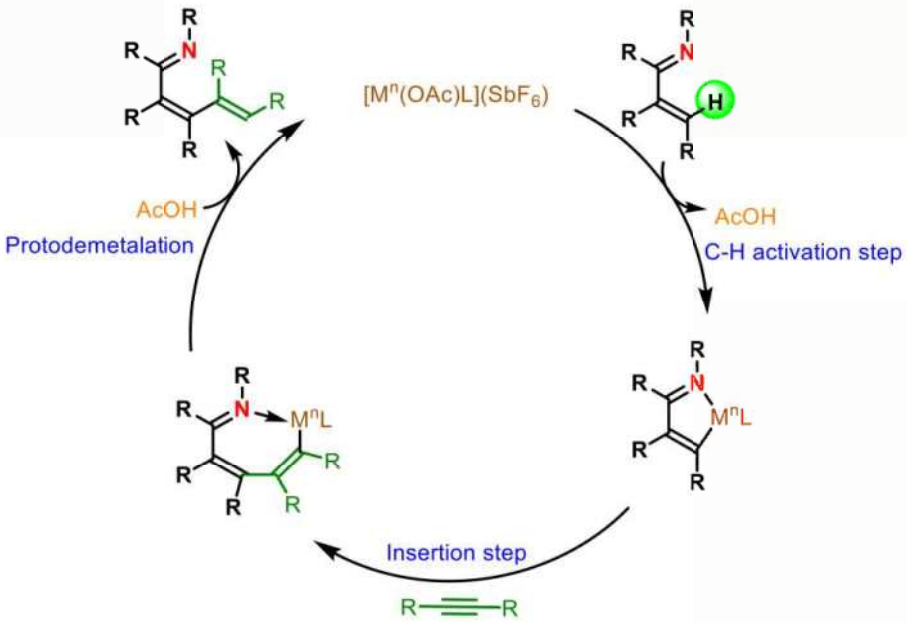

Figure-1.15: Redox-neutral process (proposed reaction pathway)

(b) Oxidative process:

By taking atom economy into account, for selective C-C bond construction, the cross-dehydrogenative coupling (CDC) process is an interesting synthetic method.[17] Li and coworkers coined the term CDC reaction to describe a reaction that uses C-H bonds to build molecules under oxidative conditions (Figure-1.16).[18] The CDC reaction has emerged as one of the most active research fields in modern organic synthesis in recent years, with numerous successful synthetic applications.[19]

The key features of oxidative process are as follows

(i) byproduct is hydrogen gas.

(ii) oxidation state of metal decreases by two unit.

(iii) it requires external oxidant to regenerate the catalytically active metal catalyst.

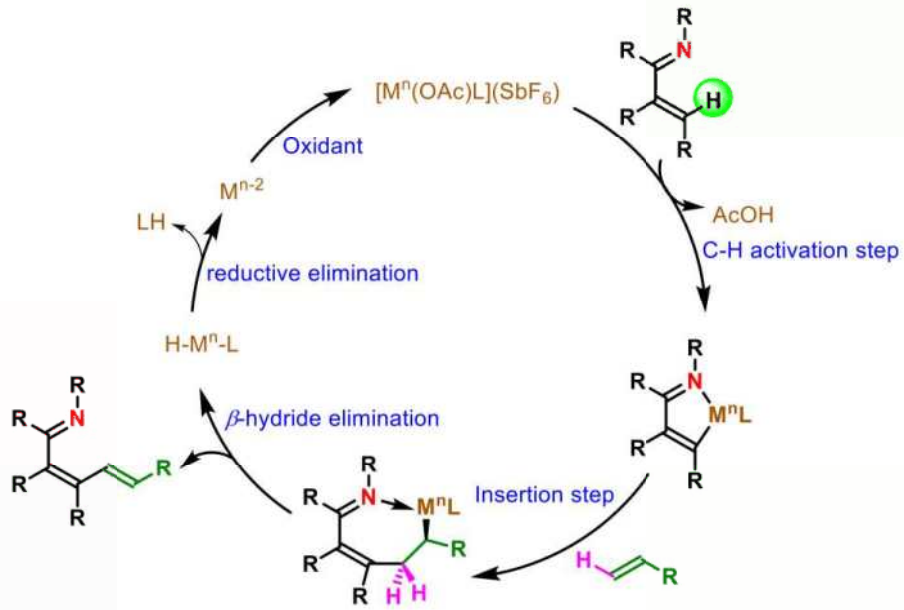

Figure-1.16: Oxidative process (proposed reaction pathway)

Bioactive libraries and the pharmaceutical industry rely heavily on heterocycles. They play an important role in our biological system. As a result, scientists are still working on developing and discovering new pharmacologically active compounds that could help to solve some of the world's most important health issues.[20] Nitrogen-heterocycles are a prevalent nucleus in a variety of bioactive natural products and drugs approved by FDA, and they play an important role in drug development and the agrochemical industry.[21]

C-H bond activation of *N*-heterocycles is an efficient way to introduce wide variety of functional groups regioselectively onto the heterocycle.[22] On the basis of their electronic properties, heterocycles can be classified into two categories, such as (a) electron-deficient heterocycles and (b) electron-rich heterocycles. Electron-deficient heterocycles are those that are less reactive than benzene towards aromatic electrophilic substitution processes; for example, pyridone, pyridine, isoquinoline, and quinoline. Electron-rich heterocycles are those that are more reactive than benzene towards aromatic electrophilic substitution, such as indole and pyrrole.

Due to the significant biological activities of 2-pyridone which is a six-membered nitrogen containing heterocycle, has attracted researchers' curiosity among all the electron deficient nitrogen-heterocycles. Pyridone is a common heteroaromatic ring found in natural products, bioactive compounds, and pharmaceuticals. Compounds that are well-known include camptothecin, milrinone, ciclopirox, fredericamycin-A, (-)-cytisine and perampanel (Figure-1.17).[23] In addition to that, recent research has identified for site selective C-H activation 2-pyridone scaffold has been used as the external ligands.[24]

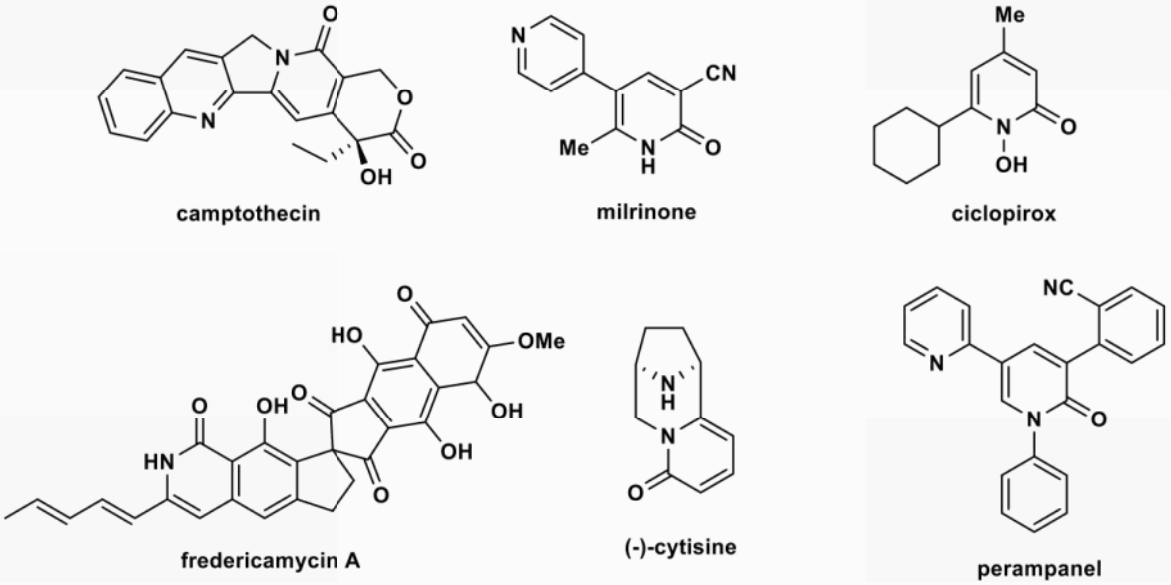

Figure-1.17: 2-pyridone in bioactive compounds and natural products

Despite the fact that the C-H functionalization technique appears to be quite useful in the synthesis of substituted pyridines.

On the pyridone ring, there are four potential reactive C-H bonds (C3-C6), and as a result the most important and difficult issue is site selectivity control. There are quite strong electronic biases in the resonance structures of 2-pyridone; the C3 and C5 positions are more electron-rich and consequently reactive toward electrophiles. Whereas the reaction with nucleophiles is more favourable at the C4 and C6 locations, which are more electron-deficient (Figure-1.18).

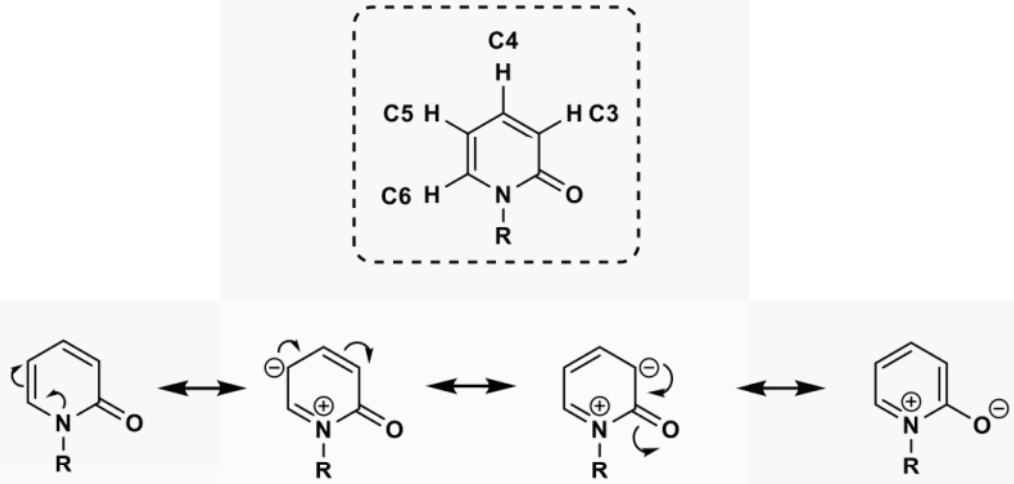

Figure-1.18: Electronic properties of 2-pyridone ring

Electronically, the 2-pyridone ring contains four distinct C-H bonds. The C3 and C5 positions of 2-pyridone have more electrons, whereas the C4 and C6 locations are electron deficient. As a result, functionalizing at the C6 position is rather difficult. In 2-pyridone, the metal catalyst can coordinate with the lone pair of electrons carried by heteroatoms and poison it.

C-H activation of electron deficient position (C4-H and C6-H) of 2-pyridone is yet to be explored, one solution is to use the DG approach, which directs the metal catalyst towards the vicinity of a specific C-H bond.

Murai and coworkers made the breakthrough discovery of ruthenium-catalyzed directed alkylation of inert C-H bonds in the aromatic ring in 1993.[25] Since then, one of the most effective solutions for resolving regioselectivity problems is the employment of directing groups.[26] In recent years alkylation,[27] alkenylation,[28] arylation,[29] allylation,[30] amination,[31] and other directing group assisted C-H bond functionalization processes have been reported.

In this thesis we have focussed on Alkylation and alkenylation.

1.7 ALKYLATION OF INERT C-H BOND:

Alkene insertion into inert C-H bonds of the arene ring is a simple method for introducing alkyl groups in aromatic ring.[32] Generally, alkylation reaction using alkene can be divided into 2 types, each of which can result in various regioselectivities (Figure-1.19).

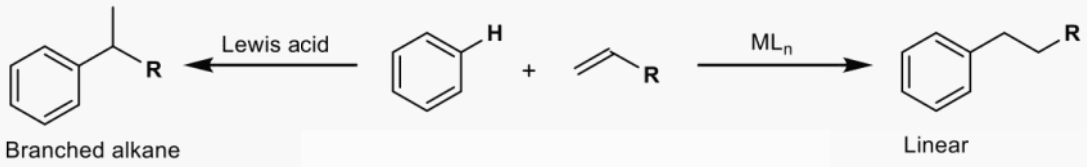

Figure-1.19: Alkylation of inert C-H bond

Alkylation reactions of the Friedel-Crafts type, Bronsted acid/Lewis acid catalysts could assist this.[33] Only electron-rich arenes and heteroarenes are suitable for the classical alkylation reaction. When an alkene is activated through a carbocationic species, it leads to Markovnikov product (branched).[34]

C-H bond activation catalyzed by transition metal typically often necessitates the directing group on the substrates, which affords linear addition product preferably.[25, 35] Murai group in 1993 have successfully demonstrated the protocol for Ru-catalyzed alkylation of acetophenone **1** with alkene **2** to form linear alkylated product **3** (Figure-1.20).[25]

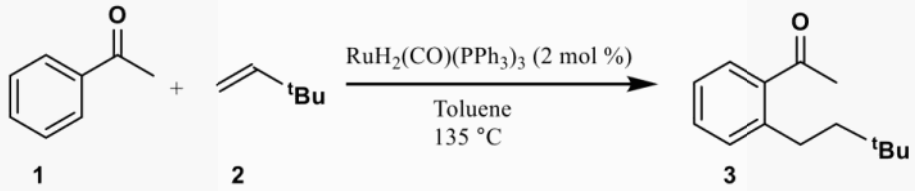

Figure-1.20: Addition of inert C-H bond to alkene

Lim and Kang developed the first rhodium-catalyzed C-H alkylation reaction.[36] Recently, Jun group have demonstrated that when *N*-benzyl aryl ketimine **4** reacts with 1-hexene **5**, catalysed by a stable Wilkinson's catalyst a linear adduct **6** was obtained (Figure-

1.21a).[37] Nakao and Hiyama group reported in 2010 that hydroheteroarylation of styrene derivative **9** by using Ni-catalyst and IMes ligand yielding a branched alkylated product **10** (Figure-1.21b).[38]

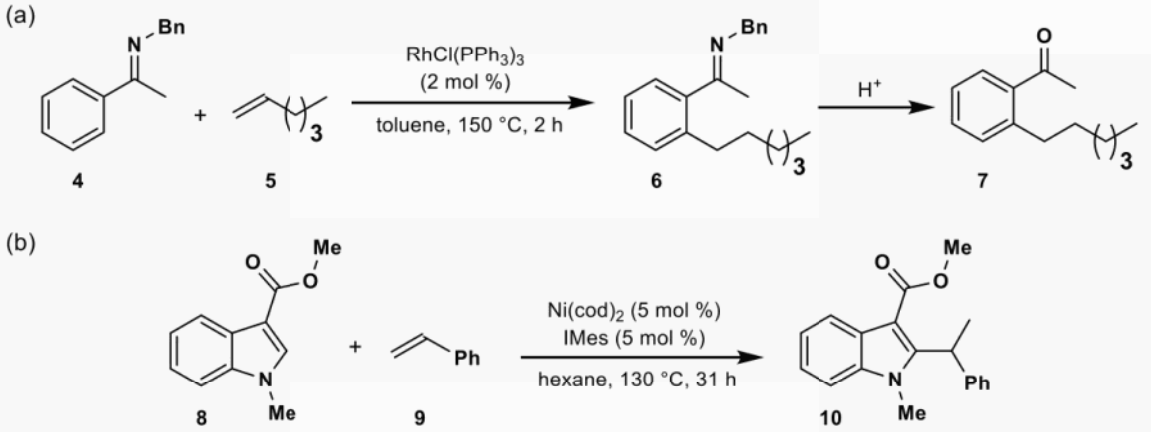

Figure-1.21: Rh, Ni-catalyzed alkylation of inert C-H bond

Yoshikai group has demonstrated the low-valent Co-catalyzed ortho alkylation of arene **11** with styrene **9** as the reaction partner under mild conditions. Interestingly the usage of different ligands can regulate the reaction's regioselectivity. The Co-PCy_3 catalysis combination resulted in a branched product **12**, whereas the Co-IMes catalysis provided a linear product **13** (Figure-1.22).[39]

The Zhang group reported in 2016 that Cp*Co(III)-catalyzed direct allylation of enamides **14** was achieved exclusively with *Z*-selectivity. (Figure-1.23a).

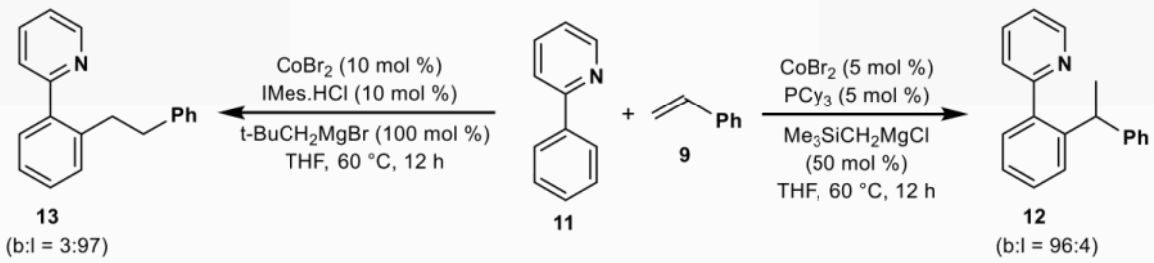

Figure-1.22: Addition of 2-aryl pyridine to olefins

Under mild conditions, this reaction proceeds efficiently and compatible to variety of functional group. Apart from allyl acetates, vinylcyclopropane and 2-vinyloxirane can also be used as allyl sources.[27a]

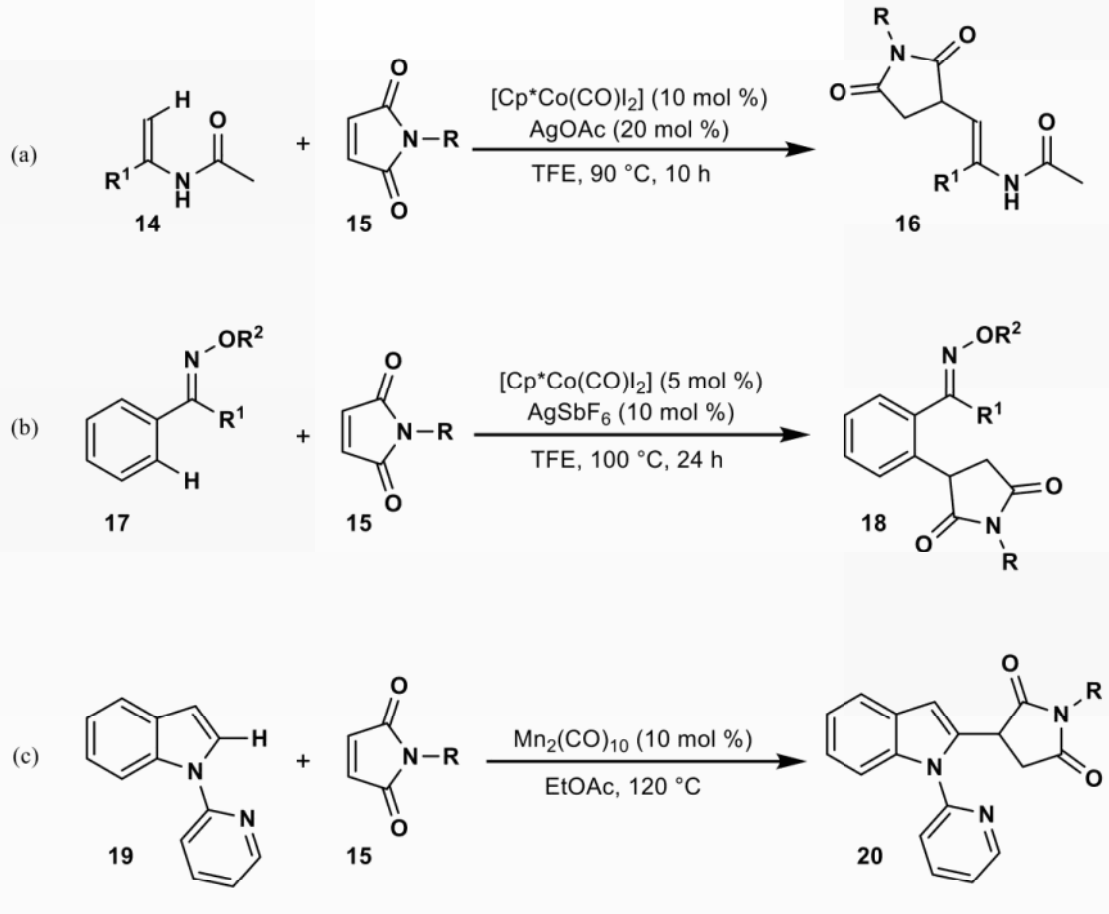

Figure-1.23: Alkylation of sp^2(C-H) bond using maleimide

Wu group revealed another example in 2017 where they have reported Oxime assisted Co-catalyzed sp^2(C-H) bond activation of the arene **17** followed by 1,4-addition to maleimide **15** (Figure-1.23b), different functional groups were well tolerated by this reaction, and numerous succinimide derivatives were efficiently generated. Only a mono selective C-H activation followed by addition product was observed by this reaction.[27b] Additionally, the Song group developed the manganese-catalyzed sp^2(C-H) activation at 2-position of indoles **19** followed by addition to maleimides **15** in the same year (Figure-1.23c). High regioselectivity and chemoselectivity was observed in this reaction.[27c] A plausible

mechanism for directing group assisted C-H alkylation was described (Figure-1.24).[40] The majority of chelation-driven processes follow a conventional reaction route except in some circumstances that may be varied. Initially substrate **I** containing heteroatom coordinates to

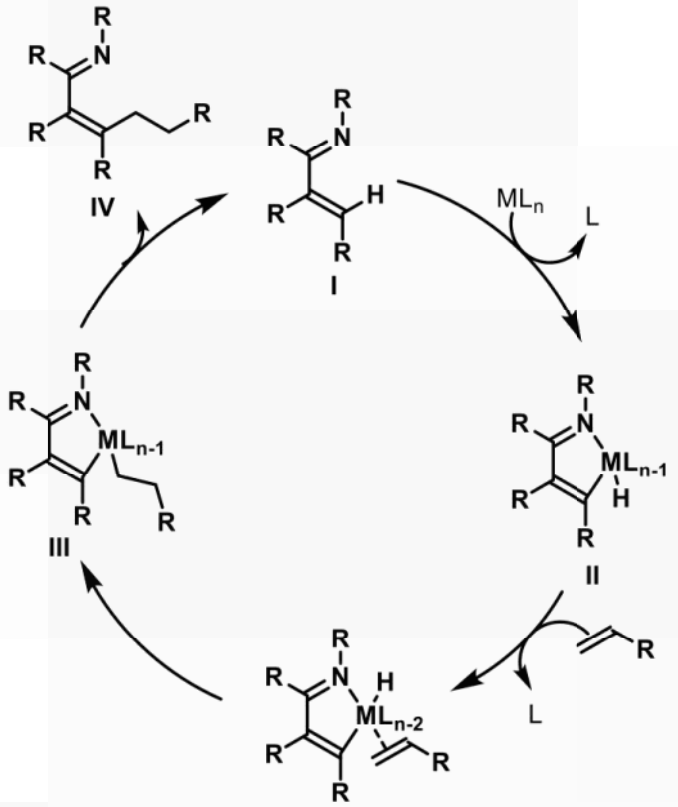

Figure-1.24 (plausible mechanism for alkylation)

the transition metal, transition metal inserts into the inert C-H bond and to give five membered metalacycle **II**. Next coordination followed by insertion of the alkene into the M–H bond of the Intermediate **II** to form intermediate **III**. Intermediate **III** undergoes reductive elimination resulting the alkylated product **IV** and regenerates the active catalyst.

1.8 ALKENYLATION OF INERT C-H BOND:

One of the most effective and straightforward atom economic methods for alkenylation of inert C-H bond is metal catalyzed addition of an C-H bond to the triple bond.[41] Compared

to Heck reactions[42] and other cross-coupling reactions,[43] this technique provides a simplified methodology.[44] In general, alkynes can be hydroarylated by two methods such as (a) activating triple bond of the alkyne and (b) activating the sp^2(C-H) bond of the arene. But here we are focussing on activation of the sp^2(C-H) bond of the arene (Figure-1.25).

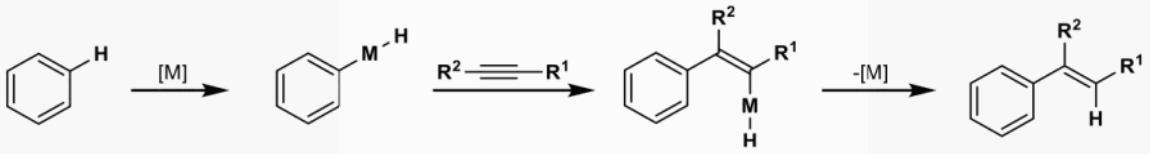

Figure-1.25: Alkenylation of inert C-H bonds

Reaction proceeds through sp^2(C-H) bond activation of the arene. The reaction provides a mixture of regioisomeric products. However, the aromatic ring contains the directing group triggers the C-H activation through chelation assistance and the regioselectivity of the reaction was controlled.

In 1994 Kisch group was reported the first low-valent Co-catalyzed hydroarylation of alkynes.[45] Here, azobenzene **21** undergo addition with diphenylacetylene **22** to give the desired alkenylated product **23** in moderate to good yields. (Figure-1.26a). Yoshikai's team revealed in 2010 that ternary catalytic systems including low-valent cobalt catalyst, Grignard reagents and phosphine ligands promote the addition of arylpyridines **11** to internal alkynes **24** with good regioselectivity and stereoselectivity (Figure-1.26b).[46] Further Yoshikai group in 2011 proposed that, using the combination of low-valent Co-catalyst,Grignard reagent and triarylphosphine ligand and pyridine promotes the directing group-aided sp^2(C-H) bond activation of an imine derivative **27** (Figure-1.26c), it inserts in to the internal alkyne forming the alkenylated product. The methodology tolerates various functional groups and also displays excellent regioselectivity.[47]

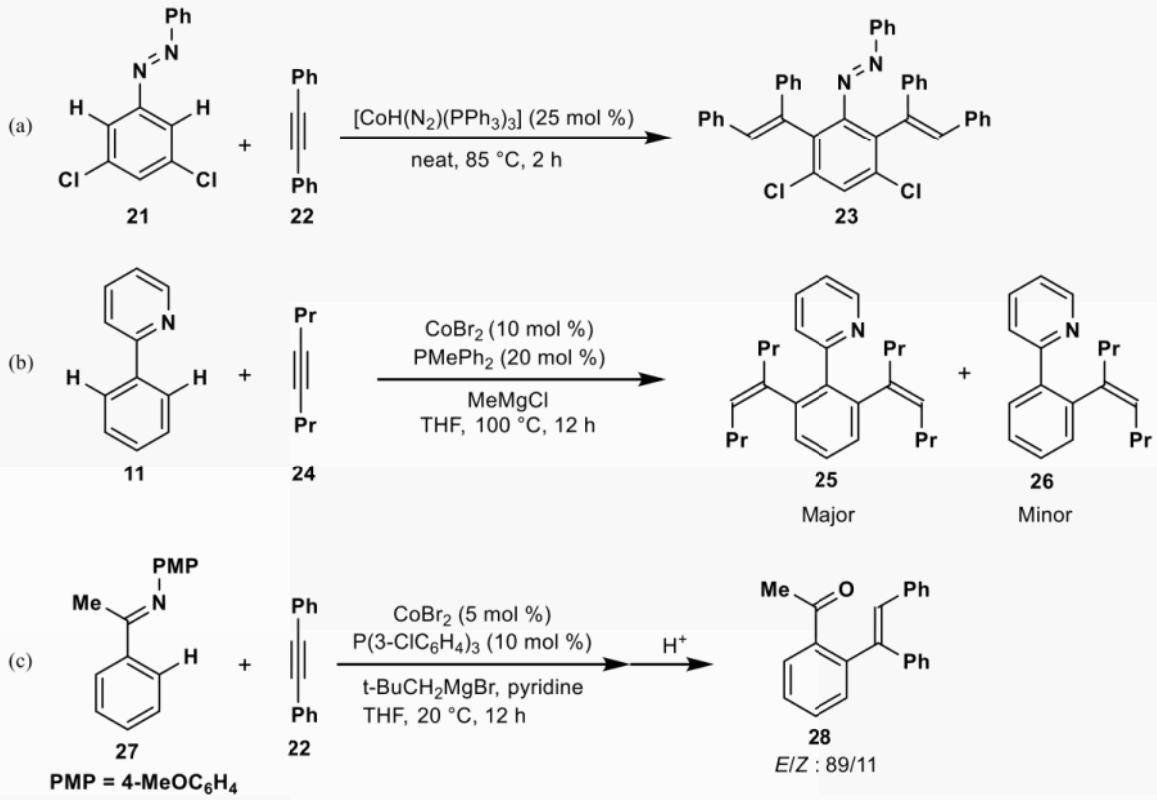

Figure-1.26: Low-valent Co-catalyzed olefination of inert C-H bond

Until 2014, alkenylation of inert C-H bond of the aromatic ring were limited to low-valent Co-catalyst, it required complex reaction conditions and the reactions is highly sensitive to moisture, which limits variety of functional group.

Matsunaga/Kanai demonstrated that in C-H activation reactions these limitations were overcome by using high-valent Co(III)-catalyst. Kanai group in 2014 have developed the Co(III)Cp* catalyst synthetic utility as compared to Rh(III)Cp* catalyst. A C2-position of indole **29** undergo selective alkenylation followed by annulation in presence of $[Co(III)Cp^*(C_6H_6)](PF_6)_2$ proceeded efficiently to provide pyrroloindolones **31** (Figure-1.27a). Here they have clearly distinguished the catalytic efficiency of Co(III)Cp* and Rh(III)Cp*.[28a] Matsunaga group in 2016 demonstrated successfully selective C-H alkenylation at C(2) position of indoles **32** with alkyne **24** as coupling partner using a catalytic

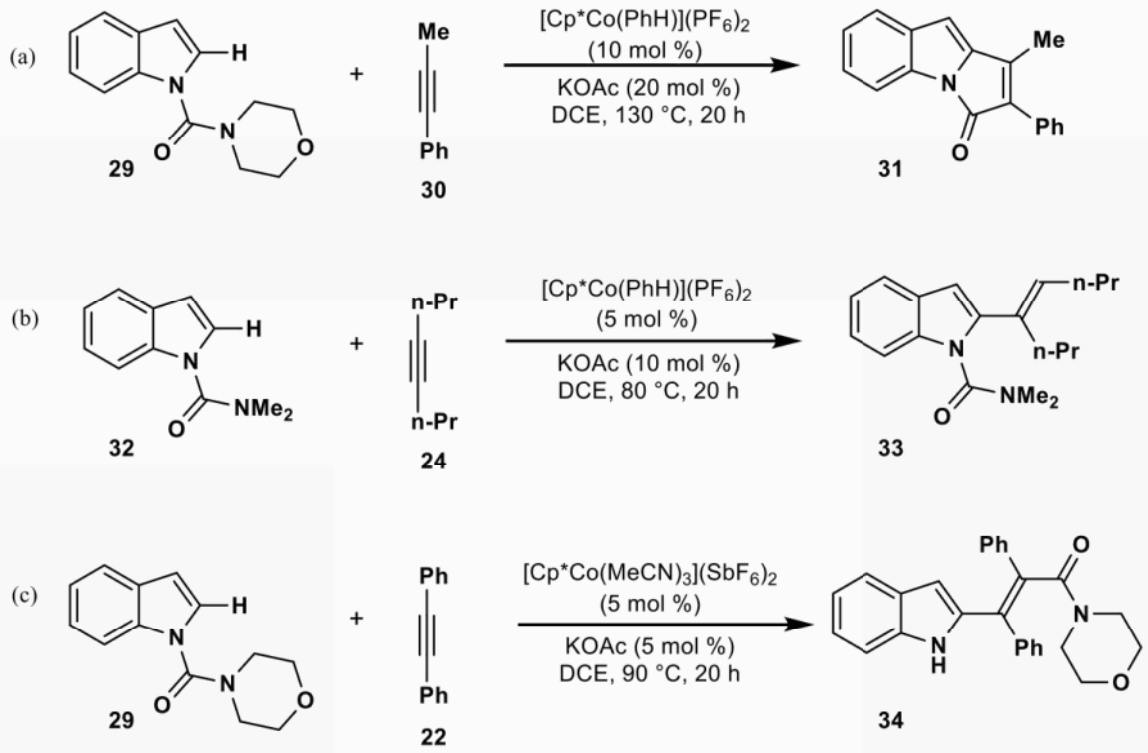

Figure-1.27: Co-catalyzed alkenylation of inert sp^2(C-H) bond

amount of $[CoCp^*(MeCN)_3](SbF_6)_2$ and base (Figure-1.27b). Various types of electronically and sterically biased internal alkynes and terminal alkyne afforded the selective alkenylated products.[28b] Further same group also revealed that, Co(III)-catalyzed sp^2(C-H) olefination at C(2) position of indole **29** followed by directing group migration to synthesize *α,β*-unsaturated amides with tetra substitution **34** (Figure-1.27c). The desired product was then transformed into two different forms of tricyclic compounds, one of which was fluorescent.[28c]

A general plausible mechanism for transition metal-catalyzed directing group assisted alkenylation of inert C-H bonds have shown (Figure-1.28).[48] sp^2(C-H) bond of the substrate **I** undergo oxidative addition by a metal catalyst to form the five membered metalacycle **II**. The next pathway is alkyne coordination followed by insertion into the M-H bond of the intermediate **II** forming intermediate **III**. Then intermediate **III** undergoes reductive

elimination forming the alkenylated product **IV** and regenerates the active catalyst for the next cycle.

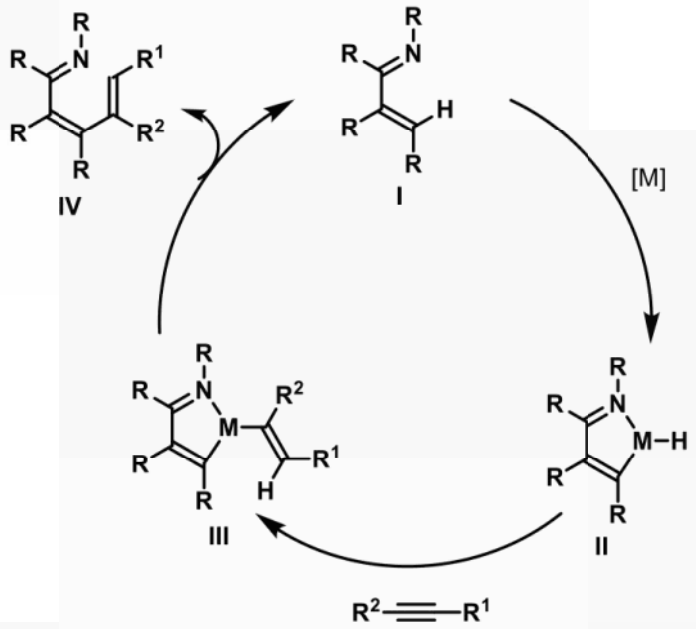

Figure-1.28: Proposed mechanism for alkenylation reaction

1.9 CONCLUSION

Formation of a C-C bond is a very important reaction in organic synthesis. Traditionally C-C bonds are formed between an aryl group using cross-coupling reactions. However, the disadvantage with such reaction is that it requires pre-functionalized substrates, which are often not commercially available. Therefore, chelation assisted direct C-H functionalization reactions offer a better alternative to cross coupling reaction. In this chapter we have discussed different elementary step involved in the catalytic cycle. Also, different processes involved in the C-H activation reaction has been discussed such as redox neutral process and oxidative process. In this regard, alkylation, alkenylation, arylation, allylation, amination, and other directing group assisted C-H bond functionalization processes have been documented. In this thesis we have demonstrated the transition metal catalyzed alkylation and alkenylation of inert C-H bond.

1.10 REFERENCES:

1. (a) Heck, R. F. Arylation, Methylation, and Carboxy alkylation of Olefins by Group VIII Metal Derivatives. *J. Am. Chem. Soc.* **1968**, *90*, 5518–5526. (b) Heck, R. F. The Mechanism of Arylation and Carbo-methoxylation of Olefins with Organopalladium Compounds. *J. Am. Chem. Soc.* **1969**, *91*, 6707–6714. (c) Heck, R. F.; Nolley, J. P. Palladium-Catalyzed Vinylic Hydrogen Substitution Reactions with Aryl, Benzyl, and Styryl Halides. *J. Org. Chem.* **1972**, *37*, 2320–2322.
2. (a) Tamao, K.; Sumitani, K.; Kumada, M. Selective Carbon-Carbon Bond Formation by Cross-Coupling of Grignard Reagents with Organic Halides. Catalysis by Nickel-Phosphine Complexes. *J. Am. Chem. Soc.* **1972**, *94*, 4374–4376. (b) Miyaura, N.; Yamada, K.; Suzuki, A. A new stereospecific cross-coupling by the palladium-catalyzed reaction of 1-alkenylboranes with 1-alkenyl or 1-alkynyl halides. *Tetrahedron Lett*. **1979**, 3437–3440. (c) King, A. O.; Okukado, N.; Negishi, E. Highly general stereo-, regio-, and chemo-selective synthesis of terminal and internal conjugated enynes by the Pd-catalysed reaction of alkynyl zinc reagents with alkenyl halides. *J. Chem. Soc.*, *Chem. Commun*. **1977**, 683–684. (d) Milstein, D.; Stille, J. K. A General, Selective, and Facile Method for Ketone Synthesis from Acid Chlorides and Organotin Compounds Catalyzed by Palladium. *J. Am. Chem. Soc.* **1978**, *100*, 3636–3638. (e) Hatanaka, Y.; Hiyama, T. Cross-coupling of organosilanes with organic halides mediated by a palladium catalyst and tris(diethylamino)sulfonium difluorotrimethylsilicate. *J. Org. Chem.* **1988**, *53*, 918–920.
3. (a) Kambe, N.; Iwasaki, T.; Terao, J. Pd-catalyzed cross-coupling reactions of alkyl halides. *Chem. Soc. Rev*. **2011**, *40*, 4937–4947. (b) Han, F. S. Transition-metal-catalyzed Suzuki–Miyaura cross-coupling reactions: a remarkable advance from palladium to nickel. *Chem. Soc. Rev*. **2013**, *42*, 5270–5298.

4. (a) Hashiguchi, B. G.; Bischof, S. M.; Konnick, M. M.; Periana, R. A. Designing Catalysts for Functionalization of Unactivated C–H Bonds Based on the C-H Activation Reaction. *Acc. Chem. Res*. **2012**, *45*, 885–898. (b) Gensch, T; Hopkinson, M. N.; Glorius, F.; Wencel-Delord, J. Mild metal-catalyzed C–H activation: examples and concepts. *Chem. Soc. Rev*. **2016**, *45*, 2900–2936.

5. (a) Murahashi, S. Synthesis of Phthalimidines from Schiff Bases and Carbon Monoxide. *J. Am. Chem. Soc*. **1955**, *77*, 6403−6404. (b) Murahashi, S.; Horiie, S. The Reaction of Azobenzene and Carbon Monoxide. *J. Am. Chem. Soc*. **1956**, *78*, 4816−4817.

6. Zhang, Y. H.; Shi, G. F.; Yu, J. Q. Carbon−Carbon σ-Bond Formation via C−H Bond Functionalization. In Comprehensive Organic Synthesis II; Knochel, P., Ed.; *Elsevier*: Amsterdam, **2014**; Chapter 3.23, pp 1101−1209.

7. (a) Xie, J.; Zhu, C. In Recent Advances in Non-Directed C(sp^3)−H Bond Functionalization: Sustainable C(sp^3)-H Bond Functionalization; *Springer: Heidelberg*, **2016**; pp 25−59. (b) Hartwig, J. F.; Larsen, M. A. Undirected, Homogeneous C-H Bond Functionalization: Challenges and Opportunities. *ACS Cent. Sci*. **2016**, *2*, 281−292. (c) Das, R.; Kapur, M. Transition-Metal-Catalyzed C−H Functionalization Reactions of π-Deficient Heterocycles. *Asian J. Org. Chem*. **2018**, *7*, 1217−1235.

8. Murai, S.; Kakiuchi, F.; Sekine, S.; Tanaka, Y.; Kamatani, A.; Sonoda, M.; Chatani, N. Efficient Catalytic Addition of Aromatic Carbon-Hydrogen Bonds to Olefins. *Nature* **1993**, *366*, 529−531.

9. (a) Huang, Z.; Lim, H. N.; Mo, F.; Young, M. C.; Dong, G. Transition Metal-Catalyzed Ketone-Directed or Mediated C-H Functionalization. *Chem. Soc. Rev*. **2015**, *44*, 7764−7786. (b) Mochida, S.; Hirano, K.; Satoh, T.; Miura, M. Rhodium Catalyzed

Regioselective Olefination Directed by a Carboxylic Group. *J. Org. Chem.* **2011**, *76*, 3024−3033. (c) Shi, Z.; Schröder, N.; Glorius, F. Rhodium(III)-Catalyzed Dehydrogenative Heck Reaction of Salicylaldehydes. *Angew. Chem., Int. Ed*. **2012**, *51*, 8092−8096. (d) Zhou, B.; Yang, Y.; Shi, J.; Feng, H.; Li, Y. Rhodium-Catalyzed Synthesis of Amides from Aldehydes and Azides by Chelation Assisted C-H Bond Activation. *Chem. Eur. J*. **2013**, *19*, 10511−10515. (e) Shi, G.; Zhang, Y. Carboxylate-Directed C-H Functionalization. *Adv. Synth. Catal*. **2014**, *356*, 1419−1442. (f) Suzuki, C.; Morimoto, K.; Hirano, K.; Satoh, T.; Miura, M. Ruthenium- and Rhodium-Catalyzed Dehydrogenative Ortho-Alkenylation of Benzylamines via Free Amino Group Directed C-H Bond Cleavage. *Adv. Synth. Catal*. **2014**, *356*, 1521−1526.

10. (a) Chen, Z.; Wang, B.; Zhang, J.; Yu, W.; Liu, Z. and Zhang, Y. Transition metal-catalyzed C–H bond functionalizations by the use of diverse directing groups. *Org. Chem. Front*. **2015**, *2*, 1107–1295. (b) Qi, Z.; Li, X. Rhodium(III)-Catalyzed Coupling of Arenes with 7-Oxa/Azabenzonorbornadienes by C−H Activation. *Angew. Chem., Int. Ed*. **2013**, *52*, 8995−9000.
11. (a) Zhang, F.; and Spring, D. R. Arene C–H functionalisation using a removable/modifiable or a traceless directing group strategy. *Chem. Soc. Rev*. **2014**, *43*, 6906–6919. (b) Chernyak, N.; Dudnik, A. S.; Huang, C.; and Gevorgyan, V. PyDipSi: A General and Easily Modifiable/Traceless Si-Tethered Directing Group for C−H Acyloxylation of Arenes. *J. Am. Chem. Soc*. **2010**, *132*, 8270–8272. (c) Yang, X. F.; Hu, X. H.; Feng, C.; Loh, T. P. Rhodium(III)-catalyzed C7-position C–H alkenylation and alkynylation of indolines. *Chem. Commun*. **2015**, *51*, 2532−2535.
12. (a) Zhang, F. L.; Hong, K.; Li, T. J.; Park H.; and Yu, J. Q. Functionalization of C(sp^3)–H bonds using a transient directing group. *Science* **2016**, *351*, 252–256. (b) Wu, Y.; Chen, Y. Q.; Liu, T.; Eastgate, M. D.; and Yu, J. Q. Pd-Catalyzed γ-C(sp^3)–H Arylation

of Free Amines Using a Transient Directing Group. *J. Am. Chem. Soc.* **2016**, *138*, 14554–14557. (c) Gandeepan, P. and Ackermann, L. Transient Directing Groups for Transformative C–H Activation by Synergistic Metal Catalysis. *Chemistry* **2018**, *4*, 199–222. (d) Jun, C. H.; Moon, C. W.; Hong, J. B.; Lim, S. G.; Chung, K. Y.; Kim, Y. H. Chelation-Assisted Rh(I)-Catalyzed ortho-Alkylation of Aromatic Ketimines or Ketones with Olefins. *Chem. Eur. J*. **2002**, *8*, 485−492.

13. Sun, H.; Guimond, N. and Huang, Y. Advances in the development of catalytic tethering directing groups for C–H functionalization reactions. *Org. Biomol. Chem*. **2016**, *14*, 8389–8397.
14. (a) Font, M.; Quibell, J. M.; Perry, G. J. P. and Larrosa, I. The use of carboxylic acids as traceless directing groups for regioselective C–H bond functionalisation. *Chem. Commun*. **2017**, *53*, 5584–5597. (b) Zhao, Q.; Poisson, T.; Pannecoucke, X. and Besset, T. The Transient Directing Group Strategy: A New Trend in Transition-Metal-Catalyzed C–H Bond Functionalization. *Synthesis* **2017**, *49*, 4808–4826. (c) Zhou, S.; Wang, M.; Wang, L.; Chen, K.; Wang, J.; Song, C.; Zhu, J. Bidentate Directing-Enabled, Traceless Heterocycle Synthesis: Cobalt-Catalyzed Access to Isoquinolines. *Org. Lett*. **2016**, *18*, 5632−5635.
15. (a) Lapointe D., Fagnou K. Overview of the Mechanistic Work on the Concerted Metallation–Deprotonation Pathway, *Chem. Lett*. **2010**, *39*, 1118–1126. (b) Ackermann L. Carboxylate-Assisted Transition-Metal Catalyzed C−H Bond Functionalizations: Mechanism and Scope, *Chem. Rev*. **2011**, *111*, 1315–1345.
16. (a) Lu, Q.; Gressies, S.; Cembellín, S.; Klauck, F. J. R.; Daniliuc, C. G.; Glorius, F. Redox-Neutral Manganese(I)-Catalyzed C-H Activation: Traceless Directing Group Enabled Regioselective Annulation. *Angew. Chem., Int. Ed.* **2017**, *56*, 12778−12782. (b) Ramesh, B.; Jeganmohan, M. Cobalt(III)-catalyzed redox-neutral [4+2]-annulation

of *N*-chlorobenzamides/acrylamides with alkylidenecyclopropanes at room temperature. *Chem. Commun*. **2021**, *57*, 3692−3695. (c) Kenny, A.; Pisarello, A.; Bird, A.; Chirila, P. G.; Hamilton, A.; Whiteoak, C. J. A challenging redox neutral Cp*Co(III)-catalysed alkylation of acetanilides with 3-buten-2-one: synthesis and key insights into the mechanism through DFT calculations. *Beilstein J. Org. Chem.* **2018**, *14*, 2366−2374.

17. (a) Yeung, C. S.; Dong, V. M. Catalytic Dehydrogenative Cross Coupling: Forming Carbon-Carbon Bonds by Oxidizing Two Carbon-Hydrogen Bonds. *Chem. Rev*. **2011**, *111*, 1215−1292. (b) Tian, T.; Li, Z. and Li, C. J. Cross-dehydrogenative coupling: a sustainable reaction for C–C bond formations, *Green Chem*. **2021**, *23*, 6789–6862.
18. Li, J. and Li, Z. P. Green chemistry: The development of cross-dehydrogenative coupling (CDC) for chemical synthesis, *Pure Appl. Chem*. **2006**, *78*, 935–945.
19. (a) Li, C. J. Cross-Dehydrogenative Coupling (CDC): Exploring C–C Bond Formations beyond Functional Group Transformations, *Acc. Chem. Res.* **2009**, *42*, 335–344. (b) Girard, S. A.; Knauber, T. and Li, C. J. The crossdehydrogenative coupling of C(sp^3)-H bonds: a versatile strategy for C-C bond formations, *Angew. Chem., Int. Ed*. **2014**, *53*, 74–100. (c) Zhang, J. S.; Liu, L.; Chen, T. and Han, L. B. Cross-Dehydrogenative Alkynylation: A Powerful Tool for the Synthesis of Internal Alkynes, *ChemSusChem*. **2020**, *13*, 4776–4794. (d) Bosque, I.; Chinchilla, R.; Gonzalez-Gomez, J. C.; Guijarro, D. and Alonso, F. Cross-dehydrogenative coupling involving benzylic and allylic C–H bonds, *Org. Chem. Front*. **2020**, *7*, 1717–1742.
20. Dua, R.; Shrivastava, S.; Sonwane, S. K.; Srivastava, S. K. Pharmacological significance of synthetic heterocycles scaffold: a review. *Adv. Biol. Res*. **2011**, *5*, 120−144.

21. Kerru, N.; Gummidi, L.; Maddila, S.; Gangu, K. K.; Jonnalagadda, S. B. A review on recent advances in nitrogen containing molecules and their biological applications, *Molecules* **2020**, *25*, 1–42.

22. Dyker, G. Transition Metal Catalyzed Coupling Reactions under C−H Activation. *Angew. Chem. Int. Ed*. **1999**, *38*, 1698–1712.

23. (a) Torres, M.; Gil, S. and Parra, M. New Synthetic Methods to 2-Pyridone Rings. *Curr. Org. Chem.* **2005**, *9*, 1757−1779. (b) Lagoja, I. M. Pyrimidine as Constituent of Natural Biologically Active Compounds. *Chem. Biodiversity* **2005**, *2*, 1–50. (c) Hibi, S.; Ueno, K.; Nagato, S.; Kawano, K.; Ito, K.; Norimine, Y.; Takenaka, O.; Hanada, T. and Yonaga, M. Discovery of 2-(2-Oxo-1-phenyl-5-pyridin-2-yl-1,2-dihydropyridin-3-yl)benzonitrile (Perampanel): A Novel, Noncompetitive α-Amino-3-hydroxy-5-methyl-4-isoxazolepropanoic Acid (AMPA) Receptor Antagonist. *J. Med. Chem*. **2012**, *55*, 10584–10600. (d) Hajek, P.; McRobbie, H. and Myers, K. Efficacy of cytisine in helping smokers quit: systematic review and meta-analysis. *Thorax*, **2013**, *68*, 1037−1042.

24. (a) Mandal, N.; Datta, A. Harnessing the Efficacy of 2-Pyridone Ligands for Pd-Catalyzed (β/γ)-C(sp^3)−H Activations. *J. Org. Chem*. **2020**, *85*, 13228−13238. (b) Liu, S.; Zhuang, Z.; Qiao, J. X.; Yeung, K. S.; Su, S.; Cherney, E. C.; Ruan, Z.; Ewing, W. R.; Poss, M. A.; Yu, J. Q. Ligand Enabled Pd(II)-Catalyzed γ-C(sp^3)−H Lactamization of Native Amides. *J. Am. Chem. Soc*. **2021**, *143*, 21657−21666. (c) Wang, Z.; Hu, L.; Chekshin, N.; Zhuang, Z.; Qian, S.; Qiao, J.; Yu, J. Q. Ligand-controlled divergent dehydrogenative reactions of carboxylic acids via C–H activation Wang et al., *Science* **2021**, *374*, 1281–1285. (d) Qian, S.; Li, Z. Q.; Li, M.; Wisniewski, S. R.; Qiao, J. X.; Richter, J. M.; Ewing, W. R.; Eastgate, M. D.; Chen, J. S.; Yu, J. Q. Ligand-Enabled

Pd(II)-Catalyzed C(sp^3)−H Lactonization Using Molecular Oxygen as Oxidant *Org. Lett*. **2020**, *22*, 3960−3963.

25. Murai, S.; Kakiuchi, F.; Sekine, S.; Tanaka, Y.; Kamatani, A.; Sonoda, M.; Chatani, N. Efficient catalytic addition of aromatic carbon-hydrogen bonds to olefins. *Nature* **1993**, *366*, 529–531.
26. Arockiam, P. B.; Bruneau, C.; Dixneuf, P. H. Ruthenium(II)-Catalyzed C–H Bond Activation and Functionalization. *Chem. Rev*. **2012**, *112*, 5879–5918.
27. (a) Yu, W.; Zhang, W.; Liu, Y.; Liu, Z.; Zhang, Y. Cobalt(III)-catalyzed cross-coupling of enamides with allyl acetates/maleimides. *Org. Chem. Front*. **2017**, *4*, 77−80. (b) Chen, X.; Ren, J.; Xie, H.; Sun, W.; Sun, M.; Wu, B. Cobalt(III)-catalyzed 1,4-addition of C−H bonds of oximes to maleimides. *Org. Chem. Front*. **2018**, *5*, 184−188. (c) Liu, S. L.; Li, Y.; Guo, J. R.; Yang, G. C.; Li, X. H.; Gong, J. F.; Song, M. P. An Approach to 3-(Indol-2-yl)succinimide Derivatives by Manganese-Catalyzed C-H Activation. *Org. Lett.* **2017**, *19*, 4042−4045.
28. (a) Ikemoto, H.; Yoshino, T.; Sakata, K.; Matsunaga, S.; Kanai, M. Pyrroloindolone Synthesis via a Cp*Co(III)-Catalyzed Redox-Neutral Directed C-H Alkenylation/Annulation Sequence. *J. Am. Chem. Soc*. **2014**, *136*, 5424−5431. (b) Tanaka, R.; Ikemoto, H.; Kanai, M.; Yoshino, T.; Matsunaga, S. Site- and Regioselective Monoalkenylation of Pyrroles with Alkynes via Cp*Co(III) Catalysis. *Org. Lett*. **2016**, *18*, 5732−5735. (c) Ikemoto, H.; Tanaka, R.; Sakata, K.; Kanai, M.; Yoshino, T.; Matsunaga, S. Stereoselective Synthesis of Tetrasubstituted Alkenes via a Cp*Co(III)-Catalyzed C−H Alkenylation/Directing Group Migration Sequence. *Angew. Chem., Int. Ed*. **2017**, *56*, 7156−7160.
29. (a) Jacob, N.; Zaid, Y.; Oliveira, J. C. A.; Ackermann, L.; Wencel-Delord, J. Cobalt Catalyzed Enantioselective C-H Arylation of Indoles. *J. Am. Chem. Soc*. **2022**, *144*,

798–806. (b) Nguyen, T. T.; Le, L. V.; Pham, H. H.; Nguyen, D. H.; Phan, N. T. S.; Le, H. V.; and Phan, A. N. Q. Cobalt-catalyzed, directed arylation of C–H bonds in *N*-aryl pyrazoles. *RSC Adv*., **2021**, *11*, 9349–9352. (c) Pandey, D. K.; Vijaykumar, M.; Punji, B. Nickel-Catalyzed C−H Arylation of Indoles with Aryl Chlorides under Neat Conditions. *J. Org. Chem*. **2019**, *84*, 12800−12808.

30. (a) Ramachandran, K.; Anbarasan, P. Cobalt-catalyzed multisubstituted allylation of the chelation-assisted C−H bond of (hetero)arenes with cyclopropenes. *Chem. Sci*. **2021**, *12*, 13442−13449. (b) Lu, Q.; Klauck, F. J. R.; Glorius, F. Manganese-catalyzed allylation via sequential C–H and C–C/C–Het bond activation. *Chem. Sci*. **2017**, *8*, 3379–3383. (c) Ni, J.; Zhao, H.; Zhang, A. Manganese(I)-Catalyzed C-H 3,3-Difluoroallylation of Pyridones and Indoles. *Org. Lett*. **2017**, *19*, 3159−3162.
31. Bera, S. S.; Maji, M. S. Carbamates: A Directing Group for Selective C−H Amidation and Alkylation under Cp*Co(III) Catalysis. *Org. Lett*. **2020**, *22*, 2615−2620.
32. (a) Trost, B. M. The Atom Economy—A Search for Synthetic Efficiency. *Science* **1991**, *254*, 1471–1477. (b) Trost, B. M. On Inventing Reactions for Atom Economy. *Acc. Chem. Res*. **2002**, *35*, 695-705. (c) Eissen, M.; Mazur, R.; Quebbemann, H. G.; Pennemann, K. H. Helv. Atom Economy and Yield of Synthesis Sequences. *Chim. Acta* **2004**, *87*, 524–535. (d) Andreatta, J. R.; McKeown, B. A.; Gunnoe, T. B. J. Transition metal catalyzed hydroarylation of olefins using unactivated substrates: Recent developments and challenges. *Organomet. Chem*. **2011**, *696*, 305–315. (e) Bair, J. S.; Schramm, Y.; Sergeev, A. G.; Clot, E.; Eisenstein, O.; Hartwig, J. F. Linear-Selective Hydroarylation of Unactivated Terminal and Internal Olefins with Trifluoromethyl-Substituted Arenes. *J. Am. Chem. Soc*. **2014**, *136*, 13098–13101.
33. (a) Kischel, J.; Jovel, I.; Mertins, K.; Zapf, A.; Beller, M. A Convenient $FeCl_3$-Catalyzed Hydroarylation of Styrenes. *Org. Lett*. **2006**, *8*, 19–22. (b) Rueping, M.;

Nachtsheim, B. J.; Scheidt, T. Efficient Metal-Catalyzed Hydroarylation of Styrenes. *Org. Lett*. **2006**, *8*, 3717–3719. (c) Wang, M. Z.; Wong, M. K.; Che, C. M. Gold(I)-Catalyzed Intermolecular Hydroarylation of Alkenes with Indoles under Thermal and Microwave-Assisted Conditions. *Chem. Eur. J*. **2008**, *14*, 8353–8364.

34. Martinez, R.; Genet, J. P.; Darses, S. Anti-Markovnikov hydroarylation of styrenes catalyzed by an in situ generated ruthenium complex. *Chem. Commun*. **2008**, 3855–3857.
35. (a) Colby, D. A.; Bergman, R. G.; Ellman, J. A. Rhodium-Catalyzed C−C Bond Formation via Heteroatom-Directed C−H Bond Activation. *Chem. Rev*. **2010**, *110*, 624–655. (b) Martinez, R.; Genet, J. P.; Darses, S. Anti-Markovnikov hydroarylation of styrenes catalyzed by an in situ generated ruthenium complex. *Chem. Commun*. **2008**, 3855–3857. (c) Martinez, R.; Chevalier, R.; Darses, S.; Genet, J. P. A Versatile Ruthenium Catalyst for C-C Bond Formation by C-H Bond Activation. *Angew. Chem. Int. Ed*. **2006**, *45*, 8232–8235. (d) Martinez, R.; Simon, M. O.; Chevalier, R.; Pautigny, C.; Genet, J. P.; Darses, S. C−C Bond Formation via C−H Bond Activation Using an in Situ-Generated Ruthenium Catalyst. *J. Am. Chem. Soc*. **2009**, *131*, 7887–7895.
36. (a) Lim, Y. G.; Kang, J. B. Rhodium-Catalyzed Coupling Reaction of 2-Vinylquinolines with Terminal Alkenes via C-H Bond Activation. *Bull. Korean Chem. Soc*. **1997**, *18*, 1213–1216. (b) Lim, Y. G.; Han, J. S.; Kang, J. B. Rhodium-Catalyzed Norbornenylation of 2-Vinylpyridines via C-H Activation. *Bull. Korean Chem. Soc*. **1998**, *19*, 1143–1145. (c) Lim, Y. G.; Han, J. S.; Koo, B. T.; Kang, J. B. Rhodium-catalyzed Coupling Reaction of 2-Vinylpyridines with Allyl Ethers. *Bull. Korean Chem. Soc*. **1999**, *20*, 1097–1100.

37. Jun, C. H.; Hong, J. B.; Kim, Y. H.; Chung, K. Y. The Catalytic Alkylation of Aromatic Imines by Wilkinson's Complex: The Domino Reaction of Hydroacylation and ortho-Alkylation. *Angew. Chem. Int. Ed*. **2000**, *39*, 3440–3442.

38. Nakao, Y.; Kashihara, N.; Kanyiva, K. S.; Hiyama, T. Nickel-Catalyzed Hydroheteroarylation of Vinylarenes. *Angew. Chem. Int. Ed*. **2010**, *49*, 4451–4454.

39. (a) Gao, K.; Yoshikai, N. Regioselectivity-Switchable Hydroarylation of Styrenes. *J. Am. Chem. Soc*. **2011**, *133*, 400–402. (b) Yoshikai, N. Cobalt-Catalyzed, Chelation-Assisted C-H Bond Functionalization. *Synlett* **2011**, *8*, 1047–1051. (c) Gao, K.; Yoshikai, N. Low-Valent Cobalt Catalysis: New Opportunities for C–H Functionalization. *Acc. Chem. Res*. **2014**, *47*, 1208–1219.

40. (a) Lyons, T. W.; Sanford, M. S. Palladium-Catalyzed Ligand-Directed C−H Functionalization Reactions. *Chem. Rev*. **2010**, *110*, 1147–1169. (b) Colby, D. A.; Bergman, R. G.; Ellman, J. A. Rhodium-Catalyzed C−C Bond Formation via Heteroatom-Directed C−H Bond Activation. *Chem. Rev*. **2010**, *110*, 624–655.

41. Kakiuchi, F.; Kochi, T. Transition-metal-catalyzed carbon-carbon bond formation via carbon-hydrogen bond cleavage. *Synthesis* **2008**, *19*, 3013–3039.

42. (a) De Meijere, A.; Meyer, F. E. Fine Feathers Make Fine Birds: The Heck Reaction in Modern Garb. *Angew. Chem. Int. Ed. Engl.* **1994**, *33*, 2379–2411. (b) Crisp, G. T. Variations on a theme-recent developments on the mechanism of the Heck reaction and their implications for synthesis. *Chem. Soc. Rev*. **1998**, *27*, 427–436. (c) Beletskaya, I. P.; Cheprakov, A. V. The Heck Reaction as a Sharpening Stone of Palladium Catalysis. *Chem. Rev*. **2000**, *100*, 3009–3066.

43. Espinet, P.; Echavarren, A. M. The Mechanisms of the Stille Reaction. *Angew. Chem. Int. Ed*. **2004**, *43*, 4704–4734.

44. Nevado, C.; Echavarren, A. M. Transition Metal-Catalyzed Hydroarylation of Alkynes. *Synthesis* **2005**, *2*, 167–182.

45. Halbritter, G.; Knoch, F.; Wolski, A.; Kisch, H. Functionalization of Aromatic Azo Compounds by the Cobalt-Catalyzed, Regioselective Double Addition of Tolane: 2,6-Distilbenylazobenzenes and 2,3-Dihydrocinnolines. *Angew. Chem., Int. Ed. Engl*. **1994**, *33*, 1603−1605.

46. Lenges, C. P.; Brookhart, M. Co(I)-Catalyzed Inter- and Intramolecular Hydroacylation of Olefins with Aromatic Aldehydes. *J. Am. Chem. Soc*. **1997**, *119*, 3165−3166.

47. Bolig, A. D.; Brookhart, M. Activation of sp^3 C−H Bonds with Cobalt(I): Catalytic Synthesis of Enamines. *J. Am. Chem. Soc*. **2007**, *129*, 14544−14545.

48. Lim, S. G.; Lee, J. H.; Moon, C. W.; Hong, J. B.; Jun, C. H. Rh(I)-Catalyzed Direct ortho-Alkenylation of Aromatic Ketimines with Alkynes and Its Application to the Synthesis of Isoquinoline Derivatives. *Org. Lett*. **2003**, *5*, 2759–2761.

Chapter 2

Redox-Neutral Co(III)-Catalyzed C-H Activation/Annulation of *α,β*-Unsaturated Oxime Ether with Alkyne: One step Access to Multi-substituted Pyridine

Chapter 2

Redox-Neutral Co(III)-Catalyzed C-H Activation/Annulation of *α,β*-Unsaturated Oxime Ether with Alkyne: One step Access to Multi-substituted Pyridine

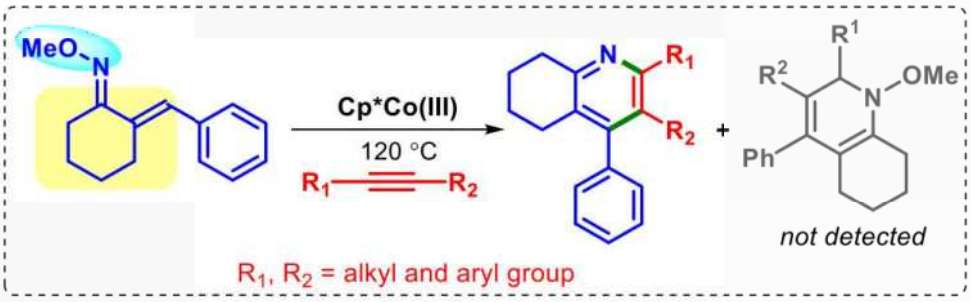

2.1 ABSTRACT: Co(III)-catalyzed annulation of *α,β*-unsaturated Oxime ether with alkyne under redox neutral conditions has been described. Without using external oxidants, multi-substituted pyridines were synthesized in moderate to good yields. A wide range of functional groups has been tolerated with the developed methodology. Notably, this transformation has been used to modify the bioactive molecule dehydropregnenolone at a late stage.

2.2 INTRODUCTION

In organic synthesis, transition metal catalyzed functionalization of C-H bonds is considered as an atom economic process.[1] Among all the heterocycles nitrogen containing heterocycles hold significance in organic synthesis, because of its presence in wide range of natural products, pharmaceuticals, and agrochemicals.[2] Hence, development of efficient synthetic methodology to obtain those molecules have received extensive importance over the years. Among all the nitrogen containing heterocycles, multisubstituted pyridine (tetrahydroquinoline) is an important structural skeleton found in many biologically active

natural products, such as haplophyllidine,[3] megistosarcimine.[4] Moreover molecules that contain tetrahydroquinoline moiety had been found to show biological activities such as anti-HIV,[5] anticancer,[6] antifungal,[7] properties (Figure 2.1). Therefore, significant efforts have been dedicated to develop methodologies for the synthesis of tetrahydroquinoline using mainly second and third row transition metal catalysts (Rh, Ir, Pd).[8,9]

Figure 2.1: Representative examples of Natural products and bioactive molecule containing tetrahydroquinoline moiety.

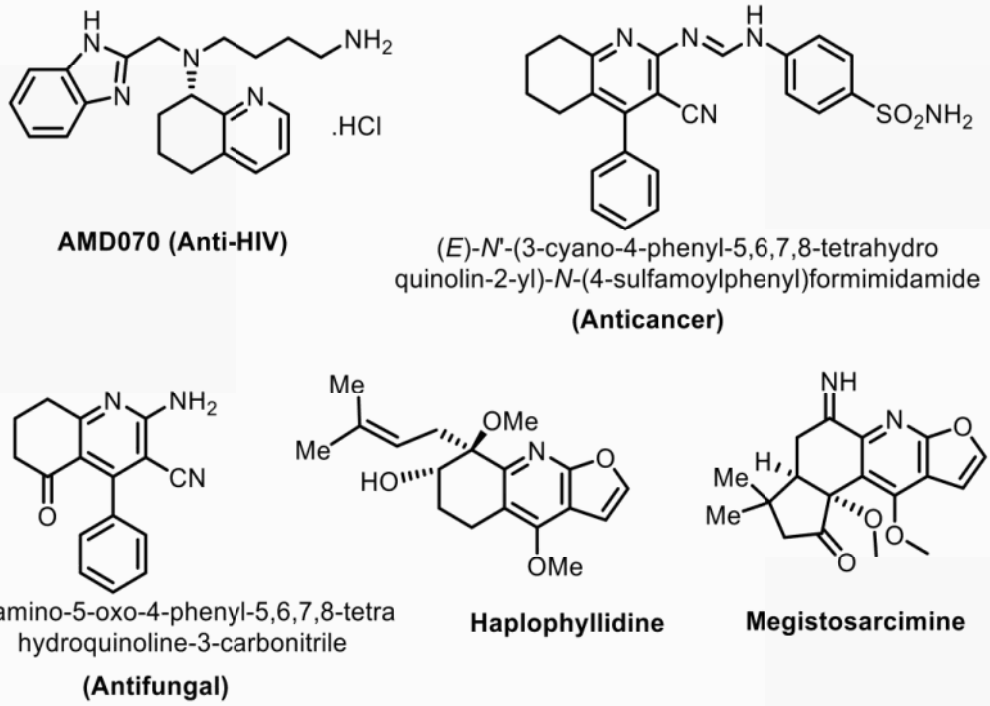

But these catalytic systems are associated with several undesirable factors (i) the use of expensive metal catalyst, (ii) harsh reaction condition, (iii) low functional group tolerance. Hence, in order to tackle the above-mentioned challenges an efficient and benign reaction conditions are of paramount importance. So far there is no report for the synthesis of tetrahydroquinoline by using cobalt catalyst. Previously, Matsunaga,[10] Ackermann,[11] Sundararaju,[12] Cheng,[13] have reported synthesis of isoquinoline from Oxime and alkyne by using Cp*Co(III) catalyst (Scheme-2.1a).

Scheme 2.1: Previous work and our work

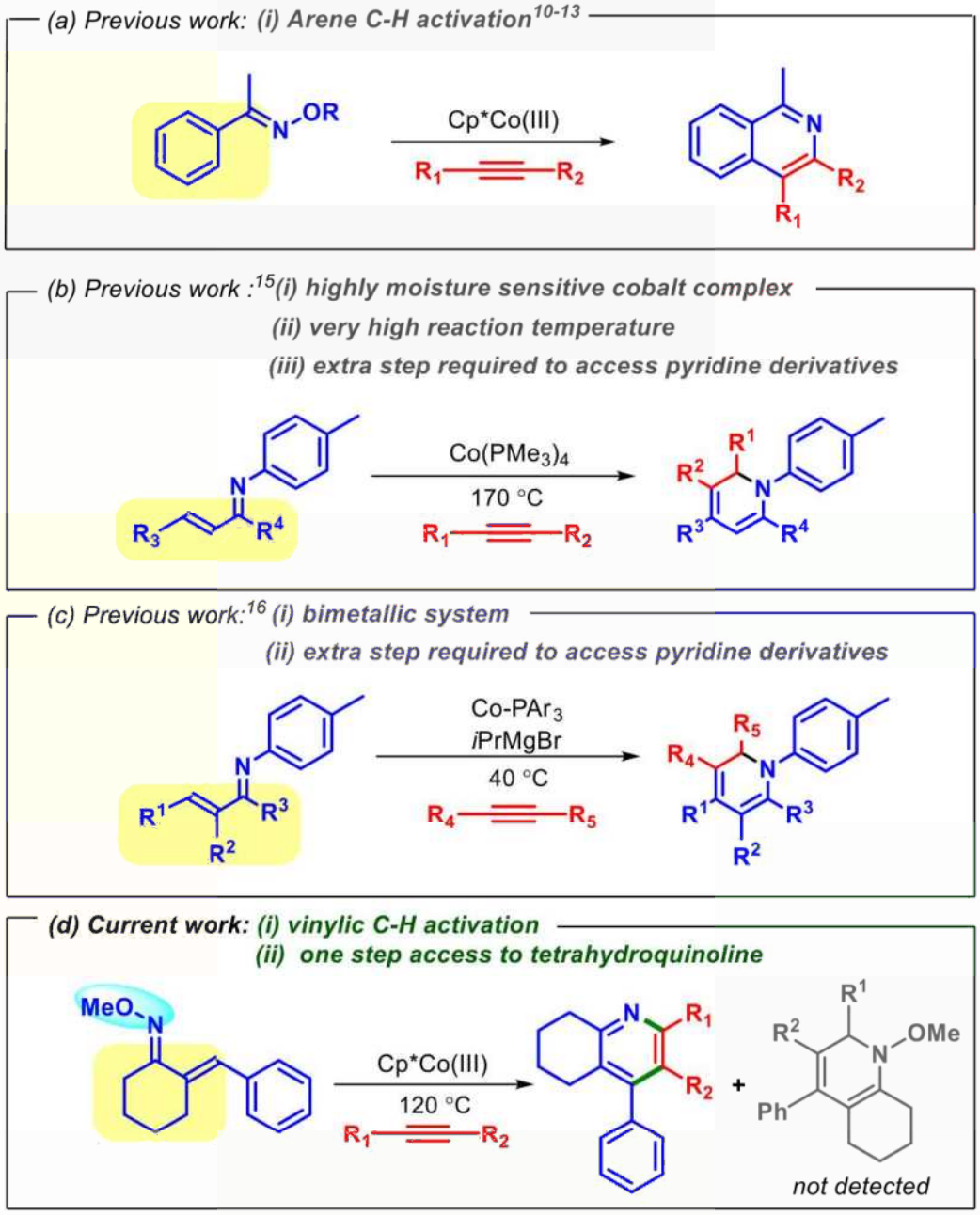

However, all the reports are based on arene C-H bond activation. The activation of non-aromatic vinylic C-H bonds is challenging and it is less explored.[14] Yoshikai and Petit groups have accomplished vinylic C-H activation of α,β-unsaturated imines using low valent cobalt catalyst and subsequent annulation with alkynes for the synthesis of dihydropyridines (Scheme-2.1b, 2.1c).[15,16] However these method suffers from some drawbacks: (a) the metal complex is highly sensitive to air, (b) requirement of high

temperature in one case, which goes against the introduction of sensitive groups, (c) necessity of extra step to access aromatic pyridine derivatives.[17] Therefore, direct synthesis of multisubstituted pyridine via olefinic C-H activation followed by annulations is still an unresolved problem.

Although there are some handful reports on Co(III)-catalyzed olefinic C-H activation,[15,16,18-22,25] to the best of our knowledge, there is no report of Co(III) catalyzed annulations of *α,β*-unsaturated Oxime ether with alkyne to synthesize multisubstituted pyridine under redox neutral condition (Scheme-2.1d). Hence it is highly desirable to develop an efficient methodology for annulations of *α,β*-unsaturated Oxime ether with alkyne using cobalt catalyst.

2.3 RESULTS AND DISCUSSION

To achieve this goal, we initiated our optimization by taking (1*E*, 2*E*)-2-benzylidenecyclohexanone *o*-methyl Oxime ether **1a** as a model substrate and diphenylacetylene **2a** as a coupling partner, [CoCp*(CO)I_2] (10 mol %) as a catalyst and $AgSbF_6$ (20 mol %) as an activator along with 1-adamantanecarboxylic acid (20 mol %) as additive in tetrahydrofuran (THF), unfortunately we did not get any product (Table 2.1, entry 1). Keeping all other reaction conditions constant we varied the solvent to dioxane and ethanol (Table 2.1, entries 2 & 3) unfortunately, we again met with failure. Gratifyingly, when we performed the reaction with HFIP as solvent, we obtained the desired product **3aa** in 9% yield (Table 2.1, entry 4). In order to improve the yield further we decided to change the additive to trifluoroacetic acid (TFA), but we obtained only 7% yield of **3aa** (Table 2.1, entry 5). Since acetate assisted bases are known to promote C-H activation reaction we decided to explore various acetate assisted bases such as NaOAc, LiOAc, AgOAc, CsOAc, KOAc (Table 2.1, entries 6-10). Among the examined additives, KOAc was found to be the most effective in producing the desired annulated product **3aa**

in 61% (Table 2.1, entry 10). For further improvement of the product yield, we screened different silver additives such as

Table 2.1. Optimization for Co-Catalyzed synthesis of multi-substituted pyridine[a]

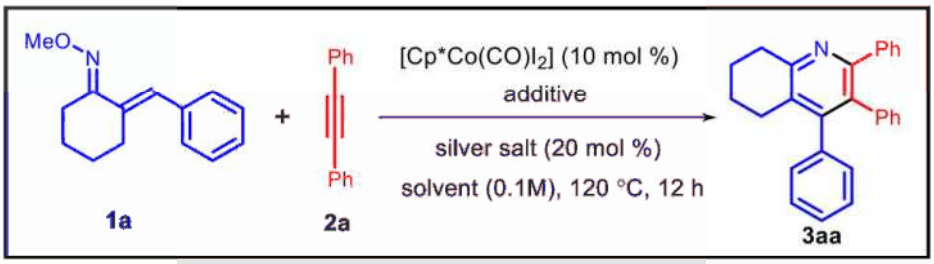

entry	silver salt (20 mol %)	additive (20 mol %)	solvent (0.1 M)	yield (%)[b]
1	$AgSbF_6$	1-AdCOOH	THF	nd
2	$AgSbF_6$	1-AdCOOH	1,4-dioxane	nd
3	$AgSbF_6$	1-AdCOOH	EtOH	nd
4	$AgSbF_6$	1-AdCOOH	HFIP	9
5	$AgSbF_6$	TFA	HFIP	7
6	$AgSbF_6$	NaOAc	HFIP	31
7	$AgSbF_6$	LiOAc	HFIP	34
8	$AgSbF_6$	AgOAc	HFIP	35
9	$AgSbF_6$	CsOAc	HFIP	37
10	$AgSbF_6$	KOAc	HFIP	61
11	$AgBF_4$	KOAc	HFIP	47
12	AgOTf	KOAc	HFIP	58
13	$AgNTf_2$	KOAc	HFIP	75
14	$AgNTf_2$	KOAc	HFIP	88[c]
15	$AgNTf_2$	KOAc	HFIP	53[d]
16	$AgNTf_2$	KOAc	HFIP	69[e]
17	$AgNTf_2$	KOAc	HFIP	nd[f]
18	$AgNTf_2$	-	HFIP	trace[g]
19	-	KOAc	HFIP	79[h]

[a]Reaction conditions: **1a** (0.112 mmol), **2a** (0.056 mmol), [Cp*Co(CO)I_2] (10 mol %), silver salt (20 mol %), additive (100 mol %), solvent (0.1 M), 120 °C for 12 h. [b]isolated yield. [c]1 equiv of additive. [d]Reaction at 60 °C. [e]5 mol % of [Cp*Co(CO)I_2]. [f]absence of cobalt catalyst. [g]absence of additive. [h]absence of $AgNTf_2$, nd = not detected.

$AgBF_4$, AgOTf, $AgNTf_2$ (Table 2.1, entries 11-13). Delightfully, $AgNTf_2$ produced the best yield of **3aa** 75% (Table 2.1, entry 13). Further when we increased the base (KOAc) equivalence from 20 mol % to 1 equivalent, we obtained 88% of the desired product **3aa** (Table 2.1, entry 14). It was found that, lower temperature and reduced catalyst loading were found to be ineffective to afford the annulation product in better yields (Table 2.1, entries 15-16). We performed few control experiments to understand the influence of catalyst, silver additive and base. In absence of catalyst no reaction could occur (Table 2.1, entry 17), in the absence of additive only a trace amount of product was formed (Table 2.1, entry 18). Whereas without silver additive 79% yield of **3aa** was obtained (Table 2.1, entry 19).

With the optimized reaction conditions in hand, the generality of the reaction was examined (Scheme-2.2). As seen before unsubstituted Oxime ether gave desired product in excellent yield (88%). The structure of **3aa** was confirmed by single-crystal X-ray analysis. *para*-halogen substituted *α,β*-unsaturated Oxime ethers (-F, -Br, -I) were found to be compatible, and produced the desired product in good to excellent yields (Scheme-2.2, **3ba**, **3ca**, **3da**). The Oxime ether with electron-donating group at the *para*-position (-Me) furnished good yield of the corresponding product (Scheme-2.2, **3ea**), whereas electron-withdrawing group ($-NO_2$) at the *para*-position gave only 23% yield of the products (Scheme-2.2, **3fa**). Heterocycle substituted Oxime ether underwent cyclization producing moderate yield of the products (Scheme-2.2, **3ga**, **3ha).** Trace amount of product was observed with *ortho*-Br-substituted Oxime ether it might be due to steric hindrance of bulky –Br group near to the reaction site (Scheme-2.2, **3ia).** Notably, the –OMe group substituted at *ortho*-position gave the desired product (Scheme-2.2, **3ja)** in 71% yield. With meta substituted Oxime ether (*meta*-OMe) the desired product was obtained in 61% yield (Scheme-2.2, **3ka)**,

Scheme 2.2: Scope of *α,β*-unsaturated Oxime ethers

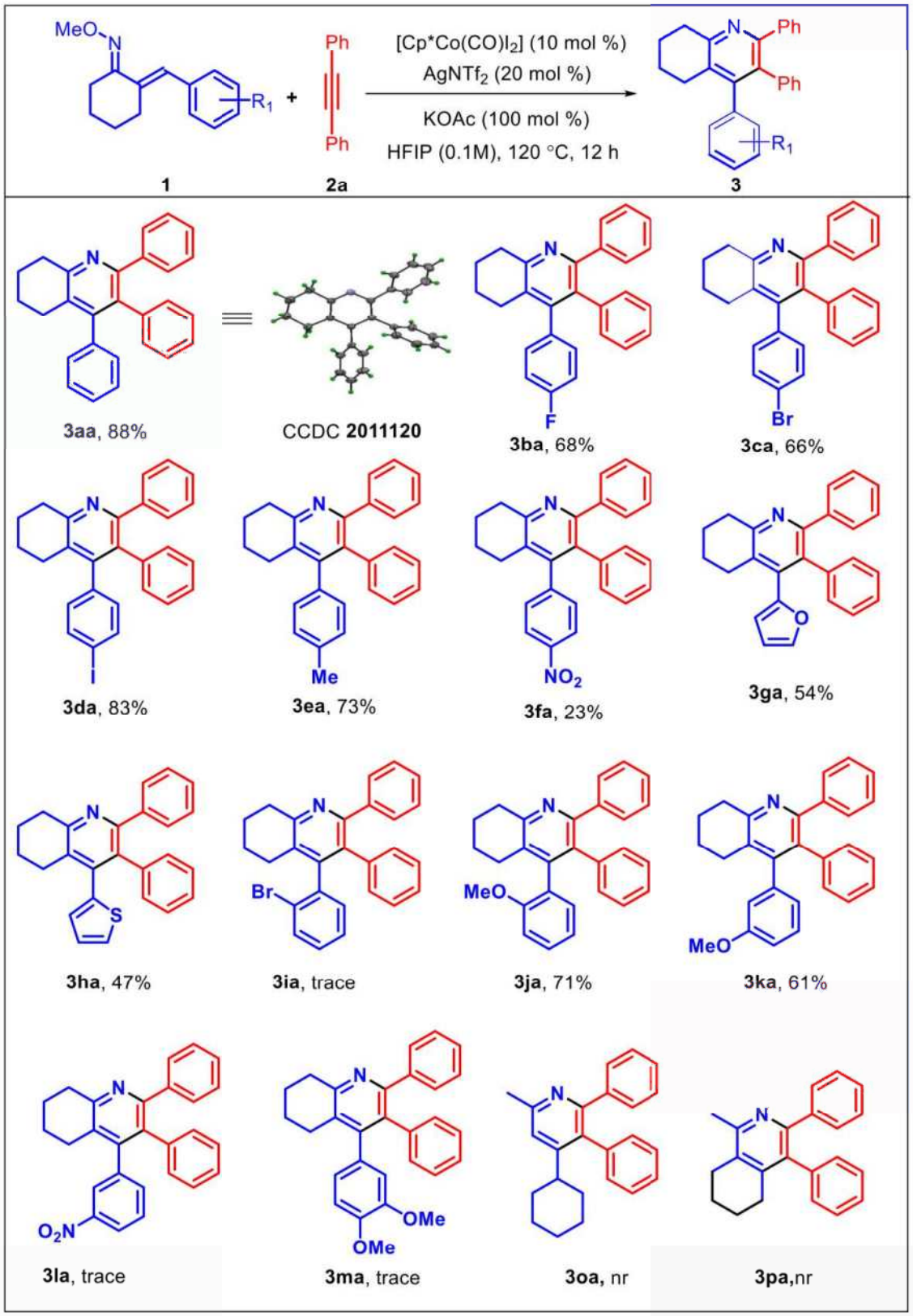

[a]Reaction conditions: **1a** (0.112 mmol), **2a** (0.056 mmol), [Cp*Co(CO)I_2] (10 mol %), $AgNTf_2$ (20 mol %), KOAc (100 mol %), HFIP (0.1 M), 120 °C for 12 h.

Scheme 2.3: Scope of Alkynes

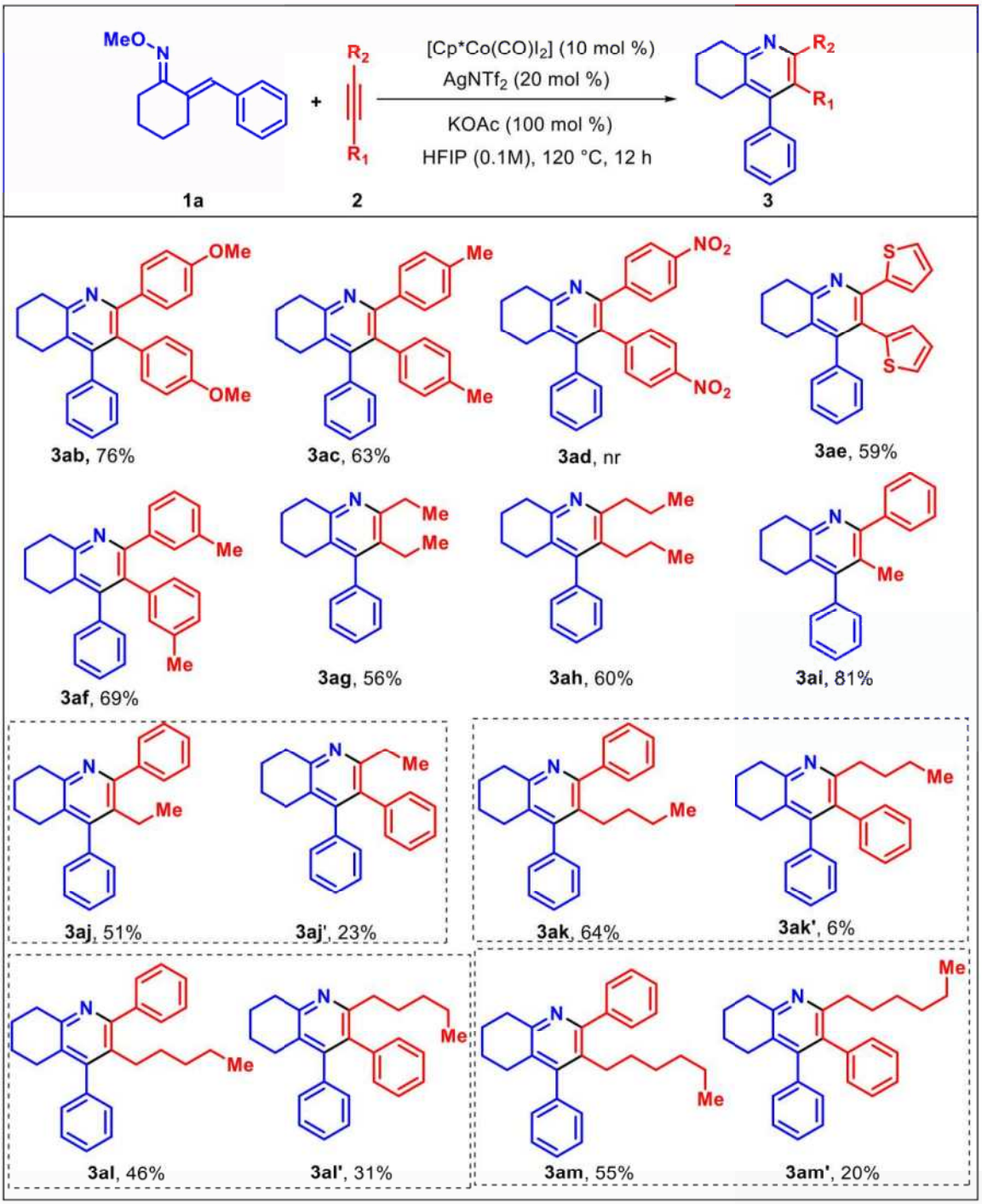

[a]Reaction conditions: **1a** (0.112 mmol), **2a** (0.056 mmol), [Cp*Co(CO)I_2] (10 mol %), $AgNTf_2$ (20 mol %), KOAc (100 mol %), HFIP (0.1 M), 120 °C for 12 h.

whereas with *meta*–NO_2 substituted Oxime ether only trace amount of product was formed (Scheme-2.2, **3la**). Di-methoxy substituted Oxime ether also gave trace amount of the product (Scheme-2.2, **3ma**). Whereas acyclic unsaturated Oxime failed to give the desired

product, it might be due to flexibility of C-C bond in acyclic unsaturated imine which might be restricting the formation of five-membered planar cobaltacycle in C-H activation step (Scheme-2.2, **3oa**, **3pa**).

Next, to extend the generality of this methodology, we examined the reaction using different alkynes (Scheme-2.3). The alkynes with electron donating groups such as -OMe and -Me at the para position furnished the corresponding annulations product in good yields (Scheme-2.3, **3ab, 3ac**). Surprisingly diphenylacetylene with electron withdrawing group (*p*-NO_2) failed to produce the annulation product **3ad**. Notably, heteroaryl alkyne such as di(2-thiophenyl)ethyne underwent cyclization in good yield (Scheme-2.3, **3ae**). The meta-methyl substituted alkyne also gave expected product in good yield (Scheme-2.3, **3af)**. Dialkyl substituted alkynes such as 3-hexyne and 4-octyne gave the products in good yields (Scheme-2.3, **3ag, 3ah**). Then, we turned our attention towards unsymmetrical aryl-alkyl alkynes. In case of 1-phenyl-1-propyne, we obtained single isomer, where the aryl ring is oriented towards the nitrogen atom of tetrahydroquinoline (Scheme-2.3, **3ai)**.[8] Other unsymmetrical alkynes such as 1-phenyl-1-butyne, 1-phenyl-1-hexyne, 1-phenyl-1-heptyne, 1-phenyl-1-octyne smoothly gave annulated product with good regioselectivity & good yields (Scheme 2.3, **3aj-3am**), wherein the aryl ring orienting towards the nitrogen atom of tetrahydroquinoline is the major product. Formation of the major regio-isomeric

Scheme 2.4: Late-stage functionalization

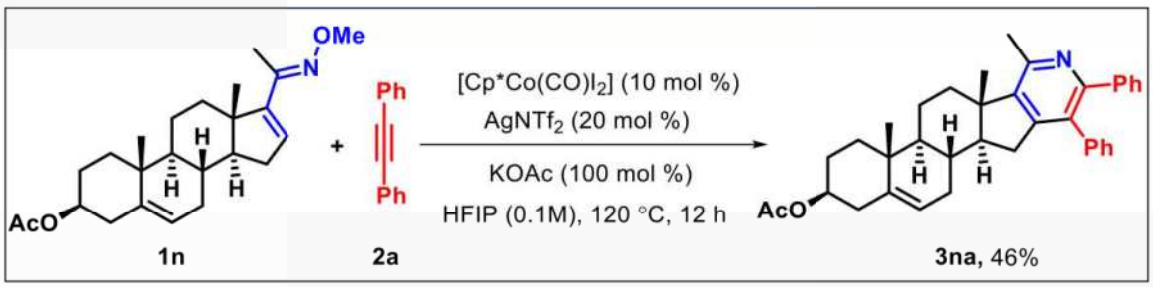

product can be rationalized with the stabilization of the intermediate-III (Scheme-2.6) by the phenyl ring through π-interaction with the metal orbitals.

The scope of the developed annulation method has been extended to complex bioactive molecule dehydropregnenolone. To our delight, the desired annulated adduct was obtained in moderate yield (Scheme-2.4, **3na**). These results indicated that the annulations protocol developed may be useful for rapid generation of the derivatives of bioactive compounds. To know the synthetic applicability on a larger scale, we performed a 1 mmol-scale reaction, which gave **3aa** in 66% yields.

Scheme 2.5: Competitive and mechanistic studies

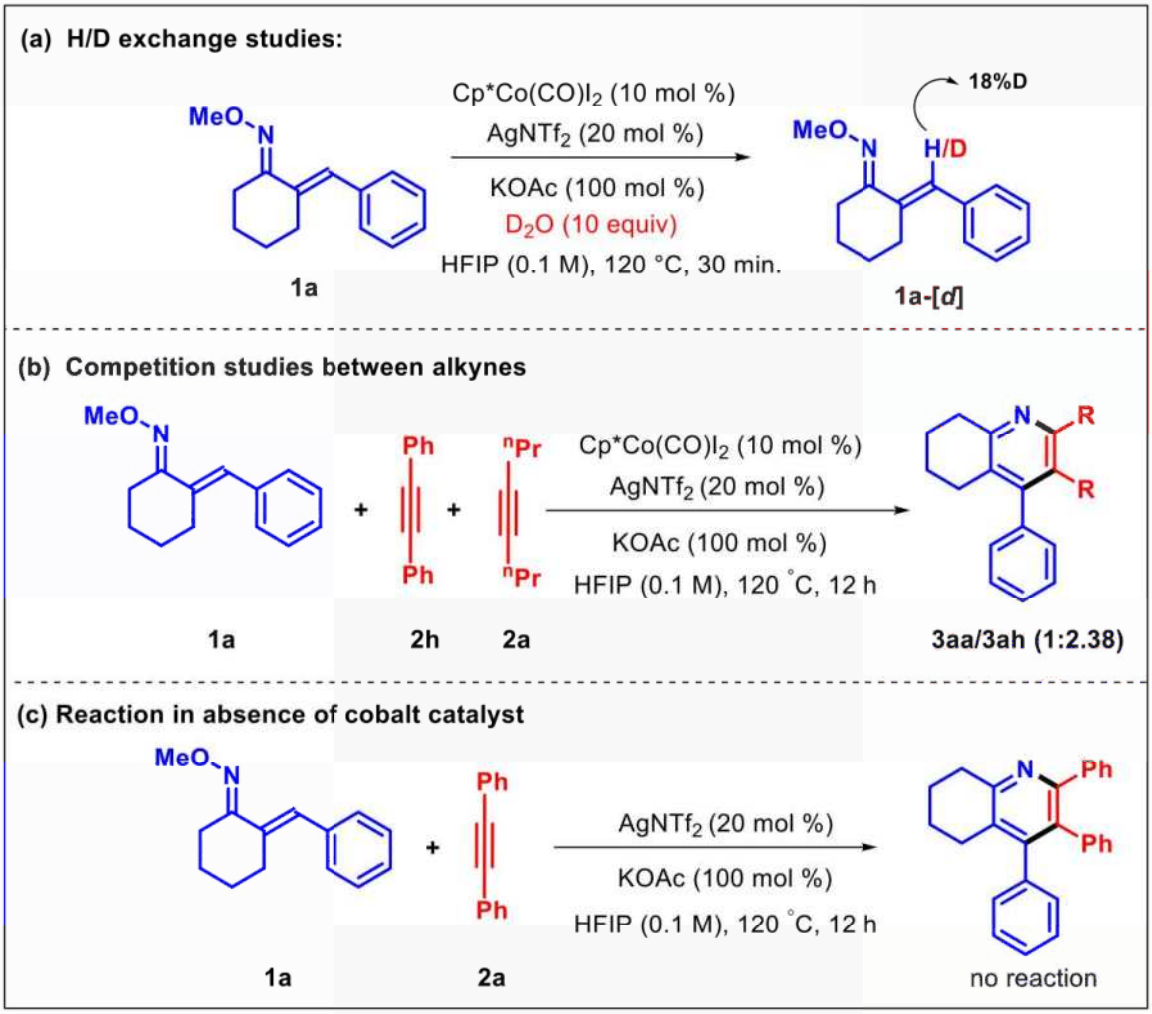

In order to have better insight of the reaction mechanism, a few mechanistic experiments were performed. The deuterium labeling experiment of Oxime ether **1a** with D_2O under the standard reaction condition showed 18% deuterium incorporation at the ortho position of the Oxime ether **1a**, which indicates an acetate assisted reversible cyclometallation pathway of the Co(III) catalyst (Scheme-2.5a). Further, an intermolecular competitive reaction between two different internal alkynes **2a** and **2h** with Oxime ether **1a** resulted, **3aa : 3ah** in 1 : 2.38 ratio. The results of the above experiment indicate that the developed annulations protocol is favorable for the electron rich alkyne (Scheme-2.5b). A control experiment was performed without cobalt catalyst, but no product was observed, which confirms the vital role of cobalt catalyst (Scheme-2.5c).

Scheme 2.6: Proposed catalytic cycle

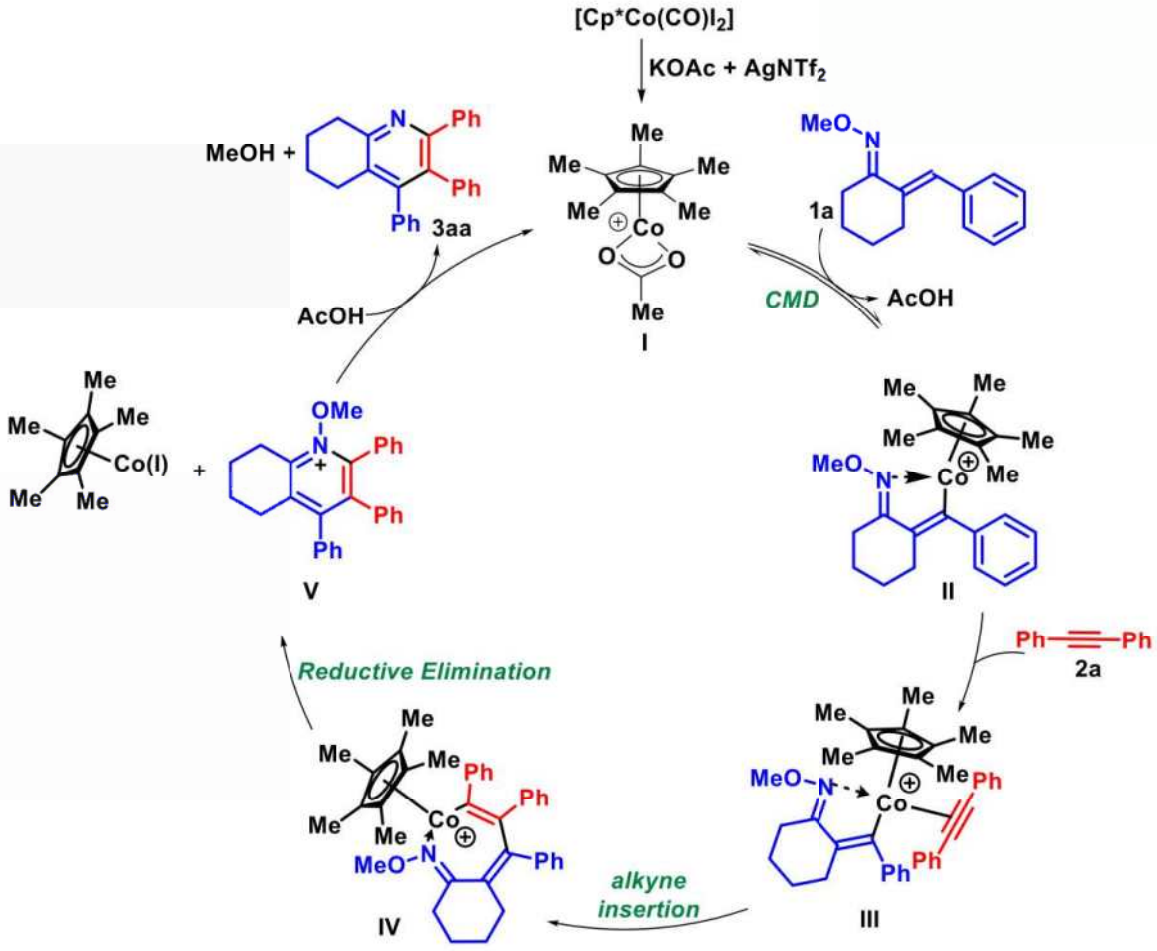

On the basis of the above mechanistic studies, and previous literature reports,[12,23,24] we propose a plausible reaction mechanism (Scheme-2.6). Initially [CoCp*(CO)I_2] undergoes decarbonylation in the presence of $AgNTf_2$ and KOAc to give the cationic complex **I**. Co-ordination of olefinic Oxime ether **1a** followed by reversible concerted cyclometallation deprotonation leads to the cobaltacycle **II**. Coordination of alkyne **2a** to the cobaltacycle **II** gives intermediate **III**, then subsequent insertion of the alkyne in to the Co-C bond of intermediate **III** affords a seven membered cobaltacycle **IV**. The intermediate **IV** undergoes C-N coupling to give $[Cp^*Co(Pyridine)(OMe)]^+$. Finally, intermediate **V** undergoes protodemetallation to give the desired product **3aa** and the catalytically active species **I** and byproduct MeOH.

2.4 CONCLUSION

In conclusion, we have successfully established an efficient methodology to access multisubstituted pyridines by annulations of α,β-unsaturated Oxime ether with alkyne using Co(III)-catalyst. The exclusive formation of multisubstituted pyridine is the most important aspect of this reaction. This approach is applicable to a variety of substrates and is compatible with a variety of functional groups. This methodology has been applied to functionalize the bioactive molecule dehydropregnenolone at a late stage.

2.5 EXPERIMENTAL SECTION

Reactions were performed using borosil sealed tube vial under N_2 atmosphere. Column chromatography was done by using 230-400 mesh silica gel of Acme synthetic chemicals company. A gradient elution was performed by using distilled petroleum ether and ethyl acetate. TLC plates detected under UV light at 254 nm and vanillin. ^1H NMR, ^{13}C NMR, recorded on Bruker AV 400 MHz and Jeol ECZ-400 R spectrometer using $CDCl_3$ as the deuterated solvent.[25] Multiplicity (s = singlet, d = doublet, t = triplet, q = quartet, quint =

quintet, sept = septet, m = multiplet, dd = double of doublet, br = broad signal), integration, and coupling constants (*J*) in hertz (Hz). HRMS signal analysis was performed using micro TOF Q-II mass spectrometer. Reagents and starting materials were purchased from Sigma Aldrich, TCI, Avra, Spectrochem and other commercially available sources, used without further purification unless otherwise noted. All aldol condensation derivatives,[26] imine derivative,[27] alkyne derivatives[28] were prepared according to the reported literature procedure.

2.5.1 Representative Procedure for the Synthesis of condensation product:[26]

The condensation reactions were performed according to a literature procedure.[26] Cycloalkanone (326 mmol, 2.91 equiv) was added to a solution of NaOH (6.52 g, 163 mmol, 1.45 equiv) in water (750 mL, 0.149 M) and stirred under ice bath for 5 min, followed by the addition of benzaldehyde (11.88 g, 112 mmol, 1.0 equiv). After 3 days of stirring,the reaction mixture was neutralized with glacial acetic acid. The product was extracted with toluene (3 x 200mL) and purified by vacuum distillation, affording both the ketones as bright yellow solids. The analytical data of these synthesized compounds were well matched with known literature data.

2.5.2 Representative Procedure for the Synthesis of (1*E*, 2*E*)-2-benzylidenecyclohexanone *o*-methyl Oxime ether:[27]

(1*E*,2*E*)-2-benzylidenecyclohexanone *o*-methyl Oxime ether was prepared according to a previously reported procedure. *α, β*–unsaturated ketone or aldehyde derivatives (5 mmol, 1.0 equiv) were taken in a 50 mL round bottom flask. Then a mixture of water (10 mL, 0.5 M) and ethanol (5 mL, 1M) was added to it. Further, alkoxylamine hydrochloride (15 mmol, 3.0 equiv) and sodium acetate (25 mmol, 5.0 equiv) were added to the suspension respectively. The resulting suspension was refluxed at the 80 ºC for 1-4 h. The progress of the reaction was regularly checked by TLC. After complete consumption of the starting

materials, additional water was added to the reaction mixture and extracted with ethyl acetate. Organic phase was dried over anhydrous sodium sulfate and concentrated under reduced pressure. Oxime ether **1a** was purified using silica gel flash column chromatography in 60-95% yield [eluent: hexane-ethyl acetate mixture (98:2 to 95:5)].

2.5.3 Representative Procedure for the synthesis of 2,3,4-triphenyl-5,6,7,8-tetrahydroquinoline.

An oven-dried Schlenk tube was equipped with a magnetic stirrer bar was charged with [Cp*Co(CO)I_2] (0.02 mmol, 0.1 equiv), potassium acetate (0.2 mmol, 100 mol %). Subsequently *o*-methyl Oxime ether **1a** (0.4 mmol, 2.0 equiv), alkyne **2** (0.2 mmol, 1.0 equiv), $AgNTf_2$ (0.04 mmol, 0.2 equiv) followed by HFIP (2 mL, 0.1 M) were added under N_2 atmosphere. The reaction mixture was vigorously stirred (750 rpm) in a preheated aluminium block at 120 ºC for 12 h. After 12 h (completion of reaction as monitored by TLC analysis), the reaction mixture was cooled to room temperature and diluted with dichloromethane and passed through a short pad of Celite, the solvent was evaporated under reduced pressure and the residue was purified by column chromatography using EtOAc/hexane (1:9) mixture on silica gel to give the pure product **3**.

2.5.4 Experimental characterization data:

(1*E*, 2*E*)-2-Benzylidenecyclohexanone o-methyl Oxime (1a):

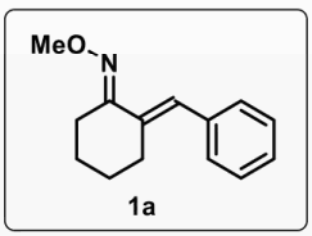

1a

Physical State: Yellow liquid (93 mg, 80% yield), R_f: 0.55 (5% EtOAc/hexane). ^{1}H NMR (400 MHz, $CDCl_3$): δ 7.26–7.21 (m, 4H), 7.16–7.12 (m, 1H), 6.85 (s, 1H), 3.86 (s, 3H), 2.58 (t, J = 6.0 Hz, 2H), 2.51 (t, J = 6.4 Hz, 2H), 1.64–1.50 (m, 4H). ^{13}C{^{1}H} NMR (100 MHz, $CDCl_3$): δ 160.1, 137.3, 135.2, 130.1, 128.4, 127.8, 127.3, 62.0, 29.3,

26.0, 25.3, 23.7. IR (KBr, cm^{-1}): 2933, 1457, 1337, 1048. HRMS (ESI) m/z: $[M + H]^+$ calcd for $C_{14}H_{18}NO$: 216.1383; found 216.1363.

(1*E*, 2*E*)-2-(4-Fluorobenzylidene)cyclohexanone o-methyl Oxime (1b):

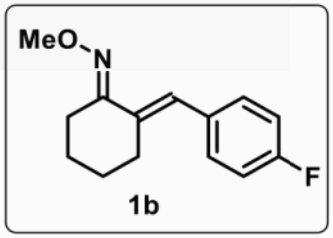

1b

Physical State: yellow liquid (78 mg, 68% yield). R_f: 0.5 (5% EtOAc/hexane). ^1H NMR (400 MHz, $CDCl_3$): δ 7.29–7.25 (m, 2H), 7.03–6.99 (m, 2H), 6.88 (s, 1H), 3.94 (s, 3H), 2.64–2.57 (m, 4H), 1.73–1.59 (m, 4H). $^{13}C\{^1H\}$ NMR (100 MHz, $CDCl_3$): δ 162.0 (d, $J_{C\text{-}F}$ = 245 Hz), 159.9, 135.0 (d, $J_{C\text{-}F}$ = 2 Hz), 133.3 (d, $J_{C\text{-}F}$ = 4 Hz), 131.6 (d, $J_{C\text{-}F}$ = 9 Hz), 126.6, 115.3 (d, $J_{C\text{-}F}$ = 22 Hz), 62.0, 29.2, 25.9, 25.2, 23.7. IR (KBr, cm^{-1}): 2935, 1600, 1505, 1223, 1156, 1048. HRMS (ESI) m/z: $[M + H]^+$ calcd for $C_{14}H_{17}FNO$: 234.1289; found 234.1301.

(1*E*, 2*E*)-2-(4-Bromobenzylidene)cyclohexanone o-methyl Oxime (1c):

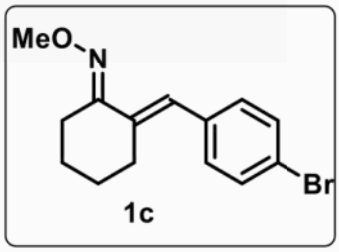

1c

Physical State: white solid (92 mg, 83% yield). mp: 61–63 °C. R_f: 0.5 (5% EtOAc/hexane). ^1H NMR (400 MHz, $CDCl_3$): δ 7.44 (d, J = 8.4 Hz, 2H), 7.17 (d, J = 8.4 Hz, 2H), 6.85 (s, 1H), 3.94 (s, 3H), 2.63–2.57 (m, 4H), 1.72–1.59 (m, 4H). $^{13}C\{^1H\}$ NMR (100 MHz, $CDCl_3$): δ 159.8, 136.2, 135.9, 131.6, 131.5, 126.5, 121.3, 62.0, 29.3, 25.9, 25.2, 23.7. IR (KBr, cm^{-1}): 2933, 1485, 1048, 870. HRMS (ESI) m/z: $[M + H]^+$ calcd for $C_{14}H_{17}BrNO$: 294.0488; found 294.0507.

(1*E*, 2*E*)-2-(4-Iodobenzylidene)cyclohexanone o-methyl Oxime (1d):

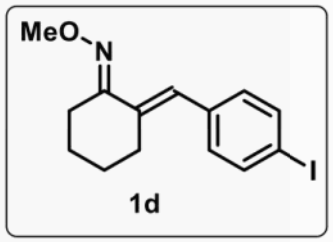

1d

Physical State: Colourless oil (80 mg, 74% yield). R_f: 0.8 (5% EtOAc/hexane). ^1H NMR (400 MHz, $CDCl_3$): δ 7.66–7.63 (m, 2H), 7.03 (d, J = 7.6 Hz, 2H), 6.83 (s, 1H), 3.94 (s, 3H), 2.63–2.56 (m, 4H), 1.68–1.56 (m, 4H). $^{13}C\{^1H\}$ NMR (100 MHz, $CDCl_3$): δ 159.7, 137.5, 136.7, 136.0, 131.8, 126.6, 93.0, 62.1, 29.4, 26.0, 25.2, 23.7. IR

(KBr, cm^{-1}): 2932, 1482, 1048, 508. HRMS (ESI) m/z: $[M + H]^+$ calcd for $C_{14}H_{17}INO$: 342.0349; found 342.0334.

(1*E*, 2*E*)-2-(4-Methylbenzylidene)cyclohexanone o-methyl Oxime (1e):

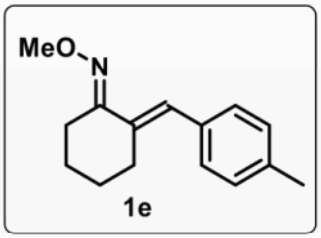

Physical State: white solid (88mg, 77% yield). mp: 58–60 °C. R_f: 0.55 (5% EtOAc/hexane). ^1H NMR (400 MHz, $CDCl_3$): δ 7.21 (d, J = 8.0 Hz, 2H), 7.13 (d, J = 8.0 Hz, 2H), 6.90 (s, 1H), 3.94 (s, 3H), 2.66 (td, J = 6.8, 1.6 Hz, 2H), 2.58 (t, J = 6.4 Hz, 2H), 2.34 (s, 3H), 1.72–1.58 (m, 4H). $^{13}C\{^1H\}$ NMR (100 MHz, $CDCl_3$): δ 160.2, 137.2, 134.4, 134.4, 130.0, 129.1, 127.8, 62.0, 29.4, 26.0, 25.2, 23.7, 21.6. IR (KBr, cm^{-1}): 2934, 1510, 1449, 1049. HRMS (ESI) m/z: $[M + H]^+$ calcd for $C_{15}H_{20}NO$: 230.1539; found 230.1561.

(1*E*, 2*E*)-2-(4-Nitrobenzylidene)cyclohexanone o-methyl Oxime (1f):

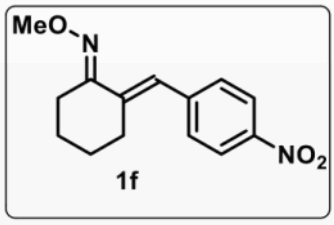

Physical State: Yellow solid (69 mg, 61% yield). mp: 92–94 °C. R_f: 0.25 (5% EtOAc/hexane). ^1H NMR (400 MHz, $CDCl_3$): δ 8.21–8.17 (m, 2H), 7.47–7.43 (m, 2H), 6.96 (s, 1H), 3.96 (s, 3H), 2.66 (td, J = 6.4, 2.0 Hz, 2H), 2.61 (t, J = 6.8 Hz, 2H), 1.74–1.63 (m, 4H). $^{13}C\{^1H\}$ NMR (100 MHz, $CDCl_3$): δ 159.2, 146.7, 144.0, 139.0, 130.6, 125.4, 123.8, 62.2, 29.6, 25.9, 25.1, 23.5. IR (KBr, cm^{-1}): 2936, 1594, 1515, 1343, 1047. HRMS (ESI) m/z: $[M + H]^+$ calcd for $C_{14}H_{17}N_2O_3$: 261.1234; found 261.1241.

(1*E*, 2*E*)-2-(Furan-2-yl-methylene)cyclohexanone o-methyl Oxime (1g):

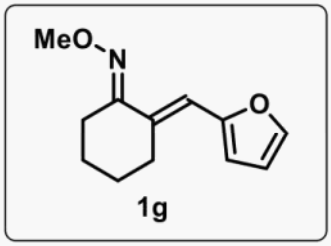

Physical State: Yellow liquid (94 mg, 81% yield). R_f: 0.5 (5% EtOAc/hexane). ^1H NMR (400 MHz, $CDCl_3$): δ 7.41 (d, J = 1.6 Hz, 1H), 6.84 (t, J = 2.0 Hz, 1H), 6.42–6.41 (m, 1H), 6.37 (d, J = 3.2 Hz, 1H), 3.93 (s, 3H), 2.78–2.74 (m, 2H), 2.58–2.54 (m, 2H), 1.68–1.65 (m, 4H). $^{13}C\{^1H\}$ NMR (100 MHz, $CDCl_3$): δ 158.9, 153.5, 142.5,

132.2, 115.5, 111.8, 111.7, 62.1, 29.3, 25.9, 24.1, 23.0. IR (KBr, cm^{-1}): 2935, 1463, 1435,1049. HRMS (ESI) m/z: $[M + H]^+$ calcd for $C_{12}H_{16}NO_2$: 206.1176; found 206.1190.

(1*E*, 2*E*)-2-(Thiophen-2-yl-methylene)cyclohexanone o-methyl Oxime (1h):

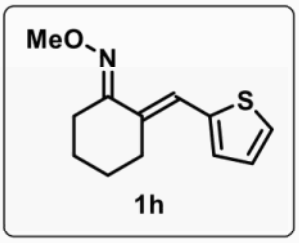

Physical State: Yellow liquid (86 mg, 75% yield). R_f: 0.5 (5% EtOAc/hexane). ^1H NMR (400 MHz, $CDCl_3$): δ 7.31 (d, J = 5.2 Hz, 1H), 7.21 (t, J = 2.0 Hz, 1H), 7.12 (d, J = 3.6 Hz, 1H), 7.04 (dd, J = 5.2, 3.6 Hz, 1H), 3.94 (s, 3H), 2.72 (m, 2H), 2.57 (t, J = 6.0 Hz, 2H), 1.70–1.66 (m, 4H). $^{13}C\{^1H\}$ NMR (100 MHz, $CDCl_3$): δ 159.2, 140.8, 131.9, 129.5, 127.3, 126.6, 120.7, 62.1, 29.4, 25.9, 24.0, 22.8. IR (KBr, cm^{-1}): 2933, 1615, 1461, 1421, 1048. HRMS (ESI) m/z: $[M + H]^+$ calcd for $C_{12}H_{16}NOS$: 222.0947; found 222.0964.

(1*E*, 2*E*)-2-(2-Bromobenzylidene)cyclohexanone o-methyl Oxime (1i):

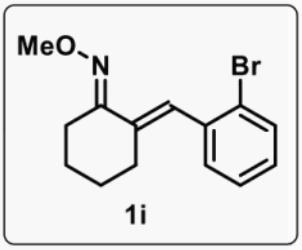

Physical State: White solid (80 mg, 72% yield). mp: 53-55 °C. R_f: 0.45 (5% EtOAc/hexane). ^1H NMR (400 MHz, $CDCl_3$): δ 7.59–7.57 (m, 1H), 7.26–7.25 (m, 2H), 7.13–7.08 (m, 1H), 6.87 (s, 1H), 3.96 (s, 3H), 2.62 (t, J = 6.8 Hz, 2H), 2.49 (td, J = 6.8, 1.6 Hz, 2H), 1.74–1.68 (m, 2H), 1.64–1.58 (m, 2H). $^{13}C\{^1H\}$ NMR (100 MHz, $CDCl_3$): δ 159.5, 137.3, 136.5, 132.9, 131.5, 128.9, 127.0, 126.9, 125.3, 62.0, 29.5, 26.0, 25.5, 24.0. IR (KBr, cm^{-1}): 2933, 1463, 1048, 1024, 746. HRMS (ESI) m/z: $[M + H]^+$ calcd for $C_{14}H_{17}BrNO$: 294.0488; found 294.0496.

(1*E*, 2*E*)-2-(2-Methoxybenzylidene)cyclohexanone o-methyl Oxime (1j):

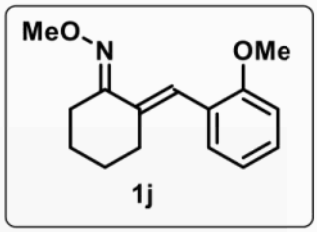

Physical State: Yellow liquid (76 mg, 66% yield). R_f: 0.3 (5% EtOAc/hexane). ^1H NMR (400 MHz, $CDCl_3$): δ 7.28–7.24 (m, 2H), 6.88–6.85 (m, 3H), 3.94 (s, 3H), 3.81 (s, 3H), 2.66 (td, J = 6.4, 1.6 Hz, 2H), 2.58 (t, J = 6.8 Hz, 2H), 1.70–1.60 (m, 4H). $^{13}C\{^1H\}$ NMR (100 MHz, $CDCl_3$): δ 160.3, 158.9, 133.4, 131.5, 130.0, 128.7, 127.5, 113.8,

113.8, 61.9, 55.5, 29.3, 26.0, 25.2, 23.7. IR (KBr, cm^{-1}): 2934, 1604, 1463, 1177, 1048. HRMS (ESI) m/z: $[M + H]^+$ calcd for $C_{15}H_{20}NO_2$: 246.1489 ; found 246.1501.

(1*E*, 2*E*)-2-(3-Methoxybenzylidene)cyclohexanone o-methyl Oxime (1k):

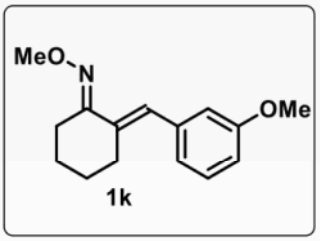

1k

Physical State: colourless oil (58 mg, 51% yield). R_f: 0.4 (5% EtOAc/hexane). ^1H NMR (400 MHz, $CDCl_3$): δ 7.16 (t, J = 7.6 Hz, 1H), 6.83 (d, J = 5.6 Hz, 2H), 6.77 (s, 1H), 6.71 (dd, J = 8.0, 2.4 Hz, 1H), 3.86 (s, 3H), 3.71 (s, 3H), 2.60–2.57 (m, 2H), 2.51 (t, J = 6.4 Hz, 2H), 1.64–1.51 (m, 4H). $^{13}C\{^1H\}$ NMR (100 MHz, $CDCl_3$): δ 159.9, 159.6, 138.6, 135.4, 129.3, 127.6, 122.6, 115.5, 112.9, 61.9, 55.5, 29.4, 25.9, 25.2, 23.7. IR (KBr, cm^{-1}): 2934, 1596, 1487, 1157, 1048. HRMS (ESI) m/z: $[M + H]^+$ calcd for $C_{15}H_{20}NO_2$: 246.1489; found 246.1508.

(1*E*, 2*E*)-2-(3-Nitrobenzylidene)cyclohexanone o-methyl Oxime (1l):

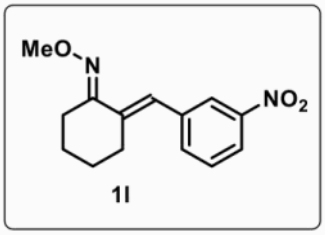

1l

Physical State: Yellow liquid (71 mg, 63% yield). R_f: 0.25 (5% EtOAc/hexane). ^1H NMR (400 MHz, $CDCl_3$): δ 8.07 (s, 1H), 7.99 (d, J = 8.4 Hz, 1H), 7.53 (d, J = 7.6 Hz, 1H), 7.41 (t, J = 8 Hz, 1H), 6.86 (s, 1H), 3.86 (s, 3H), 2.57 (t, J = 5.6 Hz, 2H), 2.52 (t, J = 6.4 Hz, 2H), 1.66–1.53 (m, 4H). $^{13}C\{^1H\}$ NMR (100 MHz, $CDCl_3$): δ 159.0, 148.3, 138.8, 137.9, 135.8, 129.2, 124.9, 124.4, 121.9, 62.0, 29.2, 25.8, 25.0, 23.4. IR (KBr, cm^{-1}): 2935, 1528, 1348, 1047. HRMS (ESI) m/z: $[M + H]^+$ calcd for $C_{14}H_{17}N_2O_3$: 261.1234; found 261.1238.

(1*E*, 2*E*)-2-(3,4-Dimethoxybenzylidene)cyclohexanone o-methyl Oxime (1m):

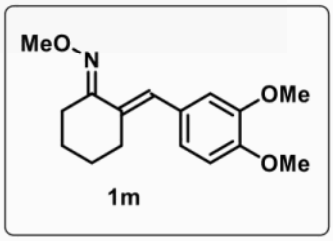

Physical State: Yellow viscous liquid (74 mg, 66% yield). R_f: 0.15 (5% EtOAc/hexane). ^{1}H NMR (400 MHz, $CDCl_3$): δ 6.92–6.82 (m, 4H), 3.94 (s, 3H), 3.88 (s, 3H), 3.86 (s, 3H), 2.68 (t, J = 5.6 Hz, 2H), 2.58 (t, J = 6.4 Hz, 2H), 1.72–1.60 (m, 4H). ^{13}C{^{1}H} NMR (100 MHz, $CDCl_3$): δ 160.2, 148.7, 148.5, 133.7, 130.3, 127.7, 122.9, 113.4, 111.1, 62.0, 56.2, 56.2, 29.4, 26.0, 25.2, 23.7. IR (KBr, cm^{-1}): 2934, 1513, 1463, 1255, 1140, 1048. HRMS (ESI) m/z: $[M + H]^+$ calcd for $C_{16}H_{22}NO_3$: 276.1594; found 276.1595.

(2*Z*, 3*E*)-4-Cyclohexylbut-3-en-2-one o-methyl Oxime (1o):

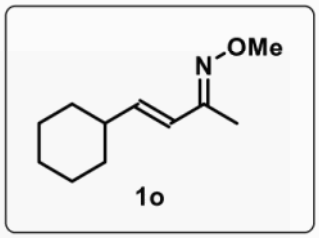

Physical State: Colourless liquid (77 mg, 60% yield). R_f: 0.6 (5% EtOAc/hexane). ^{1}H NMR (400 MHz, $CDCl_3$): δ 6.09–5.95 (m, 2H), 3.88 (s, 3H), 2.11–2.04 (m, 1H), 1.93 (s, 3H), 1.76–1.65 (m, 5H), 1.31–1.11 (m, 5H). ^{13}C{^{1}H} NMR (100 MHz, $CDCl_3$): δ 156.2, 142.0, 125.3, 61.9, 41.2, 32.9, 26.4, 26.3, 10.4. IR (KBr, cm^{-1}): 1062, 1257, 1452, 2900. HRMS (ESI) m/z: $[M + H]^+$ calcd for $C_{11}H_{20}NO$: 182.1539; found 182.1552.

(*E*)-1-(Cyclohex-1-en-1-yl)ethan-1-one o-methyl Oxime (1p):

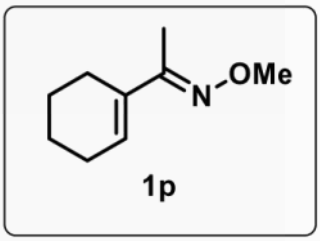

Physical State: Colourless liquid (63 mg, 51% yield). R_f:0.8 (5% EtOAc/hexane). ^{1}H NMR (400 MHz, $CDCl_3$): δ 6.13-6.10 (m, 1H), 3.88 (s, 3H), 2.30–2.27 (m, 2H), 2.18–2.15 (m, 2H), 1.93 (s, 3H), 1.66–1.59 (m, 4H). ^{13}C{^{1}H} NMR (100 MHz, $CDCl_3$): δ 156.4, 135.2, 129.3, 61.8, 26.3, 24.8, 22.8, 22.5, 10.6. IR (KBr, cm^{-1}): 1052, 1264, 1299, 1442, 2930. HRMS (ESI) m/z: $[M + H]^+$ calcd for $C_9H_{16}NO$: 154.1226; found 154.1231.

Experimental characterization data of products:

2,3,4-Triphenyl-5,6,7,8-tetrahydroquinoline (3aa):[5]

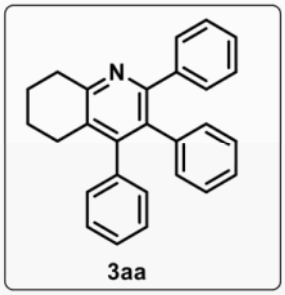

Physical State: white solid (18 mg, 88%). mp: 163–165 °C. R_f: 0.5 (10% EtOAc/hexane). ^{1}H NMR (400 MHz, $CDCl_3$): δ 7.27–7.25 (m, 2H), 7.20–7.12 (m, 6H), 6.97–6.91 (m, 5H), 6.82–6.79 (m, 2H), 3.11 (t, J = 6.8 Hz, 2H), 2.46 (t, J = 6.4 Hz, 2H), 1.95–1.89 (m, 2H), 1.77–1.74 (m, 2H). ^{13}C{^{1}H} NMR (100 MHz, $CDCl_3$): δ 156.5, 155.2, 150.1, 141.4, 138.8, 138.6, 132.9, 131.5, 130.2, 129.5, 129.2, 128.1, 127.9, 127.5, 127.3, 127.0, 126.3, 33.6, 28.2, 23.4, 23.3. IR (KBr, cm^{-1}): 3056, 2934, 1634, 1443. HRMS (ESI) m/z: $[M + H]^+$ calcd for $C_{27}H_{24}N$: 362.1903; found 362.1921.

4-(4-Fluorophenyl)-2,3-diphenyl-5,6,7,8-tetrahydroquinoline (3ba):

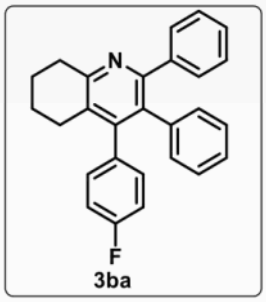

Physical State: white solid (14 mg, 68% yield). mp: 181–182 °C. R_f: 0.4 (10% EtOAc/hexane). ^{1}H NMR (400 MHz, $CDCl_3$): δ 7.26–7.24 (m, 2H), 7.15–7.13 (m, 3H), 6.97–6.86 (m, 7H), 6.79–6.77 (m, 2H), 3.11 (t, J = 6.4 Hz, 2H), 2.45 (t, J = 6.4 Hz, 2H), 1.96–1.90 (m, 2H), 1.81–1.75 (m, 2H). ^{13}C{^{1}H} NMR (100 MHz, $CDCl_3$): δ 161.9 (d, $J_{C\text{-}F}$ = 244 Hz), 156.7, 155.3, 149.2, 141.3, 138.7, 134.5 (d, $J_{C\text{-}F}$ = 3 Hz), 133.1, 131.5, 131.2 (d, $J_{C\text{-}F}$ = 8 Hz), 130.1, 129.4, 127.9, 127.7, 127.4, 126.4, 115.2 (d, $J_{C\text{-}F}$ = 22 Hz), 33.6, 28.3, 23.4, 23.3. IR (KBr, cm^{-1}): 3056, 2936, 1603, 1510, 1221. HRMS (ESI) m/z: $[M + H]^+$ calcd for $C_{27}H_{23}FN$: 380.1809; found 380.1822.

4-(4-Bromophenyl)-2,3-diphenyl-5,6,7,8-tetrahydroquinoline (3ca):

Physical State: white solid (16 mg, 66% yield). mp: 161–163 °C. R_f: 0.45 (10% EtOAc/hexane). ^{1}H NMR (400 MHz, $CDCl_3$): δ 7.33 (d, J = 8.0 Hz, 2H), 7.24 (d, J = 4.0 Hz, 2H), 7.14 (d, J = 3.6 Hz, 3H), 6.98 (d, J = 4.8 Hz, 3H), 6.84 (d, J = 8.0 Hz, 2H), 6.79

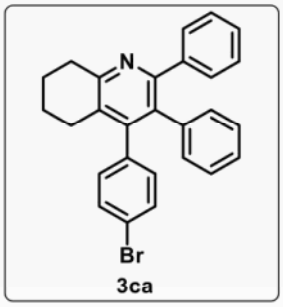

3ca

(d, J = 5.2 Hz, 2H), 3.11 (t, J = 6.4 Hz, 2H), 2.44 (t, J = 6.4 Hz, 2H), 1.96–1.91 (m, 2H), 1.80 – 1.74 (m, 2H). $^{13}C\{^1H\}$ NMR (100 MHz, $CDCl_3$): δ 156.8, 155.4, 148.9, 141.2, 138.5, 137.6, 132.8, 131.5, 131.4, 131.2, 130.1, 129.1, 127.9, 127.8, 127.4, 126.5, 121.3, 33.6, 28.3, 23.3, 23.2. IR (KBr, cm^{-1}): 3056, 2934, 1548, 1488, 1012. HRMS (ESI) m/z: $[M + H]^+$ calcd for $C_{27}H_{23}BrN$: 440.1008; found 440.1026.

4-(4-Iodophenyl)-2,3-diphenyl-5,6,7,8-tetrahydroquinoline (3da):

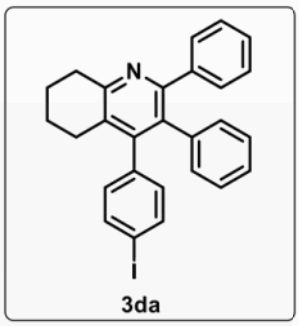

3da

Physical State: light yellow solid (23 mg, 83% yield). mp: 174–176 °C. R_f: 0.42 (10% EtOAc/hexane). ^1H NMR (400 MHz, $CDCl_3$): δ 7.53 (d, J = 8.0 Hz, 2H), 7.26–7.23 (m, 2H), 7.14–7.13 (m, 3H), 6.98–6.95 (m, 3H), 6.79–6.77 (m, 2H), 6.71 (d, J = 8.4 Hz, 2H), 3.10 (t, J = 6.4 Hz, 2H), 2.43 (t, J = 6.4 Hz, 2H), 1.96–1.89 (m, 2H), 1.80–1.75 (m, 2H). $^{13}C\{^1H\}$ NMR (100 MHz, $CDCl_3$): δ 156.8, 155.4, 148.9, 141.3, 138.5, 138.3, 137.3, 132.7, 131.5, 131.5, 130.2, 129.0, 127.9, 127.8, 127.4, 126.6, 92.8, 33.6, 28.3, 23.4, 23.3. IR (KBr, cm^{-1}): 3060, 2933, 1545, 1484, 699. HRMS (ESI) m/z: $[M + H]^+$ calcd for $C_{27}H_{23}IN$: 488.0870; found 488.0838.

2,3-Diphenyl-4-(p-tolyl)-5,6,7,8-tetrahydroquinoline (3ea):

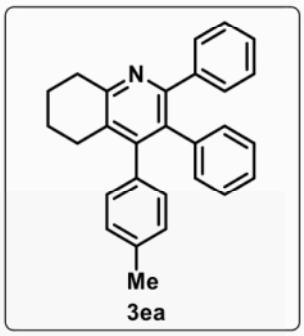

3ea

Physical State: white solid (15 mg, 73% yield). mp: 125–127 °C. R_f: 0.45 (10% EtOAc/hexane). ^1H NMR (400 MHz, $CDCl_3$): δ 7.26–7.23 (m, 2H), 7.15–7.12 (m, 3H), 6.99 (d, J = 8.0 Hz, 2H), 6.96–6.93 (m, 3H), 6.84–6.79 (m, 4H), 3.11 (t, J = 6.8 Hz, 2H), 2.46 (t, J = 6.4 Hz, 2H), 2.26 (s, 3H), 1.95–1.89 (m, 2H), 1.79–1.73 (m, 2H). $^{13}C\{^1H\}$ NMR (100 MHz, $CDCl_3$): δ 156.4, 155.2, 150.3, 141.4, 138.9, 136.6, 135.5, 133.1, 131.6, 130.2, 129.5, 129.4, 128.8, 127.9, 127.5,

127.3, 126.2, 33.6, 28.3, 23.4, 23.3, 21.5. IR (KBr, cm^{-1}): 3055, 2931, 1546, 1444. HRMS (ESI) m/z: $[M + H]^+$ calcd for $C_{28}H_{26}N$: 376.2060; found 376.2072.

4-(4-Nitrophenyl)-2,3-diphenyl-5,6,7,8-tetrahydroquinoline (3fa):

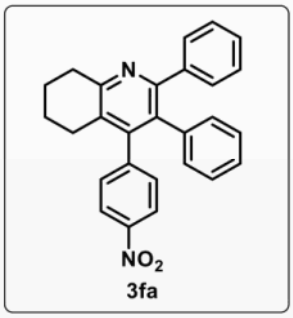

3fa

Physical State: yellow solid (5 mg, 23% yield). mp: 218–220 °C. R_f: 0.3 (10% EtOAc/hexane). ^1H NMR (400 MHz, $CDCl_3$): δ 8.07 (d, J = 8.0 Hz, 2H), 7.26 (br, 4H), 7.16 (d, J = 6.4 Hz, 4H), 6.97 (d, J = 4.8 Hz, 2H), 6.79 (d, J = 6.4 Hz, 2H), 3.13 (t, J = 6.0 Hz, 2H), 2.41 (t, J = 6.0 Hz, 2H), 1.98–1.92 (m, 2H), 1.82–1.76 (m, 2H). $^{13}C\{^1H\}$ NMR (100 MHz, $CDCl_3$): δ 157.1, 155.5, 147.9, 147.0, 146.0, 140.8, 138.0, 132.4, 131.3, 130.6, 130.1, 128.4, 128.0, 128.0, 127.7, 126.9, 123.5, 33.6, 28.2, 23.2, 23.1. IR (KBr, cm^{-1}): 3059, 2925, 1547, 1518, 1346. HRMS (ESI) m/z: $[M + H]^+$ calcd for $C_{27}H_{23}N_2O_2$: 407.1754; found 407.1752.

4-(Furan-2-yl)-2,3-diphenyl-5,6,7,8-tetrahydroquinoline (3ga):

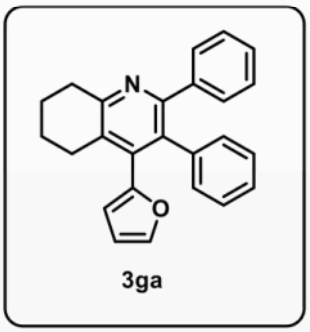

3ga

Physical State: brown solid (11 mg, 54% yield). mp: 134–136 °C. R_f: 0.5 (10% EtOAc/hexane). ^1H NMR (400 MHz, $CDCl_3$): δ 7.34 (s, 1H), 7.23 (d, J = 3.6 Hz, 2H), 7.15 (d, J = 2.8 Hz, 3H), 7.07 (d, J = 4.8 Hz, 3H), 6.89 (d, J = 4.4 Hz, 2H), 6.23 (d, J = 1.2 Hz, 1H), 5.83 (d, J = 2.8 Hz, 1H), 3.10 (t, J = 6.4 Hz, 2H), 2.69 (t, J = 6.4 Hz, 2H), 1.98–1.92 (m, 2H), 1.84–1.80 (m, 2H). $^{13}C\{^1H\}$ NMR (100 MHz, $CDCl_3$): δ 157.0, 155.5, 150.0, 142.2, 141.2, 139.5, 139.0, 133.9, 131.0, 130.8, 130.1, 127.9, 127.8, 127.4, 126.7, 111.3, 110.9, 33.5, 27.6, 23.2. IR (KBr, cm^{-1}): 3056, 2935, 1545, 1397, 1076. HRMS (ESI) m/z: $[M + H]^+$ calcd for $C_{25}H_{22}NO$: 352.1696; found 352.1693.

2,3-Diphenyl-4-(thiophen-2-yl)-5,6,7,8-tetrahydroquinoline (3ha):

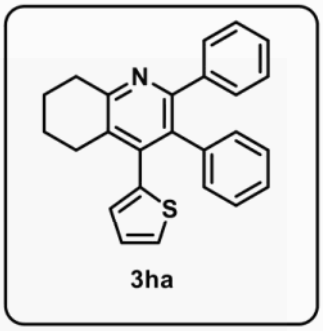

3ha

Physical State: yellow solid (10 mg, 47% yield). mp: 135–137 °C. R_f: 0.5 (10% EtOAc/hexane). ^{1}H NMR (400 MHz, $CDCl_3$): δ 7.26–7.24 (m, 2H), 7.20 (d, J = 4.8 Hz, 1H), 7.14 (d, J = 3.6 Hz, 3H), 7.02–7.01 (m, 3H), 6.90–6.86 (m, 3H), 6.68 (d, J = 3.2 Hz, 1H), 3.11 (t, J = 6.4 Hz, 2H), 2.64 (t, J = 6.4 Hz, 2H), 1.97–1.91 (m, 2H), 1.83–1.77 (m, 2H). ^{13}C{^{1}H} NMR (100 MHz, $CDCl_3$): δ 156.8, 155.3, 143.2, 141.3, 138.8, 138.6, 134.4, 131.2, 130.9, 130.1, 128.2, 127.9, 127.6, 127.4, 126.8, 126.6, 126.4, 33.6, 28.2, 23.3, 23.2. IR (KBr, cm^{-1}): 3060, 2924, 1744, 1398, 1086. HRMS (ESI) m/z: $[M + H]^+$ calcd for $C_{25}H_{22}NS$: 368.1467; found 368.1458.

4-(2-Methoxyphenyl)-2,3-diphenyl-5,6,7,8-tetrahydroquinoline (3ja):

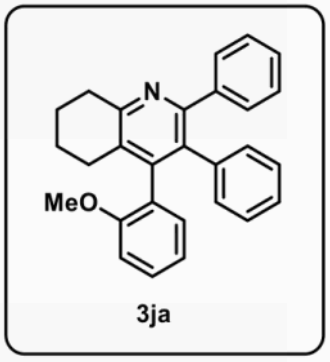

3ja

Physical State: yellow solid (16 mg, 71% yield). mp: 152–154 °C. R_f: 0.4 (10% EtOAc/hexane). ^{1}H NMR (400 MHz, $CDCl_3$): δ 7.26–7.23 (m, 2H), 7.13 (dd, J = 4.8, 1.6 Hz, 3H), 6.96–6.94 (m, 3H), 6.87 (d, J = 8.8 Hz, 2H), 6.81–6.78 (m, 2H), 6.73 (d, J = 8.8 Hz, 2H), 3.74 (s, 3H), 3.11 (t, J = 6.4 Hz, 2H), 2.48 (t, J = 6.4 Hz, 2H), 1.96–1.90 (m, 2H), 1.79–1.75 (m, 2H). ^{13}C{^{1}H} NMR (100 MHz, $CDCl_3$): δ 158.5, 156.5, 155.2, 149.9, 141.5, 139.0, 133.3, 132.6, 131.9, 131.6, 130.8, 130.6, 130.2, 129.7, 127.9, 127.6, 127.3, 126.2, 113.6, 55.4, 33.6, 28.3, 23.4, 23.3. IR (KBr, cm^{-1}): 3059, 2931, 1609, 1513, 1245. HRMS (ESI) m/z: $[M + H]^+$ calcd for $C_{28}H_{26}NO$: 392.2009; found 392.2021.

4-(3-Methoxyphenyl)-2,3-diphenyl-5,6,7,8-tetrahydroquinoline (3ka):

Physical State: Yellow solid (13 mg, 61% yield). mp: 65–67 °C. R_f: 0.4 (10% EtOAc/hexane). ^{1}H NMR (400 MHz, $CDCl_3$): δ 7.27–7.26 (m, 2H), 7.15–7.09 (m, 4H), 6.96–6.95 (m, 3H), 6.82 (d, J = 2.4 Hz, 2H), 6.69 (dd, J = 7.6, 1.8 Hz, 1H), 6.58 (d, J = 7.6

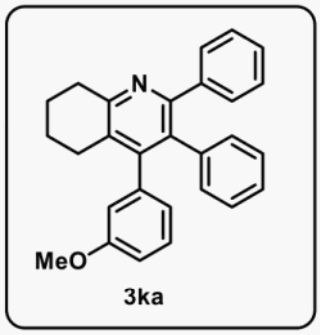

3ka

Hz, 1H), 6.48 (s, 1H), 3.64 (s, 3H), 3.11 (t, J = 6.4 Hz, 2H), 2.50 (t, J = 6.0 Hz, 2H), 1.96–1.90 (m, 2H), 1.80–1.73 (m, 2H). $^{13}C\{^1H\}$ NMR (100 MHz, $CDCl_3$): δ 159.4, 156.6, 155.2, 149.9, 141.4, 139.9, 138.8, 132.8, 131.5, 130.2, 129.2, 129.2, 127.9, 127.6, 127.3, 126.3, 122.1, 115.2, 112.8, 55.5, 33.6, 28.1, 23.4, 23.3. IR (KBr, cm-1): 3056, 2934, 1600, 1491, 1229. HRMS (ESI) m/z: $[M + H]^+$ calcd for $C_{28}H_{26}NO$: 392.2009; found 392.2020.

2,3-Bis(4-methoxyphenyl)-4-phenyl-5,6,7,8-tetrahydroquinoline (3ab):

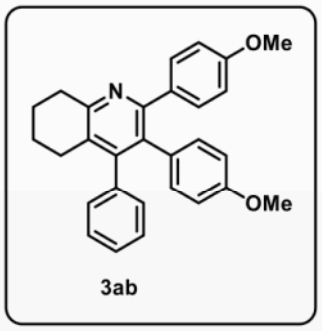

3ab

Physical State: yellow solid (18 mg, 76% yield). mp: 171–173 °C. R_f: 0.2 (10% EtOAc/hexane). ^1H NMR (400 MHz, $CDCl_3$): δ 7.22–7.14 (m, 5H), 6.95–6.93 (m, 2H), 6.71–6.68 (m, 4H), 6.52–6.49 (m, 2H), 3.74 (s, 3H), 3.65 (s, 3H), 3.09 (t, J = 6.4 Hz, 2H), 2.43 (t, J = 6.4 Hz, 2H), 1.93–1.88 (m, 2H), 1.76–1.73 (m, 2H). $^{13}C\{^1H\}$ NMR (100 MHz, $CDCl_3$): δ 158.9, 157.9, 156.2, 155.0, 150.4, 138.9, 134.2, 132.6, 132.3, 131.4, 131.3, 129.5, 128.9, 128.1, 126.9, 113.4, 113.1, 55.5, 55.3, 33.6, 28.2, 23.4, 23.3. IR (KBr, cm^{-1}): 3000, 2931, 1608, 1513, 1288, 1245. HRMS (ESI) m/z: $[M + H]^+$ calcd for $C_{29}H_{28}NO_2$: 422.2115; found 422.2108.

4-Phenyl-2,3-di-p-tolyl-5,6,7,8-tetrahydroquinoline (3ac):

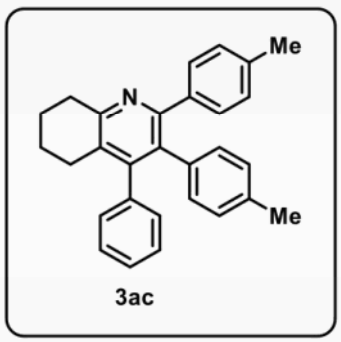

3ac

Physical State: yellow solid (14 mg, 63% yield). mp: 168–170 °C. R_f: 0.35 (10% EtOAc/hexane). ^1H NMR (400 MHz, $CDCl_3$): δ 7.24–7.17 (m, 3H), 7.08–6.96 (m, 10H), 3.07 (t, J = 6.4 Hz, 2H), 2.44 (t, J = 6.0 Hz, 2H), 2.29 (s, 3H), 2.27 (s, 3H), 1.93–1.87 (m, 2H), 1.76–1.71 (m, 2H). $^{13}C\{^1H\}$ NMR (100 MHz, $CDCl_3$): δ 157.0, 149.3, 140.1, 138.9, 138.0, 137.4, 136.5, 135.0, 132.0, 130.9, 130.4, 129.4, 129.2, 128.2, 127.3, 120.1, 92.0, 33.5, 28.4, 23.2,

23.1, 21.8, 21.5. IR (KBr, cm^{-1}): 3055, 2936, 1521, 1394. HRMS (ESI) m/z: $[M + H]^+$ calcd for $C_{29}H_{28}N$: 390.2216; found 390.2215.

4-Phenyl-2,3-di(thiophen-2-yl)-5,6,7,8-tetrahydroquinoline (3ae):

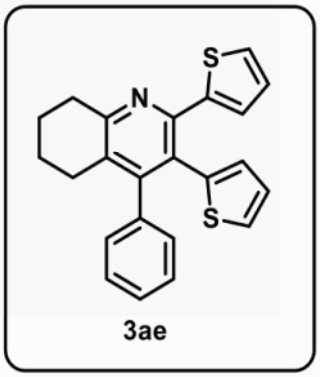

3ae

Physical State: yellow solid (12 mg, 59% yield). mp: 182–184 °C. R_f: 0.75 (10% EtOAc/hexane). ^1H NMR (400 MHz, $CDCl_3$): δ 7.26–7.17 (m, 5H), 7.02–7.00 (m, 2H), 6.82 (dd, J = 4.8, 4.0 Hz, 2H), 6.66 (dd, J = 3.2, 1.8 Hz, 1H), 6.56 (dd, J = 3.6, 1.8 Hz, 1H), 3.06 (t, J = 6.4 Hz, 2H), 2.37 (t, J = 6.4 Hz, 2H), 1.93–1.87 (m, 2H), 1.76–1.70 (m, 2H). $^{13}C\{^1H\}$ NMR (100 MHz, $CDCl_3$): δ 157.6, 152.2, 149.3, 139.4, 138.2, 130.0, 129.3, 129.1, 129.0, 128.1, 127.7, 127.5, 127.5, 127.3, 127.1, 126.9, 123.9, 33.5, 28.1, 23.3, 23.1. IR (KBr, cm^{-1}): 3100, 2934, 1491, 1436, 1389. HRMS (ESI) m/z: $[M + H]^+$ calcd for $C_{23}H_{20}NS_2$: 374.1032; found 374.1048.

4-Phenyl-2,3-di-m-tolyl-5,6,7,8-tetrahydroquinoline (3af):

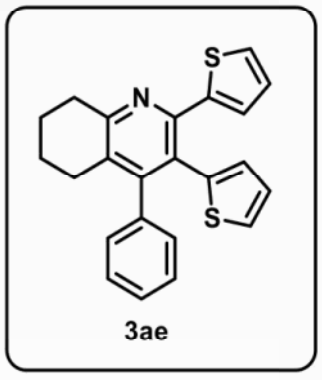

3ae

Physical State: yellow solid (15 mg, 69% yield). mp: 115–117 °C. R_f: 0.5 (10% EtOAc/hexane). ^1H NMR (400 MHz, $CDCl_3$): δ 7.20–7.12 (m, 4H), 7.00–6.93 (m, 5H), 6.82 (t, J = 7.6 Hz, 1H), 6.74 (d, J = 7.6 Hz, 1H), 6.61–6.57 (m, 2H), 3.11 (t, J = 6.8 Hz, 2H), 2.45 (d, J = 5.6 Hz, 2H), 2.23 (s, 3H), 2.03 (s, 3H), 1.94–1.90 (m, 2H), 1.79–1.73 (m, 2H). $^{13}C\{^1H\}$ NMR (100 MHz, $CDCl_3$): δ 156.3, 155.3, 150.1, 141.3, 138.8, 138.6, 137.3, 136.8, 133.1, 132.4, 130.9, 129.5, 129.1, 128.7, 128.6, 128.0, 127.5, 127.3, 127.3, 127.0, 126.9, 33.6, 28.2, 23.4, 23.3, 21.7, 21.5. IR (KBr, cm^{-1}): 3059, 2933, 1545, 1394. HRMS (ESI) m/z: $[M + H]^+$ calcd for $C_{29}H_{28}N$: 390.2216; found 390.2243.

2,3-Diethyl-4-phenyl-5,6,7,8-tetrahydroquinoline (3ag):[5]

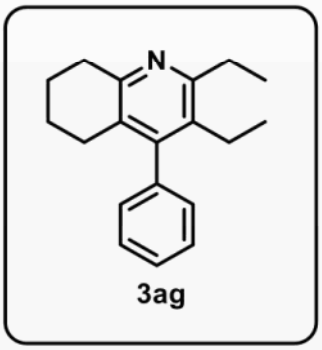

3ag

Physical State: yellow solid (8 mg, 56% yield). mp: 61–63 °C. R_f: 0.4 (10% EtOAc/hexane). ^{1}H NMR (400 MHz, $CDCl_3$): δ 7.43 (t, J = 7.2 Hz, 2H), 7.36 (t, J = 7.2 Hz, 1H), 7.09 (d, J = 8.0 Hz, 2H), 2.93 (t, J = 6.4 Hz, 2H), 2.83 (q, J = 7.6 Hz, 2H), 2.35 (q, J = 7.6 Hz, 2H), 2.21 (t, J = 6.4 Hz, 2H), 1.85–1.79 (m, 2H), 1.68–1.62 (m, 2H), 1.32 (t, J = 7.6 Hz, 3H), 0.93 (t, J = 7.6 Hz, 3H). ^{13}C{^{1}H} NMR (100 MHz, $CDCl_3$): δ 158.7, 154.1, 150.1, 139.4, 132.0, 128.7, 128.6, 128.0, 127.4, 33.2, 28.6, 27.9, 23.4, 23.3, 22.6, 15.7, 15.1. IR (KBr, cm^{-1}): 3055, 2931, 1565, 1406. HRMS (ESI) m/z: $[M + H]^+$ calcd for $C_{19}H_{24}N$: 266.1903; found 266.1894.

4-Phenyl-2,3-dipropyl-5,6,7,8-tetrahydroquinoline (3ah):

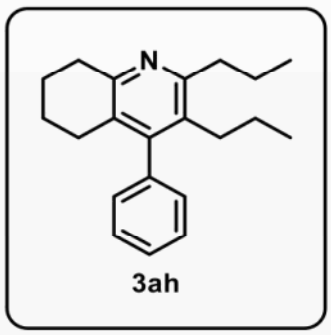

3ah

Physical State: white solid (10 mg, 60% yield). mp: 68–70 °C. R_f: 0.5 (10% EtOAc/hexane). ^{1}H NMR (400 MHz, $CDCl_3$): δ 7.44–7.33 (m, 3H), 7.08 (d, J = 8.0 Hz, 2H), 2.92 (t, J = 6.4 Hz, 2H), 2.76–2.72 (m, 2H), 2.28–2.19 (m, 4H), 1.83–1.63 (m, 6H), 1.35–1.29 (m, 2H), 1.04 (t, J = 7.2 Hz, 3H), 0.73 (t, J = 7.2 Hz, 3H). ^{13}C{^{1}H} NMR (100 MHz, $CDCl_3$): δ 157.7, 154.0, 150.2, 139.4, 130.9, 128.7, 127.9, 127.4, 37.8, 33.2, 31.9, 28.0, 24.7, 24.3, 23.4, 23.3, 14.9, 14.8. IR (KBr, cm^{-1}): 3056, 2930, 1434, 1406. HRMS (ESI) m/z: $[M + H]^+$ calcd for $C_{21}H_{28}N$: 294.2216; found 294.2215.

3-Methyl-2,4-diphenyl-5,6,7,8-tetrahydroquinoline (3ai):[5]

Physical State: white solid (13 mg, 81% yield). mp: 106–109 °C. R_f: 0.48 (10% EtOAc/hexane). ^{1}H NMR (400 MHz, $CDCl_3$): δ 7.51–7.33 (m, 8H), 7.15–7.13 (m, 2H), 3.01 (t, J = 6.4 Hz, 2H), 2.36 (t, J = 6.4 Hz, 2H), 1.91–1.84 (m, 5H), 1.74–1.68 (m, 2H).

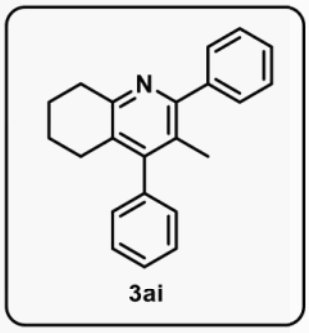

3ai

$^{13}C\{^{1}H\}$ NMR (100 MHz, $CDCl_3$): δ 156.6, 154.5, 150.9, 141.9, 139.5, 129.4, 129.1, 128.5, 128.4, 127.8, 127.6, 126.2, 33.4, 28.1, 23.3, 18.0. IR (KBr, cm^{-1}): 3031, 1562, 1402, 1263. HRMS (ESI) m/z: $[M + H]^+$ calcd for $C_{22}H_{22}N$: 300.1747; found 300.1763.

3-Ethyl-2,4-diphenyl-5,6,7,8-tetrahydroquinoline (3aj):

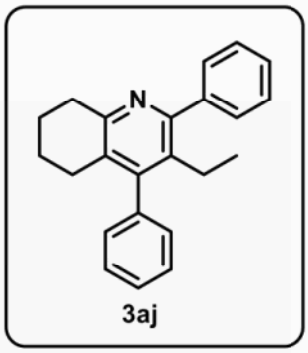

3aj

Physical State: white solid (9 mg, 51% yield). mp: 125–127 °C. R_f: 0.75 (10% EtOAc/DCM). ^1H NMR (400 MHz, $CDCl_3$): δ 7.47–7.33 (m, 8H), 7.18–7.16 (m, 2H), 2.99 (t, J = 6.4 Hz, 2H), 2.36–2.29 (m, 4H), 1.89–1.83 (m, 2H), 1.73–1.67 (m, 2H), 0.70 (t, J = 7.6 Hz, 3H). $^{13}C\{^{1}H\}$ NMR (100 MHz, $CDCl_3$): δ 156.9, 154.3, 150.5, 142.0, 139.0, 132.6, 129.6, 129.1, 128.8, 128.5, 127.7, 127.6, 33.3, 28.1, 23.3, 23.1, 15.4. IR (KBr, cm^{-1}): 3059, 2872, 1557, 1441, 1401. HRMS (ESI) m/z: $[M + H]^+$ calcd for $C_{23}H_{24}N$: 314.1903; found 314.1928.

2-Ethyl-3,4-diphenyl-5,6,7,8-tetrahydroquinoline (3aj'):

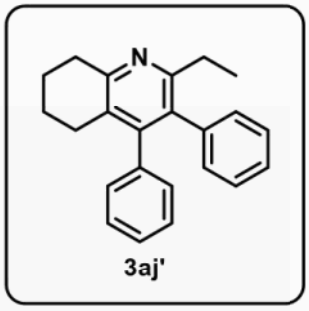

3aj'

Physical State: colourless liquid (4 mg, 23% yield). R_f: 0.5 (10% EtOAc/DCM). ^1H NMR (400 MHz, $CDCl_3$): δ 7.17–7.07 (m, 6H), 6.98–6.96 (m, 2H), 6.91–6.89 (m, 2H), 3.03 (t, J = 6.4 Hz, 2H), 2.59 (q, J = 7.2 Hz, 2H), 2.37 (t, J = 6.4 Hz, 2H), 1.93–1.87 (m, 2H), 1.73–1.71 (m, 2H), 1.12 (t, J = 7.6 Hz, 3H). $^{13}C\{^{1}H\}$ NMR (100 MHz, $CDCl_3$): δ 158.3, 156.1, 149.7, 139.0, 138.7, 133.3, 130.5, 129.3, 128.0, 127.8, 127.7, 126.9, 126.7, 33.4, 29.6, 28.0, 23.4, 23.4, 15.0. IR (KBr, cm^{-1}): 3059, 2932, 1492, 1432, 1401. HRMS (ESI) m/z: $[M + H]^+$ calcd for $C_{23}H_{24}N$: 314.1903; found 314.1896.

3-Butyl-2,4-diphenyl-5,6,7,8-tetrahydroquinoline and 2-butyl-3,4-diphenyl-5,6,7,8-tetrahydroquinoline (3ak and 3ak'):

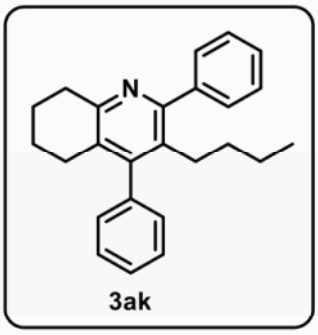

3ak

Physical State: colourless liquid (13 mg, 70% yield). R_f: 0.45 (10% EtOAc/hexane). ^{1}H NMR (400 MHz, $CDCl_3$): δ 7.46–7.33 (m, 8H), 7.17–7.15 (m, 2H), 2.99 (t, J = 6.8 Hz, 2H), 2.33–2.26 (m, 4H), 1.89–1.83 (m, 2H), 1.73–1.67 (m, 2H), 1.11–1.04 (m, 2H), 0.88–0.81 (m, 2H), 0.46 (t, J = 7.2 Hz, 3H). ^{13}C{^{1}H} NMR (100 MHz, $CDCl_3$): δ 157.0, 154.2, 150.6, 142.0, 139.0, 131.5, 129.5, 129.2, 128.8, 128.7, 128.4, 127.7, 127.5, 33.3, 32.9, 29.4, 28.1, 23.3, 23.3, 22.8, 13.5. IR (KBr, cm^{-1}): 3055, 2931, 1556, 1492, 1431, 1400. HRMS (ESI) m/z: $[M + H]^+$ calcd for $C_{25}H_{28}N$: 342.2216; found 342.2235.

3-Pentyl-2,4-diphenyl-5,6,7,8-tetrahydroquinoline (3al):

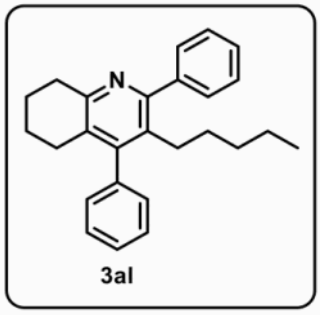

3al

Physical State: colourless liquid (9 mg, 46% yield). R_f: 0.4 (10% EtOAc/hexane). ^{1}H NMR (400 MHz, $CDCl_3$): δ 7.46–7.32 (m, 8H), 7.17–7.15 (m, 2H), 2.99 (t, J = 6.4 Hz, 2H), 2.34–2.26 (m, 4H), 1.89–1.83 (m, 2H), 1.74–1.68 (m, 2H), 1.14–1.07 (m, 2H), 0.89–0.80 (m, 4H), 0.60 (t, J = 6.8 Hz, 3H). ^{13}C{^{1}H} NMR (100 MHz, $CDCl_3$): δ 157.1, 154.3, 150.6, 142.2, 139.1, 131.5, 129.4, 129.2, 128.8, 128.8, 128.4, 127.7, 127.5, 33.4, 32.0, 30.4, 29.8, 28.1, 23.4, 23.3, 22.0, 13.9. IR (KBr, cm^{-1}): 3057, 2928, 1556, 1431, 1401. HRMS (ESI) m/z: $[M + H]^+$ calcd for $C_{26}H_{30}N$: 356.2373; found 356.2387.

2-Pentyl-3,4-diphenyl-5,6,7,8-tetrahydroquinoline (3al'):

Physical State: yellow liquid (6 mg, 31% yield). R_f: 0.5 (10% EtOAc/hexane). ^{1}H NMR (400 MHz, $CDCl_3$): δ 7.16–7.06 (m, 6H), 6.97–6.94 (m, 2H), 6.91–6.89 (m, 2H), 3.02 (t, J = 6.4 Hz, 2H), 2.57–2.53 (m, 2H), 2.36 (t, J = 6.4 Hz, 2H), 1.92–1.86 (m, 2H), 1.73–1.68

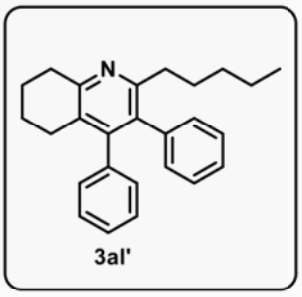

(m, 2H), 1.60–1.52 (m, 2H), 1.17–1.14 (m, 4H), 0.79–0.75 (m, 3H). $^{13}C\{^{1}H\}$ NMR (100 MHz, $CDCl_3$): δ 157.4, 156.0, 149.6, 139.0, 138.8, 133.5, 130.6, 129.3, 128.0, 127.8, 127.6, 126.9, 126.6, 36.5, 33.5, 32.2, 30.4, 28.0, 23.4, 22.6, 14.2. IR (KBr, cm^{-1}): 3059, 2929, 1555, 1442, 1400. HRMS (ESI) m/z: $[M + H]^+$ calcd for $C_{26}H_{30}N$: 356.2373; found 356.2370.

3-Hexyl-2,4-diphenyl-5,6,7,8-tetrahydroquinoline (3am):

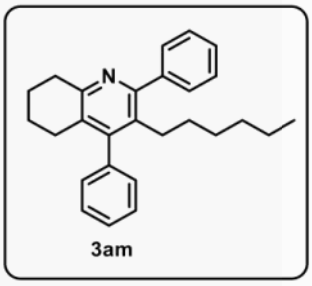

Physical State: yellow liquid (11 mg, 55% yield). R_f: 0.4 (10% EtOAc/hexane). ^{1}H NMR (400 MHz, $CDCl_3$): δ 7.47–7.34 (m, 8H), 7.17–7.15 (m, 2H), 3.03 (t, J = 6.4 Hz, 2H), 2.34–2.26 (m, 4H), 1.87–1.83 (m, 2H), 1.73–1.69 (m, 2H), 1.11–1.07 (m, 2H), 0.98–0.95 (m, 2H), 0.83–0.79 (m, 4H), 0.69 (t, J = 7.2 Hz, 3H). $^{13}C\{^{1}H\}$ NMR (100 MHz, $CDCl_3$): δ 157.0, 154.2, 150.6, 142.0, 139.0, 131.5, 129.5, 129.2, 128.8, 128.7, 128.4, 127.7, 127.5, 33.3, 31.1, 30.6, 29.7, 29.3, 28.1, 23.3, 23.3, 22.5, 14.2. IR (KBr, cm^{-1}): 3062, 2928, 1545, 1441, 1431, 1400. HRMS (ESI) m/z: $[M + H]^+$ calcd for $C_{27}H_{32}N$: 370.2529; found 370.2548.

2-Hexyl-3,4-diphenyl-5,6,7,8-tetrahydroquinoline (3am'):

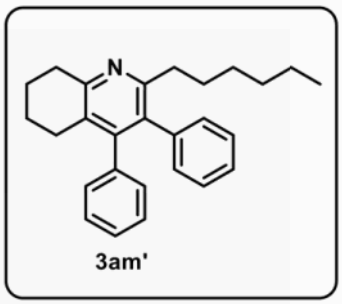

Physical State: yellow liquid (4 mg, 20% yield). R_f: 0.5 (10% EtOAc/hexane). ^{1}H NMR (400 MHz, $CDCl_3$): δ 7.17–7.06 (m, 6H), 6.97–6.95 (m, 2H), 6.91–6.89 (m, 2H), 3.03 (t, J = 6.8 Hz, 2H), 2.57–2.53 (m, 2H), 2.36 (t, J = 6.4 Hz, 2H), 1.93–1.86 (m, 2H), 1.74–1.73 (m, 2H), 1.58–1.50 (m, 2H), 1.19–1.09 (m, 6H), 0.79 (t, J = 6.8 Hz, 3H). $^{13}C\{^{1}H\}$ NMR (100 MHz, $CDCl_3$): δ 157.4, 155.9, 149.7, 138.9, 138.8, 133.5, 130.6, 129.3, 128.0, 127.8, 127.6, 126.9, 126.6, 36.4,

33.4, 31.8, 30.7, 29.6, 28.0, 23.3, 23.4, 22.8, 14.4. IR (KBr, cm^{-1}): 3062, 2929, 1555, 1442, 1431, 1400. HRMS (ESI) m/z: $[M + H]^+$ calcd for $C_{27}H_{32}N$: 370.2529; found 370.2521.

(4S,6aR,6bS,8aS,13aS,13bR)-6a,8a,9-trimethyl-11,12-diphenyl-3,4,5,6,6a,6b,7,8,8a,13,13a,13b-dodecahydro-1H-naphtho[2',1':4,5]indeno[1,2-c]pyridin-4-yl acetate (3na):

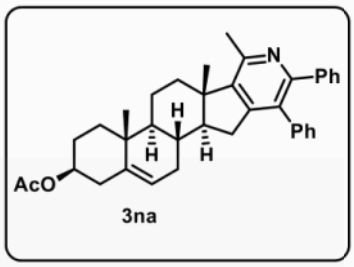

3na

Physical State: white solid (14 mg, 46% yield). mp: 208–210 °C. R_f: 0.2 (10% EtOAc/hexane).^{1}H NMR (400 MHz, $CDCl_3$): δ 7.28–7.21 (m, 5H), 7.16–7.14 (m, 3H), 7.06 (d, J = 7.6 Hz, 2H), 5.36 (d, J = 4.8 Hz, 1H), 4.64–4.57 (m, 1H), 2.64 (s, 3H), 2.53–2.40 (m, 3H), 2.34 (d, J = 6.8 Hz, 2H), 2.03 (s, 3H), 1.99–1.88 (m, 3H), 1.82–1.70 (m, 4H), 1.67–1.57 (m, 3H), 1.28–1.16 (m, 2H), 1.13 (s, 3H), 1.10 (s, 3H). $^{13}C\{^1H\}$ NMR (100 MHz, $CDCl_3$): δ 170.9, 154.8, 152.5, 151.3, 145.2, 141.1, 140.3, 139.0, 131.4, 130.4, 130.3, 128.3, 127.9, 127.4, 127.0, 122.4, 74.1, 57.3, 50.5, 46.2, 38.4, 37.2, 37.1, 36.3, 32.5, 31.9, 31.0, 28.1, 22.7, 21.8, 21.2, 19.6, 17.0. IR (KBr, cm^{-1}): 3056, 2956, 1730, 1562, 1378, 1244, 1034. HRMS (ESI) m/z: $[M + H]^+$ calcd for $C_{37}H_{42}NO_2$: 532.3210; found 532.3192.

NMR spectra of 2,3,4-Triphenyl-5,6,7,8-tetrahydroquinoline (3aa):

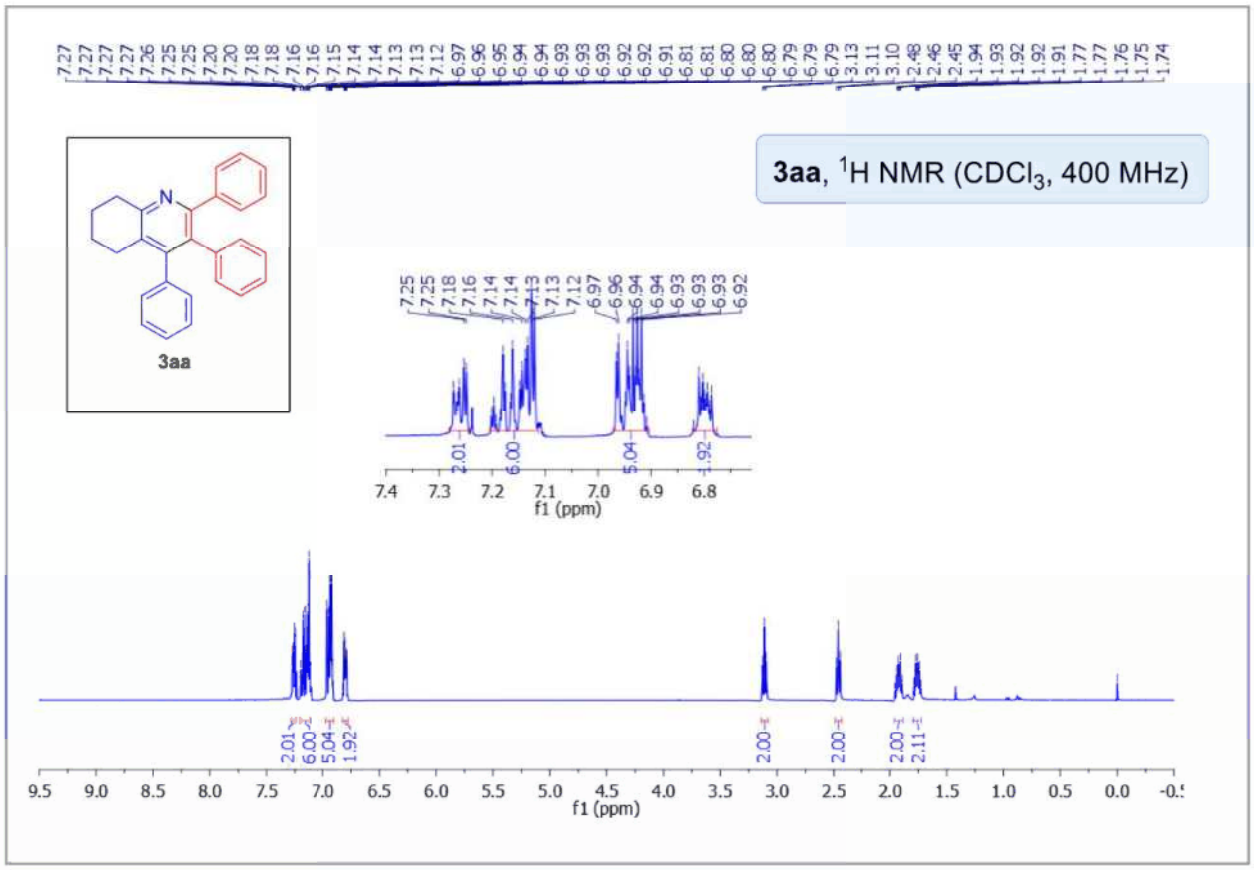

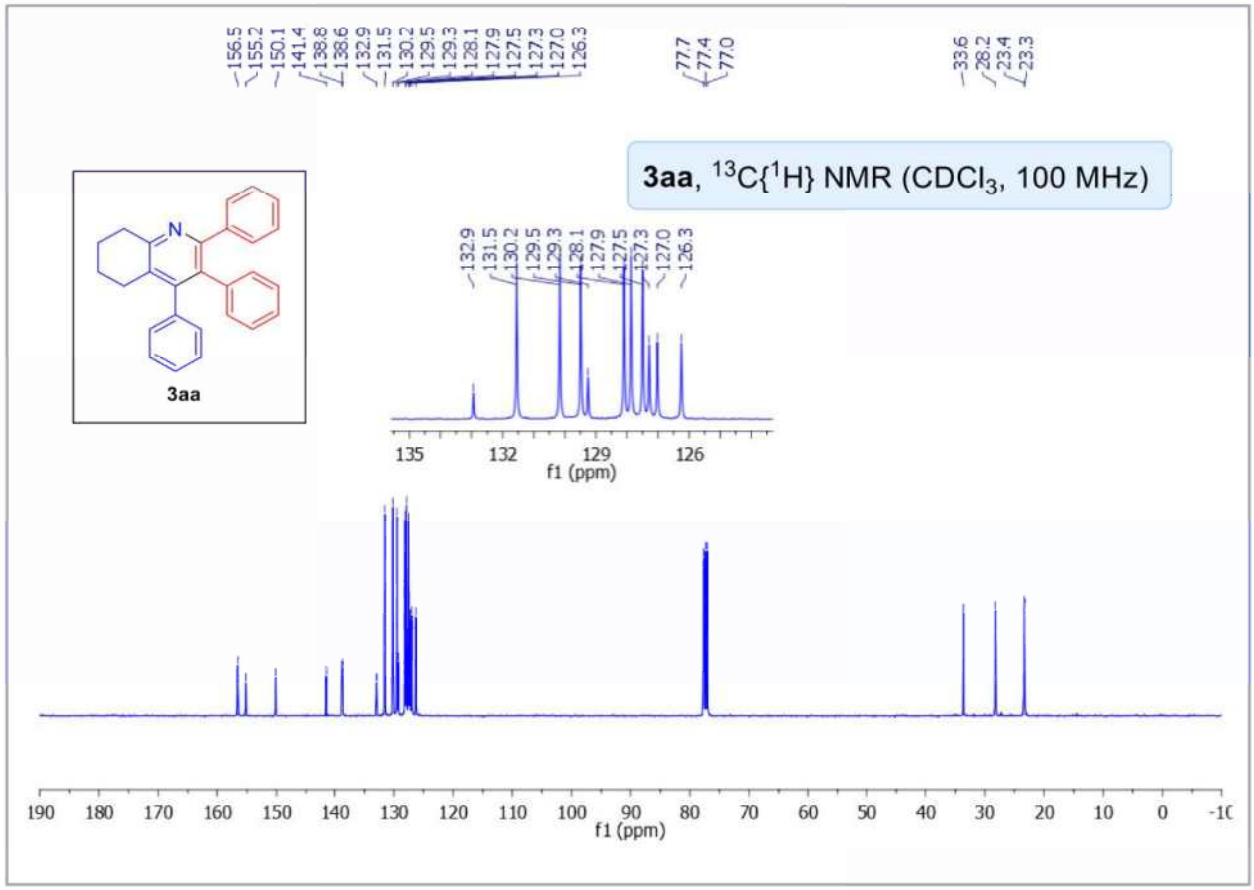

NMR spectra of 3-Methyl-2,4-diphenyl-5,6,7,8-tetrahydroquinoline (3ai):

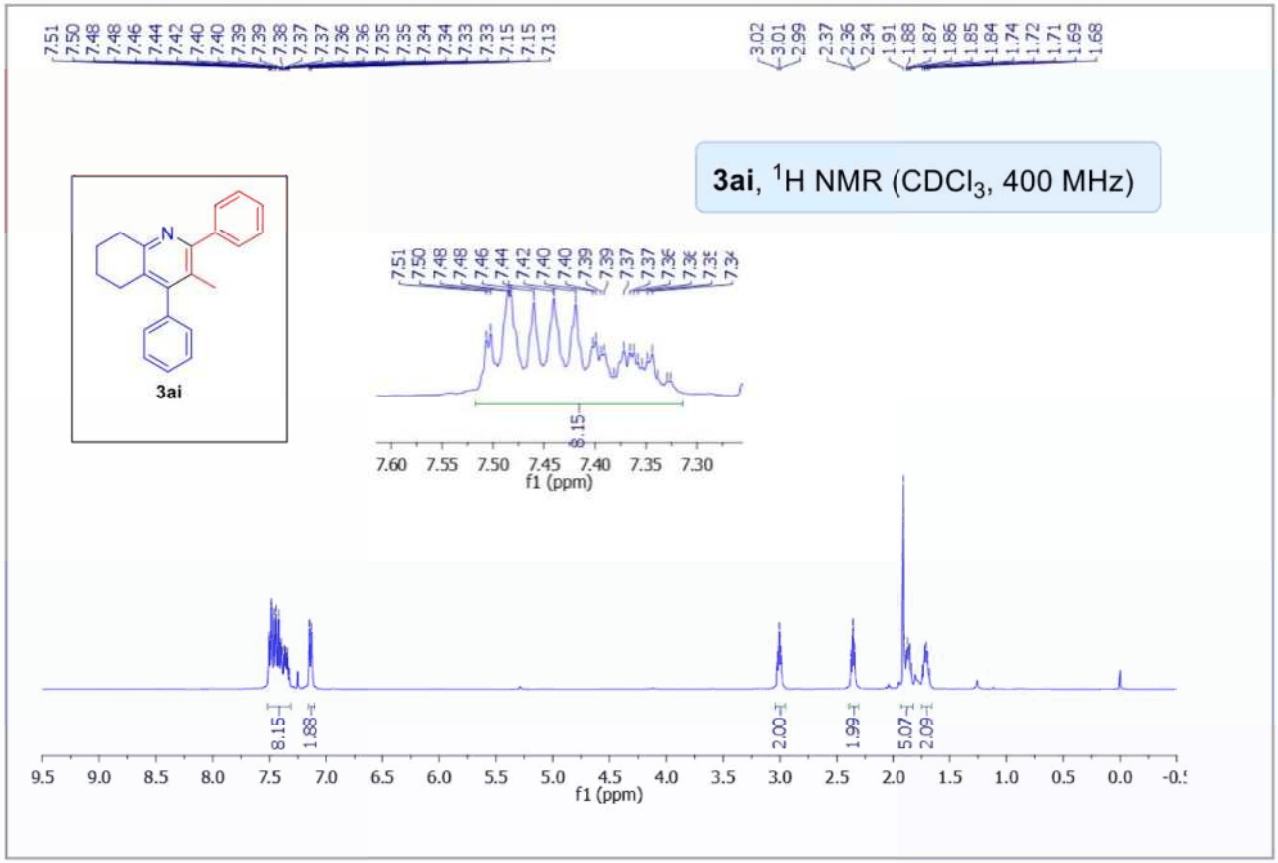

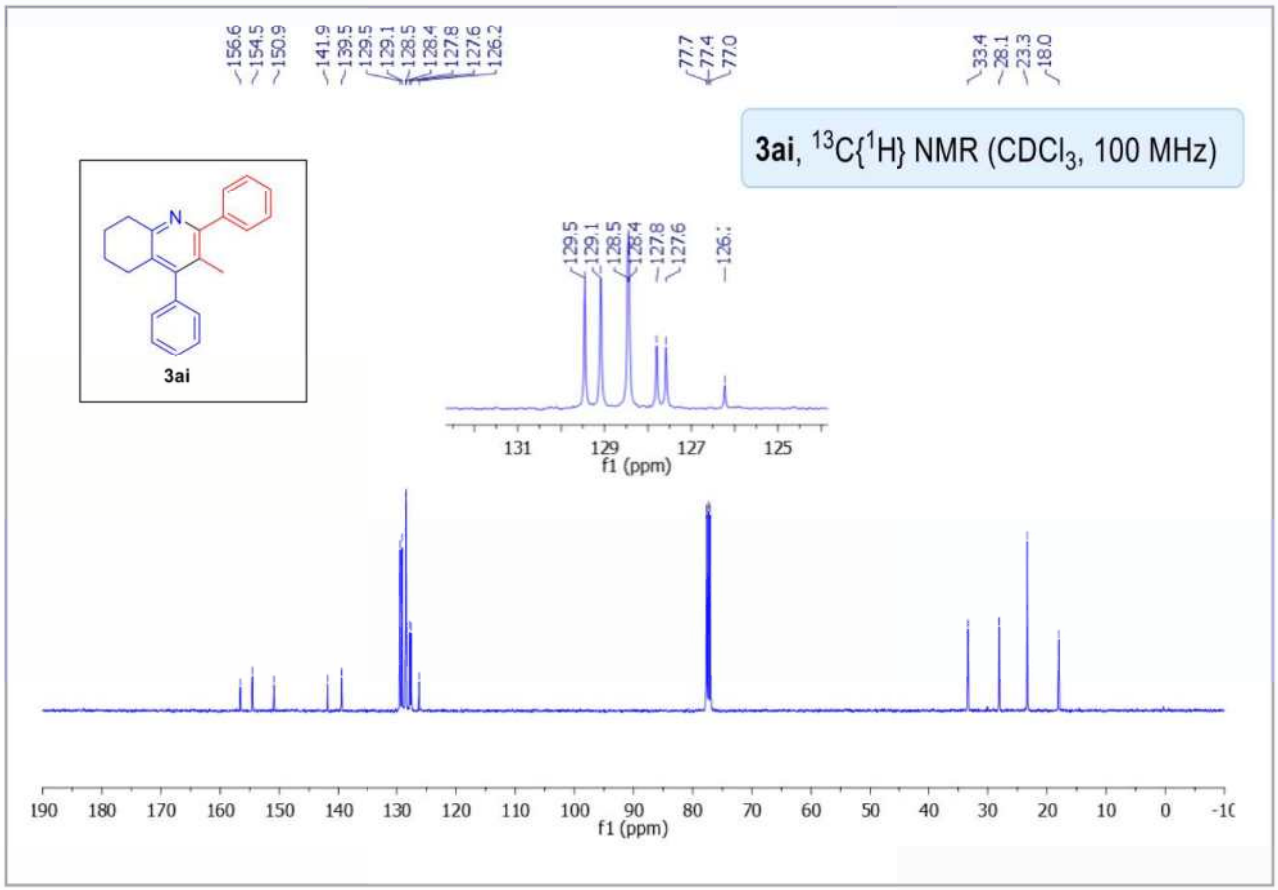

^{1}H-^{13}C HMBC confirms the product 3ai.

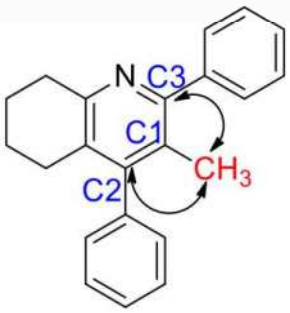

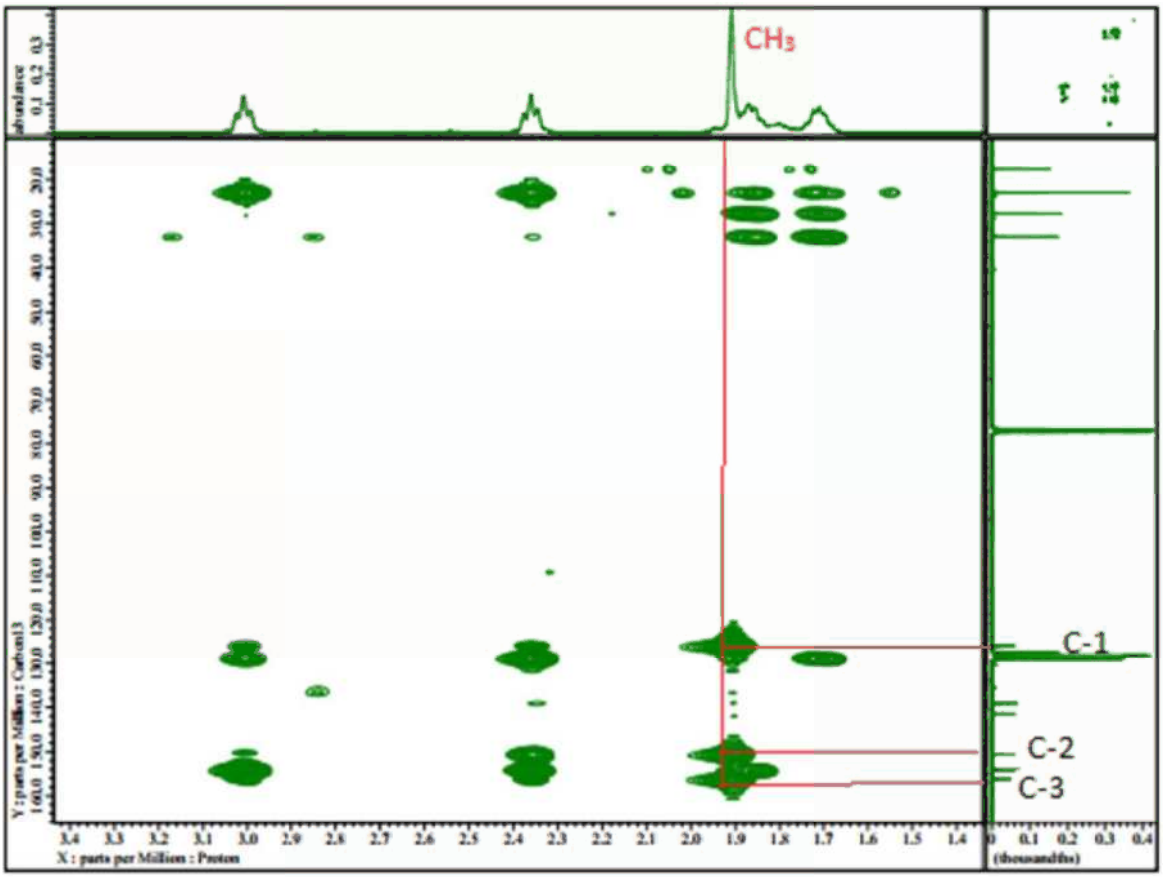

Crystal structure of 3aa

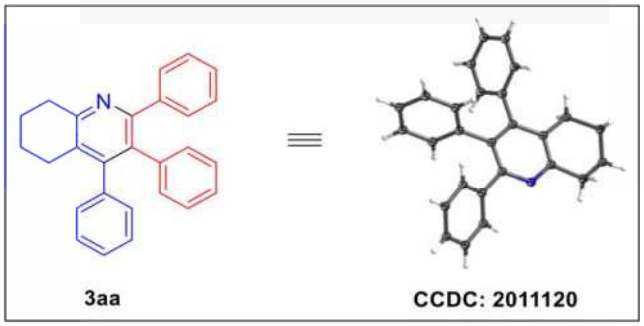

Datablock pcr_srm_anuu - ellipsoid plot

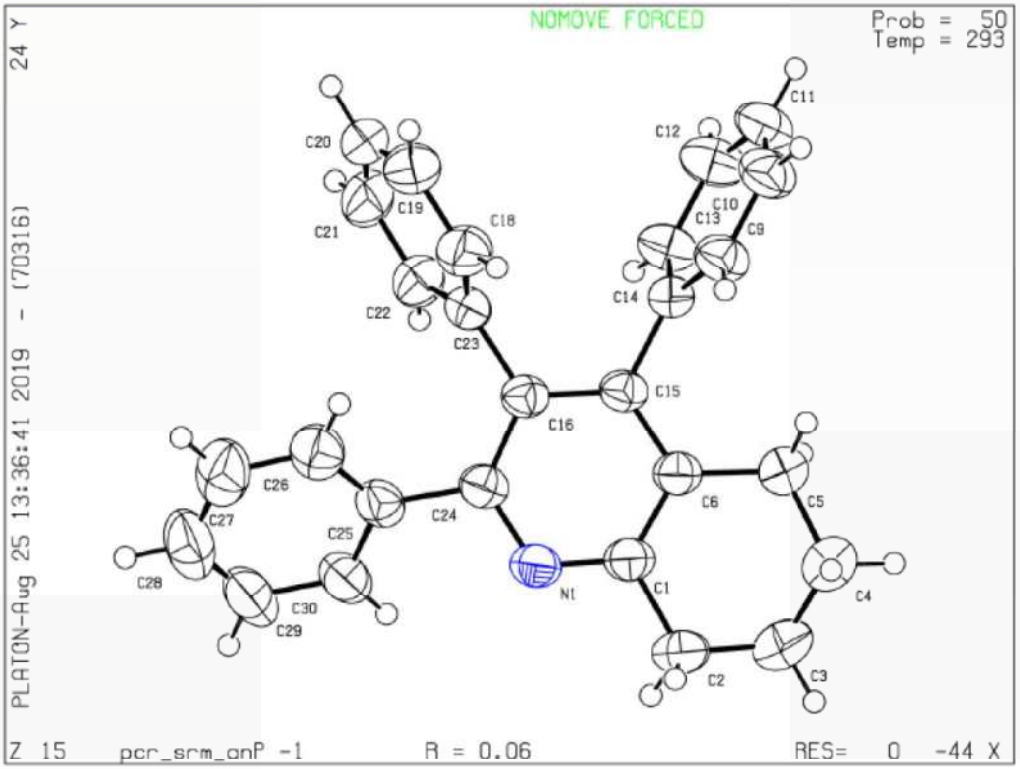

2.6 REFERENCES

1. (a) Yoshino, T.; Matsunaga, S. (Pentamethylcyclopentadienyl)cobalt(III)-Catalyzed C-H Bond Functionalization: From Discovery to Unique Reactivity and Selectivity. *Adv. Synth. Catal.* **2017**, *359*, 1245−1262. (b) Gandeepan, P.; Müller, T.; Zell, D.; Cera, G.; Warratz, S.; Ackermann, L. 3d Transition Metals for C−H Activation. *Chem. Rev*. **2019**, *119*, 2192. (c) Moselage, M.; Li, J.; Ackermann, L. Cobalt-Catalyzed C−H Activation. *ACS Catal*. **2016**, *6*, 498−525.
2. Zhang, B.; Studer, A. Recent Advances in the Synthesis of Nitrogen Heterocycles via Radical Cascade Reactions Using Isonitriles as Radical Acceptors. *Chem. Soc. Rev.* **2015**, *44*, 3505–3521.
3. Bessonova, I. A. Acetylhaplophyllidine, a new alkaloid from haplophyllum perforatum. *Chem. Nat. Compd.* **1999**, *35*, 589−590.
4. Papageorgiou, M.; Fokialakis, N.; Mitaku, S.; Skaltsounis, A. L.; Tillequin, F.; Sevenet, T. Two New Alkaloids from the Bark of Sarcomelicope megistophylla. *J. Nat. Prod*. **2000**, *63*, 385−386.
5. J. B. Crawford, G. Chen, D. Gauthier, T. Wilson, B. Carpenter, I. R. Baird, E. McEachern, A. Kaller, C. Harwig, B. Atsma, R. T. Skerlj, G. J. Bridger. AMD070, a CXCR4 Chemokine Receptor Antagonist: Practical Large-Scale Laboratory Synthesis. Org. *Process Res. Dev.* **2008**, *12*, 823−830.
6. M. M. Ghorab, F. A. Ragab, M. M. Hamed. Design, synthesis and anticancer evaluation of novel tetrahydroquinoline derivatives containing sulfonamide moiety. *Eur. J. Med. Chem*. **2009**, *44*, 4211−4217.
7. A. R. Gholap, K. S. Toti, F. Shirazi, R. Kumari, M. Bhat, M. V. Deshpande, K. V. Srinivasan. Synthesis and evaluation of antifungal properties of a series of the novel 2-

amino-5-oxo-4-phenyl-5,6,7,8-tetrahydroquinoline-3-carbonitrile and its analogues. *Bioorg. Med. Chem.* **2007**, *15*, 6705−6715.

8. Parthasarathy, K.; Cheng, C. H. Easy Access to Isoquinolines and Tetrahydroquinolines from Ketoximes and Alkynes via Rhodium-Catalyzed C-H Bond Activation. *J. Org. Chem.* **2009**, *74*, 9359–9364.
9. Pita, B.; Masaguer, C. F.; Raviña, E. New Synthetic Approaches to CNS Drugs. A Straightforward, Efficient Synthesis of Tetrahydroindol-4-Ones and Tetrahydroquinolin-5-Ones via Palladium-Catalyzed Oxidation of Hydroxyenaminones. *Tetrahedron Lett.* **2002**, *43*, 7929–7932.
10. Sun, B.; Yoshino, T.; Kanai, M.; Matsunaga, S. Cp∗Co(III) Catalyzed Site-Selective C-H Activation of Unsymmetrical O-Acyl Oximes: Synthesis of Multisubstituted Isoquinolines from Terminal and Internal Alkynes. *Angew. Chemie Int. Ed.* **2015**, *54*, 12968–12972.
11. Wang, H.; Koeller, J.; Liu, W.; Ackermann, L. Cobalt(III)-Catalyzed C-H/N-O Functionalizations: Isohypsic Access to Isoquinolines. *Chem. Eur. J.* **2015**, *21*, 15525–15528.
12. Sen, M.; Kalsi, D.; Sundararaju, B. Cobalt(III)-Catalyzed Dehydrative [4+2] Annulation of Oxime with Alkyne by C-H and N-OH Activation. *Chem. Eur. J.* **2015**, *21*, 15529–15533.
13. Muralirajan, K.; Kuppusamy, R.; Prakash, S.; Cheng, C. H. Easy Access to 1-Amino and 1-Carbon Substituted Isoquinolines via Cobalt-Catalyzed C-H/N-O Bond Activation. *Adv. Synth. Catal.* **2016**, *358*, 774–783.
14. Wang, K.; Hu, F.; Zhang, Y.; Wang, J. Directing Group-Assisted Transition-Metal-Catalyzed Vinylic C-H Bond Functionalization. *Sci. China Chem.* **2015**, *58*, 1252–1265.

15. Yamakawa, T.; Yoshikai, N. Annulation of α,β -Unsaturated Imines and Alkynes via Cobalt-Catalyzed Olefinic C-H Activation. *Org. Lett*. **2013**, *15*, 196−199.

16. Fallon, B. J.; Garsi, J.-B.; Derat, E.; Amatore, M.; Aubert, C.; Petit, M. Synthesis of 1,2-Dihydropyridines Catalyzed by Well-Defined Low-Valent Cobalt Complexes: C−H Activation Made Simple. *ACS Catal*. **2015,** *5***,** 7493−7497.

17. Colby, D. A.; Bergman, R. G.; Ellman, J. A.; Berkeley, L. Synthesis of Dihydropyridines and Pyridines from Imines and Alkynes via C-H Activation. *J. Am. Chem. Soc*. **2008**, *130*, 3645–3651.

18. (a) Yu, W.; Zhang, W.; Liu, Y.; Zhou, Y.; Liu, Z.; Zhang, Y. Cobalt(III)-Catalyzed Synthesis of Pyrroles from Enamides and Alkynes. *RSC Adv.* **2016**, *6*, 24768–24772. (b) Lade, D. M.; Pawar, A. B. Cp∗Co(III)-Catalyzed Vinylic C-H Bond Activation under Mild Conditions: Expedient Pyrrole Synthesis: Via (3 + 2) Annulation of Enamides and Alkynes. *Org. Chem. Front.* **2016**, *3*, 836–840. (c) Yu, W.; Zhang, W.; Liu, Y.; Liu, Z.; Zhang, Y. Cobalt(III)-catalyzed cross-coupling of enamides with allyl acetates/maleimides. *Org. Chem. Front.* **2017**, *4*, 77−80.

19. (a) Yu, D. G.; Gensch, T.; De Azambuja, F.; Vásquez-Céspedes, S.; Glorius, F. Co(III)-Catalyzed C-H Activation/Formal S_N-Type Reactions: Selective and Efficient Cyanation, Halogenation, and Allylation. *J. Am. Chem. Soc.* **2014**, *136*, 17722–17725. (b) Chen, X.; Hu, X.; Deng, Y.; Jiang, H.; Zeng, W. A [4 + 1] Cyclative Capture Access to Indolizines via Cobalt(III)-Catalyzed Csp^2-H bond Functionalization. *Org. Lett.* **2016**, *18*, 4742–4745. (c) Prakash, S.; Muralirajan, K.; Cheng, C. H. Simple Cobalt-Catalyzed Oxidative Annulation of Nitrogen-Containing Arenes with Alkynes: An Atom-Economical Route to Heterocyclic Quaternary Ammonium Salts. *Angew. Chemie Int. Ed.* **2016***, 55,* 1844−1848.

20. (a) Gandeepan, P.; Rajamalli, P.; Cheng, C. H. Diastereoselective [3+2] Annulation of Aromatic/Vinylic Amides with Bicyclic Alkenes through Cobalt-Catalyzed C-H Activation and Intramolecular Nucleophilic Addition. *Angew. Chemie Int. Ed.* **2016**, *55*, 4308–4311. (b) Kawai, K.; Bunno, Y.; Yoshino, T.; Matsunaga, S. Weinreb Amide Directed Versatile C-H Bond Functionalization under (η^5-Pentamethylcyclopentadienyl)cobalt(III) Catalysis. *Chem. Eur. J.* **2018**, *24*, 10231−10237. (c) Zhang, L. B.; Hao, X. Q.; Zhang, S. K.; Liu, Z. J.; Zheng, X. X.; Gong, J. F.; Niu, J. L.; Song, M. P. Cobalt-Catalyzed C(sp^2)-H Alkoxylation of Aromatic and Olefinic Carboxamides. *Angew. Chemie Int. Ed.* **2015**, *54*, 272−275. (d) Hu, L.; Gui, Q.; Chen, X.; Tan, Z.; Zhu, G. Cobalt-promoted selective arylation of benzamide and acrylamides with arylboronic acids. *Org. Biomol. Chem.* **2016**, *14*, 11070-11075. (e) Gensch, T.; Vasquez-Cespedes, S.; Yu, D. G.; Glorius, F. Cobalt(III)-Catalyzed Directed C−H Allylation. *Org. Lett.* **2015**, *17*, 3714−3717. (f) Grigorjeva, L.; Daugulis, O. Cobalt-Catalyzed Aminoquinoline-Directed Coupling of sp^2 C−H Bonds with Alkenes. *Org. Lett.* **2014**, *16*, 4684-4687. (g) Sauermann, N.; Meyer, T. H.; Tian, C.; Ackermann, L. Electrochemical Cobalt-Catalyzed C−H Oxygenation at Room Temperature. *J. Am. Chem. Soc.* **2017**, *139*, 18452-18455.

21. (a) Liu, X. G.; Zhang, S. S.; Jiang, C. Y.; Wu, J. Q.; Li, Q.; Wang, H. Cp∗Co(III)-Catalyzed Annulations of 2-Alkenylphenols with CO: Mild Access to Coumarin Derivatives. *Org. Lett.* **2015**, *17*, 5404–5407. (b) Kuppusamy, R.; Muralirajan, K.; Cheng, C. H. Cobalt(III)-Catalyzed [5 + 1] Annulation for 2H-Chromenes Synthesis via Vinylic C-H Activation and Intramolecular Nucleophilic Addition. *ACS Catal.* **2016**, *6*, 3909–3913. (c) Ghorai, J.; Reddy, A. C. S.; Anbarasan, P. Cobalt(III)-Catalyzed Intramolecular Cross-Dehydrogenative C-H/X-H Coupling: Efficient Synthesis of Indoles and Benzofurans. Chem. *Eur. J.* **2016**, *22*, 16042−16046.

22. Hummel, J. R.; Ellman, J. A. Cobalt(III)-Catalyzed Synthesis of Indazoles and Furans by C-H Bond Functionalization/Addition/Cyclization Cascades. *J. Am. Chem. Soc.* **2015**, *137*, 490–498.

23. Wang, J.; Zha, S.; Chen, K.; Zhu, J. Cp*Co(III)-Catalyzed, N-N Bond-Based Redox-Neutral Synthesis of Isoquinolines. *Org. Chem. Front.* **2016**, *3*, 1281–1285.

24. Li, J.; Ackermann, L. Cobalt(III)-Catalyzed Aryl and Alkenyl C-H Aminocarbonylation with Isocyanates and Acyl Azides. *Angew. Chemie Int. Ed.* **2015**, *54*, 8551–8554.

25. Gottlieb, H. E.; Kotlyar, V.; Nudelman, A. NMR chemical shifts of common laboratory solvents as trace impurities. *J. Org. Chem.* **1997**, *62*, 7512-7515.

26. Warner, M. C.; Nagendiran, A.; Bogár, K.; Bäckvall, J. E. Enantioselective Route to Ketones and Lactones from Exocyclic Allylic Alcohols via Metal and Enzyme Catalysis. *Org. Lett*. **2012**, *14*, 5094–5097.

27. D. Das, G. Sahoo, A. Biswas and R. Samanta. Rh(III)-Catalyzed Synthesis of Highly Substituted 2-Pyridones using Fluorinated Diazomalonate. *Chem. Asian J*., **2020**, *15*, 360-364.

28. Nishihara, Y.; Ikegashira, K.; Hirabayashi, K.; Ando, J. I.; Mori, A.; Hiyama, T. Coupling Reactions of Alkynylsilanes Mediated by a Cu(I) Salt: Novel Syntheses of Conjugate Diynes and Disubstituted Ethynes. *J. Org. Chem*. **2000**, *65*, 1780–1787.

Chapter 3

Cobalt(III)-Catalyzed C-6 Alkenylation of 2-Pyridones by Using Terminal Alkyne with High Regioselectivity

Chapter 3

Cobalt(III)-Catalyzed C-6 Alkenylation of 2-Pyridones by Using Terminal Alkyne with High Regioselectivity

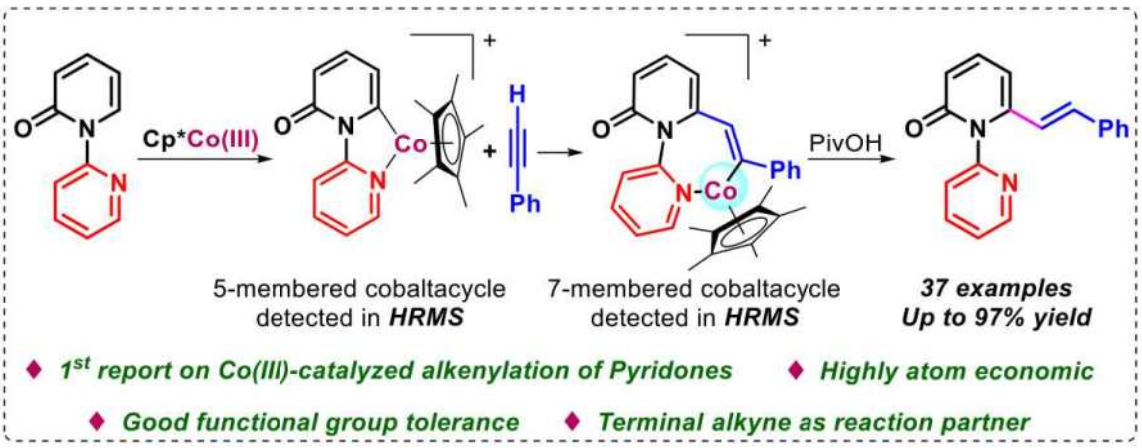

3.1 ABSTRACT: For the first time, Co(III)-catalyzed C-6 alkenylation of 2-pyridones with terminal alkyne as coupling partner has been demonstrated with high regioselectivity. The reaction conditions can be used with a variety of substrates and also shows good functional group tolerance. Reaction proceeds through cyclometallation, alkyne insertion followed by protodemetalation steps. High resolution mass spectrometry was also used to detect the formation of five and seven membered cobaltacycle intermediates.

3.2 INTRODUCTION

2-Pyridone is a nitrogen-containing heterocycle found in a wide range of biologically active natural products (Figure-3.1). It is also valued as an important synthetic intermediate[1] as it can be easily converted to piperidines, pyridines, indolizidines and quinolizidines.[2] Controlling the reactivity in 2-pyridone ring which has four reactive centers (C3, C4, C5, C6) is the most challenging issue in the C-H functionalization of 2-pyridones. C-H functionalization at the electron deficient C(6)-H position was relatively difficult as compared to C(3)-H,[3] C(4)-H,[4] C(5)-H.[5] C(6) carbon of 2-pyridone is often functionalized

(C-C bond) in many bio-active molecules. Therefore, C-C bond forming reaction at C-6 position of 2-pyridone has attracted significant attention lately.[6] For the C-H bond functionalization reaction to be greener and sustainable, the metal used should be cost effective and earth abundant.[7] Pioneering work by Matsunaga and Kanai has made Cp*Co(III) as excellent metal catalyst for such greener reaction.[8,9]

Figure 3.1: Representative examples of natural products and bioactive molecules containing C-6 substituted 2-pyridone moiety.

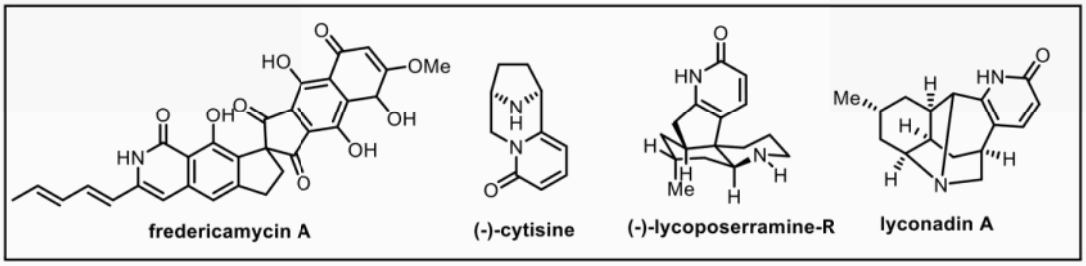

In particular, C(6)-H alkenylation is gaining more importance in recent years.[10] Recently, Walsh group[6b] reported a useful decarboxylative C-6 alkenylation of 2-pyridone with polyenyl carboxylic acid (Scheme-3.1a) using an expensive and moisture sensitive Rh catalyst at elevated temperature. Miura group[6c] also reported a Rh catalyzed alkenylation of 2-pyridone by using styrene as the coupling partner (Scheme-3.1b). Though Miura's approach is atom economical and performed at lower temperature, it still suffers from few drawbacks, such as, use of expensive catalyst and stoichiometric amount of external oxidant, which makes the reaction less sustainable for industrial use. Use of internal alkynes under rhodium catalyst enabled double C-H bond activation and produced the corresponding quinolones (Scheme-3.1c).[11] In general, directed C-H alkenylation reactions are performed by using internal alkynes.[12] Terminal alkynes are generally not preferred for C-H alkenylation as it is less compatible[12b-e] with cobalt catalyst because of the acidic terminal proton which leads to homocoupled product[10] under oxidative condition. Many research groups have already reported this homocoupling problem with

Scheme 3.1: Previous work and our work

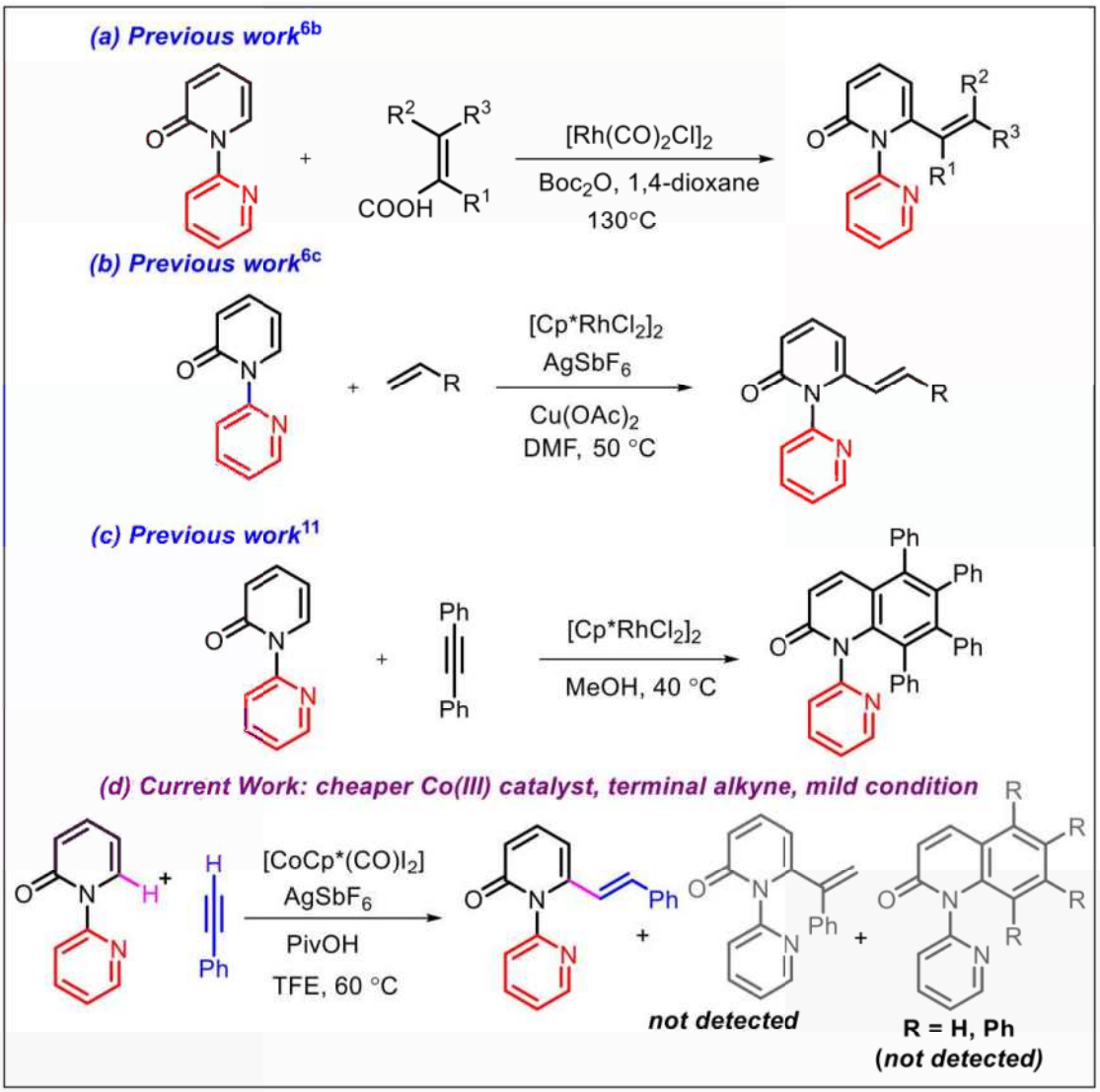

terminal alkynes under cobalt catalysis.[13] This hinders the synthesis of many C-6 substituted (C-C bonded) moieties using cobalt catalyzed C-H activation strategy. In recent years activation of C-H bond using more abundant and less expensive first row transition metals are gaining prominence.[14] Therefore, use of first row metal catalyst such as cobalt along with terminal alkynes is a challenging but attractive proposal for C(6)-H alkenylation of 2-pyridones. Herein, we report the first, Cp*Co(III)-catalyzed highly regioselective C-6 alkenylation of 2-pyridone with terminal alkynes under mild conditions.[15] To the best of

our knowledge, there is no report of Co(III)-catalyzed alkenylation of 2-pyridones with terminal alkynes.[16]

3.3 RESULTS AND DISCUSSION

Optimization conditions for the alkenylation of 2-pyridones are summarized in Table 3.1. We initiated our optimization by taking 2*H*-[1,2'-bipyridin]-2-ones **1a** and phenyl acetylene **2a** as the reactants with 5 mol % of Cp*Co(CO)I_2 and 10 mol % of $AgSbF_6$ as an activator, along with 1 equiv of 1-AdCOOH in DCE at 60 °C for 12 h. This reaction failed to give the desired product **3aa** (Table 3.1, entry 1). We then screened solvents such as toluene, tetrahydrofuran (THF), hexafluoroisopropanol (HFIP) and trifluoroethanol (TFE). While toluene and THF failed to give the product **3aa** (Table 3.1, entry 2 & 3), fluorinated solvents such as HFIP and TFE gave positive results with isolated yields of **3aa** in 37% and 64% respectively (Table 3.1, entry 4 & 5). It has been reported elsewhere in the literature that fluorinated solvents have magical influence on C-H activation reactions.[17] Therefore, we continued our optimization with the fluorinated solvent TFE and varied different acid additives such as *para*-toluenesulfonic acid (PTSA), acetic acid, trifluoroacetic acid and pivalic acid (PivOH) (Table 3.1, entries 6-9). Delightfully, with PivOH the yield of the product raised to 94%. Surprisingly when HFIP was used as solvent with PivOH lower yield of **3aa** (57%) was obtained (Table 3.1, entry 10). Changing the silver salts to AgOTf, $AgBF_4$ and $AgNTf_2$ were not helpful (Table 3.1, entries 11-13). Further lowering of the temperature to room temperature reduced the yield of the product **3aa** drastically to 46% (Table 3.1, entry 14). Several control experiments were performed to ascertain the role of silver salt, acid additive and cobalt catalyst. Reaction in the absence of $AgSbF_6$ furnished the product **3aa** in only 20% yield (Table 3.1, entry 15). Absence of either PivOH or Cp*Co catalyst did not produce the alkenylated product **3aa** (Table 3.1, entries 16-17), this clearly proves that both catalyst and acid additive are playing key role

in this reaction. Finally, 5 mol % of Cp*Co(III) catalyst, 10 mol % of $AgSbF_6$, with 1 equivalent of pivalic acid and TFE as solvent (0.1 M) at 60 °C was found to be the best optimized reaction condition (Table 3.1, entry 9).

Table 3.1. Optimization for Co(III)-Catalyzed C-6 Alkenylation of 2-pyridones[a]

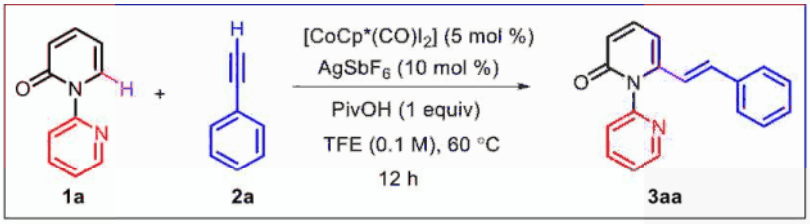

entry	silver salt (10 mol %)	additive (1 equiv)	solvent (0.1 M)	yield of **3aa** (%)[b]
1	$AgSbF_6$	1-AdCOOH	DCE	nd
2	$AgSbF_6$	1-AdCOOH	Toluene	nd
3	$AgSbF_6$	1-AdCOOH	THF	nd
4	$AgSbF_6$	1-AdCOOH	HFIP	37
5	$AgSbF_6$	1-AdCOOH	TFE	64
6	$AgSbF_6$	PTSA	TFE	nd
7	$AgSbF_6$	CH_3COOH	TFE	22
8	$AgSbF_6$	CF_3COOH	TFE	61
9	$AgSbF_6$	PivOH	TFE	94
10	$AgSbF_6$	PivOH	HFIP	57
11	AgOTf	PivOH	TFE	48
12	$AgBF_4$	PivOH	TFE	10
13	$AgNTf_2$	PivOH	TFE	86
14[c]	$AgSbF_6$	PivOH	TFE	46
15[d]	-	PivOH	TFE	20
16[e]	$AgSbF_6$	-	TFE	nd
17[f]	$AgSbF_6$	PivOH	TFE	nd

[a]Reaction conditions: **1a** (0.058 mmol), **2a** (0.069 mmol), [Cp*Co(CO)I_2] (5 mol %), silver salt (10 mol %), additive (1 equiv), solvent (0.1 M), at 60 °C for 12 h. [b]isolated yield. [c]at rt. [d]without silver salt. [e]without acid additive. [f]in absence of cobalt catalyst. nd = not detected.

With the unsubstituted 2*H*-[1,2'-bipyridin]-2-ones giving excellent yield (94%) of **3aa** (Scheme-3.2), we continued exploring the substrate scope with the same optimized conditions. Halogen substituted at C(3)-position of 2*H*-[1,2'-bipyridin]-2-ones (-Cl, -Br)

were found to be compatible, and produced the desired product in very good yields

Scheme 3.2: Scope for the Synthesis of Alkenylated Derivatives[a]

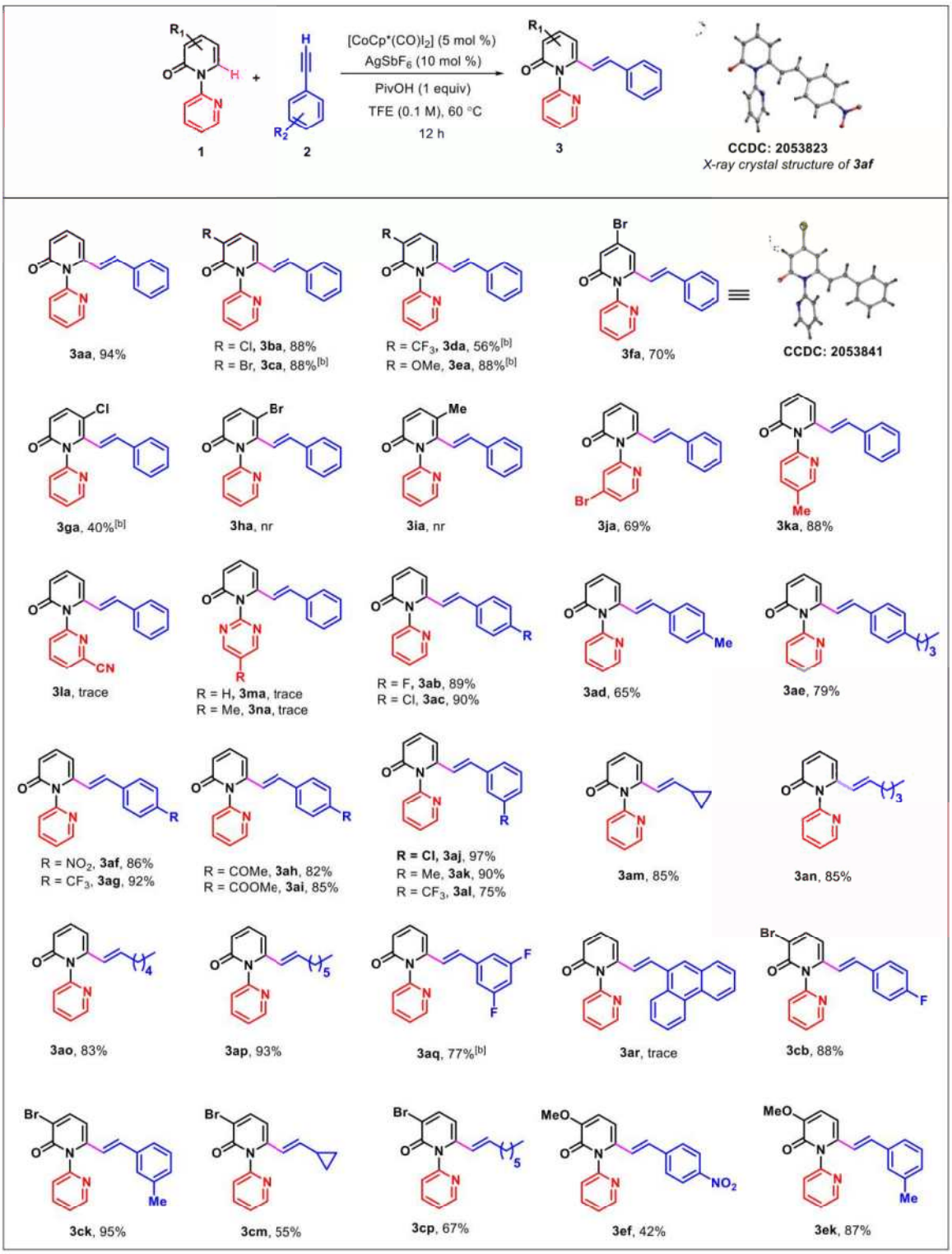

[a]Reaction conditions: **1a** (1.0 equiv), **2a** (1.2 equiv), [Cp*Co(CO)I_2] (5 mol %), $AgSbF_6$ (10 mol %), PivOH (1 equiv), TFE (0.1 M w.r.t. **1a**), 60 °C for 12 h, [b]reaction at 120 °C.

(Scheme-3.2, **3ba**, **3ca**). The 2*H*-[1,2'-bipyridin]-2-ones with electron-withdrawing group at the 3-position (-CF_3) furnished 56% yield of the corresponding product (Scheme-3.2, **3da**), whereas, electron-donating group (-OMe) at the C(3)-position gave 88% yield of the product (Scheme-3.2, **3ea**). Bromo (-Br) substituent at the C(4)-position did not alter the reactivity (Scheme-3.2, **3fa).** The structure of **3fa** was confirmed by single-crystal X-ray analysis. Chloro (-Cl group) substituent at C(5)-position gave the desired product (Scheme-3.2, **3ga)** in 40% yield. Sterically demanding substituent (-Br, -Me) at 5-position did not give any product even at high temperature, it might be due to steric hindrance of the –Br group and -Me group near to the reaction site (Scheme-3.2, **3ha, 3ia).** Similarly, different substituent on the pyridine ring were also examined, all the pyridine derivatives (4-Br, 5-Me) that were examined led to the formation of alkenylated products **3ja**, **3ka** in 69% and 88% yield respectively. The introduction of a -CN group at the C6-position of the pyridine gave only trace amount of the desired product. This might be due to electron withdrawing nature of -CN group decreasing the electron density on the nitrogen atom of pyridine ring which chelates with metal. Instead of pyridine, other chelating groups like pyrimidine, 5-Me substituted pyrimidine were also studied, which gave trace amount of desired product. We further studied the scope of terminal alkynes **2**. The alkynes with halogen groups such as -F and -Cl at the para position furnished the corresponding alkenylated product with excellent yields (Scheme-3.2, **3ab, 3ac**). Phenylacetylene with electron donating group (*p*-Me, *p*-^{n}butyl) also gave the alkenylated product (Scheme-3.2, **3ad, 3ae**) in good yield. Phenylacetylene with electron withdrawing substituents (*p*-NO_2, *p*-CF_3, *p*-COMe, *p*-COOMe) also underwent alkenylation and produced excellent yields (Scheme-3.2, **3af, 3ag, 3ah, 3ai**). The structure of **3af** was confirmed by single-crystal X-ray analysis. The *meta* substituted (*m*-Cl, *m*-Me, *m*-CF_3) phenyl acetylene also gave expected product in good to excellent yields (Scheme-3.2, **3aj, 3ak, 3al)**. In addition, aliphatic alkyne is also

compatible with the reaction conditions, affording the alkenylated products in good yields (Scheme-3.2, **3am, 3an, 3ao, 3ap**). Notably, alkyne bearing the strained cyclopropyl ring (**3am**) was also compatible under the reaction condition. Then, we turned our attention towards disubstituted phenyl acetylenes, *bis*-F substituted phenyl acetylene forming the corresponding alkenylated product in good yields (Scheme-3.2, **3aq**). Unfortunately, with 9-ethynylphenanthrene, only trace amount of alkenylated product was obtained (Scheme-3.2, **3ar**). We further extended the scope of this reaction with substitutions on both 2-pyridone **1** and aryl/aliphatic alkyne **2**. It is encouraging to note that C(3)-Br substituted 2*H*-[1,2'-bipyridin]-2-ones reacted with different substituted aromatic and aliphatic alkynes resulting in good to excellent yields of desired products (Scheme-3.2, **3cb**, **3ck**, **3cm** and **3cp**). 2*H*-[1,2'-bipyridin]-2-ones bearing a (-OMe) group at the C-3 position also provided the alkenylated product in good yields (Scheme-3.2, **3ef** and **3ek**). Overall, this methodology was found very general and compatible with a wide variety of substrate combinations.

To show the synthetic applicability of this methodology, a 1 mmol scale reaction was performed **3aa** was obtained in good yield. As shown in Scheme-3.3a, **3aa** can be hydrogenated at room temperature to obtained the saturated analogue piperidin-2-one **4** in 75% yield. Pyridine directing group can be easily removed from the alkenylated product **3aa** by using the reagent combination MeOTf and $NaBH_4$ to form the C-6-alkenylated 2-pyridone products **5**, **6** ,**7** in 65%, 59%, 72% yield respectively (Scheme-3.3b).[22] Several control experiments were performed to understand the reaction mechanism. H/D exchange reaction was performed under standard reaction condition along with 10 equivalents of methanol-d^4 in the absence of coupling partner (Scheme-3.3c). A 10% deuterium incorporation was observed in 30 minutes indicating the reversibility of C-H activation step. The competitive and parallel experiment (Scheme-3.3d) showed that **1a** reacts slightly

Scheme 3.3: Synthetic Utility and Mechanistic Studies

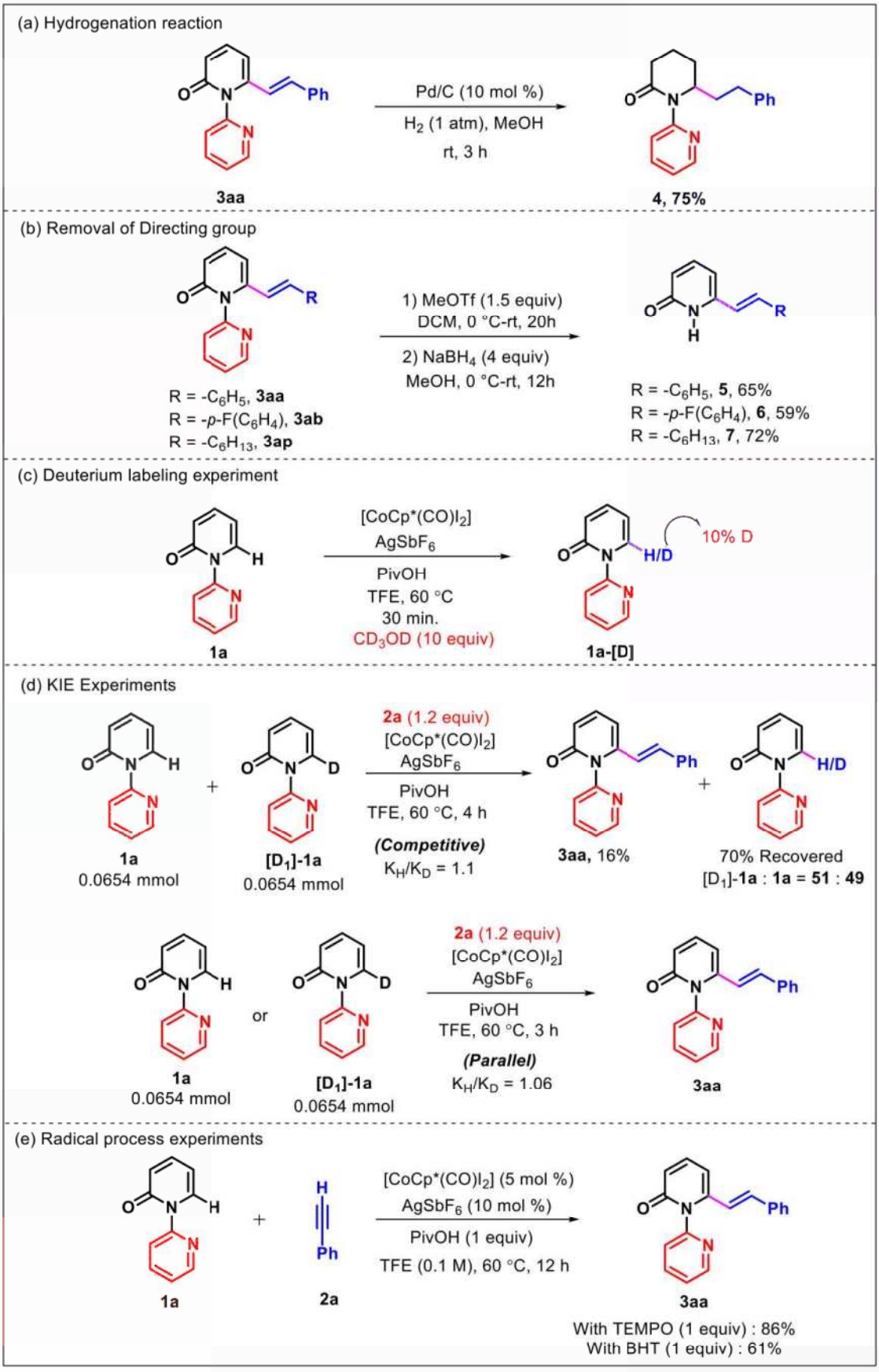

faster than deuterio-**1a**. This value suggesting that the C-H bond cleavage might not be involved in the rate determining step.[18] To understand whether this reaction goes by radical or ionic mechanism a radical quench experiments were conducted using radical scavengers such as 2,2,6,6-tetramethylpiperidinyloxy (TEMPO) and 3,5-di-tert-4-butylhydroxytoluene (BHT). In both the cases, yield of the product **3aa** (86% and 61%) did not diminish significantly, which indicates an ionic pathway (Scheme-3.3e). We have also detected two cationic intermediates (**B** and **D**) through high resolution mass spectrometry (HRMS) (refer to see page no. 107).

On the basis of the above mechanistic studies, and previous literature reports,[19] we propose a plausible reaction mechanism as follows (Scheme-3.4). Initially [CoCp*(CO)I_2] gets

Scheme 3.4: Plausible Mechanism

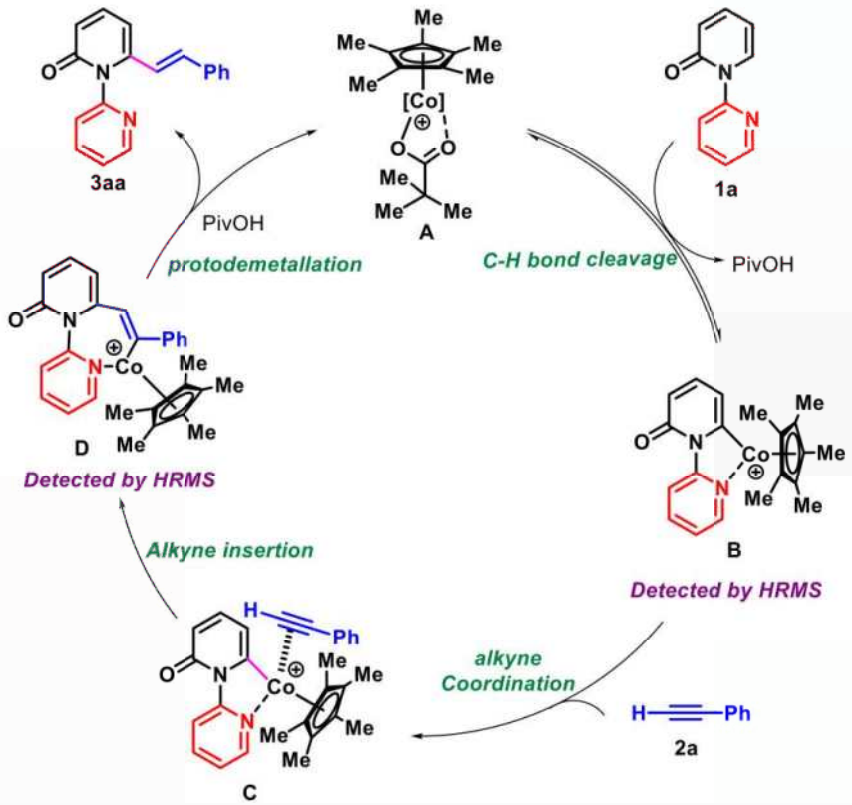

converted to cationic complex **A** in the presence of $AgSbF_6$ and PivOH. Coordination to nitrogen atom of the pyridine ring in **1a** followed by reversible concerted metallation

deprotonation leads to the cobaltacycle **B**. Coordination of alkyne **2a** to the cobaltacycle **B** gives intermediate **C**, then subsequent insertion of the alkyne in to the Co-C bond of intermediate **C** affords a seven membered cobaltacycle **D**. The intermediate **D** undergoes protodemetallation to give alkenylated product **3aa** and regenerates the catalytically active species **A**.

3.4 CONCLUSION

In conclusion, we have developed a cost-effective Co(III)-catalyzed C(6)-H alkenylation of 2-pyridones by using terminal alkyne with high regioselectivity. Under mild conditions, this methodology produced alkenylated compounds with good functional group tolerance. As compared to previous approaches, this methodology is significantly atom economical. This methodology opens the door for C-(6) alkenylation of 2-pyridones.

3.5 EXPERIMENTAL SECTION

Reactions were performed using borosil sealed tube vial under N_2 atmosphere. Column chromatography was done by using 230-400 mesh silica gel of Acme synthetic chemicals company. A gradient elution was performed by using distilled petroleum ether and EtOAc. Merck TLC Silica gel 60 F254 aluminium plates were used. TLC plates detected under UV light at 254 nm and vanillin. ^{1}H NMR, ^{13}C NMR and ^{19}F NMR were recorded on Bruker AV 400 and 700 MHz spectrometer using $CDCl_3$ as the deuterated solvent.[20] Multiplicity (s = singlet, d = doublet, t = triplet, q = quartet, quint = quintet, m = multiplet, dd = doublet of doublet, br = broad signal), integration, and coupling constants (*J*) in hertz (Hz). HRMS signal analysis was performed using micro TOF Q-II mass spectrometer. Reagents and starting materials were purchased from Sigma Aldrich, TCI, Avra, Spectrochem and other commercially available sources, used without further purification unless otherwise noted. All 2-pyridones were prepared according to the reported literature procedure.[21]

3.5.1 Representative Procedure for the Synthesis of 2*H*-[1,2'-bipyridin]-2-ones.[21]

Substrates 2*H*-[1,2'-bipyridin]-2-ones were prepared according to the reported procedures.[21] All substrates **1** (except **1e, 1j, 1l, 1n**) are known compounds and their spectral data were in agreement with the corresponding literature values. To a mixture of 2-hydroxypyridine (1 equiv), copper (I) iodide (0.05 equiv), and potassium phosphate (2 equiv) in toluene (0.75 M) were added *N*, *N'*-dimethylethylenediamine (0.1 equiv) and 2-bromopyridine (2 equiv) in round bottom flask and the resulting mixture was stirred at 120 ºC for 20 h under N_2. It was allowed to cool to room temperature and then quenched with water. A small amount of ethylenediamine (2.5 M) was added to dissolve the residual copper salts into the aqueous phase. The aqueous layers were extracted with EtOAc several times. The combined organic layers were dried over anhydrous Na_2SO_4 and the solvent was evaporated under reduced pressure. The product was purified by silica gel column chromatography using EtOAc/DCM (v/v, 1/1) afforded 2*H*-[1,2'-bipyridin]-2-one in 55% to 75% yield.

3.5.2 Representative Procedure for the Synthesis of (*E*)-6-styryl-2*H*-[1,2'-bipyridin]-2-one.

An oven-dried Schlenk tube equipped with a magnetic stirrer bar was charged with [Cp*Co(CO)I_2] (0.05 equiv) and pivalic acid (1 equiv). Subsequently 2*H*-[1,2'-bipyridin]-2-one **1** (1 equiv), terminal alkyne **2** (1.2 equiv), $AgSbF_6$ (0.1 equiv) followed by TFE (0.1 M) were added under N_2 atmosphere. The reaction mixture was vigorously stirred (750 rpm) in a preheated aluminum block at 60 ºC for 12 h. After 12 h (completion of reaction as monitored by TLC analysis), the reaction mixture was cooled to room temperature and diluted with DCM and passed through a short pad of celite, the solvent was evaporated under reduced pressure and the residue was purified by column chromatography using EtOAc/DCM (1:1) mixture on silica gel to give the pure product **3**.

3.5.3 Experimental characterization data of 2*H*-[1,2'-bipyridin]-2-one:

3-Methoxy-2*H*-[1,2'-bipyridin]-2-one (1e):

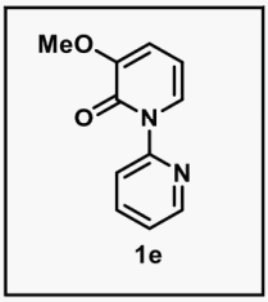

1e

Physical state: brown liquid (80 mg for 0.791 mmol scale, 50% yield). R_f: 0.45 (50 % EtOAc/DCM). ^{1}H NMR (400 MHz, $CDCl_3$): δ 8.55 (dd, J = 4.0, 0.8 Hz, 1H), 7.94 (d, J = 8.4 Hz, 1H), 7.84 (td, J = 7.2, 1.6 Hz, 1H), 7.50 (dd, J = 7.2, 1.6 Hz, 1H), 7.33–7.30 (m, 1H), 6.67 (dd, J = 7.6, 1.6 Hz, 1H), 6.24 (t, J = 7.2 Hz, 1H), 3.86 (s, 3H). ^{13}C{^{1}H} NMR (100 MHz, $CDCl_3$): δ 158.2, 152.2, 150.8, 149.1, 138.1, 127.2, 123.4, 121.9, 112.7, 105.4, 56.3. IR (KBr, cm^{-1}): 2843, 1661, 1610, 1249, 1285. HRMS (ESI) m/z: $[M + H]^+$ calcd for $C_{11}H_{11}N_2O_2$, 203.0815; found 203.0816.

4'-Bromo-2*H*-[1,2'-bipyridin]-2-one (1j):

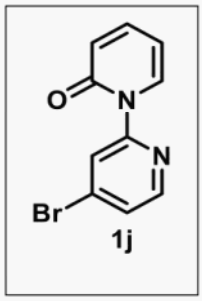

1j

Physical state: colourless liquid (130 mg for 1.052 mmol scale, 50% yield). R_f: 0.7 (50 % EtOAc/Hexane). ^{1}H NMR (400 MHz, $CDCl_3$): δ 8.37 (d, J = 5.2 Hz, 1H), 8.22 (d, J = 1.6 Hz, 1H), 7.87 (dd, J = 7.2, 1.6 Hz, 1H), 7.47 (dd, J = 5.6, 1.6 Hz, 1H), 7.41–7.37 (m, 1H), 6.63 (d, J = 9.2 Hz, 1H), 6.29 (td, J = 6.8, 1.2 Hz, 1H). ^{13}C{^{1}H} NMR (100 MHz, $CDCl_3$): δ 162.2, 152.6, 149.4, 140.6, 135.8, 133.9, 126.7, 124.9, 122.4, 106.7. IR (KBr, cm^{-1}): 3051, 1666, 1602, 756. HRMS (ESI) m/z: $[M + H]^+$ calcd for $C_{10}H_8BrN_2O$, 250.9815; found 250.9813.

2-Oxo-2*H*-[1,2'-bipyridine]-6'-carbonitrile (1l):

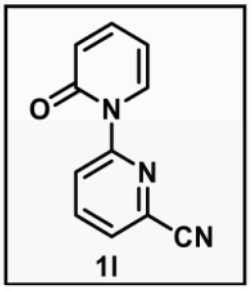

1l

Physical state: white solid (146 mg for 1.052 mmol scale, 71% yield). mp: 185–187 °C. R_f: 0.2 (50 % EtOAc/Hexane). ^{1}H NMR (400 MHz, $CDCl_3$): δ 8.35 (dd, J = 8.4, 0.8 Hz, 1H), 8.00–7.95 (m, 2H), 7.72 (dd, J = 7.2, 0.8 Hz, 1H), 7.45– 7.40 (m, 1H), 6.65 (d, J = 9.2 Hz, 1H),

6.35 (td, J = 7.2, 1.2 Hz, 1H). $^{13}C\{^1H\}$ NMR (100 MHz, $CDCl_3$): δ 162.3, 153.0, 141.1, 139.1, 135.4, 132.8, 127.9, 125.5, 122.7, 116.7, 107.3. IR (KBr, cm^{-1}): 3081, 2235, 1675, 1602, 1447. HRMS (ESI) m/z: $[M + H]^+$ calcd for $C_{11}H_8N_3O$, 198.0662; found 198.0656.

1-(5-Methylpyrimidin-2-yl)pyridin-2(1*H*)-one (1n):

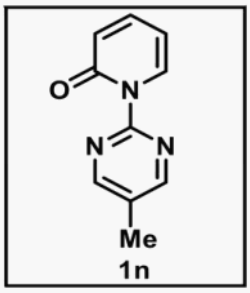

1n

Physical state: white solid (66 mg for 1.58 mmol scale, 22% yield). mp: 84–86 °C. R_f: 0.6 (50 % EtOAc/Hexane). ^1H NMR (400 MHz, $CDCl_3$): δ 8.44 (s, 2H), 8.34 (dd, J = 5.2, 1.2 Hz, 1H), 7.80 (td, J = 8.0, 2.0 Hz, 1H), 7.18–7.15 (m, 1H), 7.12 (d, J = 8.0 Hz, 1H), 2.29 (s, 3H).$^{13}C\{^1H\}$ NMR (100 MHz, $CDCl_3$): δ 163.2, 161.3, 160.0, 148.6, 140.1, 126.7, 121.1, 115.0, 15.0. IR (KBr, cm^{-1}): 2927, 1589, 1413, 1238. HRMS (ESI) m/z: $[M + Na]^+$ calcd for $C_{10}H_9N_3ONa$, 210.0638; found 210.0631.

Experimental characterization data of products:

(*E*)-6-Styryl-2*H*-[1,2'-bipyridin]-2-one (3aa):[6b]

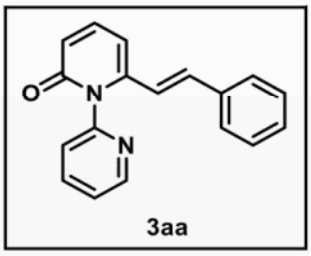

3aa

Physical state: yellow solid (30 mg for 0.116 mmol scale, 94% yield). mp: 102–110 °C. R_f: 0.2 (50% EtOAc/DCM). ^1H NMR (400 MHz, $CDCl_3$): δ 8.62 (ddd, J = 5.2, 2.0, 0.8 Hz, 1H), 7.84 (td, J = 7.6, 2.0 Hz, 1H), 7.38–7.28 (m, 3H), 7.20–7.17 (m, 3H), 7.12–7.10 (m, 2H), 6.95 (d, J = 16.0 Hz, 1H), 6.53 (t, J = 8.4 Hz, 2H), 6.11 (d, J = 16.0 Hz, 1H). $^{13}C\{^1H\}$ NMR (100 MHz, $CDCl_3$): δ 163.5, 152.0, 150.3, 146.7, 140.3, 139.1, 136.0, 134.6, 129.3, 129.1, 127.3, 124.5, 124.4, 121.2, 120.1, 104.3. IR (KBr, cm^{-1}): 2925, 1673, 1579, 1149.

(*E*)-3-Chloro-6-styryl-2*H*-[1,2'-bipyridin]-2-one (3ba):[6b]

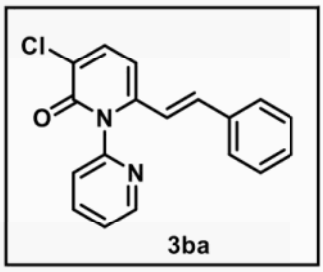

3ba

Physical state: yellow liquid (27 mg for 0.099 mmol scale, 88% yield). R_f: 0.7 (50% EtOAc/DCM). ^{1}H NMR ($CDCl_3$, 400 MHz): δ 8.69 (dd, J = 4.8, 1.6 Hz, 1H), 7.92 (td, J = 7.6, 2.0 Hz, 1H), 7.61 (d, J = 7.6 Hz, 1H), 7.44 (dd, J = 7.2, 4.8 Hz, 1H), 7.39 (d, J = 7.6 Hz, 1H), 7.27–7.26 (m, 2H), 7.19–7.17 (m, 3H), 7.01 (d, J = 16.0 Hz, 1H), 6.55 (d, J = 7.6 Hz, 1H), 6.16 (d, J = 16.0 Hz, 1H). ^{13}C{^{1}H} NMR ($CDCl_3$, 100 MHz): δ 159.7, 151.8, 150.4, 145.6, 139.2, 138.2, 135.9, 135.1, 129.5, 129.2, 127.4, 125.4, 124.7, 124.4, 120.7, 103.6. IR (KBr, cm^{-1}): 2929, 1661, 1614, 1064, 748.

(*E*)-3-Bromo-6-styryl-2*H*-[1,2'-bipyridin]-2-one (3ca):[6b]

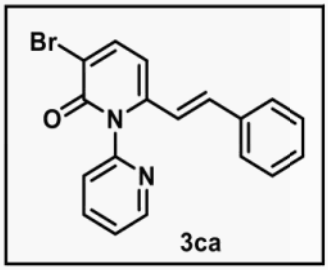

3ca

Physical state: yellow solid (37 mg for 0.118 mmol scale, 88% yield). mp: 146–149 °C. R_f: 0.5 (50% EtOAc/DCM). ^{1}H NMR ($CDCl_3$, 400 MHz): δ 8.67 (dd, J = 4.4, 0.8 Hz, 1H), 7.91 (td, J = 7.6, 2.0 Hz, 1H), 7.81 (d, J = 7.6 Hz, 1H), 7.45–7.42 (m, 1H), 7.37 (d, J = 8.0 Hz, 1H), 7.27–7.26 (m, 2H), 7.19–7.17 (m, 3H), 7.04 (d, J = 16.0 Hz, 1H), 6.50 (d, J = 8.0 Hz, 1H), 6.13 (d, J = 16.0 Hz, 1H). ^{13}C{^{1}H} NMR ($CDCl_3$, 100 MHz): δ 159.5, 151.6, 150.2, 146.3, 142.1, 139.2, 135.7, 135.1, 129.4, 129.1, 127.3, 124.7, 124.2, 120.4, 115.1, 104.1. IR (KBr, cm^{-1}): 3055, 1657, 1614, 1434, 692.

(*E*)-6-Styryl-3-(trifluoromethyl)-2*H*-[1,2'-bipyridin]-2-one (3da):[6b]

Physical state: yellow solid (24 mg for 0.125 mmol scale, 56% yield). mp: 152–154 °C. R_f: 0.7 (50% EtOAc/DCM). ^{1}H NMR ($CDCl_3$, 400 MHz): δ 8.70 (dd, J = 4.4, 1.2 Hz, 1H), 7.94 (td, J = 8.0, 2.0 Hz, 1H), 7.83 (d, J = 7.6 Hz, 1H), 7.46 (dd, J = 7.2, 5.2 Hz, 1H), 7.43 (d, J = 8.0 Hz, 1H), 7.31–7.29 (m, 3H), 7.23–7.20 (m, 2H), 7.15 (d, J = 16.0 Hz, 1H), 6.65 (d, J

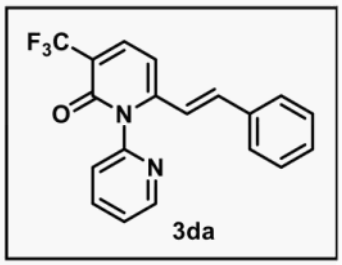

= 7.6 Hz, 1H), 6.20 (d, J = 15.6 Hz, 1H). $^{13}C\{^1H\}$ NMR ($CDCl_3$, 100 MHz): δ 159.4, 150.9, 150.8, 150.5, 139.4 (q, $J_{C\text{-}F}$ = 4.8 Hz), 139.2, 137.3, 135.3, 130.0, 129.2, 127.6, 124.9, 124.5, 123.1 (q, $J_{C\text{-}F}$ = 269.5 Hz), 120.1, 119 (q, $J_{C\text{-}F}$ = 31.3 Hz), 102.1. $^{19}F\{^1H\}$ NMR ($CDCl_3$, 376 MHz): δ -65.4. IR (KBr, cm^{-1}): 3011, 1682, 1548, 1409, 1320.

(*E*)-3-Methoxy-6-styryl-2*H*-[1,2'-bipyridin]-2-one (3ea):

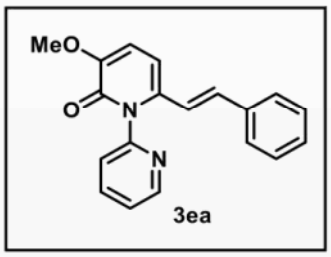

Physical state: brown liquid (40 mg for 0.149 mmol scale, 88% yield). R_f: 0.2 (50% EtOAc/DCM). ^1H NMR ($CDCl_3$, 400 MHz): δ 8.67 (dd, J = 4.8, 0.8 Hz, 1H), 7.90 (td, J = 7.6, 2.0 Hz, 1H), 7.43–7.38 (m, 2H), 7.27–7.22 (m, 3H), 7.17–7.15 (m, 2H), 6.87 (d, J = 16.0 Hz, 1H), 6.74 (d, J = 8.0 Hz, 1H), 6.54 (d, J = 8.0 Hz, 1H), 6.13 (d, J = 16.0 Hz, 1H), 3.86 (s, 3H). $^{13}C\{^1H\}$ NMR ($CDCl_3$, 100 MHz): δ 158.7, 151.8, 150.1, 149.6, 139.1, 137.7, 136.4, 132.0, 128.9, 128.7, 127.0, 124.5, 124.4, 121.1, 113.4, 103.6, 56.3. IR (KBr, cm^{-1}): 2937, 1660, 1601, 1434, 1266. HRMS (ESI) m/z: $[M + H]^+$ calcd for $C_{19}H_{17}N_2O_2$, 305.1285; found 305.1287.

(*E*)-4-Bromo-6-styryl-2*H*-[1,2'-bipyridin]-2-one (3fa):[6b]

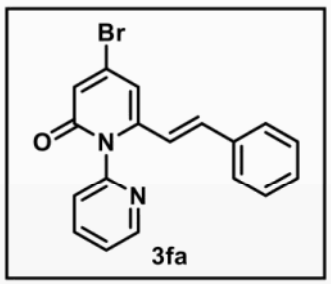

Physical state: yellow solid (28 mg for 0.113 mmol scale, 70% yield). mp: 225–228 °C. R_f: 0.2 (50% EtOAc/Hexane). ^1H NMR ($CDCl_3$, 400 MHz): δ 8.69 (dd, J = 4.8, 1.2 Hz, 1H), 7.92 (td, J = 7.6, 1.6 Hz, 1H), 7.46–7.43 (m, 1H), 7.37 (d, J = 8.0 Hz, 1H), 7.29–7.26 (m, 3H), 7.21–7.18 (m, 2H), 7.06 (d, J = 16.0 Hz, 1H), 6.85 (d, J = 2.0 Hz, 1H), 6.75 (d, J = 2.0 Hz, 1H), 6.13 (d, J = 16.0 Hz, 1H). $^{13}C\{^1H\}$ NMR ($CDCl_3$, 100 MHz): δ 162.3, 151.3, 150.4, 146.6, 139.3, 136.8, 136.1, 135.5,

129.7, 129.2, 127.5, 124.7, 124.4, 121.7, 119.8, 108.4. IR (KBr, cm^{-1}): 2924, 1650, 1515, 1433, 694.

(*E*)-5-Chloro-6-styryl-2*H*-[1,2'-bipyridin]-2-one (3ga):[6b]

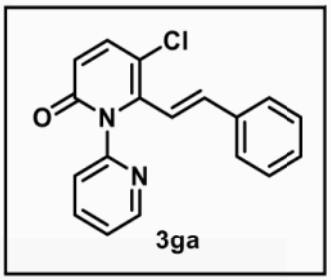

3ga

Physical state: yellow liquid (12 mg for 0.097 mmol scale, 40% yield). R_f: 0.3 (50% EtOAc/DCM). ^1H NMR ($CDCl_3$, 400 MHz): δ 8.65 (d, J = 3.6 Hz, 1H), 7.88 (t, J = 7.6 Hz, 1H), 7.48 (d, J = 9.6 Hz, 1H), 7.41–7.35 (m, 2H), 7.28–7.26 (m, 3H), 7.16–7.14 (m, 2H), 6.77 (d, J = 16.8 Hz, 1H), 6.60 (d, J = 9.6 Hz, 1H), 6.32 (d, J = 16.8 Hz, 1H). $^{13}C\{^1H\}$ NMR ($CDCl_3$, 100 MHz): δ 162.4, 150.3, 142.6, 139.7, 139.1, 129.5, 129.1, 128.9, 128.6, 127.1, 124.6, 124.5, 123.7, 121.6, 121.1, 118.8. IR (KBr, cm^{-1}): 2923, 1674, 1521, 1432, 821.

(*E*)-4'-Bromo-6-styryl-2*H*-[1,2'-bipyridin]-2-one (3ja):

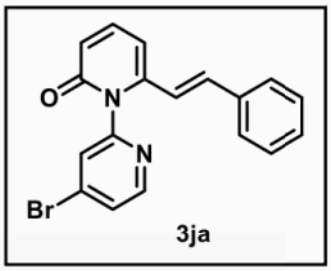

3ja

Physical state: yellow liquid (29 mg for 0.12 mmol scale, 69% yield). R_f: 0.2 (50% EtOAc/Hexane). ^1H NMR ($CDCl_3$, 700 MHz): δ 8.51 (d, J = 4.2 Hz, 1H), 7.61–7.59 (m, 2H), 7.44 (t, J = 7.7 Hz, 1H), 7.31–7.28 (m, 3H), 7.22 (d, J = 7.7 Hz, 2H), 7.05 (d, J = 15.4 Hz, 1H), 6.59 (d, J = 7.0 Hz, 2H), 6.19 (d, J = 16.1 Hz, 1H). $^{13}C\{^1H\}$ NMR ($CDCl_3$, 175 MHz): δ 163.4, 152.7, 150.6, 146.5, 140.5, 135.8, 135.1, 135.0, 129.5, 129.2, 128.1, 128.0, 127.4, 120.8, 120.1, 104.5. IR (KBr, cm^{-1}): 3053, 1661, 1531, 1388, 795. HRMS (ESI) m/z: $[M + Na]^+$ calcd for $C_{18}H_{13}BrN_2ONa$, 375.0103; found 375.0100.

(*E*)-5'-Methyl-6-styryl-2*H*-[1,2'-bipyridin]-2-one (3ka):

Physical state: yellow liquid (27 mg for 0.107 mmol scale, 88% yield). R_f: 0.1 (50% EtOAc/Hexane). ^1H NMR ($CDCl_3$, 700 MHz): δ 8.50 (d, J = 1.4 Hz, 1H), 7.71 (dd, J = 8.4, 2.1 Hz, 1H), 7.43 (dd, J = 9.1, 7.0 Hz, 1H), 7.29–7.26 (m, 4H), 7.21 (d, J = 7.0 Hz, 2H),

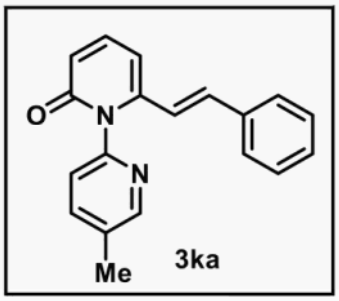

3ka

7.03 (d, J = 16.1 Hz, 1H), 6.59 (dd, J = 18.2, 9.8 Hz, 2H), 6.23 (d, J = 15.4 Hz, 1H), 2.43 (s, 3H). $^{13}C\{^1H\}$ NMR ($CDCl_3$, 100 MHz): δ 163.7, 150.6, 149.5, 146.8, 140.2, 139.7, 136.1, 134.6, 134.3, 129.2, 129.1, 127.4, 123.7, 121.3, 120.1, 104.2, 18.5. IR (KBr, cm^{-1}): 2924, 1659, 1532, 1477. HRMS (ESI) m/z: $[M + H]^+$ calcd for $C_{19}H_{17}N_2O$, 289.1335; found 289.1347.

(*E*)-6-(4-Fluorostyryl)-2*H*-[1,2'-bipyridin]-2-one (3ab):[6b]

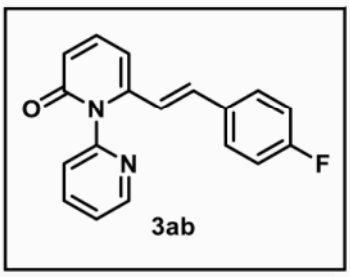

3ab

Physical state: yellow solid (30 mg for 0.115 mmol scale, 89% yield). mp: 165–167 °C. R_f: 0.18 (50% EtOAc/DCM). ^1H NMR (400 MHz, $CDCl_3$): δ 8.60 (dd, J = 4.8, 0.8 Hz, 1H), 7.82 (td, J = 8.0, 2.0 Hz, 1H), 7.35–7.29 (m, 3H), 7.08–7.04 (m,2H), 6.90–6.84 (m, 3H), 6.49 (dd, J = 16.0, 9.2 Hz, 2H), 6.00 (d, J = 16.0 Hz,1H). $^{13}C\{^1H\}$ NMR (100 MHz, $CDCl_3$): δ 163.3 (d, $J_{C\text{-}F}$ = 248.6 Hz), 163.5, 152.0, 150.3, 146.4, 140.2, 139.1, 133.3, 132.2 (d, $J_{C\text{-}F}$ = 2.8 Hz), 129.0 (d, $J_{C\text{-}F}$ = 8.0 Hz), 128.6, 124.5 (d, $J_{C\text{-}F}$ = 4.4 Hz), 120.9, 120.1, 116.1 (d, $J_{C\text{-}F}$ = 21.8 Hz), 104.2. $^{19}F\{^1H\}$ NMR (CDCl3, 376 MHz): δ -111.6. IR (KBr, cm^{-1}): 2986, 1667, 1532, 1225, 1435.

(*E*)-6-(4-Chlorostyryl)-2*H*-[1,2'-bipyridin]-2-one (3ac):[6b]

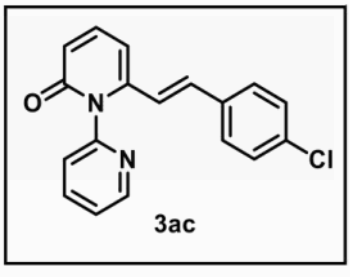

3ac

Physical state: yellow solid (30 mg for 0.108 mmol scale, 90% yield). mp: 189–190 °C. R_f: 0.19 (50% EtOAc/Hexane). ^1H NMR (400 MHz, $CDCl_3$): δ 8.70 (d, J = 4.0 Hz, 1H), 7.92 (t, J = 7.6 Hz, 1H), 7.46–7.39 (m, 3H), 7.23 (d, J = 8.4 Hz, 2H), 7.11 (d, J = 8.4 Hz, 2H), 6.96 (d, J = 16.0 Hz, 1H), 6.64–6.58 (m, 2H), 6.15 (d, J = 16.0 Hz, 1H). $^{13}C\{^1H\}$ NMR (100 MHz, $CDCl_3$): δ 163.6, 151.8, 150.3, 146.3, 140.3, 139.2, 135.0, 134.4, 133.3, 129.3, 128.4, 124.5, 121.7, 120.3, 104.5. IR (KBr, cm^{-1}): 2982, 1651, 1532, 1086, 808.

(*E*)-6-(4-Methylstyryl)-2*H*-[1,2'-bipyridin]-2-one (3ad):[6b]

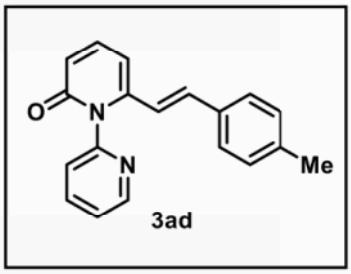

3ad

Physical state: yellow solid (22 mg for 0.117 mmol scale, 65% yield). mp: 108–110 °C. R_f: 0.2 (50% EtOAc/DCM). ^{1}H NMR (400 MHz, $CDCl_3$): δ 8.70 (d, J = 4.0 Hz, 1H), 7.91 (td, J = 7.6, 1.6 Hz, 1H), 7.45–7.38 (m, 3H), 7.08 (s, 4H), 7.00 (d, J = 16.0 Hz, 1H), 6.59 (t, J = 8.4 Hz, 2H), 6.12 (d, J = 16.0 Hz, 1H), 2.31 (s, 3H). ^{13}C{^{1}H} NMR (100 MHz, $CDCl_3$): δ 163.6, 152.1, 150.3, 146.9, 140.3, 139.5, 139.1, 134.7, 133.2, 129.8, 127.3, 124.5, 124.4, 120.1, 119.8, 104.1, 21.6. IR (KBr, cm^{-1}): 2930, 1661, 1532, 1433, 1466.

(*E*)-6-(4-Butylstyryl)-2*H*-[1,2'-bipyridin]-2-one (3ae):

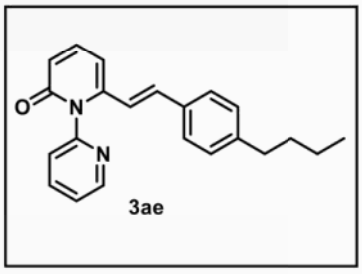

3ae

Physical state: yellow liquid (30 mg for 0.115 mmol scale, 79% yield). R_f: 0.19 (50% EtOAc/DCM). ^{1}H NMR (400 MHz, $CDCl_3$): δ 8.70 (dd, J = 4.8, 1.6 Hz, 1H), 7.91 (td, J = 7.6, 1.6 Hz, 1H), 7.45–7.36 (m, 3H), 7.09 (d, J = 2.8 Hz, 4H), 7.00 (d, J = 16.0 Hz, 1H), 6.59 (t, J = 8.4 Hz, 2H), 6.13 (d, J = 16.0 Hz, 1H), 2.56 (t, J = 7.6 Hz, 2H), 1.58–1.51 (m, 2H), 1.36-1.29 (m, 2H), 0.90 (t, J = 7.2 Hz, 3H). ^{13}C{^{1}H} NMR (100 MHz, $CDCl_3$): δ 163.6, 152.2, 150.4, 146.9, 144.6, 140.3, 139.1, 134.7, 133.5, 129.2, 127.3, 124.5, 124.4, 120.2, 119.9, 104.1, 35.7, 33.7, 22.6, 14.2. IR (KBr, cm^{-1}): 2858, 1662, 1532, 1433. HRMS (ESI) m/z: $[M + Na]^+$ calcd for $C_{22}H_{22}N_2ONa$, 353.1624; found 353.1631.

(*E*)-6-(4-Nitrostyryl)-2*H*-[1,2'-bipyridin]-2-one (3af):[6b]

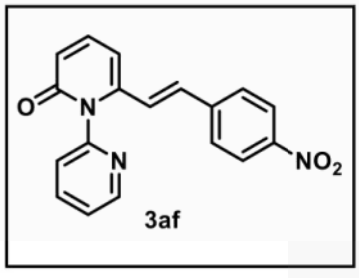

3af

Physical state: yellow solid (40 mg for 0.145 mmol scale, 86% yield). mp: 202–204 °C. R_f: 0.15 (50% EtOAc/DCM). ^{1}H NMR (400 MHz, $CDCl_3$): δ 8.70 (d, J = 4.8 Hz, 1H), 8.14 (d, J = 8.8 Hz, 2H), 7.96 (td, J = 7.6, 1.6 Hz, 1H), 7.49–7.44

(m, 3H), 7.32 (d, J = 8.4 Hz, 2H), 7.05 (d, J = 16.0 Hz, 1H), 6.66 (dd, J = 16.0, 9.2 Hz, 2H), 6.34 (d, J = 16.0 Hz, 1H). $^{13}C\{^1H\}$ NMR (100 MHz, $CDCl_3$): δ 163.3, 151.6, 150.3, 147.8, 145.4, 142.2, 140.1, 139.2, 131.7, 127.8, 125.4, 124.7, 124.6, 124.4, 121.4, 105.2. IR (KBr, cm^{-1}): 2926, 1686, 1530, 1341.

(*E*)-6-(4-(Trifluoromethyl)styryl)-2*H*-[1,2'-bipyridin]-2-one (3ag):[6b]

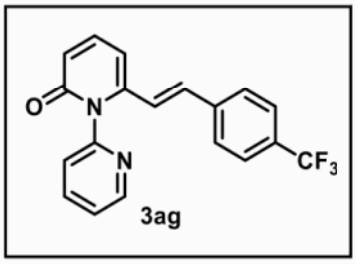

3ag

Physical state: yellow solid (32 mg for 0.101 mmol scale, 92% yield). mp: 65–70 °C. R_f: 0.2 (100% EtOAc). ^1H NMR (400 MHz, $CDCl_3$): δ 8.70 (d, J = 4.0 Hz, 1H), 7.93 (dt, J = 7.8, 1.2 Hz, 1H), 7.52 (d, J = 8.0 Hz, 2H), 7.47–7.41 (m, 3H), 7.29–7.26 (m, 2H), 7.03 (d, J = 16.0 Hz, 1H), 6.66–6.60 (m, 2H), 6.27 (d, J = 16.0 Hz, 1H). $^{13}C\{^1H\}$ NMR (100 MHz, $CDCl_3$): δ 163.4, 151.9, 150.4, 145.9, 140.1, 139.4, 139.2, 132.8, 130.8 (q, $J_{C\text{-}F}$ = 32.5 Hz), 127.4 (q, $J_{C\text{-}F}$ = 75.6 Hz), 127.4, 126.0 (q, $J_{C\text{-}F}$ = 3.6 Hz), 124.6, 124.2 (q, $J_{C\text{-}F}$ = 270.2 Hz), 123.7, 120.9, 104.8. $^{19}F\{^1H\}$ NMR (376 MHz, $CDCl_3$): δ -62.8. IR (KBr, cm^{-1}): 3055, 1666, 1532, 1324, 1110, 1067. HRMS (ESI) m/z: $[M + H]^+$ calcd for $C_{19}H_{14}F_3N_2O$, 343.1053; found 343.1042.

(*E*)-6-(4-Acetylstyryl)-2*H*-[1,2'-bipyridin]-2-one (3ah):[6b]

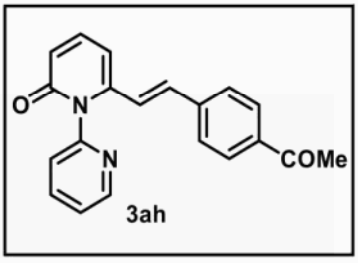

3ah

Physical state: yellow solid (28 mg for 0.108 mmol scale, 82% yield). mp: 193–196 °C. R_f: 0.15 (50% EtOAc/DCM). ^1H NMR (400 MHz, $CDCl_3$): δ 8.70 (d, J = 4.8 Hz, 1H), 7.95 (td, J = 7.6, 1.6 Hz, 1H), 7.86 (d, J = 8.0 Hz, 2H), 7.48–7.42 (m, 3H), 7.26 (d, J = 8.4 Hz, 2H), 7.05 (d, J = 16.0 Hz, 1H), 6.64 (dd, J = 9.2, 6.0 Hz, 2H), 6.29 (d, J = 16.0 Hz, 1H), 2.56 (s, 3H). $^{13}C\{^1H\}$ NMR (100 MHz, $CDCl_3$): δ 197.5, 163.4, 151.8, 150.3, 145.9, 140.4, 140.1, 139.1, 137.2, 133.1, 129.1, 127.3, 124.5, 124.5, 123.6, 120.8, 104.8, 26.9. IR (KBr, cm^{-1}): 2918, 1651, 1532, 1267.

(*E*)-Methyl 4-(2-(2-oxo-2*H*-[1,2'-bipyridin]-6-yl)vinyl)benzoate (3ai):[6b]

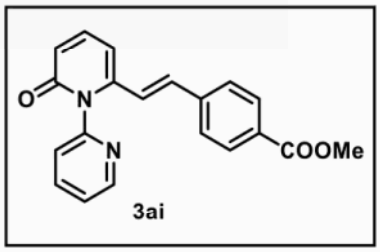

3ai

Physical state: pale green solid (33 mg for 0.116 mmol scale, 85% yield). mp: 126–133 °C. R_f: 0.1 (100% EtOAc). ^{1}H NMR (400 MHz, $CDCl_3$): δ 8.71 (d, J = 3.6 Hz, 1H), 7.96–7.92 (m, 3H), 7.47–7.41 (m, 3H), 7.24 (d, J = 8.0 Hz, 2H), 7.03 (d, J = 16.0 Hz, 1H), 6.66–6.61 (m, 2H), 6.28 (d, J = 16.0 Hz, 1H), 3.90 (s, 3H). ^{13}C{^{1}H} NMR (100 MHz, $CDCl_3$): δ 166.8, 163.4, 151.9, 150.4, 146.1, 140.3, 140.2, 139.2, 133.3, 130.5, 130.4, 127.2, 124.6, 123.6, 120.9, 104.8, 52.5. IR (KBr, cm^{-1}): 2922, 1715, 1661, 1535, 1435, 1288, 1108. HRMS (ESI) m/z: $[M + H]^+$ calcd for $C_{20}H_{17}N_2O_3$, 333.1234; found 333.1205.

(*E*)-6-(3-Chlorostyryl)-2*H*-[1,2' bipyridin]-2-one (3aj):

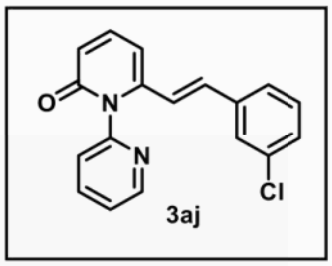

3aj

Physical state: yellow solid (35 mg for 0.116 mmol scale, 97% yield). mp: 165–172 °C. R_f: 0.25 (100% EtOAc). ^{1}H NMR (400 MHz, $CDCl_3$): δ 8.70 (d, J = 3.2 Hz, 1H), 7.94 (dt, J = 7.8, 1.6 Hz, 1H), 7.48–7.40 (m, 3H), 7.24–7.18 (m, 2H), 7.15 (s, 1H), 7.06 (td, J = 6.8, 1.6 Hz, 1H), 6.95 (d, J = 16.0 Hz, 1H), 6.65–6.59 (m, 2H), 6.18 (d, J = 15.6 Hz, 1H). ^{13}C{^{1}H} NMR (100 MHz, $CDCl_3$): δ 163.5, 151.9, 150.4, 146.1, 140.2, 139.2, 137.9, 135.1, 133.1, 130.3, 129.2, 127.2, 125.4, 124.6, 124.5, 122.6, 120.7, 104.7. IR (KBr, cm^{-1}): 3063, 2929, 1670, 1577, 1540, 1432, 794. HRMS (ESI) m/z: $[M + H]^+$ calcd for $C_{18}H_{14}ClN_2O$, 309.0789; found 309.0789.

(*E*)-6-(3-Methylstyryl)-2*H*-[1,2'-bipyridin]-2-one (3ak):

Physical state: yellow solid (30 mg for 0.115 mmol scale, 90% yield). mp: 122–125 °C. R_f: 0.12 (50% EtOAc/DCM). ^{1}H NMR (400 MHz, $CDCl_3$): δ 8.61 (d, J = 3.6 Hz, 1H), 7.83 (t, J = 7.6 Hz, 1H), 7.36–7.27 (m, 3H), 7.09–6.88 (m, 5H), 6.53–6.48 (m, 2H), 6.08 (d, J = 15.6 Hz, 1H), 2.20 (s, 3H). ^{13}C{^{1}H} NMR (100 MHz, $CDCl_3$): δ 163.5, 152.0, 150.3, 146.7,

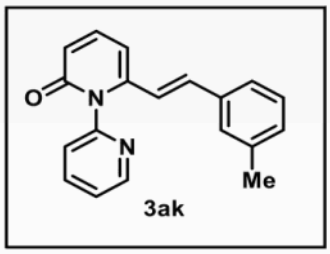

3ak

140.2, 139.1, 138.6, 135.9, 134.8, 130.0, 128.9, 128.2, 124.4, 124.4, 124.2, 120.9, 119.9, 104.2, 21.5. IR (KBr, cm^{-1}): 2965, 1660, 1579, 1531, 1433. HRMS (ESI) m/z: $[M + H]^+$ calcd for $C_{19}H_{17}N_2O$, 289.1335; found, 289.1330.

(*E*)-6-(3-(Trifluoromethyl)styryl)-2*H*-[1,2'-bipyridin]-2-one (3al):

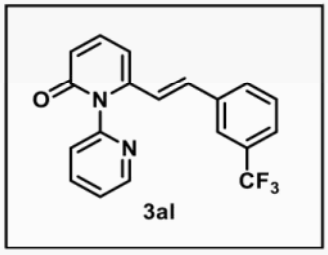

3al

Physical state: yellow solid (29 mg for 0.113 mmol scale, 75 % yield). mp: 171–174 °C. R_f: 0.1 (50% EtOAc/Hexane). ^1H NMR (400 MHz, $CDCl_3$): δ 8.70 (dd, J = 5.2, 1.2 Hz, 1H), 7.94 (td, J = 7.6, 2.0 Hz, 1H), 7.51–7.34 (m, 7H), 7.02 (d, J = 16.0 Hz, 1H), 6.64 (d, J = 9.2 Hz, 1H), 6.59 (d, J = 7.2 Hz, 1H), 6.25 (d, J = 16.0 Hz, 1H). $^{13}C\{^1H\}$ NMR (100 MHz, $CDCl_3$): δ 163.4, 151.9, 150.3, 146.0, 140.2, 139.2, 136.8, 132.9, 131.6 (q, $J_{C\text{-}F}$ = 32.0 Hz), 130.0, 129.6, 125.7, 124.6, 124.2, 124.1, 124.1 (q, $J_{C\text{-}F}$ = 271.0 Hz), 123.1, 120.8, 104.7. $^{19}F\{^1H\}$ NMR ($CDCl_3$, 376 MHz): δ -62.9. IR (KBr, cm^{-1}): 3011, 1651, 1535, 1337, 1111. HRMS (ESI) m/z: $[M + H]^+$ calcd for $C_{19}H_{14}F_3N_2O$, 343.1053; found 343.1032.

(*E*)-6-(2-Cyclopropylvinyl)-2*H*-[1,2'-bipyridin]-2-one (3am):

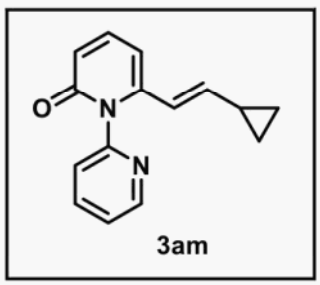

3am

Physical state: yellow liquid (23 mg for 0.113 mmol scale, 85% yield). R_f: 0.1 (50% EtOAc/DCM). ^1H NMR (400 MHz, $CDCl_3$): δ 8.69 (d, J = 4.4 Hz, 1H), 7.91 (td, J = 7.6, 1.6 Hz, 1H), 7.42 (dd, J = 7.2, 4.8 Hz, 1H), 7.37–7.33 (m, 2H), 6.51 (d, J = 9.2 Hz, 1H), 6.34 (d, J = 7.2 Hz, 1H), 5.69 (dd, J = 15.2, 9.2 Hz, 1H), 5.56 (d, J = 15.6 Hz, 1H), 1.33–1.25 (m, 1H), 0.80–0.75 (m, 2H), 0.45–0.41 (m, 2H). $^{13}C\{^1H\}$ NMR (100 MHz, $CDCl_3$): δ 163.6, 152.2, 150.2, 146.9, 142.6, 140.3, 139.0, 124.4, 124.3, 120.3, 118.8, 103.2, 15.2, 8.3. IR (KBr, cm^{-1}): 3005, 1652, 1575, 1532, 1433. HRMS (ESI) m/z: $[M + H]^+$ calcd for $C_{15}H_{15}N_2O$, 239.1179; found 239.1188.

(*E*)-6-(Hex-1-en-1-yl)-2*H*-[1,2'-bipyridin]-2-one (3an):

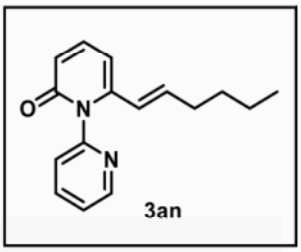

3an

Physical state: brown oil (25 mg for 0.115 mmol scale, 85% yield). R_f: 0.12 (50% EtOAc/DCM). ^{1}H NMR (400 MHz, $CDCl_3$): δ 8.67 (d, J = 4.0 Hz, 1H), 7.90 (td, J = 7.6, 1.6 Hz, 1H), 7.42-7.40 (m, 1H), 7.38–7.36 (m, 1H), 7.33 (d, J = 7.6 Hz, 1H), 6.55 (d, J = 9.2 Hz, 1H), 6.39 (d, J = 6.8 Hz, 1H), 6.23–6.15 (m, 1H), 5.50 (d, J = 15.2 Hz, 1H), 1.99 (dd, J = 13.2, 6.4 Hz, 2H), 1.29–1.25 (m, 2H), 1.22–1.17 (m, 2H), 0.81 (t, J = 7.2 Hz, 3H). ^{13}C{^{1}H} NMR (100 MHz, $CDCl_3$): δ 163.7, 152.1, 150.2, 147.1, 140.5, 139.0, 138.5, 124.4, 124.3, 123.3, 119.3, 103.9, 32.7, 30.8, 22.2, 14.1. IR (KBr, cm^{-1}): 2932, 1661, 1537, 1434. HRMS (ESI) m/z: $[M + H]^+$ calcd for $C_{16}H_{19}N_2O$, 255.1492; found 255.1492.

(*E*)-6-(Hept-1-en-1-yl)-2*H*-[1,2'-bipyridin]-2-one (3ao):[6b]

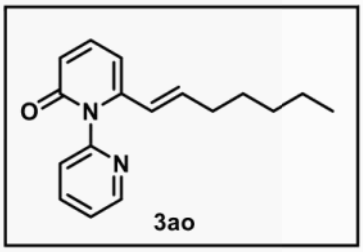

3ao

Physical state: brown oil (26 mg for 0.116 mmol scale, 83% yield). R_f: 0.2 (50% EtOAc/DCM). ^{1}H NMR (400 MHz, $CDCl_3$): δ 8.60 (dd, J = 5.2, 2.0 Hz, 1H), 7.82 (td, J = 7.6, 2.0 Hz, 1H), 7.35–7.25 (m, 3H), 6.48 (d, J = 9.2 Hz, 1H), 6.31 (d, J = 7.2 Hz, 1H), 6.16–6.08 (m, 1H), 5.42 (d, J = 15.6 Hz, 1H), 1.91 (q, J = 7.2 Hz, 2H), 1.25–1.18 (m, 3H), 1.16–1.12 (m, 2H), 1.11–1.09 (m, 1H), 0.77 (t, J = 7.2 Hz, 3H). ^{13}C{^{1}H} NMR (100 MHz, $CDCl_3$): δ 163.7, 152.2, 150.2, 147.1, 140.5, 138.9, 138.6, 124.4, 124.3, 123.3, 119.3, 103.9, 33.0, 31.4, 28.4, 22.7, 14.3. IR (KBr, cm^{-1}): 2925, 1716, 1537, 1434.

(*E*)-6-(Oct-1-en-1-yl)-2*H*-[1,2'-bipyridin]-2-one (3ap):

Physical state: brown oil (30 mg for 0.114 mmol scale, 93% yield). R_f: 0.13 (50% EtOAc/DCM). ^{1}H NMR (400 MHz, $CDCl_3$): δ 8.60 (d, J = 4.4 Hz, 1H), 7.82 (t, J = 7.6 Hz, 1H), 7.34–7.24 (m, 3H), 6.47 (d, J = 9.2 Hz, 1H), 6.30 (d, J = 7.2 Hz, 1H), 6.15–6.08 (m, 1H), 5.42 (d, J = 15.6 Hz, 1H), 1.90 (dd, J = 14.0, 7.2 Hz, 2H), 1.22–1.09 (m, 8H), 0.78 (t,

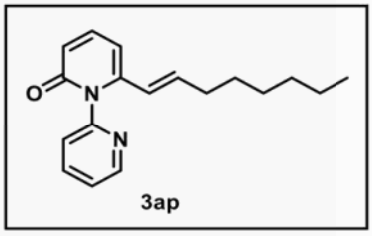

3ap

J = 6.8 Hz, 3H). $^{13}C\{^1H\}$ NMR (100 MHz, $CDCl_3$): δ 163.6, 152.2, 150.2, 147.1, 140.4, 138.9, 138.5, 124.4, 124.3, 123.3, 119.3, 103.9, 33.1, 31.9, 28.9, 28.7, 22.9, 14.4. IR (KBr, cm^{-1}): 2954, 1667, 1537, 1433. HRMS (ESI) m/z: $[M + H]^+$ calcd for $C_{18}H_{23}N_2O$, 283.1805; found 283.1802.

(*E*)-6-(3,5-Difluorostyryl)-2*H*-[1,2'-bipyridin]-2-one (3aq):

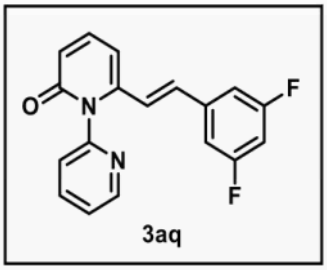

3aq

Physical state: yellow solid (28 mg for 0.117 mmol scale, 77% yield). mp: 152–158 °C. R_f: 0.5 (60% EtOAc/Hexane). ^1H NMR (400 MHz, $CDCl_3$): δ 8.70 (d, J = 4.0 Hz, 1H), 7.95 (dt, J = 7.6, 2.0 Hz, 1H), 7.49–7.42 (m, 3H), 6.91 (d, J = 16.0 Hz, 1H), 6.73–6.65 (m, 4H), 6.61 (d, J = 6.8 Hz, 1H), 6.19 (d, J = 16.0 Hz, 1H). $^{13}C\{^1H\}$ NMR (100 MHz, $CDCl_3$): δ 163.5 (dd, $J_{C\text{-}F}$ = 247.0 Hz, $J_{C\text{-}F}$ = 13.0 Hz), 163.4, 151.6, 150.4, 145.7, 140.4, 139.3, 139.2 (t, $J_{C\text{-}F}$ = 9.0 Hz), 132.3 (t, $J_{C\text{-}F}$ = 3.0 Hz), 124.7, 124.5, 123.7, 120.8, 110.0 (dd, $J_{C\text{-}F}$ = 18.0 Hz, $J_{C\text{-}F}$ = 7.0 Hz), 105.3, 104.5 (t, $J_{C\text{-}F}$ = 25.0 Hz). $^{19}F\{^1H\}$ NMR (376 MHz, $CDCl_3$): δ -109.4. IR (KBr, cm^{-1}): 3051, 2923, 1670, 1617, 1590, 1532, 1433, 1118, 838. HRMS (ESI) m/z: $[M + H]^+$ calcd for $C_{18}H_{13}F_2N_2O$, 311.0990; found 311.0991.

(*E*)-3-Bromo-6-(4-fluorostyryl)-2*H*-[1,2'-bipyridin]-2-one (3cb):

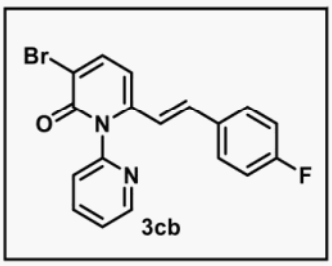

3cb

Physical state: yellow solid (12 mg for 0.036 mmol scale, 88% yield). mp: 200–202 °C. R_f: 0.6 (50% EtOAc/Hexane). ^1H NMR ($CDCl_3$, 400 MHz): δ 8.69 (d, J = 3.6 Hz, 1H), 7.93 (td, J = 7.6, 1.6 Hz, 1H), 7.83 (d, J =7.6 Hz, 1H), 7.47–7.44 (m, 1H), 7.40 (d, J = 8.0 Hz, 1H), 7.18–7.15 (m, 2H), 7.03–6.94 (m, 3H), 6.49 (d, J = 7.6 Hz, 1H), 6.05 (d, J = 16.0 Hz, 1H). $^{13}C\{^1H\}$ NMR ($CDCl_3$, 100 MHz): δ 163.4 (d, $J_{C\text{-}F}$ = 248.6 Hz), 159.6, 151.8, 150.3, 146.2, 142.1, 139.2, 133.9, 132.1,

129.1 (d, $J_{C\text{-}F}$ = 8.2 Hz), 124.5 (d, $J_{C\text{-}F}$ = 41.0 Hz), 120.4, 116.2 (d, $J_{C\text{-}F}$ = 21.8 Hz), 115.4, 104.1. $^{19}F\{^1H\}$ NMR ($CDCl_3$, 376 MHz): δ -111.1. IR (KBr, cm^{-1}): 2917, 1686, 1518, 1225, 750. HRMS (ESI) m/z: $[M + Na]^+$ calcd for $C_{18}H_{12}BrFN_2ONa$, 393.0009; found 393.0005.

(*E*)-3-Bromo-6-(3-methylstyryl)-2*H*-[1,2'-bipyridin]-2-one (3ck):

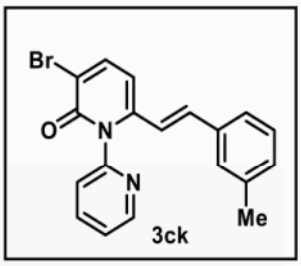

Physical state: yellow oil (13 mg for 0.037 mmol scale, 95% yield). R_f: 0.4 (40% EtOAc/Hexane). ^1H NMR ($CDCl_3$, 400 MHz): δ 8.68 (dd, J = 4.8, 1.2 Hz, 1H), 7.91 (td, J = 7.6, 2.0 Hz, 1H), 7.81 (d, J = 7.6 Hz, 1H), 7.45–7.42 (m, 1H), 7.38 (d, J = 7.6 Hz, 1H), 7.15 (t, J = 7.6 Hz, 1H), 7.07 (d, J = 7.6 Hz, 1H), 7.02–6.97 (m, 3H), 6.48 (d, J = 7.6 Hz, 1H), 6.13 (d, J = 16.0 Hz, 1H), 2.29 (s, 3H). $^{13}C\{^1H\}$ NMR ($CDCl_3$, 100 MHz): δ 159.7, 151.8, 150.3, 146.5, 142.1, 139.2, 138.8, 135.8, 135.4, 130.4, 129.0, 128.3, 124.7, 124.4, 124.3, 120.4, 115.2, 104.1, 21.6. IR (KBr, cm^{-1}): 2917, 1661, 1519, 1733, 782. HRMS (ESI) m/z: $[M + H]^+$ calcd for $C_{19}H_{16}BrN_2O$, 367.0441; found 367.0417.

(*E*)-3-Bromo-6-(2-cyclopropylvinyl)-2*H*-[1,2'-bipyridin]-2-one (3cm):

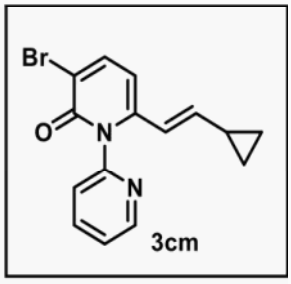

Physical state: yellow solid (8 mg for 0.045 mmol scale, 55% yield). mp: 145–150 °C. R_f: 0.4 (50% EtOAc/Hexane). ^1H NMR ($CDCl_3$, 400 MHz): δ 8.68 (d, J = 4.0 Hz, 1H), 7.92 (td, J = 8.0, 2.0 Hz, 1H), 7.74 (d, J = 7.6 Hz, 1H), 7.46–7.43 (m, 1H), 7.34 (d, J = 8.0 Hz, 1H), 6.26 (d, J = 7.6 Hz, 1H), 5.72 (dd, J = 15.6, 9.2 Hz, 1H), 5.53 (d, J = 15.6 Hz, 1H), 1.32–1.26 (m, 1H), 0.82–0.77 (m, 2H), 0.48–0.44 (m, 2H). $^{13}C\{^1H\}$ NMR ($CDCl_3$, 100 MHz): δ 159.7, 151.8, 150.2, 146.6, 143.6, 142.3, 139.3, 124.7, 124.3, 119.7, 113.7, 103.2, 15.5, 8.6. IR (KBr, cm^{-1}): 3009, 1651, 1520, 1634, 783. HRMS (ESI) m/z: $[M + H]^+$ calcd for $C_{15}H_{14}BrN_2O$, 317.0284; found 317.0276.

(*E*)-3-Bromo-6-(oct-1-en-1-yl)-2*H*-[1,2'-bipyridin]-2-one (3cp):

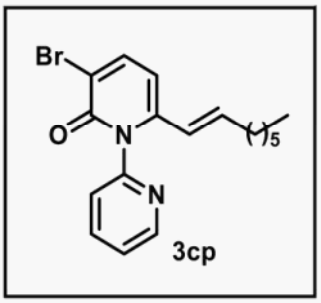

Physical state: colorless liquid (10 mg for 0.041 mmol scale, 67% yield). R_f: 0.6 (50% EtOAc/Hexane). ^{1}H NMR ($CDCl_3$, 400 MHz): δ 8.65 (d, J = 4.8 Hz, 1H), 7.90 (td, J = 7.6, 1.6 Hz, 1H), 7.75 (d, J = 8.0 Hz, 1H), 7.41 (dd, J = 7.2, 5.2 Hz, 1H), 7.32 (d, J = 8.0 Hz, 1H), 6.30 (d, J = 8.0 Hz, 1H), 6.27–6.19 (m, 1H), 5.47 (d, J =15.6 Hz, 1H), 2.01–1.95 (m, 2H), 1.28–1.24 (m, 4H), 1.18–1.16 (m, 4H), 0.85 (t, J = 6.8 Hz, 3H). ^{13}C{^{1}H} NMR ($CDCl_3$, 100 MHz): δ 159.7, 151.9, 150.2, 146.8, 142.3, 139.3, 139.1, 124.6, 124.2, 122.8, 114.4, 103.8, 33.2, 31.9, 28.9, 28.6, 22.9, 14.4. IR (KBr, cm^{-1}): 2925, 1661, 1588, 1523, 785. HRMS (ESI) m/z: $[M + H]^+$ calcd for $C_{18}H_{22}BrN_2O$, 361.0910; found 361.0928.

(*E*)-3-Methoxy-6-(4-nitrostyryl)-2*H*-[1,2'-bipyridin]-2-one (3ef):

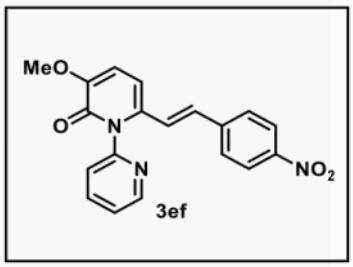

Physical state: red solid (7 mg for 0.047 mmol scale, 42% yield). mp: 240–244 °C. R_f: 0.4 (50% EtOAc/DCM). ^{1}H NMR ($CDCl_3$, 400 MHz): δ 8.68 (dd, J = 4.8, 1.2 Hz, 1H), 8.11 (d, J = 8.8 Hz, 2H), 7.95 (td, J = 7.6, 2 Hz, 1H), 7.48–7.44 (m, 2H), 7.29–7.26 (m, 2H), 6.88 (d, J = 16.0 Hz, 1H), 6.74 (d, J = 8.0 Hz, 1H), 6.61 (d, J = 8.0 Hz, 1H), 6.29 (d, J =16.0 Hz, 1H), 3.90 (s, 3H). ^{13}C{^{1}H} NMR ($CDCl_3$, 100 MHz): δ 158.5, 154.9, 151.6, 150.6, 150.2, 147.5, 142.8, 139.2, 136.5, 129.1, 127.4, 125.6, 124.7, 124.4, 112.9, 105.0, 56.5. IR (KBr, cm^{-1}): 2959, 1667, 1590, 1510, 1341. HRMS (ESI) m/z: $[M + H]^+$ calcd for $C_{19}H_{16}N_3O_4$, 350.1135; found 350.1129.

(*E*)-3-Methoxy-6-(3-methylstyryl)-2*H*-[1,2'-bipyridin]-2-one (3ek):

Physical state: yellow solid (14 mg for 0.05 mmol scale, 87% yield). mp: 140–145 °C. R_f: 0.5 (60% EtOAc/DCM). ^{1}H NMR ($CDCl_3$, 400 MHz): δ 8.67 (dd, J = 4.8, 1.6 Hz, 1H), 7.89

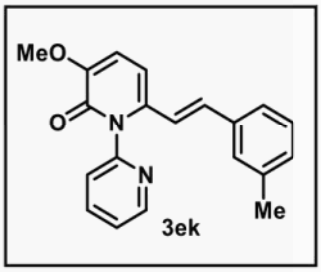

3ek

(td, J =7.6, 1.6 Hz, 1H), 7.43–7.37 (m, 2H), 7.13 (t, J = 7.6 Hz, 1H), 7.04–6.95 (m, 3H), 6.83 (d, J = 16.0 Hz, 1H), 6.74 (d, J = 8.0 Hz, 1H), 6.52 (d, J = 7.6 Hz, 1H), 6.11 (d, J = 16.0 Hz, 1H), 3.86 (s, 3H), 2.27 (s, 3H). $^{13}C\{^1H\}$ NMR ($CDCl_3$, 100 MHz): δ 158.7, 151.8, 150.1, 149.5, 139.1, 138.6, 137.9, 136.3, 132.3, 129.5, 128.8, 127.9, 124.5, 124.4, 124.0, 120.9, 113.6, 103.6, 56.3, 21.6. IR (KBr, cm^{-1}): 2912, 1661, 1602, 1434, 1273. HRMS (ESI) m/z: $[M + Na]^+$ calcd for $C_{20}H_{18}N_2O_2Na$, 341.1260; found 341.1265.

(S)-6-Phenethyl-1-(pyridin-2-yl)piperidin-2-one (4):[6b]

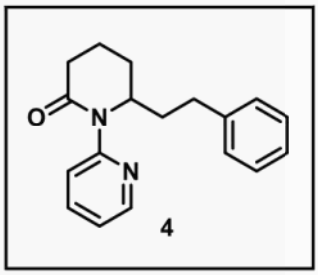

4

Physical state: colourless liquid (38 mg for 0.182 mmol scale, 75% yield). R_f: 0.7 (50% EtOAc/Hexane). ^1H NMR ($CDCl_3$, 400 MHz): δ 8.45 (d, J = 3.6 Hz, 1H), 7.70 (td, J = 8.0, 1.6 Hz, 1H), 7.51 (d, J = 8.4 Hz, 1H), 7.22 (t, J = 6.8 Hz, 2H), 7.17–7.12 (m, 2H), 7.01 (d, J = 7.2 Hz, 2H), 4.68–4.62 (m, 1H), 2.66–2.43 (m, 4H), 2.11–1.73 (m, 6H). $^{13}C\{^1H\}$ NMR ($CDCl_3$, 100 MHz): δ 171.1, 154.0, 148.7, 141.5, 137.4, 128.7, 128.4, 126.2, 123.6, 121.6, 56.5, 35.5, 33.3, 32.3, 26.9, 17.9. IR (KBr, cm^{-1}): 2947, 1656, 1455, 1403.

(*E*)-6-Styrylpyridin-2(1*H*)-one (5):[6b]

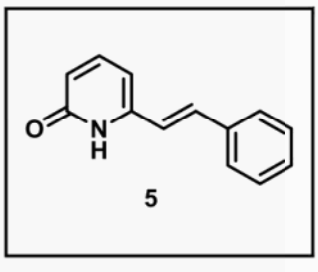

5

Physical state: yellow solid (14 mg for 0.109 mmol scale, 65% yield). mp: 205–210 °C. R_f: 0.25 (5 % MeOH/DCM). ^1H NMR ($CDCl_3$, 400 MHz): δ 12.63 (s, 1H), 7.61–7.56 (m, 3H), 7.46–7.31 (m, 4H), 6.81 (d, J = 16.8 Hz, 1H), 6.53 (d, J = 8.8 Hz, 1H), 6.35 (d, J = 6.8 Hz, 1H). $^{13}C\{^1H\}$ NMR ($CDCl_3$, 100 MHz): δ 165.5, 144.5, 141.7, 136.2, 134.0, 129.3, 129.1, 127.6, 120.9, 119.3, 106.8. IR (KBr, cm^{-1}): 3419, 2927, 1645, 1634.

(*E*)-6-(4-Fluorostyryl)pyridin-2(1*H*)-one (6):

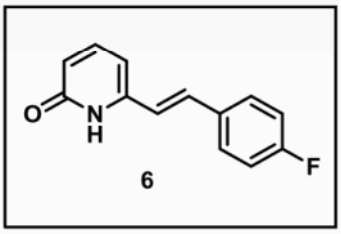

6

Physical state: white solid (15 mg for 0.119 mmol scale, 59% yield). mp: 190–192 °C. R_f: 0.1 (20 % EtOAc/Hexane). ^{1}H NMR ($CDCl_3$, 400 MHz): δ 12.33 (s, 1H), 7.56–7.50 (m, 3H), 7.44 (dd, J = 9.2, 7.2 Hz, 1H), 7.08 (t, J = 8.4 Hz, 2H), 6.71 (d, J = 16.8 Hz, 1H), 6.53 (d, J = 9.2 Hz, 1H), 6.33 (d, J = 7.2 Hz, 1H). ^{13}C{^{1}H} NMR ($CDCl_3$, 100 MHz): δ 165.6, 163.4 (d, $J_{C\text{-}F}$ = 247.8 Hz), 144.4, 141.8, 132.9, 132.4 (d, $J_{C\text{-}F}$ = 3.3 Hz), 129.3 (d, $J_{C\text{-}F}$ = 8.2 Hz), 120.6 (d, $J_{C\text{-}F}$ = 2.4 Hz), 119.3, 116.2 (d, $J_{C\text{-}F}$ = 21.7 Hz), 106.9. ^{19}F{^{1}H} NMR (376 MHz, $CDCl_3$): δ -111.7. IR (KBr, cm^{-1}): 2932, 1651, 1590, 971. HRMS (ESI) m/z: $[M + Na]^+$ calcd for $C_{13}H_{10}FNONa$, 238.0639; found 238.0636.

(*E*)-6-(Oct-1-en-1-yl)pyridin-2(1*H*)-one (7):

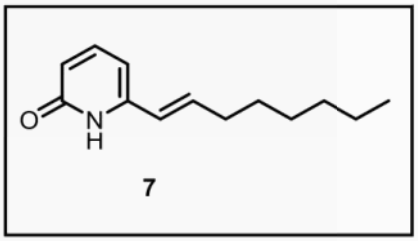

7

Physical state: colourless liquid (22 mg for 0.149 mmol scale, 72% yield). R_f: 0.55 (50 % EtOAc/Hexane). ^{1}H NMR ($CDCl_3$, 400 MHz): δ 12.05 (s, 1H), 7.35 (dd, J = 9.2, 7.2 Hz, 1H), 6.65–6.61 (m, 1H), 6.42 (d, J = 8.8 Hz, 1H), 6.17–6.13 (m, 2H), 2.25 (q, J = 6.8 Hz, 2H), 1.51–1.44 (m, 2H), 1.39–1.26 (m, 6H), 0.89 (t, J = 6.8 Hz, 3H). ^{13}C{^{1}H} NMR ($CDCl_3$, 100 MHz): δ 165.4, 144.7, 141.7, 137.8, 123.2, 118.4, 105.0, 33.4, 32.0, 29.2, 29.1, 22.9, 14.4. IR (KBr, cm^{-1}): 2926, 1647, 1591, 1462. HRMS (ESI) m/z: $[M + H]^+$ calcd for $C_{13}H_{20}NO$, 206.1539; found 206.1533.

NMR spectra of 3-Methoxy-2*H*-[1,2'-bipyridin]-2-one (1e):

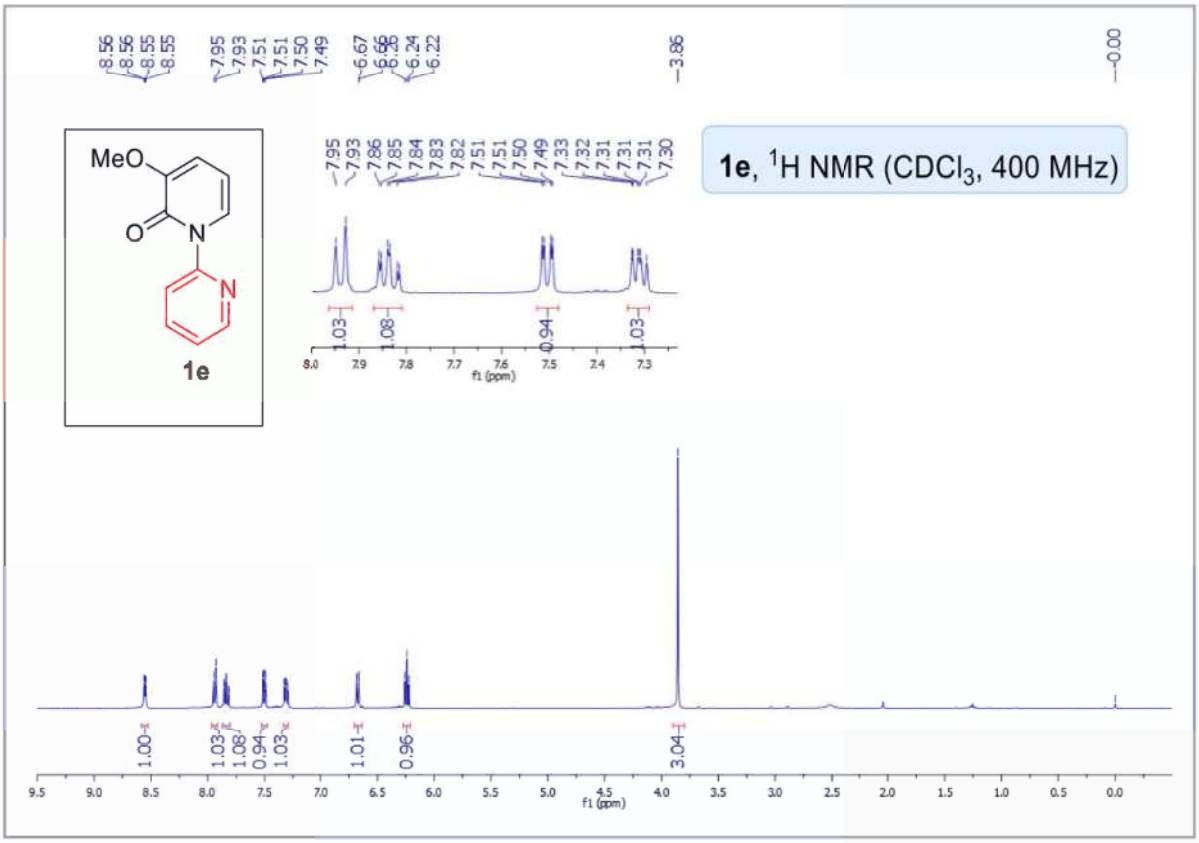

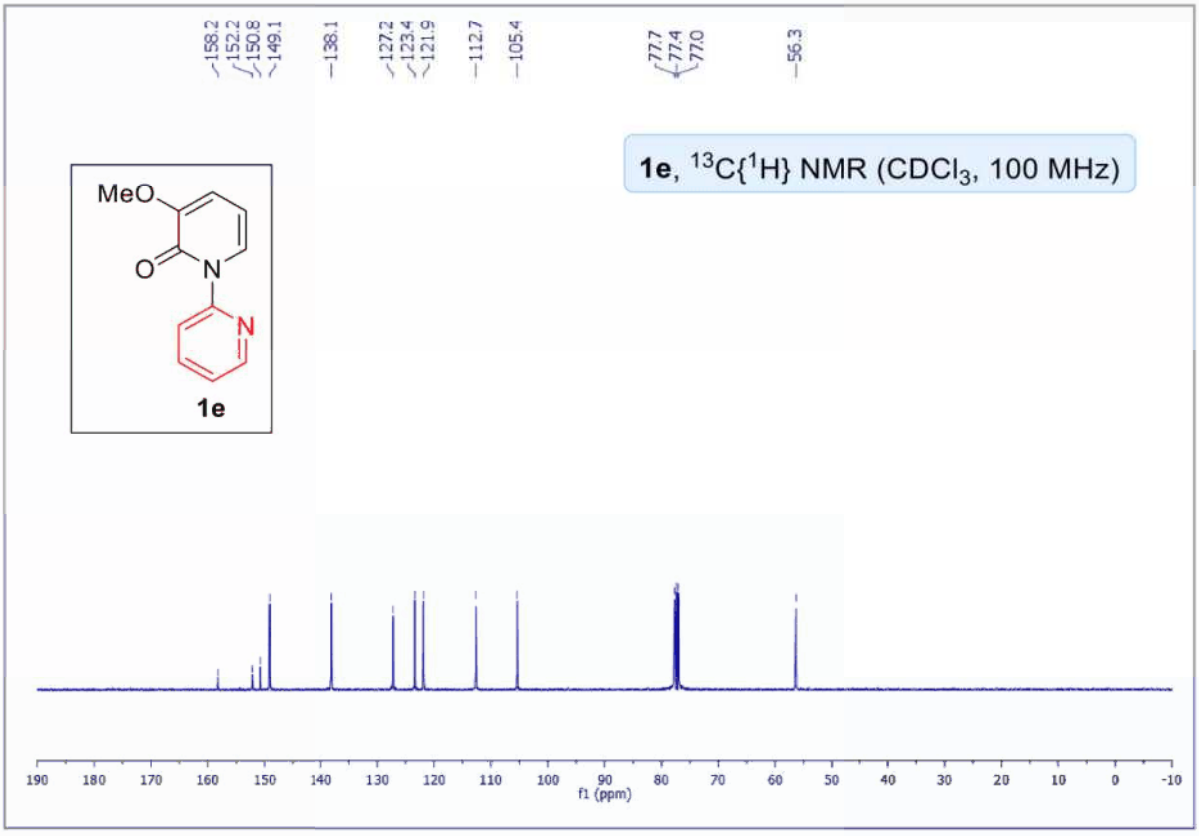

NMR spectra of (*E*)-6-Styryl-2*H*-[1,2'-bipyridin]-2-one (3aa):

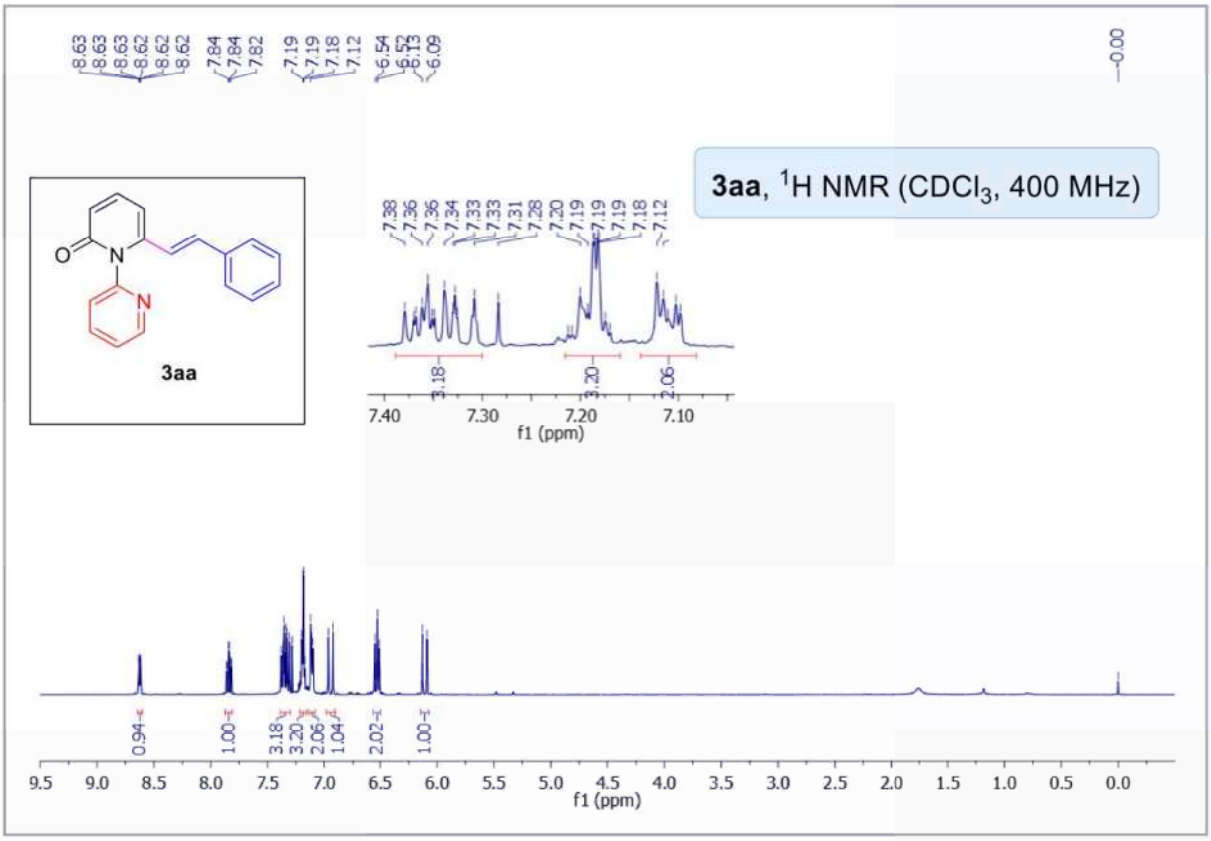

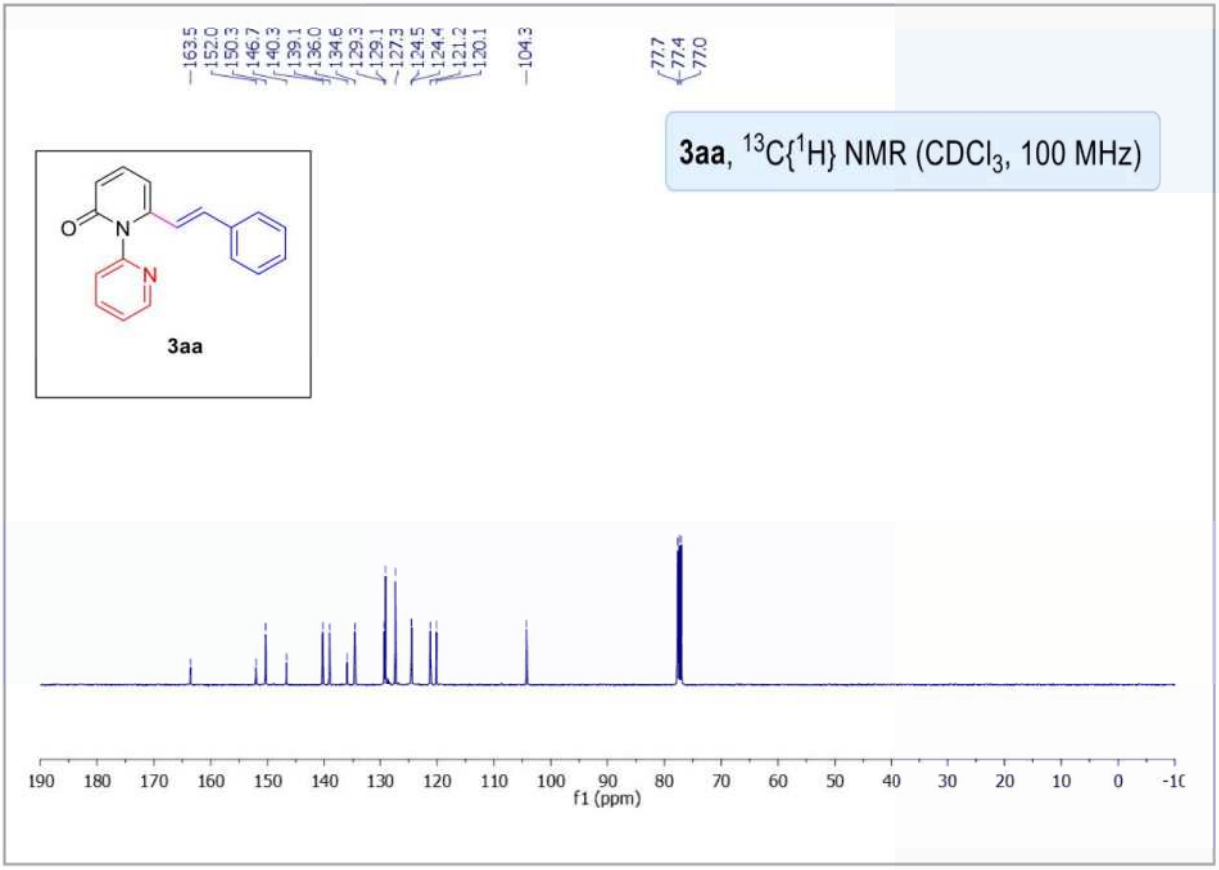

NMR spectra of (S)-6-Phenethyl-1-(pyridin-2-yl)piperidin-2-one (4):

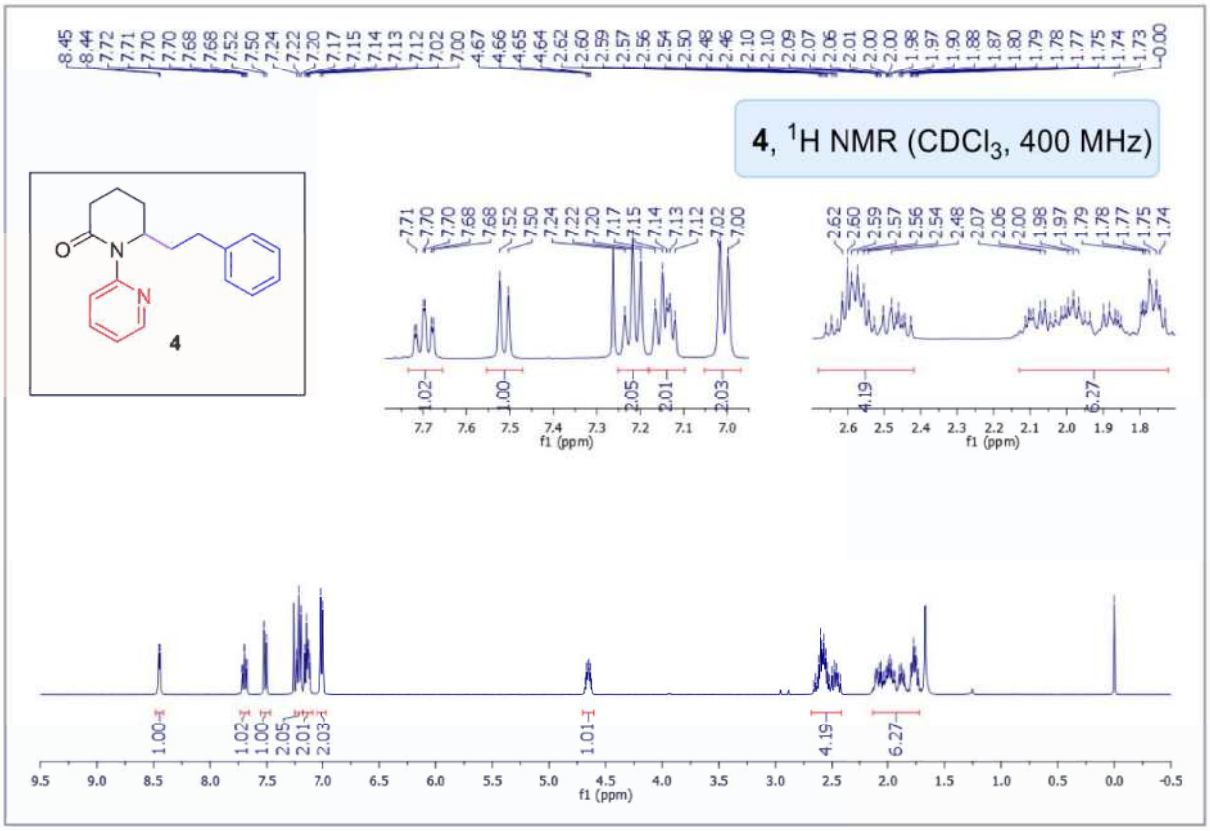

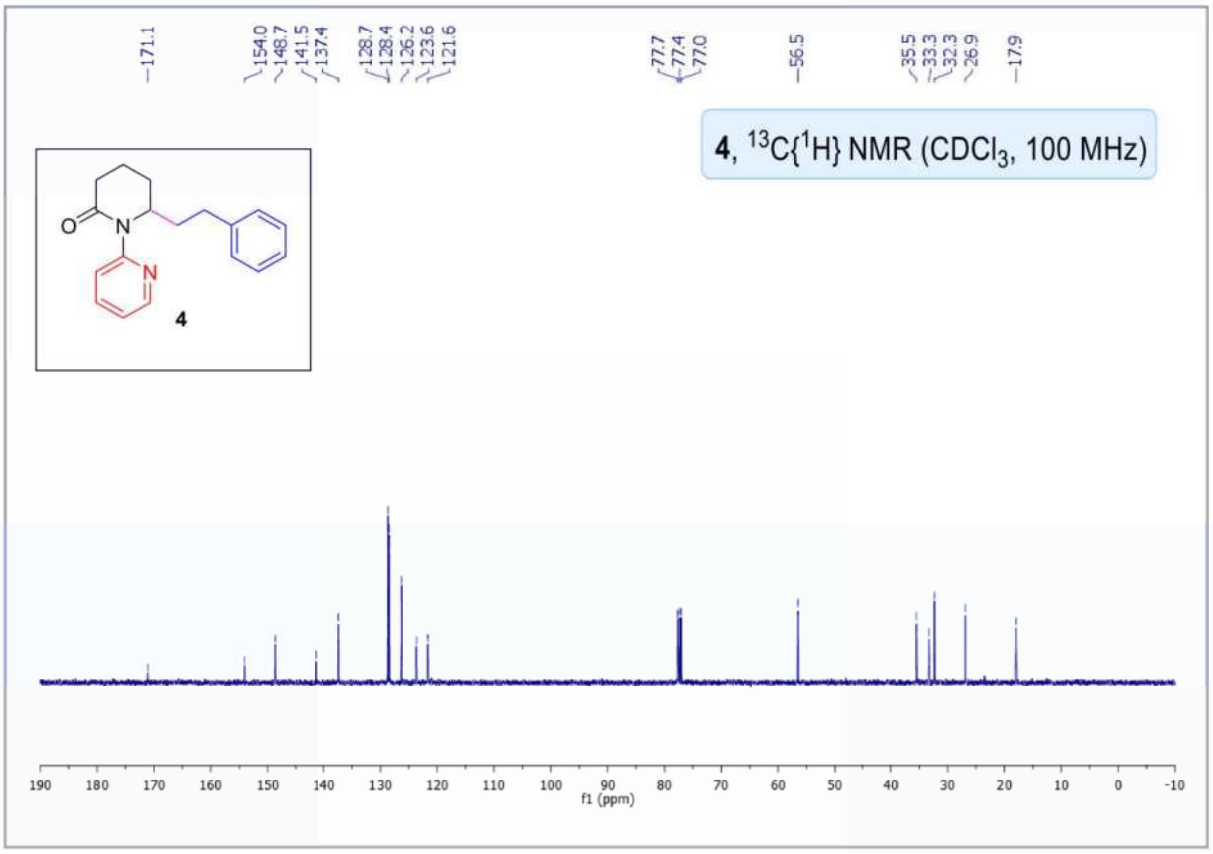

NMR spectra of (*E*)-6-Styrylpyridin-2(1*H*)-one (5):

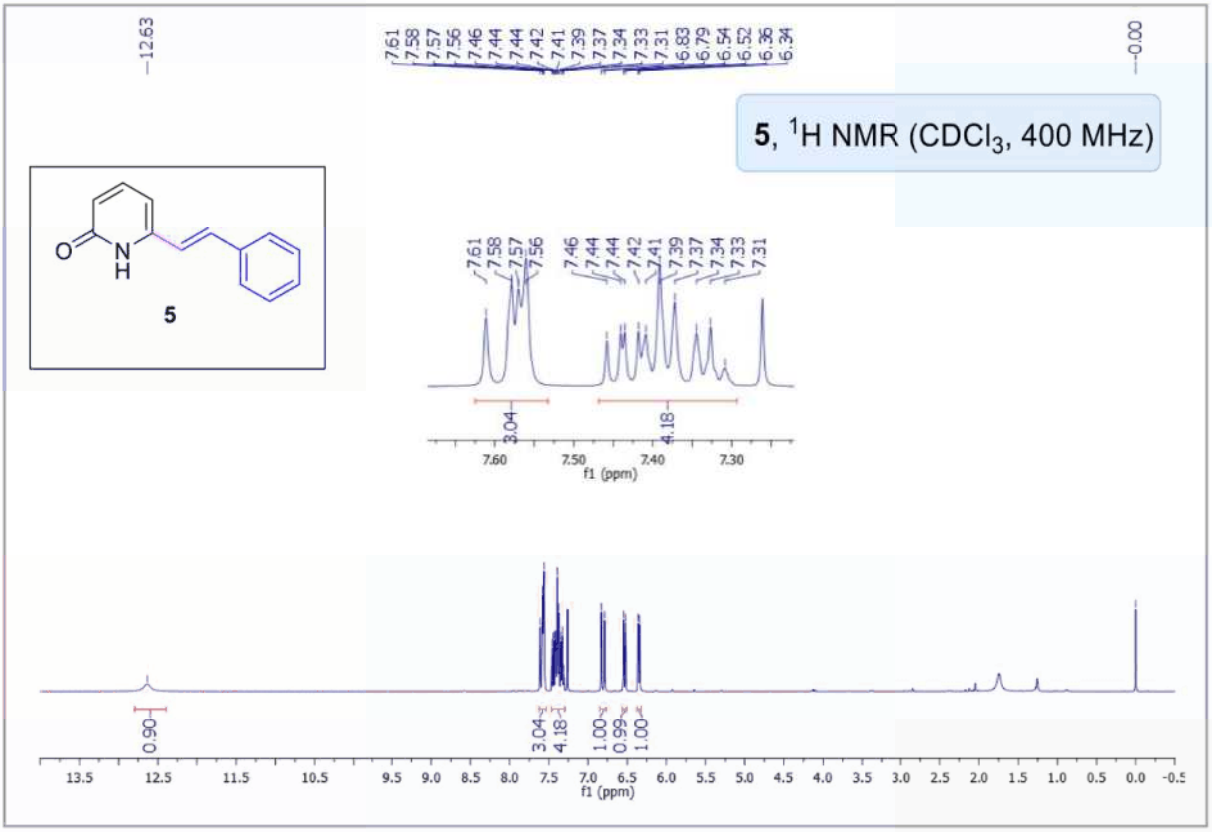

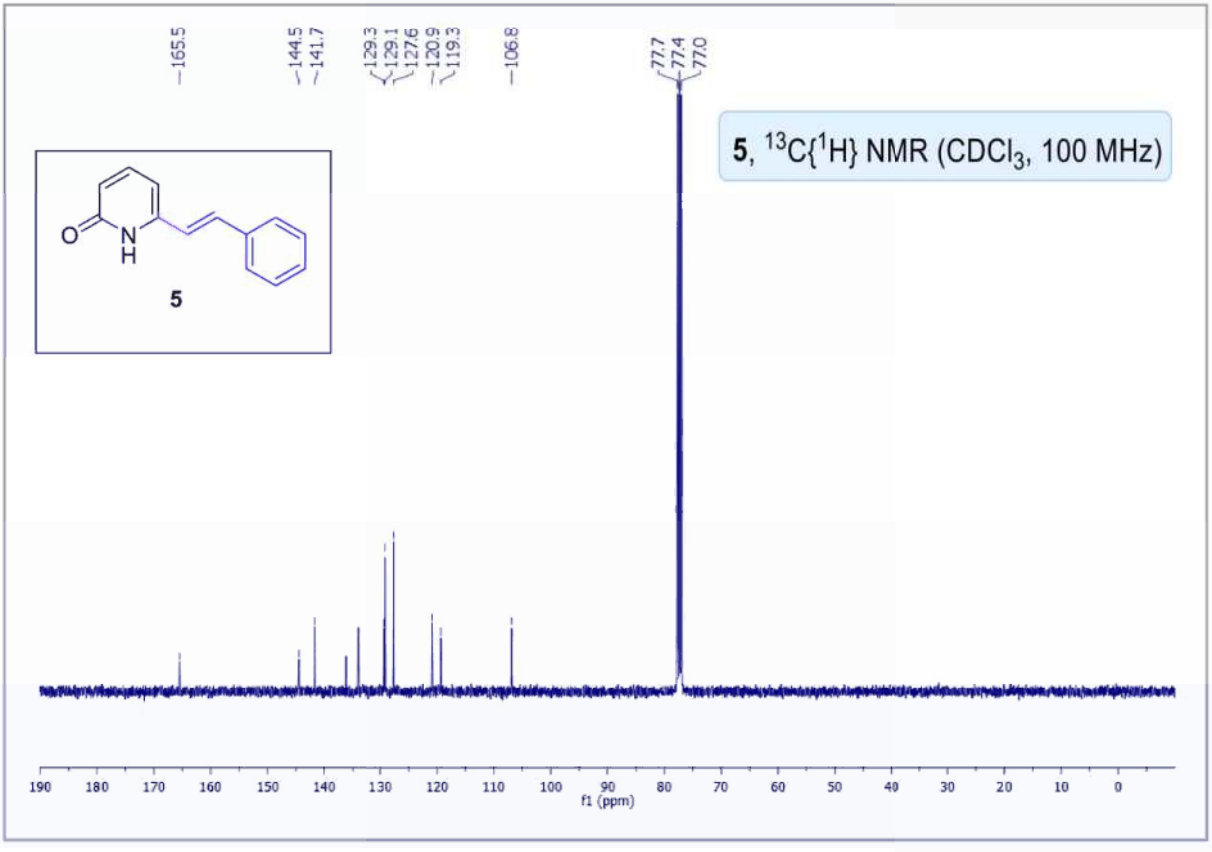

Detection of intermediate (B and D) through HRMS:

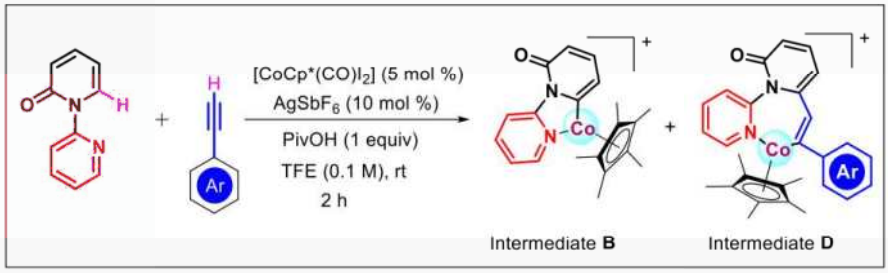

Intermediate B HRMS:

HRMS (ESI) m/z: calcd for $C_{20}H_{22}CoN_2O$ $[M]^+$: 365.1059; found: 365.1093.

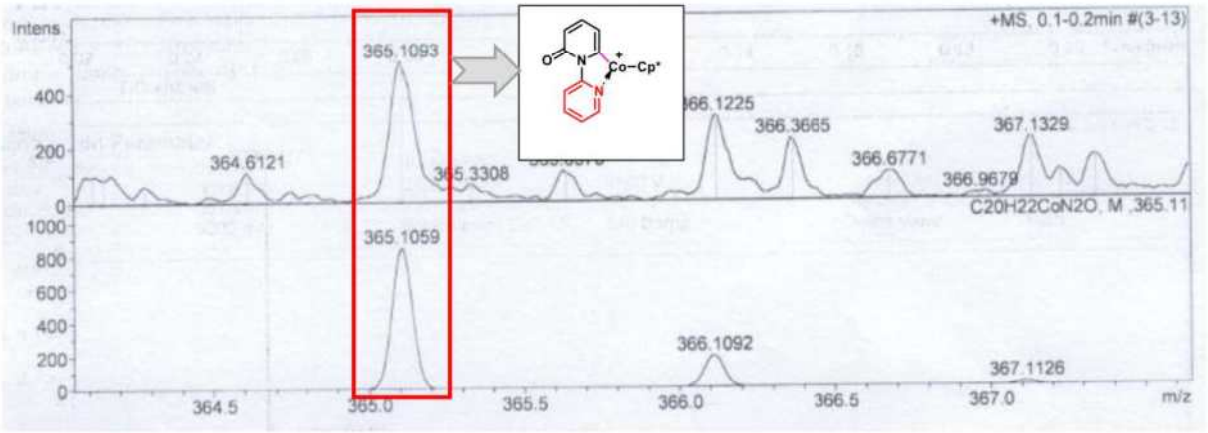

Intermediate D HRMS:

HRMS (ESI) m/z: calcd for $C_{28}H_{28}CoN_2O$ $[M]^+$: 467.1528; found: 467.1502.

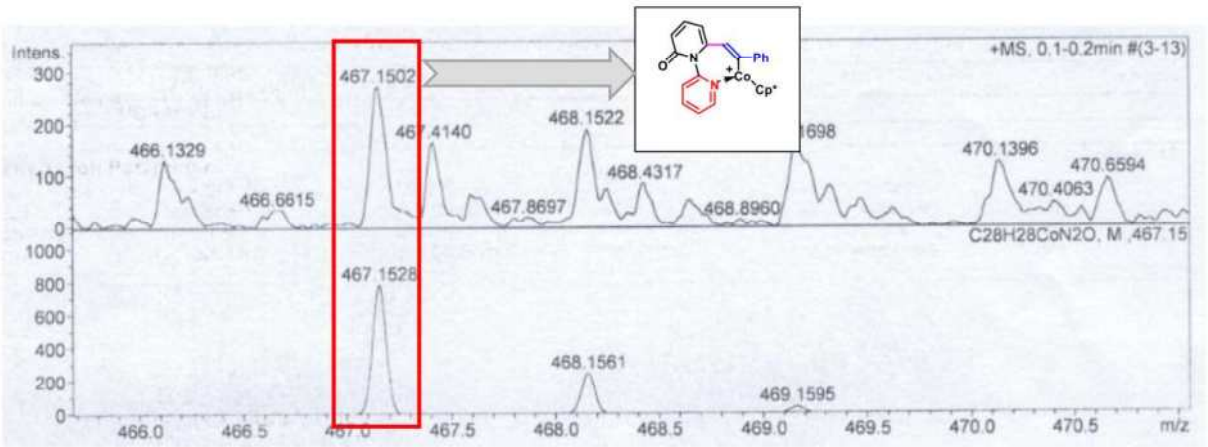

Crystal structure of 3fa

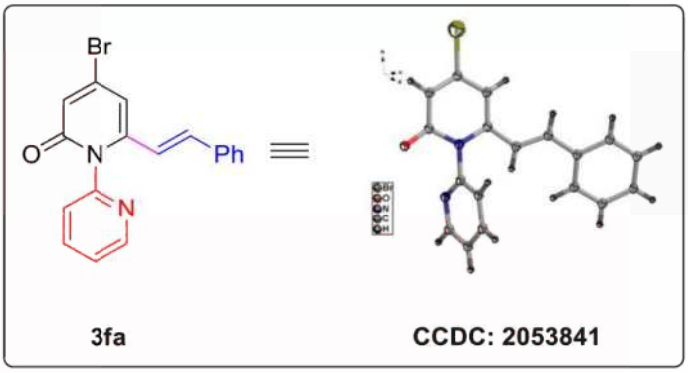

Datablock pcr-lkg-296 - ellipsoid plot

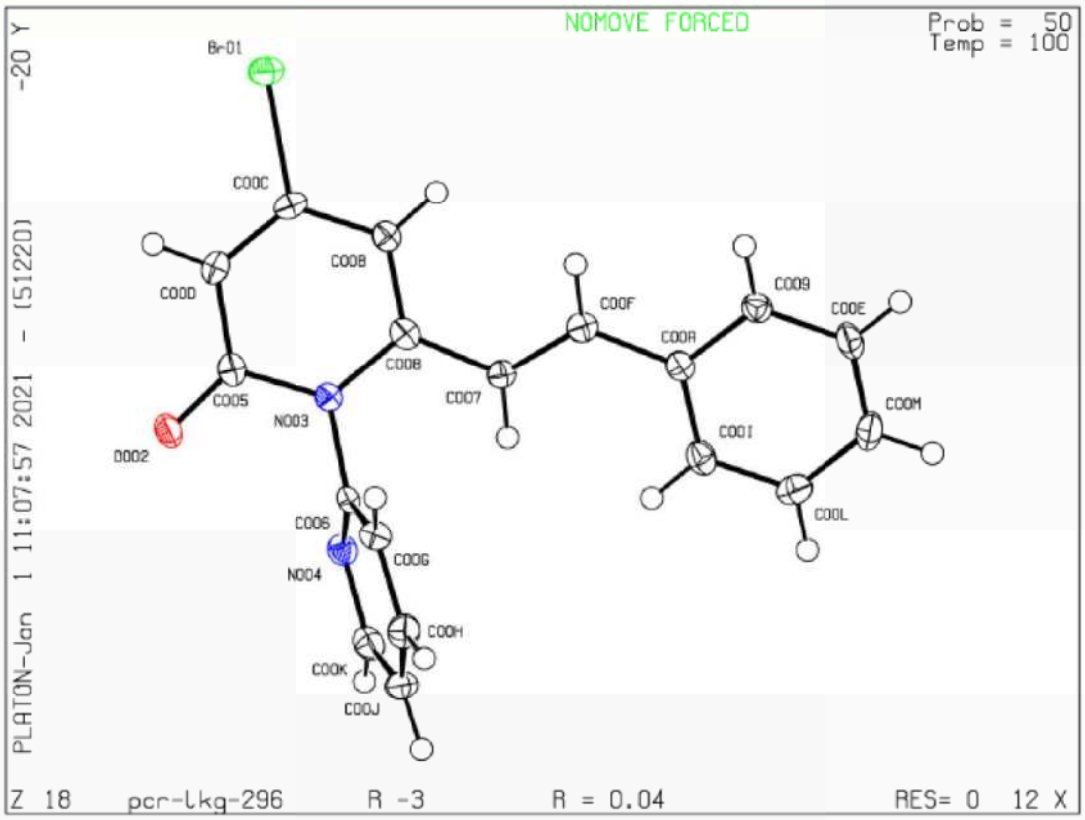

Crystal structure of 3af

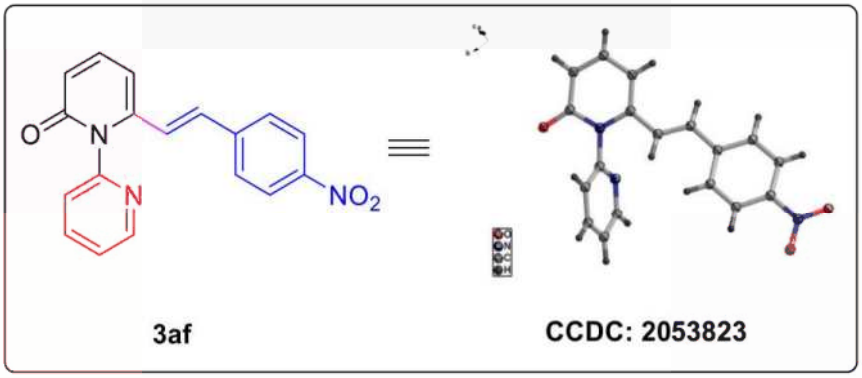

Datablock pcr-srm-631 - ellipsoid plot

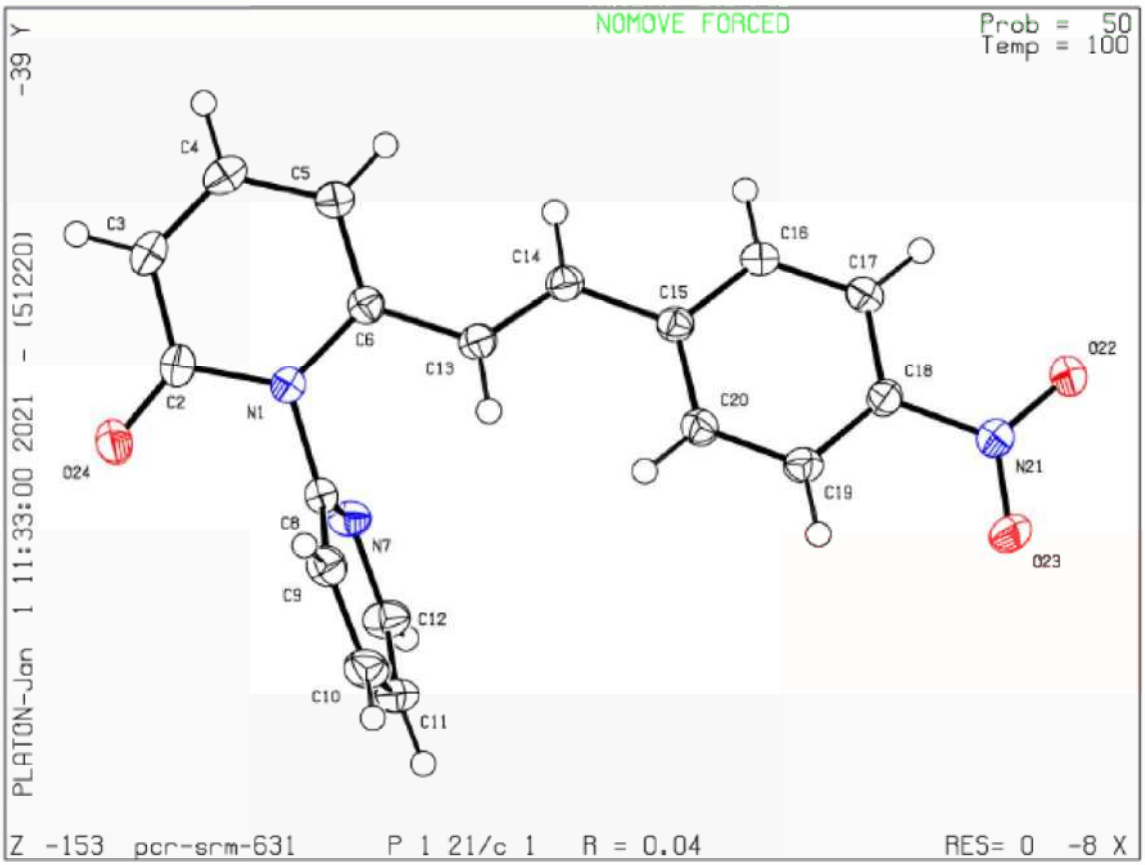

3.6 REFERENCES

1. (a) Torres, M.; Gil, S.; Parra, M. New Synthetic Methods to 2-pyridone Rings. *Curr. Org. Chem*, **2005**, *9*, 1757−1779. (b) Lagoja, I. M. Pyrimidine as Constituent of Natural Biologically Active Compounds. *Chem. Biodiversity,* **2005**, *2*, 1−50. (c) Jessen, H. J.; Gademann, K. 4-Hydroxy-2-pyridone alkaloids: Structures and synthetic approaches. *Nat. Prod. Rep*. **2010**, *27*, 1168−1185.
2. Katritzky, A. R.; Rees, C. W. Comprehensive heterocyclic chemistry: the structure, reactions, synthesis and uses of heterocyclic compounds. *Pergamon Press, Oxford*, **1984**, *vol. 8*.
3. (a) Nakatani, A.; Hirano, K.; Satoh, T.; Miura, M. Nickel-Catalyzed Direct Alkylation of Heterocycles with α-Bromo Carbonyl Compounds: C3-Selective Functionalization of 2-pyridones. *Chem. Eur. J.* **2013**, *19*, 7691−7695. (b) Nakatani, A.; Hirano, K.; Satoh, T.; Miura, M. Manganese-mediated C3-selective direct alkylation and arylation of 2-pyridones with diethyl malonates and arylboronic acids. *J. Org. Chem.* **2014**, *79*, 1377−1385. (c) Modak, A.; Rana, S.; Maiti, D. Iron-Catalyzed Regioselective Direct Arylation at the C-3 Position of N-Alkyl-2-pyridone. *J. Org. Chem.* **2015**, *80*, 296−303. (d) Anagnostaki, E. E.; Fotiadou, A. D.; Demertzidou, V.; Zografos, A. L. Palladium catalyzed C3-arylation of 4-hydroxy-2-pyridones. *Chem. Commun*. **2014**, *50*, 6879−6882. (e) Min, M.; Kim, Y.; Hong, S. Regioselective palladium-catalyzed olefination of coumarins via aerobic oxidative Heck reactions. *Chem. Commun.* **2013**, *49*, 196−198. (f) Cheng, D.; Gallagher, T. Direct and Regioselective C−H Alkenylation of Tetrahydropyrido[1,2-a]pyrimidines. *Org. Lett.* **2009**, *11*, 2639−2641. (g) Dutta, U.; Deb, A.; Lupton, D.

W.; Maiti, D. The regioselective iodination of quinolines, quinolones, pyridones, pyridines and uracil. *Chem. Commun.* **2015**, *51*, 17744−17747.

4. Miura, W.; Hirano, K.; Miura, M. Iridium-Catalyzed Site-Selective C–H Borylation of 2-pyridones. *Synthesis* **2017**, *49*, 4745−4752.
5. (a) Itahara, T.; Ouseto, F. Alkenylation of 1-methyl-2-pyridone and 2-formylfuran with methyl acrylate and palladium acetate. *Synthesis* **1984**, *6*, 488−489. (b) Chen, Y.; Wang, F.; Jia, A.; Li, X. Palladium-catalyzed selective oxidative olefination and arylation of 2-pyridones. *Chem. Sci.* **2012** , *3*, 3231−3236.
6. (a) Kwon, S.; Kang, D.; Hong, S. Rh(I)-Catalyzed Site-Selective Decarbonylative Alkenylation and Arylation of Quinolones under Chelation Assistance. *Eur. J. Org. Chem.* **2015**, 3671−3678. (b) Zhao, H.; Xu, X.; Luo, Z.; Cao, L.; Li, B.; Li, H.; Xu, L.; Fan, Q.; Walsh, P. J. Rhodium(I)-Catalyzed C6-Selective C-H Alkenylation and Polyenylation of 2-pyridones with Alkenyl and Conjugated Polyenyl Carboxylic Acids. *Chem. Sci.* **2019**, *10*, 10089−10096. (c) Hazra, S.; Hirano, K.; Miura, M. Solvent-Controlled Rhodium-Catalyzed C6-Selective C-H Alkenylation and Alkylation of 2-pyridones with Acrylates. *Asian J. Org. Chem.* **2019**, *8*, 1097−1101. (d) Zhu, C.; Kuniyil, R.; Ackermann, L. Manganese(I)-Catalyzed C-H Activation/Diels-Alder/retro-Diels-Alder Domino Alkyne Annulation featuring Transformable Pyridines. *Angew. Chem., Int. Ed.* **2019**, *58*, 5338−5342. (e) Zheng, G.; Sun, J.; Xu, Y.; Zhai, S.; Li, X. Mn-Catalyzed DehydrocyanativeTransannulation of Heteroarenes and Propargyl Carbonates through C-H Activation: Beyond the Permanent Directing Effects of Pyridines/Pyrimidines. *Angew. Chem., Int. Ed.* **2019**, *58*, 5090−5094. (f) Zhu, C.; Kuniyil, R.; Jei, B. B.; Ackermann, L. Domino C−H Activation/Directing Group Migration/Alkyne Annulation: Unique Selectivity by d^6-Cobalt(III) Catalysts. *ACS*

Catal. **2020**, *10*, 4444−4450. (g) Nakao, Y.; Idei, H.; Kanyiva, K. S.; Hiyama, T. Direct Alkenylation and Alkylation of pyridone Derivatives by Ni/$AlMe_3$ Catalysis. *J. Am. Chem. Soc*. **2009**, *131*, 15996–15997. (h) Wang, H.; Pesciaioli, F.; Oliveira, J. C. A.; Warratz, S.; Ackermann, L. Synergistic Manganese(I) C-H Activation Catalysis in Continuous Flow: Chemoselective Hydroarylation. *Angew. Chem., Int. Ed.* **2017**, *56*, 15063−15067.

7. For selected reviews on C−H bond functionalization with first row transition metals, see: (a) Kulkarni, A.; Daugulis, O. Direct Conversion of Carbon-Hydrogen into Carbon-Carbon Bonds by First-Row Transition-Metal Catalysis. *Synthesis* **2009**, *24*, 4087−4109. (b) Nakamura, E.; Yoshikai, N. Low-Valent Iron-Catalyzed C−C Bond Formation−Addition, Substitution, and C−H Bond Activation. *J. Org. Chem*. **2010**, *75*, 6061−6067. (c) Gao, K.; Yoshikai, N. Low-Valent Cobalt Catalysis: New Opportunities for C–H Functionalization. *Acc. Chem. Res.* **2014**, *47*, 1208−1219. (d) Su, B.; Cao, Z.-C.; Shi, Z.-J. Exploration of Earth-Abundant Transition Metals (Fe, Co, and Ni) as Catalysts in Unreactive Chemical Bond Activations. *Acc. Chem. Res.* **2015**, *48*, 886−896. (e) Miao, J.; Ge, H. Recent Advances in First-Row-Transition-Metal-Catalyzed DehydrogenativeCoupling of C(sp^3)–H Bonds. Eur. *J. Org. Chem.* **2015**, 7859−7868. (f) Liu, W.; Ackermann, L. Manganese-Catalyzed C–H Activation. *ACS Catal.* **2016**, *6*, 3743−3752. (g) Pototschnig, G.; Maulide, N.; Schnü rch, M. Direct Functionalization of C-H Bonds by Iron, Nickel, and Cobalt Catalysis. *Chem. Eur. J.* **2017**, *23*, 9206−9232. (h) Rajesh, N.; Barsu, N.; Sundararaju, B. Recent advances in C(sp^3)-H bond carbonylation by first row transition metals. *Tetrahedron Lett*. **2018**, *59*, 862−868.

8. Yoshino, T.; Ikemoto, H.; Matsunaga, S.; Kanai, M. Cp*Co(III)-Catalyzed C2-Selective Addition of Indoles to Imines. *Chem. Eur. J.* **2013**, *19*, 9142−9146.

9. For reviews on Cp*Co(III) catalyzed C−H bond functionalization, see: (a) Yoshino, T.; Matsunaga, S. (Pentamethylcyclopentadienyl)cobalt(III)-Catalyzed C–H Bond Functionalization: From Discovery to Unique Reactivity and Selectivity. *Adv. Synth. Catal.* **2017**, *359*, 1245−1262. (b) Wang, S.; Chen, S.-Y.; Yu, X.-Q. C–H functionalization by high-valent Cp*Co(III) catalysis. *Chem. Commun*. **2017**, *53*, 3165−3180. (c) Usman, M.; Ren, Z.-H.; Wang, Y.-Y.; Guan, Z. H. Recent Developments in Cobalt Catalyzed Carbon–Carbon and Carbon–Heteroatom Bond Formation via C–H Bond Functionalization. *Synthesis* **2017**, *49*, 1419−1443. (d) Moselage, M.; Li, J.; Ackermann, L. Cobalt-Catalyzed C–H Activation. *ACS Catal*. **2016**, *6*, 498−525. (e) Yoshikai, N. Cp*Co(III)-Catalyzed C-H Activation of (Hetero)arenes:Expanding the Scope of Base-Metal-Catalyzed C-H Functionalizations. *ChemCatChem* **2015**, *7*, 732−734. (f) Wei, D.; Zhu, X.; Niu, J.-L.; Song, M. P. High Valent Cobalt-Catalyzed C-H Functionalization Based on Concerted Metalation–Deprotonation and Single-Electron-Transfer Mechanisms. *ChemCatChem* **2016**, *8*, 1242−1263. (g) Hyster, T. High-Valent Co(III)- and Ni(II)-Catalyzed C–H Activation. *Catal. Lett*. **2015**, *145*, 458−467.

10. (a) For a recent review, see: Boyarskiy, V. P.; Ryabukhin, D. S.; Bokach, N. A.; Vasilyev, A. V. Alkenylation of Arenes and Heteroarenes with Alkynes. *Chem. Rev*. **2016**, *116*, 5894−5986. (b) Ali, W.; Prakash, G.; Maiti, D. Recent development in transition metal-catalysed C-H olefination. *Chemical Science*. **2021**, *12*, 2735−2759. (c) Ma, W.; Gandeepan, P.; Li, J.; Ackermann, L. Recent advances in positional-selective alkenylations: removable guidance for twofold C−H activation. *Org. Chem. Front*. **2017**, *4*, 1435−1467.

11. Biswas, A.; Giri, D.; Das, D.; De, A.; Patra, S. K.; Samanta, R. A Mild Rhodium Catalyzed Direct Synthesis of Quinolones from pyridones: Application in the Detection of Nitroaromatics. *J. Org. Chem*. **2017**, *82*, 10989−10996.

12. (a) Bera, S. S.; Debbarma, S.; Ghosh, A. K.; Chand, S.; Maji, M. S. Cp*Co(III)−Catalyzed syn-Selective C−H Hydroarylation of Alkynes Using Benzamides: An Approach Toward Highly Conjugated Organic Frameworks. *J. Org. Chem.* **2017**, *82*, 420−430. (b) Yu, Y.; Wu, Q.; Liu, D.; Hu, L.; Yu, L.; Tan, Z.; Zhu, G. Synthesis of Benzofulvenes via Cp*Co(III)-Catalyzed C−H Activation and Carbocyclization of Aromatic Ketones with Internal Alkynes. *J. Org. Chem*. **2019**, *84*, 7449−7458. (c) Ding, Z.; Yoshikai, N. Cobalt-Catalyzed Addition of Azoles to Alkynes. *Org. Lett.* **2010**, *12*, 4180−4183. (d) Zhang, Z. Z.; Liu, B.; Xu, J. W.; Yan, S. Y.; Shi, B. F. Indole Synthesis via Cobalt(III)-Catalyzed Oxidative Coupling of N-Arylureas and Internal Alkynes. *Org. Lett*. **2016**, *18*, 1776−1779. (e) Tao, L. M.; Li, C. H.; Chen, J.; Liu, H. Cobalt(III)-Catalyzed Oxidative Annulation of Benzaldehydes with Internal Alkynes via C−H Functionalization in Poly(ethylene glycol). *J. Org. Chem.* **2019**, *84*, 6807−6812.

13. (a) Krafft, M. E.; Hirosawa, C.; Dalal, N.; Ramsey, C.; Stiegman, A. Cobalt-catalyzed homocoupling of terminal alkynes: synthesis of 1,3-diynes. *Tetrahedron Lett*. **2001**, *42*, 7733−7736. (b) Mayer, M.; Czaplik, W. M.; Jacobi von Wangelin, A. Cobalt-Catalyzed Biaryl Coupling Reactions. *Synlett.* **2009**, *18*, 2919−2923. (c) Roslan, I. I.; Sun, J.; Chuah, G.-K.; Jaenicke, S. Cobalt(II)-Catalyzed Electrophilic Alkynylation of 1,3-Dicarbonyl Compounds To Form Polysubstituted Furans via π-π Activation. *Adv. Synth. Catal.* **2015**, *357*, 719−726. (d) Xu, D.; Sun, Q.; Quan, Z.; Wang, C.; Sun, W. Cobalt-Catalyzed Dimerization and Homocoupling of Terminal Alkynes. *Asian J. Org. Chem*. **2018**, *7*, 155−159. (e) Hilt, G.; Hengst, C.; Arndt, M.

The Unprecedented Cobalt-Catalysed Oxidative Glaser Coupling under Reductive Conditions. *Synthesis* **2009**, *3*, 395−398.

14. Gandeepan, P.; Müller, T.; Zell, D.; Cera, G.; Warratz, S.; Ackermann, L. 3d Transition Metals for C−H Activation. *Chem. Rev*. **2019**, *119*, 2192−2452.
15. (a) Dalton, T.; Faber, T.; Glorius, F. C-H Activation : Toward Sustainability and Applications. *ACS Cent. Sci.* **2021**, *7*, 245−261. (b) Gensch, T.; Hopkinson, M. N.; Glorius, F.; Wencel-Delord, J. Mild Metal-Catalyzed C−H Activation: Examples and Concepts. *Chem. Soc. Rev.* **2016**, *45*, 2900−2936.
16. Wan, Shanhong.; Luo, Zhenli.; Xu, Xin.; Yu, Haiyang.; Li, Jiajie.; Pan, Yixiao.; Zhang, Xin.; Xu, Lijin.; Cao, Rui. Manganese(I)-Catalyzed Site Selective C6-Alkenylation of 2-pyridones using Alkynes via C-H Activation. *Adv. Synth. Catal.* **2021**, *363*, 1−9.
17. Sinha, S. K.; Bhattacharya, T.; Maiti, D. Role of Hexafluoroisopropanol in C-H Activation. React. *Chem. Eng.* **2019**, *4*, 244−253.
18. Simmons, E. M.; Hartwig, J. F. On the Interpretation of Deuterium Kinetic Isotope Effects in C-H Bond Functionalizations by Transition Metal Complexes. *Angew. Chem. Int. Ed.* **2012**, *51*, 3066–3072.
19. Tanaka, R.; Ikemoto, H.; Kanai, M.; Yoshino, T.; Matsunaga, S. Site- and Regioselective Monoalkenylation of Pyrroles with Alkynes via Cp*Co(III) Catalysis. *Org. Lett*. **2016**, *18*, 5732−5735.
20. Gottlieb, H. E.; Kotlyar, V.; Nudelman, A. NMR chemical shifts of common laboratory solvents as trace impurities. *J. Org. Chem.* **1997**, *62*, 7512−7515.
21. Li, T.; Wang, Z.; Xu, K.; Liu, W.; Zhang, X.; Mao, W.; Guo, Y.; Ge, X.; Pan, F. Rhodium Catalyzed/Copper-Mediated Tandem C(sp^2)-H Alkynylation and Annulation: Synthesis of 11-Acylated Imidazo[1,2-a:3,4-a']dipyridin5-ium-4-

olates from 2H-[1,2'-Bipyridin]-2-ones and Propargyl Alcohols. *Org. Lett.* **2016**, *18*, 1064−1067.

22. Das, D.; Samanta, R. Iridium(III)-Catalyzed Regiocontrolled Direct Amidation of Isoquinolones and pyridones. *Adv. Synth. Catal*. **2018**, *360*, 379−384.

Chapter 4

Pyridone directed selective Ru catalyzed olefination of sp^2(C-H) bond by using acrylate as reacting partner: Creation of drug analogues

Chapter 4

Pyridone directed selective Ru catalyzed olefination of sp^2(C-H) bond by using acrylate as reacting partner: Creation of drug analogues

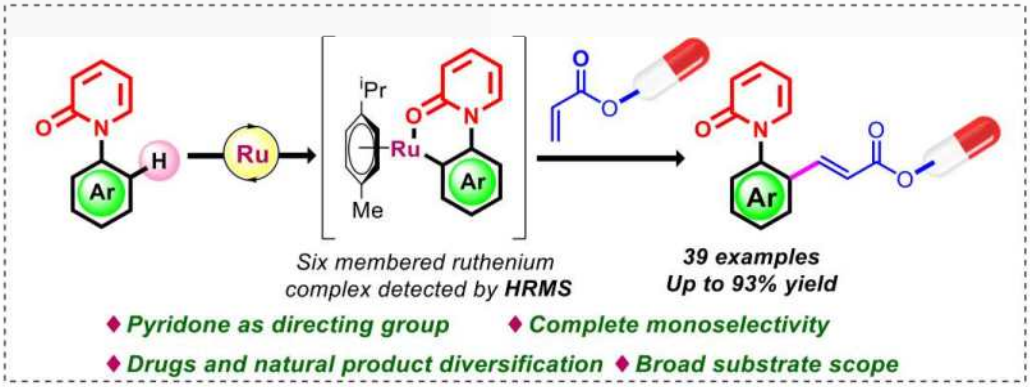

4.1 ABSTRACT: We have demonstrated the ruthenium-catalyzed regioselective sp^2(C-H) mono-alkenylation of *N*-arylpyridones by using acrylate as the coupling partner, where the pyridone was acting as a weakly coordinating directing group. Importantly, several drug analogues such as pirfenidone, naproxen, ibuprofen, geraniol, umbelliferone, pregnenolone, and estrone have been successfully synthesised using the current methodology. This approach works well with the substrates bearing wide range of functional groups and can produce upto 93% yield. By using HRMS, a six-membered ruthenacycle was also detected.

4.2 INTRODUCTION

N-arylpyridones which are present in pharmaceutically active compounds has many biological activities.[1] A wide range of *N*-arylpyridone moieties present in marketed drugs such as anti-inflammatory drug (pirfenidone) for idiopathic pulmonary fibrosis treatment (Figure 4.1).[1a,2]

Therefore, approaches for synthesizing and modifying these heterocycles are useful for developing drugs and increasing their biological activity.[3] The pyridone heterocycle is located next to an aromatic ring in these biologically active compounds. As a result, these structures are gaining interest for use as directing groups in C-H functionalization reaction.

Transition metal catalyzed C-H functionalization has been a common approach for forming C-C bonds.[4] In this approach, inert C-H bonds are converted into highly reactive functional groups. Using this concept, derivatization of biologically active molecules such as *N*-arylpyridones will be a very interesting strategy.

Figure 4.1: Pharmaceutically active compounds containing the *N*-arylpyridones.

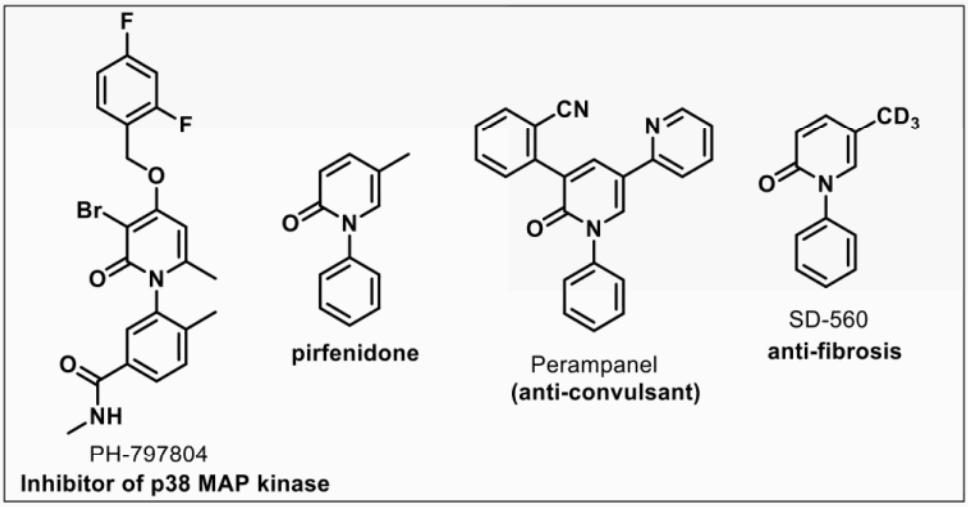

In the field of catalysis minor tuning of the substrate's electronic and steric nature can lead to very different pathways.[5] Depending on the combination of reagents, catalyst systems and directing group used often it gives very different products.[6] So far there are only two reports on the C–H functionalization of *N*-arylpyridone by using Rhodium and Palladium catalyst (Scheme-4.1a, 4.1b).[3b,3c] The reaction of *N*-arylpyridones with acrylates in the presence of a Pd catalyst gives the different product in terms of substitution. It may be because the reaction

is going through electrophilic metalation pathway. According to the literature precedences, metal and reagent (acid/base/oxidants/additive/solvents) combinations play a crucial role in

Scheme 4.1: Previous work and our work

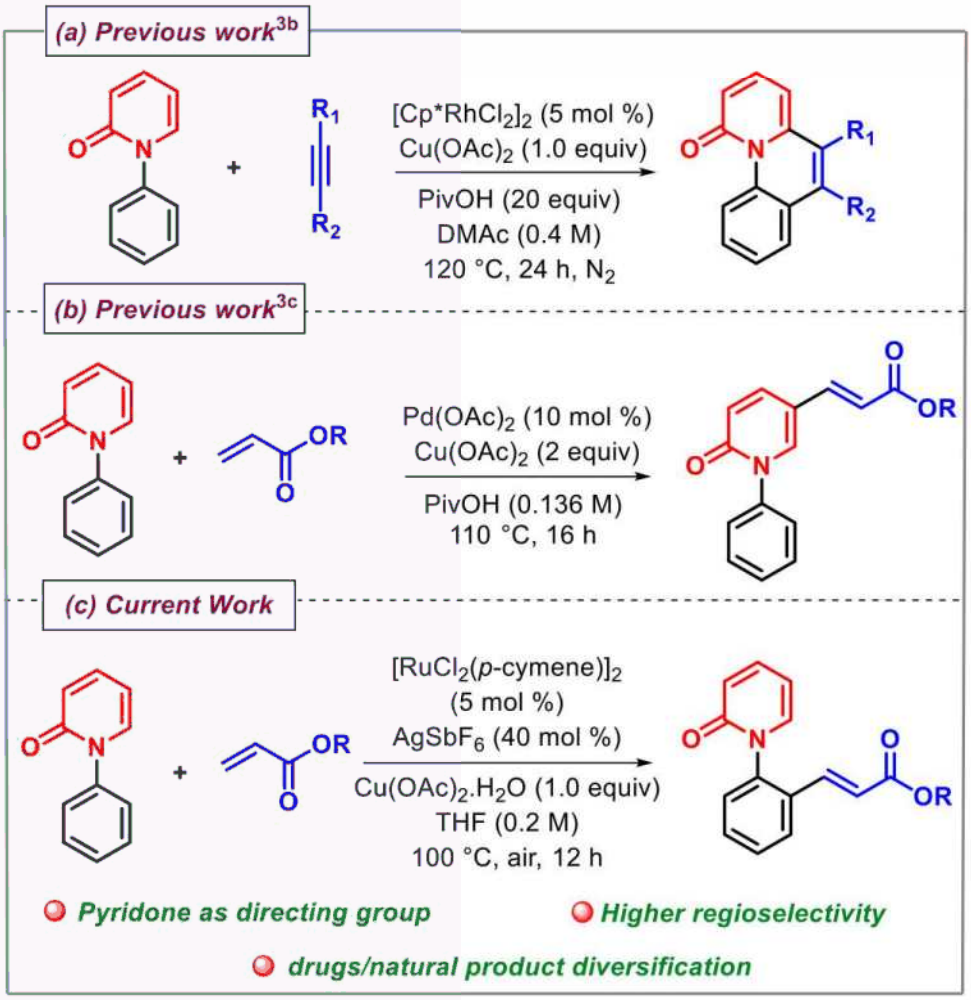

dictating the outcome of the reaction. Therefore, we were curious to see the reactivity of *N*-arylpyridones with ruthenium catalyst using acrylate as reacting partner. Herein, the first Ru-catalyzed alkenylation[7] of *ortho* C-H bond of *N*-phenylpyridone by using acrylate as reacting partner was reported which is completely new product compared to the previously reported Pd catalyzed C-H alkenylation of *N*-phenylpyridone (Scheme 4.1b).

Table 4.1. Optimization for Ru catalyzed olefination of sp^2(C-H) bond[a]

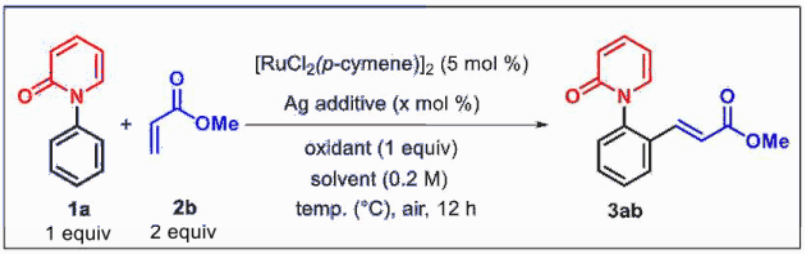

entry	additive	oxidant	solvent	yield of **3aa**[b]
1	$AgSbF_6$	$Cu(OAc)_2.H_2O$	DMF	22%
2	$AgSbF_6$	$Cu(OAc)_2.H_2O$	Dioxane	56%
3	$AgSbF_6$	$Cu(OAc)_2.H_2O$	DCE	54%
4	$AgSbF_6$	$Cu(OAc)_2.H_2O$	THF	74%
5[c]	$AgSbF_6$	$Cu(OAc)_2.H_2O$	THF	14%
6[d]	$AgSbF_6$	$Cu(OAc)_2.H_2O$	THF	90%
7[d]	AgOTf	$Cu(OAc)_2.H_2O$	THF	76%
8[d]	$AgBF_4$	$Cu(OAc)_2.H_2O$	THF	80%
9[d]	$AgNTf_2$	$Cu(OAc)_2.H_2O$	THF	85%
10[d]	$AgSbF_6$	Ag_2CO_3	THF	41%
11[d]	$AgSbF_6$	$Cu(OAc)_2$	THF	59%
12[d]	$AgSbF_6$	CuO	THF	82%
13[e]	$AgSbF_6$	$Cu(OAc)_2.H_2O$	THF	68%
14[d,f]	$AgSbF_6$	$Cu(OAc)_2.H_2O$	THF	82%
15[d]	-	$Cu(OAc)_2.H_2O$	THF	22%
16[d]	$AgSbF_6$	-	THF	27%
17[d,g]	$AgSbF_6$	$Cu(OAc)_2.H_2O$	THF	nd
18[d,h]	$AgSbF_6$	$Cu(OAc)_2.H_2O$	THF	71%
19[d,i]	$AgSbF_6$	$Cu(OAc)_2.H_2O$	THF	83%
20[d,j]	$AgSbF_6$	$Cu(OAc)_2.H_2O$	THF	87%
21[d,k]	$AgSbF_6$	$Cu(OAc)_2.H_2O$	THF	59%

[a]Reaction conditions: **1a** (1 equiv, 0.2 mmol), **2b** (2 equiv, 0.4 mmol), $[RuCl_2(p\text{-cymene})]_2$ (5 mol %), $AgSbF_6$ (20 mol %), $Cu(OAc)_2.H_2O$ (1 equiv, 0.2 mmol), THF (0.2 M) at 100 °C

under air for 12 h. [b]isolated yield. [c]under N_2. [d]$AgSbF_6$ (40 mol %). [e]Reaction was carried out at 80 °C. [f]Reaction was carried out at 120 °C. [g]reaction without catalyst. [h]20 mol% $Cu(OAc)_2.H_2O$ was used, [i]40 mol% $Cu(OAc)_2.H_2O$ was used, [j]2 equiv $Cu(OAc)_2.H_2O$ was used. [k]$Pd(OAc)_2$ was used instead of $[RuCl_2(p\text{-cymene})]_2$. nd = not detected.

4.3 RESULTS AND DISCUSSION

We started the optimization for alkenylation of *N*-phenylpyridones, by taking 1-phenylpyridin-2(1*H*)-one **1a** as the substrate and acrylate **2b** as the reaction partner with $[RuCl_2(p\text{-cymene})]_2$ (5 mol %) as the catalyst, $AgSbF_6$ (20 mol %) as the additive and $Cu(OAc)_2.H_2O$ (1 equiv) as oxidant in DMF at 100 °C under air for 12 h, but we got only 22% yield of the desired product (Table 4.1, entry 1). After getting the product, we experimented with a variety of solvents such as dioxane, DCE and THF (Table 4.1, entries 2-4). To our delight, we observed 74% yield using THF as the solvent. We also attempted this reaction under nitrogen atmosphere, however the yield of the product dropped drastically to 14% (Table 4.1, entry 5). By keeping other parameter fixed, when we increased the loading of $AgSbF_6$ to 40 mol %, the yield of the product raised to 90% (Table 4.1, entry 6). We then examined with different silver additives such as AgOTf, $AgBF_4$ and $AgNTf_2$ and found that they all yielded lesser than $AgSbF_6$ (Table 4.1, entries 7-9). Finally, to see how the oxidants affect the results, we explored a variety of oxidants (Ag_2CO_3, $Cu(OAc)_2$, CuO) and found inferior results in all cases (Table 4.1, entries 10-12). When the reaction temperature was lowered, or raised, the product yield was reduced (Table 4.1, entries 13-14). Further, control experiments were performed to have better understanding of the effects of additives, oxidants, and catalysts (Table 4.1, entries 15-17). The desired product was not found in the absence of the catalyst (Table 4.1, entry 17) and in the absence of the additive/oxidant lower yields of the product were obtained (Table 4.1, entries 15-16). From this control experiment, it is revealed that additive, oxidant, and catalyst all are

essential in this process. Further, we screened the loading of $Cu(OAc)_2.H_2O$ (20 mol%, 40 mol%, 2 equiv). With 20 mol % and 40 mol % loading of $Cu(OAc)_2.H_2O$ lower yield was observed whereas with 2 equivalents almost similar reactivity as that of 1 equivalent of $Cu(OAc)_2.H_2O$ was observed. (Table 4.1, entries 18-20). We tried this reaction with $Pd(OAc)_2$ and obtained 59% of the alkenylated product (Table 4.1, entry 21).

After obtaining the optimum reaction conditions for alkenylation of *N*-phenylpyridones, we investigated the scope of different substituted 1-phenylpyridin-2(1*H*)-one **1** (Scheme 4.2) under the standard reaction conditions using benzylacrylate as reacting partner. Neutral 1-phenylpyridin-2(1*H*)-one **1a** delivered the desired product **3aa** in 62% yield. Then, upon varying the different electron donating substituent (-OMe, -Me) at the *p*-position of phenyl ring, it gave 60% and 67% of the alkenylated product **3ba**, **3ca** respectively. After that, we examined the effect of halogen group (-Cl) at the *p*-position which resulted in 74% yield of product **3da**. Electron withdrawing group at the *p*-position ($-NO_2$, -COMe) gave the desired product **3ea** and **3fa** in 59% and 53% yield respectively. Substrate bearing a fluoro substituent at the *m*-position of the phenyl ring gave a mixture of regioisomers (**3ga**:**3g'a**/1:1.5). It might be due to fluorine atom exerting considerable secondary directing group effect through which it is coordinating to metal and stabilizing the intermediate.[8] In addition to that, when we tried few more reactions with *m*-substituted substrates (-OMe, -Me and $-CF_3$), in all the cases the alkenylation occurred selectively at less hindered position (**3ha**, **3ia** and **3ja)** in good yields (72%, 69% and 76%). This could be due to the steric hindrance of the *m*-substituted substrates, that are not allowing the metal to activate the C-H bond at the more hindered site. Furthermore, substrates bearing amino and methyl group at ortho position of the benzene ring gave only a trace amount of desired product. Whereas, methoxy group at the *ortho*-position of the benzene

ring gave the alkenylated product **3ma** in moderate yield. We also examined the impact of methyl substituent on the directing group, which gave the product **3na** in 63% yield.

Then, we explored the effect of different acrylate derivatives **2** (Scheme 4.2). 1-phenylpyridin-2(1*H*)-one **1a** reacted well with various acrylates having different alkyl group and furnished 52-91% yield of the desired product **3ab-3ag**. Under the same reaction conditions, acrylates with a free -OH group also tolerated well and gave the corresponding product **3ah** in 70% yield. Moreover, acrylates with an electronically biased phenyl ring reacted smoothly to give the product **3ai** in 85% yield. In addition, we tried our methodology with acrylonitrile, which yielded the target product **3aj** with mixture of both *E* and *Z* isomers (1:1.7) in 88% yield.[9] In addition, we also tested the effect of different electron donating substituent on the *N*-phenylpyridone (-Me and -OMe) with different acrylate (**2i** and **2h**). In both cases we obtained corresponding product **3ci**, **3bh** in 78% and 66% yield respectively. *N*-phenylpyridone containing different halogen group at the *p*-position (-F and -Cl) reacted well with methacrylate leading to product **3sb**, **3db** in 93% and 85% yield respectively. Under the standard reaction conditions maleimide and quinone were found to be unreactive. Notably, by using alkyne as the reacting partner, 19% of the alkenylated product **3as** was observed. Our methodology is not limited to *N*-arylpyridone. Indeed, other substrates such as carbonyl protected indoline, carbonyl protected aniline gave alkenylated product **3pa**, **3qa** in 57%, 61% respectively.

A variety of olefins synthesized from the core structure of drug molecules (Scheme 4.3) were used to demonstrate the efficacy of this methodology (Ibuprofen, Geraniol, Naproxen, Umbelliferone, Estrogen and Pregnenolone). Good yields (53%-84%) of the product **3ak-3ap** was observed in all cases. Additionally, the drug molecule pirfenidone was subjected to our

Scheme 4.2: Scope of 1-phenylpyridin-2(1*H*)-ones and acrylates for the Synthesis of alkenylated products

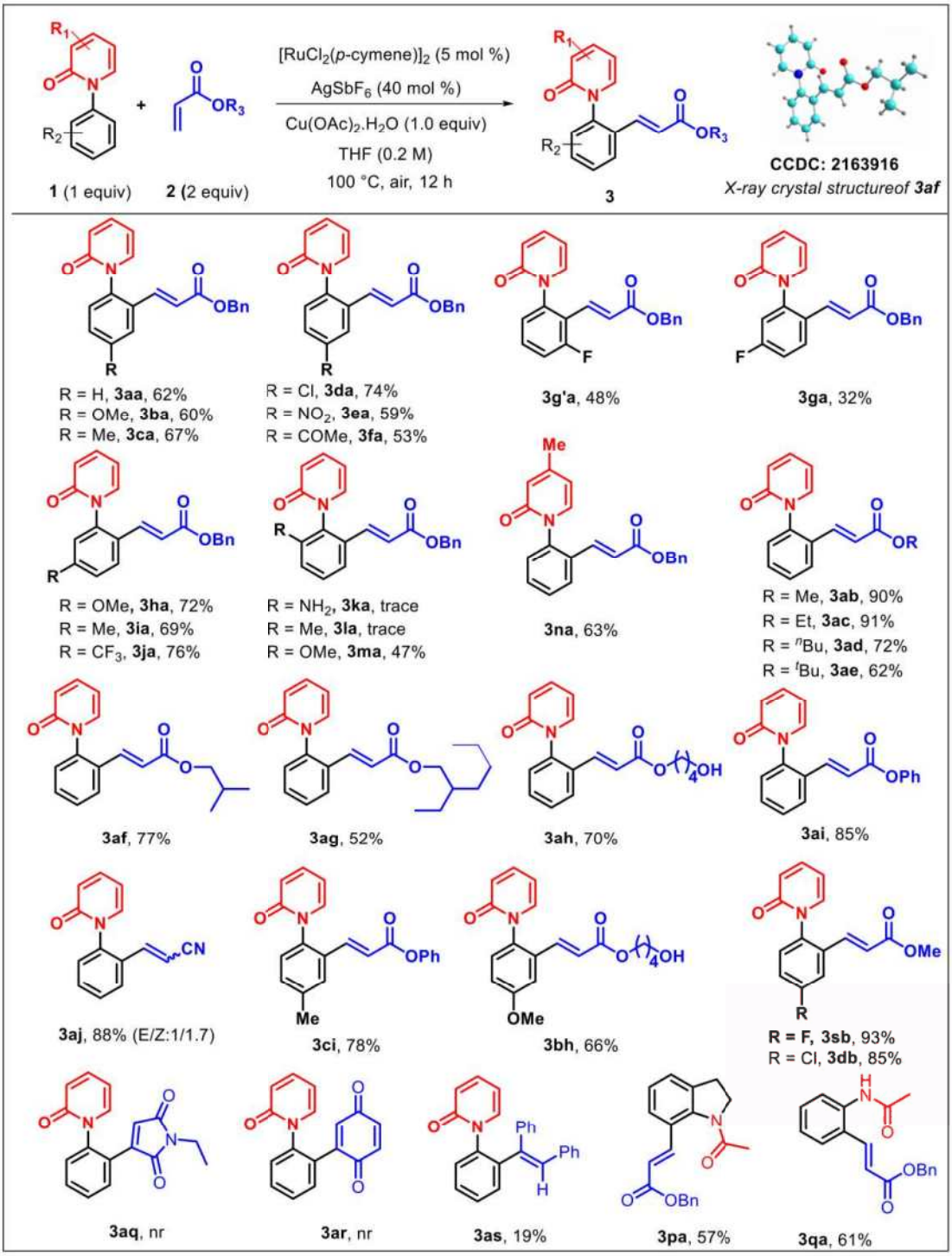

[a]Reaction conditions: **1a** (1.0 equiv), **2a** (2.0 equiv), $[RuCl_2(p\text{-cymene})]_2$ (5 mol %), $AgSbF_6$ (40 mol %), $Cu(OAc)_2.H_2O$ (1 equiv), THF (0.2 M), 100 °C under air for 12 h.

Scheme 4.3: Scope of olefins derived from drugs and natural products

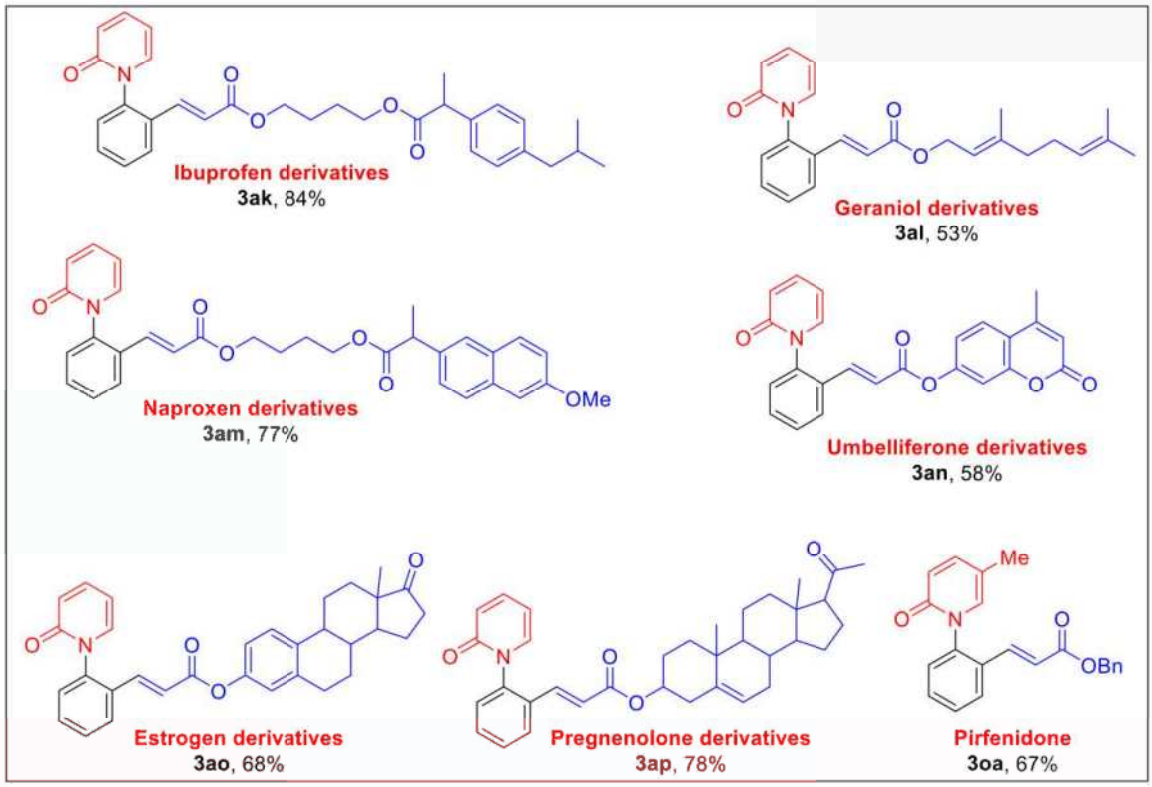

methodology using benzyl acrylate as the reacting partner which gave the desired product **3oa** in 67% yield.

To gain insight into the reaction mechanism some experiments was conducted (Scheme 4.4). The reaction was performed with D_2O and the starting material *N*-phenylpyridone has been recovered with 13% D incorporation at ortho position (Scheme 4.4a). It suggests that C–H activation pathway is reversible in nature. In order to ascertain whether the reaction proceeds through a radical pathway, the reaction was performed in the presence of 1 equiv of TEMPO and BHT. In both cases we obtained good yield of product **3ab** (59% and 83%, Scheme 4.4b). This demonstrates that the reaction is going through a non-radical pathway. Most crucially, high resolution mass spectrometer (HRMS) was used to detect the six-membered ruthenium complex, which confirms our proposed catalytic cycle (Scheme 4.4c). To demonstrate the synthetic usefulness, a 1 mmol scale reaction was conducted, which gave the product **3ab** (184 mg) in 72% yield (Scheme 4.4d). In addition to that, the

Scheme 4.4: Mechanistic studies and synthetic utility

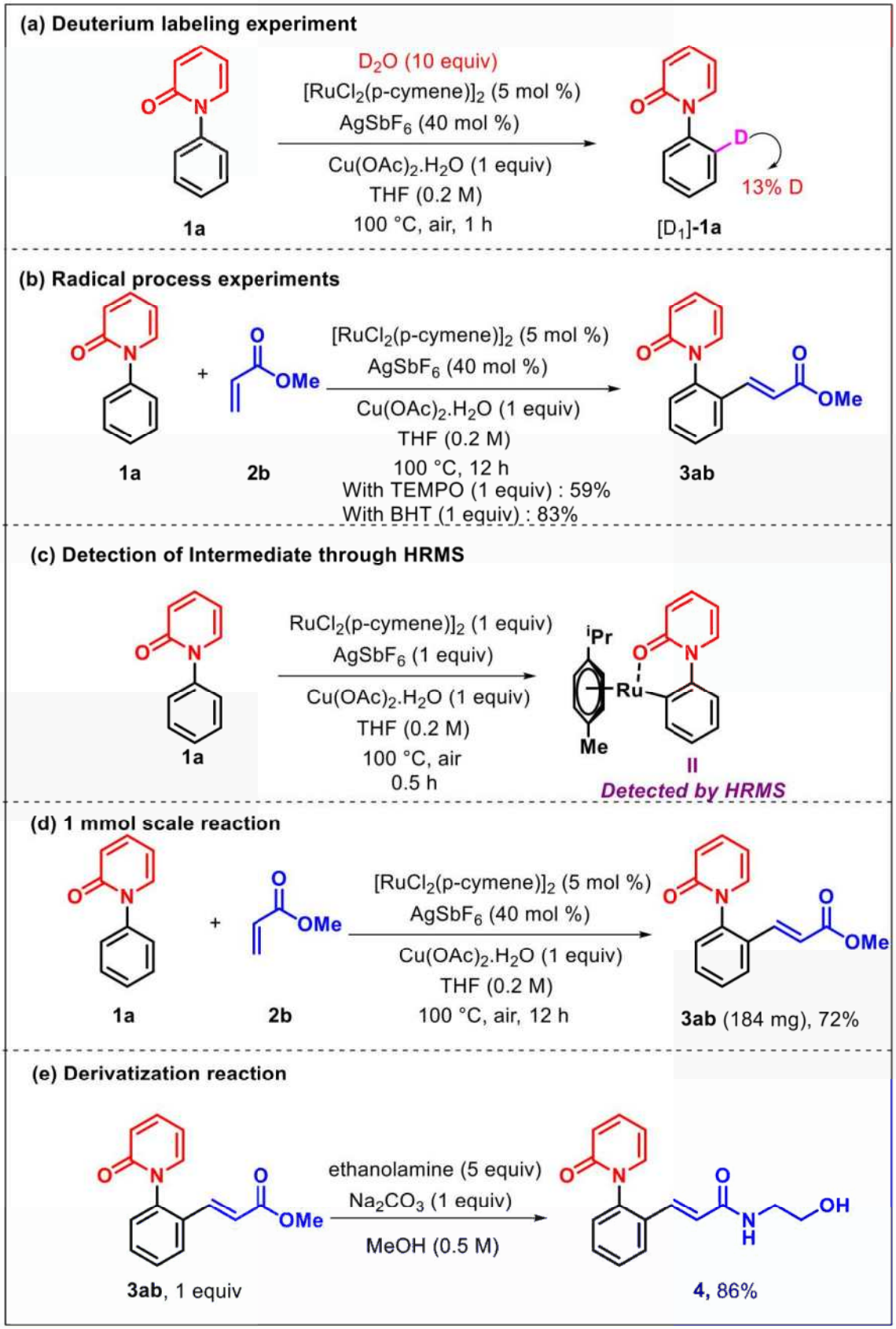

ester group present in **3ab** converted into secondary amide **4** with an 86% yield (Scheme 4.4e).

Based on mechanistic experiment and earlier literature reports,[10] a plausible reaction mechanism was proposed for the alkenylation of *N*-phenylpyridone (Scheme 4.5). Active catalyst **I** is formed in the presence of $Cu(OAc)_2.H_2O$ and $AgSbF_6$. The first step involves coordination of *N*-phenylpyridone **1a** with an active ruthenium catalyst followed by C-H metalation leading to the formation of a six membered ruthenium complex **II** (detected by HRMS) (refer to see page no. 157). Coordination followed by insertion of acrylate **2** with intermediate **II** gives intermediate **III**. Finally *β*-hydride elimination forming the desired product **3**, and the active catalyst is regenerated by reoxidation using $Cu(OAc)_2.H_2O$ and air.

Scheme 4.5: Proposed Catalytic cycle

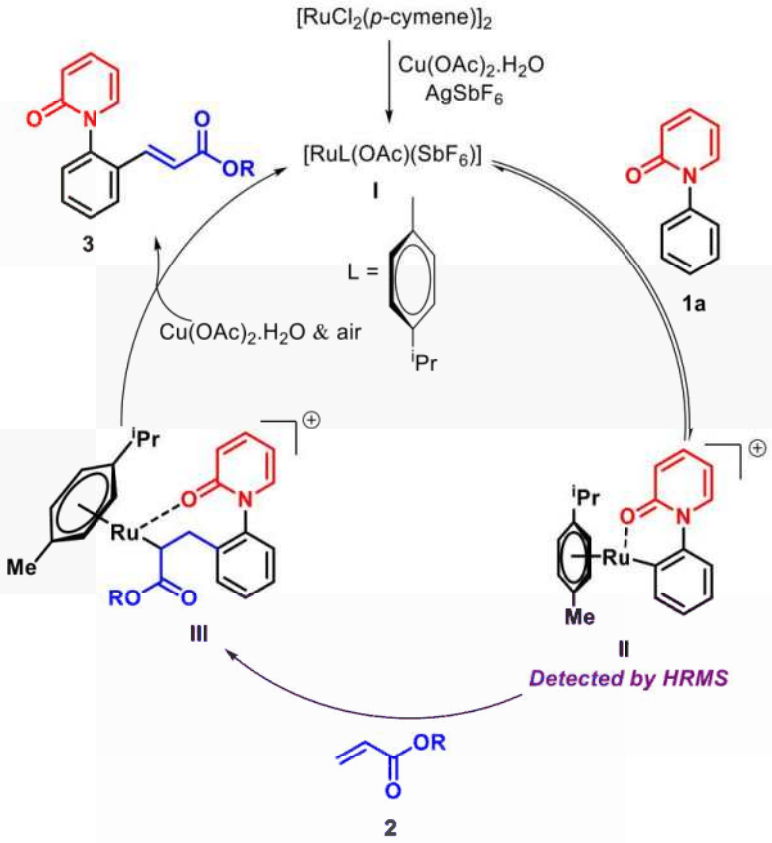

In above case $Cu(OAc)_2.H_2O$ is acting as the terminal oxidant, whereas in absence of $Cu(OAc)_2.H_2O$ (in presence of air) 27% of the alkenylated product was forming. Based on the earlier literature[11] reports we proposed the plausible mechanism for the alkenylation of *N*-phenylpyridone in presence of air (Scheme 4.6). The mechanism proceeds via removal of AgCl precipitate from the $[RuCl_2(p\text{-cymene})]_2$ complex in presence of $AgSbF_6$ forming the active ruthenium catalyst. The first step involves coordination of *N*-phenylpyridone **1a** with an active ruthenium catalyst followed by C–H metalation leading to the formation of a six membered ruthenium complex **II** (detected by HRMS). Coordination followed by insertion of acrylate **2** with intermediate **II** gives intermediate **III**. Finally, *β*-hydride

Scheme 4.6: Plausible Mechanism in presence of air

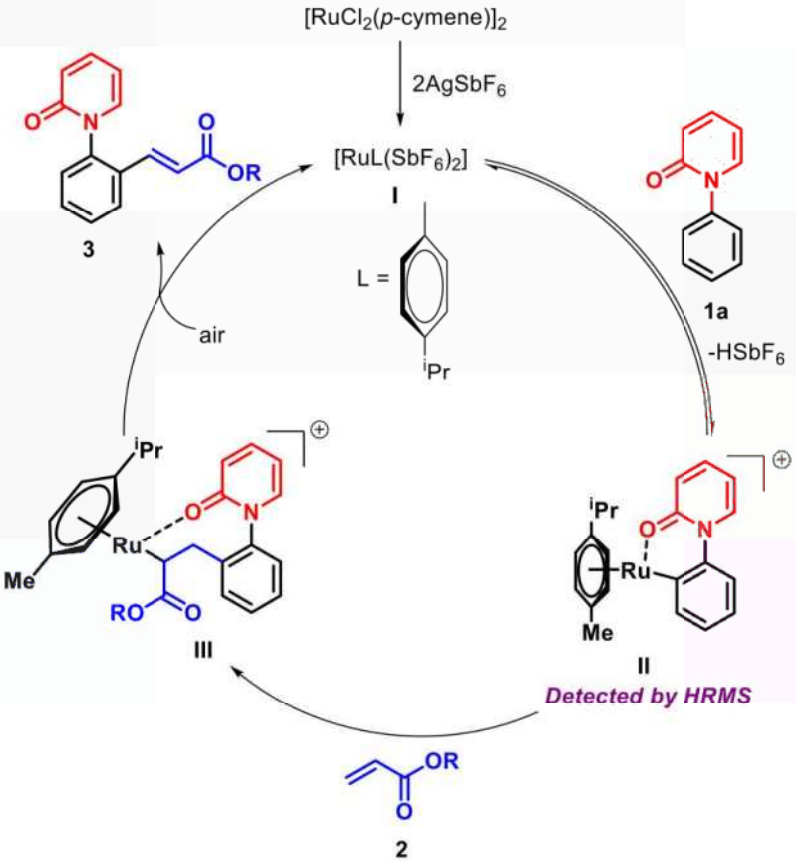

elimination gives the alkenylated product and Ru(II)-hydrido complex. Ru-hydrido complex undergoes reductive elimination to form Ru(0) intermediate, which is oxidized in

presence of air regenerates the active Ru(II) catalyst for the next catalytic cycle**.** Oxygen in the atmosphere assists in recycling the oxidant.

4.4 CONCLUSION

In conclusion, using pyridone as a weakly chelating directing group, a less expensive ruthenium catalyzed C-H alkenylation method was developed. This approach has been demonstrated with a variety of substrates. To prove the usefulness of the methodology, a variety of olefins derived from drug molecules (geraniol, ibuprofen, naproxen, umbelliferone, pregnenolone, estrogen, pirfenidone) was tested. Most crucially, by HRMS the six-membered ruthenacycle was detected, which confirming our proposed catalytic cycle.

4.5 EXPERIMENTAL SECTION[12]

Reactions were performed using borosil sealed tube vial under air atmosphere. Column chromatography was done by using 230-400 mesh silica gel of Acme synthetic chemicals company. A gradient elution was performed by using distilled petroleum ether and ethyl acetate. Merck TLC Silica gel 60 F_{254} aluminum plates were used. TLC plates detected under UV light at 254 nm and vanillin. ^{1}H NMR, $^{13}C\{^{1}H\}$ NMR and ^{19}F NMR were recorded on Bruker AV 400 and 700 MHz spectrometer using $CDCl_3$ as the deuterated solvent.[13] Multiplicity (s = singlet, d = doublet, t = triplet, q = quartet, m = multiplet, dd = doublet of doublets, br = broad signal), integration, and coupling constants (*J*) in hertz (Hz). HRMS signal analysis was performed using micro TOF Q-II mass spectrometer. Reagents and starting materials were purchased from Sigma Aldrich, TCI, Avra, Spectrochem and other commercially available sources, used without further purification unless otherwise noted. All *N*-phenylpyridones were prepared according to the reported literature procedure.[14]

4.5.1 General procedure for the synthesis of *1-phenylpyridin-2(1H)-one*:[14] Substrates 1-phenylpyridin-2(1*H*)-ones were prepared according to the reported procedures. All substrates **1** (except **1c**, **1e-1o**, **1s**) are known compounds, and their spectral data were in agreement with the corresponding literature values.

To a 25 ml Schlenk tube were added substituted pyridine-2(1*H*)-ones (0.6 mmol, 1.0 equiv), aryl iodides (1.2 mmol, 2.0 equiv), anhydrous potassium carbonate (0.6 mmol, 1.0 equiv), CuI (0.06 mmol, 0.1 equiv) and anhydrous dimethylformamide (0.67 M). The mixture was stirred at 150 °C under N_2 for 6 h. After that, reaction was cooled down to room temperature, the solvent was removed under reduced pressure and the residue was purified by column chromatography on silica gel using EtOAc:Hexane gradient elution to give the corresponding product **1**.

4.5.2 General procedure for the synthesis of acrylate:[15] The mixture of alcohols (1.0 mmol, 1.0 equiv) and Et_3N (1.5 mmol, 1.5 equiv) in dry DCM (0.3 M) was cooled to 0 °C in an ice-water bath and acryloyl chloride (1.2 mmol, 1.2 equiv) was added dropwise. The mixture was warmed to room temperature and stirred overnight. The solvent was removed under reduced pressure and the residue was purified by column chromatography on silica gel using EtOAc:Hexane gradient elution to give the corresponding product **2**.

4.5.3 General procedure for the synthesis of alkyl (*E*)-3-(2-(2-oxopyridin-1(2*H*)-yl)phenyl)acrylate:

To a flame-dried teflon-screw-capped tube was equipped with a magnetic stir bar, $[RuCl_2(p\text{-cymene})]_2$ (0.01 mmol, 5 mol%), THF (0.2 M), 1-phenylpyridin-2(1*H*)-one **1** (0.2 mmol, 1.0 equiv), acrylate **2** (0.4 mmol, 2.0 equiv), $Cu(OAc)_2.H_2O$ (0.2 mmol, 1.0 equiv) were added sequentially under air and $AgSbF_6$ (0.08 mmol, 40 mol%) were added inside the glove box and sealed. The sealed tube was directly put into a pre-heated aluminum block at 100 °C and stirred for 12 h. After completion of the reaction, the resulting mixture

was cooled down to room temperature, diluted with EtOAc, filtered through a short pad of celite. The filtrate was pre-absorbed on silica gel and concentrated by rotary evaporator. The crude product was purified by silica gel column chromatography (DCM:EtOAc = 50:50) to afford the product **3**.

4.5.4 Experimental characterization data for starting materials:

1-(4-Fluorophenyl)pyridin-2(1*H*)-one (1s):

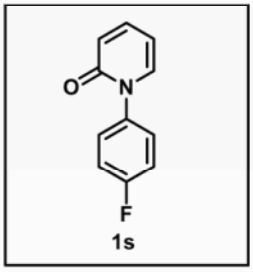

1s

Physical state: brown solid (75 mg, 66% yield). mp: 140–142 °C. *Rf*: 0.7 (50% EtOAc/DCM). ^{1}H NMR (700 MHz, $CDCl_3$): δ 7.41–7.39 (m, 1H), 7.37–7.35 (m, 2H), 7.31 (dd, J = 7.0, 1.4 Hz, 1H), 7.18–7.16 (m, 2H), 6.64 (d, J = 9.1 Hz, 1H), 6.25 (t, J = 7.0 Hz, 1H). ^{13}C{^{1}H} NMR (175 MHz, $CDCl_3$): δ 162.9 (d, $J_{C\text{-}F}$ = 318.5 Hz), 161.7, 140.3, 138.1, 137.1 (d, $J_{C\text{-}F}$ = 12.6 Hz), 128.6 (d, $J_{C\text{-}F}$ = 35.0 Hz), 122.1, 116.5 (d, $J_{C\text{-}F}$ = 91.7 Hz), 106.3. ^{19}F NMR (376 MHz, $CDCl_3$): δ -112.7. IR (KBr, cm^{-1}): 3038, 1653, 1582, 1136, 762. HRMS (ESI) m/z: $[M + H]^+$ calcd for $C_{11}H_9NOF$, 190.0663; found, 190.0664.

1-(*p*-Tolyl)pyridin-2(1*H*)-one (1c):

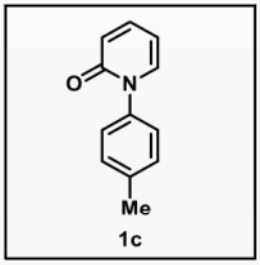

1c

Physical state: colorless solid (104 mg, 94% yield). mp: 138–140 °C. *Rf*: 0.5 (50% EtOAc/DCM). ^{1}H NMR ($CDCl_3$, 400 MHz): δ 7.40–7.36 (m, 1H), 7.33–7.24 (m, 5H), 6.65 (d, J = 9.2 Hz, 1H), 6.22 (t, J = 6.4 Hz, 1H), 2.40 (s, 3H). ^{13}C{^{1}H} NMR ($CDCl_3$, 100 MHz): δ 162.9, 140.1, 138.8, 138.7, 138.4, 130.2, 126.6, 122.1, 106.1, 21.4. IR (KBr, cm^{-1}): 3031, 1668, 1588, 1276. HRMS (ESI) m/z: $[M + H]^+$ calcd for $C_{12}H_{12}NO$, 186.0913; found, 186.0922.

1-(4-Nitrophenyl)pyridin-2(1*H*)-one (1e):

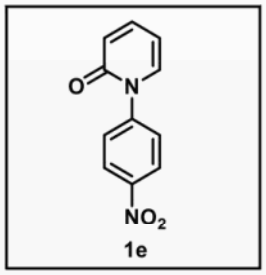

1e

Physical state: yellow solid (67 mg, 52% yield). mp: 193–195 °C. R_f: 0.6 (50% EtOAc/DCM). ^{1}H NMR ($CDCl_3$, 400 MHz): δ 8.36 (d, J = 8.8 Hz, 2H), 7.63 (d, J = 8.8 Hz, 2H), 7.47–7.42 (m, 1H), 7.35–7.33 (m, 1H), 6.68 (d, J = 9.2 Hz, 1H), 6.33 (t, J = 6.8 Hz, 1H). ^{13}C{^{1}H} NMR ($CDCl_3$, 100 MHz): δ 162.1, 147.6, 146.3, 140.7, 137.0, 128.0, 125.0, 122.6, 107.1. IR (KBr, cm^{-1}): 3073, 1673, 1532, 1346, 1284. HRMS (ESI) m/z: $[M + H]^+$ calcd for $C_{11}H_9N_2O_3$, 217.0608; found, 217.0605.

1-(4-Acetylphenyl)pyridin-2(1*H*)-one (1f):

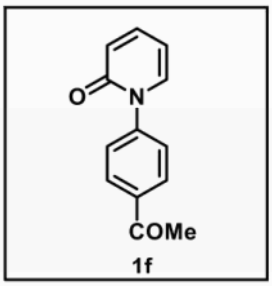

1f

Physical state: brown solid (86 mg, 67% yield). mp: 160–162 °C. R_f: 0.3 (50% EtOAc/DCM). ^{1}H NMR ($CDCl_3$, 700 MHz): δ 8.08 (d, J = 8.4 Hz, 2H), 7.50 (d, J = 8.4 Hz, 2H), 7.43–7.41 (m, 1H), 7.34 (dd, J = 6.3, 1.4 Hz, 1H), 6.66 (d, J = 9.1 Hz, 1H), 6.29 (t, J = 6.3 Hz, 1H), 2.64 (s, 3H). ^{13}C{^{1}H} NMR ($CDCl_3$, 175 MHz): δ 197.2, 162.3, 144.9, 140.4, 137.5, 137.0, 129.7, 127.1, 122.4, 106.7, 27.0. IR (KBr, cm^{-1}): 3054, 1669, 1608, 1531, 1263. HRMS (ESI) m/z: $[M + H]^+$ calcd for $C_{13}H_{12}NO_2$, 214.0863; found, 214.0853.

1-(3-Fluorophenyl)pyridin-2(1*H*)-one (1g):

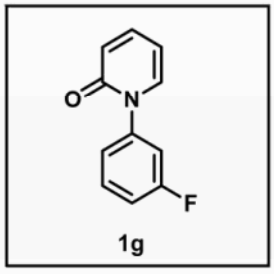

1g

Physical state: colorless solid (64 mg, 56% yield). mp: 113–115 °C. R_f: 0.75 (50% EtOAc/DCM). ^{1}H NMR ($CDCl_3$, 400 MHz): δ 7.47–7.37 (m, 2H), 7.31 (dd, J = 6.8, 2.0 Hz, 1H), 7.17–7.09 (m, 3H), 6.62 (d, J = 9.2 Hz, 1H), 6.20 (t, J = 6.8 Hz, 1H). ^{13}C{^{1}H} NMR ($CDCl_3$, 100 MHz): δ 162.7 (d, $J_{C\text{-}F}$ = 246.3 Hz), 162.2, 142.2 (d, $J_{C\text{-}F}$ = 9.8 Hz), 140.2, 137.7, 130.7 (d, $J_{C\text{-}F}$ = 9.0 Hz), 122.4 (d, $J_{C\text{-}F}$ = 3.2 Hz),

122.0, 115.7 (d, $J_{C\text{-}F}$ = 20.8 Hz), 114.6 (d, $J_{C\text{-}F}$ = 23.8 Hz), 106.3. ^{19}F NMR (376 MHz, $CDCl_3$): δ -111.0. IR (KBr, cm^{-1}): 3083, 1673, 1537, 1262, 689. HRMS (ESI) m/z: $[M + H]^+$ calcd for $C_{11}H_9FNO$, 190.0663; found, 190.0652.

1-(3-Methoxyphenyl)pyridin-2(1*H*)-one (1h):

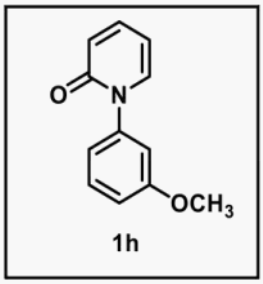

1h

Physical state: brown solid (62 mg, 51% yield). mp: 83–85 °C. R_f: 0.5 (50% EtOAc/DCM). ^1H NMR ($CDCl_3$, 400 MHz): δ 7.40–7.35 (m, 2H), 7.32 (d, J = 6.8 Hz, 1H), 6.96–6.92 (m, 3H), 6.63 (d, J = 9.6 Hz, 1H), 6.22 (t, J = 6.8 Hz, 1H), 3.81 (s, 3H). $^{13}C\{^1H\}$ NMR ($CDCl_3$, 100 MHz): δ 162.5, 160.3, 142.1, 140.1, 138.2, 130.2, 121.9, 118.8, 114.6, 112.5, 106.0, 55.6. IR (KBr, cm^{-1}): 2959, 1662, 1584, 1293. HRMS (ESI) m/z: $[M + H]^+$ calcd for $C_{12}H_{12}NO_2$, 202.0868; found, 202.0863.

1-(m-Tolyl)pyridin-2(1H)-one (1i):

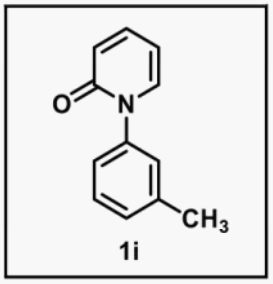

1i

Physical state: yellow solid (48 mg, 43% yield). mp: 68–70 °C. R_f: 0.55 (50% EtOAc/DCM). ^1H NMR ($CDCl_3$, 700 MHz): δ 7.40–7.36 (m, 2H), 7.32 (dd, J = 7.0, 2.1 Hz, 1H), 7.23 (d, J = 7.7 Hz, 1H), 7.19 (s, 1H), 7.16 (d, J = 7.7 Hz, 1H), 6.65 (d, J = 9.1 Hz, 1H), 6.22 (t, J = 7.0 Hz, 1H), 2.41 (s, 3H). $^{13}C\{^1H\}$ NMR ($CDCl_3$, 175 MHz): δ 162.8, 141.3, 140.1, 139.8, 138.4, 129.7, 129.5, 127.5, 123.9, 122.2, 106.1, 21.7. IR (KBr, cm^{-1}): 2959, 1721, 1536, 1287. HRMS (ESI) m/z: $[M + H]^+$ calcd for $C_{12}H_{12}NO$, 186.0919; found, 186.0914.

1-(3-(Trifluoromethyl)phenyl)pyridin-2(1*H*)-one (1j):

Physical state: colorless solid (86 mg, 60% yield). mp: 76–78 °C. R_f: 0.7 (50% EtOAc/DCM). ^1H NMR ($CDCl_3$, 400 MHz): δ 7.68–7.61 (m, 4H), 7.44–7.40 (m, 1H), 7.34–7.32 (m, 1H), 6.65 (d, J = 9.6 Hz, 1H), 6.28 (t, J = 6.8 Hz, 1H). $^{13}C\{^1H\}$ NMR ($CDCl_3$, 100 MHz): δ 162.3, 141.5, 140.5, 137.6, 132.0 (q, $J_{C\text{-}F}$ = 32.9 Hz), 130.5, 130.2, 125.5 (q, $J_{C\text{-}F}$ =

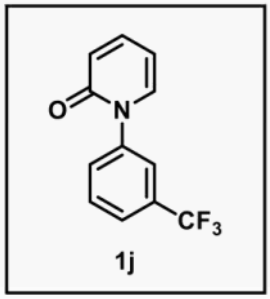

1j

3.7 Hz), 123.9 (q, $J_{C\text{-}F}$ = 3.7 Hz), 123.7 (q, $J_{C\text{-}F}$ = 270.8 Hz), 122.2, 106.7. ^{19}F NMR (376 MHz, $CDCl_3$): δ -62.6. IR (KBr, cm^{-1}): 2959, 1659, 1447, 1331, 810. HRMS (ESI) m/z: $[M + H]^+$ calcd for $C_{12}H_9F_3NO$, 240.0636; found, 240.0632.

1-(2-Aminophenyl)pyridin-2(1*H*)-one (1k):

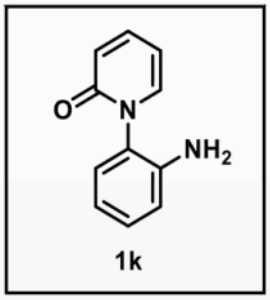

1k

Physical state: pink liquid (25 mg, 22% yield). R_f: 0.65 (50% EtOAc/Hexane). ^{1}H NMR ($CDCl_3$, 400 MHz): δ 8.22 (d, J = 4.4 Hz, 1H), 7.67 (t, J = 8.4 Hz, 1H), 7.07–6.97 (m, 3H), 6.86 (t, J = 8.0 Hz, 2H), 6.79 (t, J = 7.6 Hz, 1H), 3.77 (s, 2H). $^{13}C\{^1H\}$ NMR ($CDCl_3$, 175 MHz): δ 163.8, 148.4, 141.3, 139.8, 139.5, 126.3, 122.5, 119.3, 118.8, 117.2, 110.8. IR (KBr, cm^{-1}): 3360, 2962, 1726, 1430, 1193. HRMS (ESI) m/z: $[M + Na]^+$ calcd for $C_{11}H_{10}N_2ONa$, 209.0685; found, 209.0699.

1-(o-Tolyl)pyridin-2(1*H*)-one (1l):

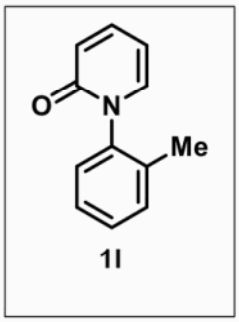

1l

Physical state: colorless solid (71 mg, 64% yield). mp: 73–75 °C. R_f: 0.3 (50% EtOAc/Hexane). ^{1}H NMR ($CDCl_3$, 400 MHz): δ 7.44–7.40 (m, 1H), 7.34–7.30 (m, 3H), 7.20–7.17 (m, 2H), 6.67 (d, J = 9.2 Hz, 1H), 6.24 (t, J = 6.8 Hz, 1H), 2.16 (s, 3H). $^{13}C\{^1H\}$ NMR ($CDCl_3$, 100 MHz): δ 162.5, 140.5, 140.3, 138.3, 135.3, 131.4, 129.4, 127.4, 127.4, 122.2, 106.1, 17.8. IR (KBr, cm^{-1}): 2959, 1721, 1534, 1278. HRMS (ESI) m/z: $[M + Na]^+$ calcd for $C_{12}H_{11}NONa$, 208.0733; found, 208.0731.

1-(2-Methoxyphenyl)pyridin-2(1*H*)-one (1m):

Physical state: colorless solid (57 mg, 47% yield). mp: 129–131 °C. R_f: 0.5 (50% EtOAc/DCM). ^{1}H NMR (400 MHz, $CDCl_3$): δ 7.43–7.37 (m, 2H), 7.26 (d, J = 6.8 Hz, 1H), 7.20 (dd, J = 6.8, 1.6 Hz, 1H), 7.07–7.03 (m, 2H), 6.65 (d, J = 9.2 Hz, 1H), 6.20 (t, J = 6.8

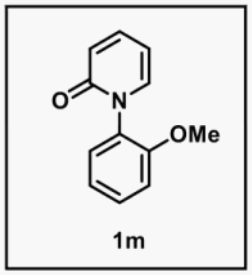

1m

Hz, 1H), 3.81 (s, 3H). $^{13}C\{^{1}H\}$ NMR (100 MHz, $CDCl_3$): δ 162.7, 154.5, 140.2, 139.2, 130.6, 129.9, 128.8, 122.0, 121.2, 112.7, 105.7, 56.2. IR (KBr, cm^{-1}): 3019, 1660, 1505, 1240. HRMS (ESI) m/z: $[M + H]^+$ calcd for $C_{12}H_{12}NO_2$, 202.0863; found, 202.0861.

4-Methyl-1-phenylpyridin-2(1*H*)-one (1n):

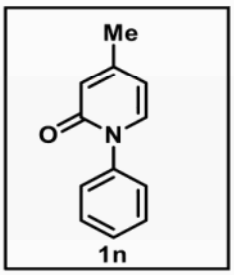

1n

Physical state: colorless solid (104 mg, 94% yield). mp: 114–116 °C. R_f: 0.3 (50% EtOAc/Hexane). ^{1}H NMR (400 MHz, $CDCl_3$): δ 7.48 (t, J = 7.2 Hz, 2H), 7.42–7.36 (m, 3H), 7.23 (d, J = 7.2 Hz, 1H), 6.47 (s, 1H), 6.09 (dd, J = 6.8, 1.6 Hz, 1H), 2.23 (s, 3H). $^{13}C\{^{1}H\}$ NMR (175 MHz, $CDCl_3$): δ 162.7, 151.9, 141.2, 137.1, 129.6, 128.7, 126.9, 120.4, 108.9, 21.7. IR (KBr, cm^{-1}): 3054, 1677, 1532, 1282. HRMS (ESI) m/z: $[M + H]^+$ calcd for $C_{12}H_{12}NO$, 186.0913; found, 186.0912.

5-Methyl-1-phenylpyridin-2(1*H*)-one (1o):

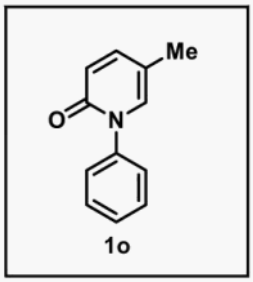

1o

Physical state: colorless solid (90 mg, 81% yield). mp: 109–111 °C. R_f: 0.5 (50% EtOAc/Hexane). ^{1}H NMR (700 MHz, $CDCl_3$): δ 7.47 (t, J = 7.7 Hz, 2H), 7.41–7.36 (m, 3H), 7.26 (dd, J = 9.8, 2.8 Hz, 1H), 7.11 (s, 1H), 6.60 (d, J = 9.1 Hz, 1H), 2.09 (s, 3H). $^{13}C\{^{1}H\}$ NMR (175 MHz, $CDCl_3$): δ 162.0, 142.8, 141.4, 135.6, 129.5, 128.6, 126.8, 121.7, 115.1, 17.2. IR (KBr, cm^{-1}): 3063, 1667, 1532, 1282. HRMS (ESI) m/z: $[M + Na]^+$ calcd for $C_{12}H_{11}NONa$, 208.0733; found, 208.0734.

4-((2-(4-Isobutylphenyl)propanoyl)oxy)butyl acrylate (2k):

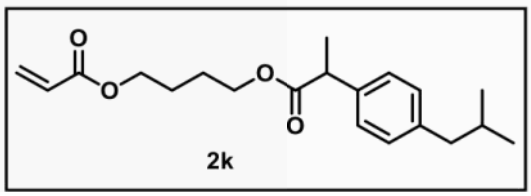

2k

Physical state: colorless liquid (292 mg, 88% yield). R_f: 0.4 (10% EtOAc/Hexane). ^{1}H NMR (700 MHz, $CDCl_3$): δ 7.19 (d, J = 8.4 Hz, 2H),

7.08 (d, J = 7.7 Hz, 2H), 6.38 (d, J = 17.5 Hz, 1H), 6.12–6.08 (m, 1H), 5.81 (d, J = 10.5 Hz, 1H), 4.12–4.08 (m, 4H), 3.68 (q, J = 7.0 Hz, 1H), 2.44 (d, J = 7.7 Hz, 2H), 1.86–1.82 (m, 1H), 1.69–1.60 (m, 4H), 1.49 (d, J = 7.0 Hz, 3H), 0.89 (d, J = 7.0 Hz, 6H). $^{13}C\{^1H\}$ NMR (175 MHz, $CDCl_3$): δ 175.0, 166.5, 140.8, 138.1, 131.0, 129.6, 128.8, 127.4, 64.4, 64.3, 45.5, 45.3, 30.5, 25.6, 25.5, 22.7, 18.7. IR (KBr, cm^{-1}): 2955, 2865, 1732, 1407, 1186. HRMS (ESI) m/z: $[M + Na]^+$ calcd for $C_{20}H_{28}O_4Na$, 355.1880; found, 355.1875.

4-((2-(6-Methoxynaphthalen-2-yl)propanoyl)oxy)butyl acrylate (2m):

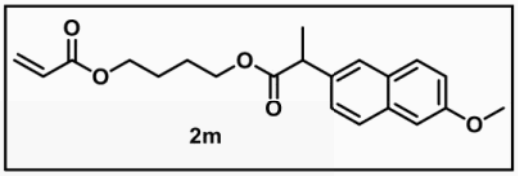

2m

Physical state: colorless liquid (267 mg, 75% yield). R_f: 0.45 (10% EtOAc/Hexane). ^1H NMR (700 MHz, $CDCl_3$): δ 7.69–7.66 (m, 3H), 7.39 (d, J = 8.4 Hz, 1H), 7.14–7.09 (m, 2H), 6.35 (d, J = 16.8 Hz, 1H), 6.08–6.04 (m, 1H), 5.78 (d, J = 10.5 Hz, 1H), 4.11–4.07 (m, 4H), 3.88 (s, 3H), 3.84 (q, J = 7.0 Hz, 1H), 1.66–1.57 (m, 7H). $^{13}C\{^1H\}$ NMR (175 MHz, $CDCl_3$): δ 174.9, 166.4, 157.9, 135.9, 133.9, 130.9, 129.5, 129.2, 128.7, 127.4, 126.4, 126.2, 119.2, 105.8, 64.4, 64.2, 55.5, 45.7, 25.5, 25.4, 18.7. IR (KBr, cm^{-1}): 2962, 2900, 1732, 1606, 1182. HRMS (ESI) m/z: $[M + Na]^+$ calcd for $C_{21}H_{24}O_5Na$, 379.1516; found, 379.1513.

Experimental characterization data for alkenylated products:

Benzyl (*E*)-3-(2-(2-oxopyridin-1(2*H*)-yl)phenyl)acrylate (3aa):

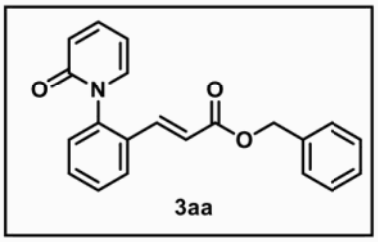

3aa

Physical state: yellow solid (41 mg, 62% yield). mp: 117–119 °C. R_f: 0.6 (50% EtOAc/DCM). ^1H NMR ($CDCl_3$, 400 MHz): δ 7.77–7.75 (m, 1H), 7.54–7.43 (m, 4H), 7.36–7.26 (m, 6H), 7.17 (dd, J = 6.8, 2.0 Hz, 1H), 6.68 (d, J = 9.6 Hz, 1H), 6.45 (d, J = 15.6 Hz, 1H), 6.26 (t, J = 6.8 Hz, 1H), 5.18 (s, 2H). $^{13}C\{^1H\}$ NMR ($CDCl_3$, 100 MHz): δ 166.3, 162.7, 140.7, 140.5, 139.4, 138.3, 136.2, 131.9, 131.6, 129.8, 128.8,

128.6, 128.5, 128.4, 127.8, 122.4, 121.3, 106.5, 66.7. IR (KBr, cm^{-1}): 3068, 3038, 1676, 1564, 1279. HRMS (ESI) m/z: $[M + Na]^+$ calcd for $C_{21}H_{17}NO_3Na$, 354.1101; found, 354.1091.

Benzyl (*E*)-3-(5-methoxy-2-(2-oxopyridin-1(2*H*)-yl)phenyl)acrylate (3ba):

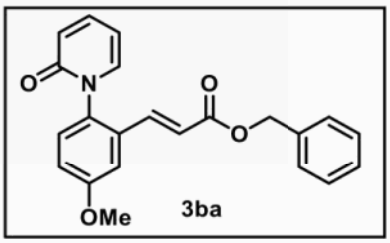

3ba

Physical state: colorless solid (43 mg, 60% yield). mp: 106–108 °C. R_f: 0.48 (50% EtOAc/DCM). ^1H NMR ($CDCl_3$, 700 MHz): δ 7.46–7.43 (m, 1H), 7.40 (d, J = 15.4 Hz, 1H), 7.37–7.31 (m, 5H), 7.22 (dd, J = 6.3, 3.5 Hz, 2H), 7.17 (dd, J = 7.0, 2.1 Hz, 1H), 7.04 (dd, J = 9.1, 2.8 Hz, 1H), 6.68 (d, J = 9.1 Hz, 1H), 6.44 (d, J = 16.1 Hz, 1H), 6.25 (t, J = 6.3 Hz, 1H), 5.18 (s, 2H), 3.86 (s, 3H). $^{13}C\{^1H\}$ NMR ($CDCl_3$, 175 MHz): δ 166.3, 163.1, 160.2, 140.7, 139.5, 138.7, 136.1, 133.6, 132.8, 129.7, 128.9, 128.6, 128.5, 122.3, 121.4, 117.5, 112.2, 106.4, 66.8, 56.0. IR (KBr, cm^{-1}): 3078, 2955, 1659, 1579, 1248. HRMS (ESI) m/z: $[M + Na]^+$ calcd for $C_{22}H_{19}NO_4Na$, 384.1206; found, 384.1232.

Benzyl (*E*)-3-(5-methyl-2-(2-oxopyridin-1(2*H*)-yl)phenyl)acrylate (3ca):

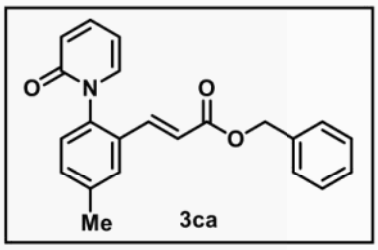

3ca

Physical state: colorless solid (46 mg, 67% yield). mp: 135–137 °C. R_f: 0.7 (50% EtOAc/DCM). ^1H NMR ($CDCl_3$, 700 MHz): δ 7.56 (s, 1H), 7.46–7.41 (m, 2H), 7.37–7.32 (m, 6H), 7.19–7.16 (m, 2H), 6.68 (d, J = 9.1 Hz, 1H), 6.44 (d, J = 16.1 Hz, 1H), 6.25 (t, J = 6.3 Hz, 1H), 5.18 (s, 2H), 2.42 (s, 3H). $^{13}C\{^1H\}$ NMR ($CDCl_3$, 175 MHz): δ 166.4, 162.9, 140.7, 139.9, 139.6, 138.5, 138.1, 136.2, 132.4, 131.5, 128.9, 128.5, 128.4, 128.3, 128.3, 122.3, 121.0, 106.4, 66.7, 21.6. IR (KBr, cm^{-1}): 3068, 2958, 1712, 1662, 1589, 1281. HRMS (ESI) m/z: $[M + Na]^+$ calcd for $C_{22}H_{19}NO_3Na$, 368.1257; found, 368.1253.

Benzyl (*E*)-3-(5-chloro-2-(2-oxopyridin-1(2*H*)-yl)phenyl)acrylate (3da):

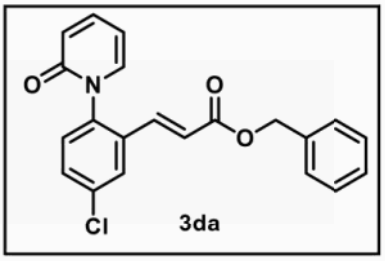

Physical state: brown solid (54 mg, 74% yield). mp: 144–146 °C. *Rf*: 0.6 (50% EtOAc/DCM). ^{1}H NMR ($CDCl_3$, 700 MHz): δ 7.75 (s, 1H), 7.51–7.47 (m, 2H), 7.40–7.35 (m, 5H), 7.28 (d, J = 8.4 Hz, 2H), 7.16 (dd, J = 6.3, 1.4 Hz, 1H), 6.70 (d, J = 9.1 Hz, 1H), 6.48 (d, J = 16.1 Hz, 1H), 6.30 (t, J = 7.0 Hz, 1H), 5.21 (s, 2H). ^{13}C{^{1}H} NMR ($CDCl_3$, 175 MHz): δ 166.0, 162.6, 140.9, 138.8, 138.2, 138.0, 136.0, 135.9, 133.6, 131.5, 130.0, 128.9, 128.6, 128.5, 127.8, 122.6, 122.5, 106.8, 66.9. IR (KBr, cm^{-1}): 3064, 2923, 1713, 1668, 1171, 977. HRMS (ESI) m/z: [M + Na]$^{+}$ calcd for $C_{21}H_{16}ClNO_3Na$, 388.0711; found, 388.0708.

Benzyl (*E*)-3-(5-nitro-2-(2-oxopyridin-1(2*H*)-yl)phenyl)acrylate (3ea):

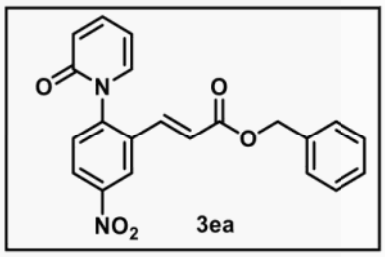

Physical state: yellow solid (44 mg, 59% yield). mp: 168–170 °C. *Rf*: 0.7 (50% EtOAc/DCM). ^{1}H NMR ($CDCl_3$, 700 MHz): δ 8.62 (s, 1H), 8.35 (dd, J = 9.1, 2.8 Hz, 1H), 7.50 (d, J = 9.1 Hz, 1H), 7.51–7.49 (m, 1H), 7.44 (d, J = 16.1 Hz, 1H), 7.39–7.33 (m, 5H), 7.15 (dd, J = 7.0, 2.1 Hz, 1H), 6.70 (d, J = 9.8 Hz, 1H), 6.63 (d, J = 15.4 Hz, 1H), 6.34 (t, J = 6.3 Hz, 1H), 5.21 (s, 2H). ^{13}C{^{1}H} NMR ($CDCl_3$, 175 MHz): δ 165.6, 162.1, 148.4, 145.1, 141.3, 137.3, 137.1, 135.8, 134.0, 130.3, 128.9, 128.7, 128.6, 125.7, 124.1, 123.0, 122.7, 107.2, 67.2. IR (KBr, cm^{-1}): 3078, 2952, 1718, 1675, 1348, 1284. HRMS (ESI) m/z: [M + Na]$^{+}$ calcd for $C_{21}H_{16}N_2O_5Na$, 399.0951; found, 399.0945.

Benzyl (*E*)-3-(5-acetyl-2-(2-oxopyridin-1(2*H*)-yl)phenyl)acrylate (3fa):

Physical state: colorless liquid (44 mg, 59% yield). *Rf*: 0.45 (50% EtOAc/DCM). ^{1}H NMR ($CDCl_3$, 700 MHz): δ 8.34 (s, 1H), 8.08 (dd, J = 8.4, 1.4 Hz, 1H), 7.49–7.43 (m, 3H), 7.38–7.34 (m, 5H), 7.16 (d, J = 6.3 Hz, 1H), 6.70 (d, J = 9.8 Hz, 1H), 6.58 (d, J = 16.1 Hz, 1H),

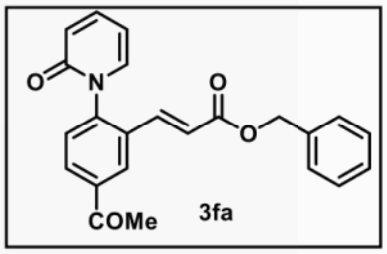

3fa

6.31 (t, J = 6.3 Hz, 1H), 5.20 (s, 2H), 2.66 (s, 3H). $^{13}C\{^{1}H\}$ NMR ($CDCl_3$, 175 MHz): δ 196.8, 166.1, 162.4, 143.9, 141.0, 138.6, 138.1, 137.6, 136.0, 132.6, 131.0, 129.2, 128.9, 128.7, 128.5, 127.9, 122.6, 122.6, 106.9, 67.0, 27.1. IR (KBr, cm^{-1}): 3069, 3034, 1716, 1661, 1532, 1281. HRMS (ESI) m/z: $[M + Na]^+$ calcd for $C_{23}H_{19}NO_4Na$, 396.1206; found, 396.1181.

Benzyl (*E*)-3-(2-fluoro-6-(2-oxopyridin-1(2*H*)-yl)phenyl)acrylate (3ga):

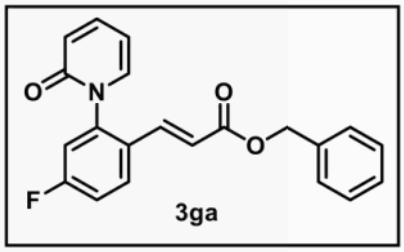

3ga

Physical state: colorless liquid (22 mg, 32% yield). R_f: 0.85 (50% EtOAc/DCM). ^{1}H NMR ($CDCl_3$, 700 MHz): δ 7.76 (dd, J = 9.1, 6.3 Hz, 1H), 7.48–7.45 (m, 1H), 7.39–7.32 (m, 6H), 7.23–7.20 (m, 1H), 7.16 (d, J = 6.3 Hz, 1H), 7.07 (dd, J = 8.4, 2.1 Hz, 1H), 6.69 (d, J = 9.8 Hz, 1H), 6.40 (d, J = 16.1 Hz, 1H), 6.29 (t, J = 6.3 Hz, 1H), 5.18 (s, 2H). $^{13}C\{^{1}H\}$ NMR ($CDCl_3$, 175 MHz): δ 166.3, 164.0 (d, $J_{C\text{-}F}$ = 254.0 Hz), 162.4, 141.7 (d, $J_{C\text{-}F}$ = 10.0 Hz), 141.0, 138.4, 137.8, 136.1, 129.6 (d, $J_{C\text{-}F}$ = 9.2 Hz), 128.9, 128.6, 128.5, 128.4 (d, $J_{C\text{-}F}$ = 3.9 Hz), 122.6, 121.1 (d, $J_{C\text{-}F}$ = 1.8 Hz), 117.4 (d, $J_{C\text{-}F}$ = 21.6 Hz), 116.4 (d, $J_{C\text{-}F}$ = 23.4 Hz), 106.8, 66.8. ^{19}F NMR (376 MHz, $CDCl_3$): δ -107.5. IR (KBr, cm^{-1}): 3066, 2966, 1718, 1669, 1168, 764. HRMS (ESI) m/z: $[M + H]^+$ calcd for $C_{21}H_{17}FNO_3$, 350.1187; found, 350.1178.

Benzyl (*E*)-3-(4-fluoro-2-(2-oxopyridin-1(2*H*)-yl)phenyl)acrylate (3g'a):

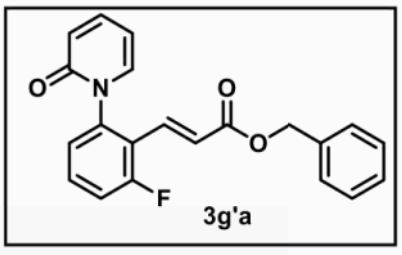

3g'a

Physical state: colorless liquid (34 mg, 48% yield). R_f: 0.75 (50% EtOAc/DCM). ^{1}H NMR ($CDCl_3$, 400 MHz): δ 7.48–7.41 (m, 2H), 7.37–7.32 (m, 5H), 7.30–7.21 (m, 2H), 7.15–7.11 (m, 2H), 6.66 (d, J = 9.2 Hz, 1H), 6.59 (d, J = 16.4 Hz, 1H), 6.26 (t, J = 6.8 Hz, 1H), 5.18 (s, 2H). $^{13}C\{^{1}H\}$ NMR ($CDCl_3$, 175 MHz): δ 166.6, 162.5, 162.3 (d, $J_{C\text{-}F}$ = 256.4 Hz), 141.8 (d, $J_{C\text{-}F}$ = 5.1 Hz), 141.0, 137.9,

136.1, 133.6, 131.6 (d, $J_{C\text{-}F}$ = 10.6 Hz), 128.9, 128.6, 128.5, 125.5 (d, $J_{C\text{-}F}$ = 13.7 Hz), 124.5 (d, $J_{C\text{-}F}$ = 3.3 Hz), 122.5, 121.0 (d, $J_{C\text{-}F}$ = 13.0 Hz), 117.6 (d, $J_{C\text{-}F}$ = 23.0 Hz), 106.8, 66.8. ^{19}F NMR (376 MHz, $CDCl_3$): δ -108.3. IR (KBr, cm^{-1}): 3084, 3035, 1718, 1667, 1172, 753. HRMS (ESI) m/z: $[M + Na]^+$ calcd for $C_{21}H_{16}FNO_3Na$, 372.1006; found, 372.0998.

Benzyl (*E*)-3-(4-methoxy-2-(2-oxopyridin-1(2*H*)-yl)phenyl)acrylate (3ha):

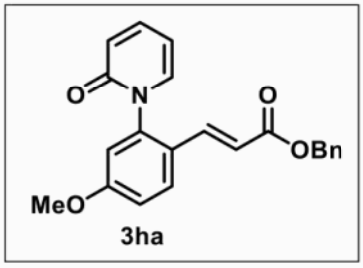

3ha

Physical state: colorless liquid (52 mg, 72% yield). R_f: 0.6 (50% EtOAc/DCM). ^{1}H NMR ($CDCl_3$, 700 MHz): δ 7.70 (d, J = 9.1 Hz, 1H), 7.47–7.44 (m, 1H), 7.38–7.31 (m, 6H), 7.17 (dd, J = 7.0, 2.1 Hz, 1H), 7.02 (dd, J = 8.4, 2.1 Hz, 1H), 6.81 (d, J = 2.8 Hz, 1H), 6.69 (d, J = 9.1 Hz, 1H), 6.33 (d, J = 15.4 Hz, 1H), 6.26 (td, J = 6.3, 1.4 Hz, 1H), 5.17 (s, 2H), 3.85 (s, 3H). ^{13}C{^{1}H} NMR ($CDCl_3$, 175 MHz): δ 166.7, 162.7, 162.2, 141.9, 140.7, 139.1, 138.2, 136.4, 129.1, 128.9, 128.5, 128.4, 124.2, 122.5, 118.8, 116.3, 113.7, 106.5, 66.6, 56.1. IR (KBr, cm^{-1}): 2957, 1684, 1553, 1366, 1165. HRMS (ESI) m/z: $[M + Na]^+$ calcd for $C_{22}H_{19}NO_4Na$, 384.1206; found, 384.1223.

Benzyl (*E*)-3-(4-methyl-2-(2-oxopyridin-1(2*H*)-yl)phenyl)acrylate (3ia):

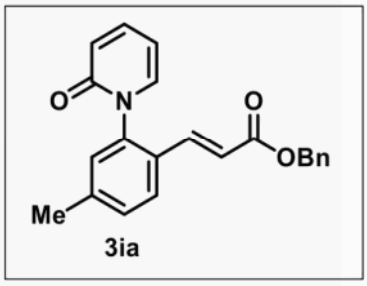

3ia

Physical state: colorless solid (48 mg, 69% yield). mp: 97–99 °C. R_f: 0.7 (50% EtOAc/DCM). ^{1}H NMR ($CDCl_3$, 700 MHz): δ 7.65 (d, J = 7.7 Hz, 1H), 7.46–7.43 (m, 1H), 7.41 (d, J = 16.1 Hz, 1H), 7.36–7.31 (m, 5H), 7.28 (d, J = 8.4 Hz, 1H), 7.16 (dd, J = 7.0, 2.1 Hz, 1H), 7.11 (s, 1H), 6.68 (d, J = 9.1 Hz, 1H), 6.41 (d, J = 15.4 Hz, 1H), 6.25 (t, J = 6.3 Hz, 1H), 5.17 (s, 2H), 2.41 (s, 3H). ^{13}C{^{1}H} NMR ($CDCl_3$, 175 MHz): δ 166.5, 162.8, 142.5, 140.7, 140.5, 139.4, 138.3, 136.3, 130.7, 129.1, 129.0, 128.8, 128.5, 128.4, 127.7, 122.4, 120.2, 106.4, 66.6, 21.6. IR (KBr, cm^{-1}): 2959, 1687, 1556, 1371, 1225. HRMS (ESI) m/z: $[M + H]^+$ calcd for $C_{22}H_{20}NO_3$, 346.1443; found, 346.1438.

Benzyl (*E*)-3-(2-(2-oxopyridin-1(2*H*)-yl)-4-(trifluoromethyl)phenyl)acrylate (3ja):

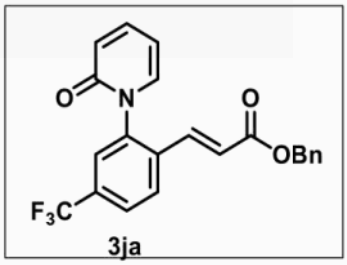

3ja

Physical state: colorless liquid (61 mg, 76% yield). R_f: 0.5 (30% EtOAc/DCM). ^{1}H NMR ($CDCl_3$, 700 MHz): δ 7.87 (d, J = 8.4 Hz, 1H), 7.74 (d, J = 8.4 Hz, 1H), 7.58 (s, 1H), 7.49–7.44 (m, 2H), 7.38–7.33 (m, 4H), 7.26 (s, 1H), 7.17 (d, J = 6.3 Hz, 1H), 6.69 (d, J = 9.1 Hz, 1H), 6.53 (d, J = 16.1 Hz, 1H), 6.31 (t, J = 6.3 Hz, 1H), 5.20 (s, 2H). ^{13}C{^{1}H} NMR ($CDCl_3$, 175 MHz): δ 165.9, 162.4, 141.1, 140.7, 138.1, 137.7, 136.0, 135.8, 133.3 (q, $J_{C\text{-}F}$ = 33.1 Hz), 128.9, 128.7, 128.5, 128.5, 126.7 (q, $J_{C\text{-}F}$ = 3.5 Hz), 126.0 (q, $J_{C\text{-}F}$ = 3.7 Hz), 123.7, 123.4 (q, $J_{C\text{-}F}$ = 270.9 Hz), 122.6, 107.0, 67.0. ^{19}F NMR (376 MHz, $CDCl_3$): δ -62.8. IR (KBr, cm^{-1}): 2958, 1684, 1598, 1499, 1333, 1282. HRMS (ESI) m/z: $[M + Na]^+$ calcd for $C_{22}H_{16}F_3NO_3Na$, 422.0974; found, 422.0958.

Benzyl (*E*)-3-(3-amino-2-(2-oxopyridin-1(2*H*)-yl)phenyl)acrylate (3ka):

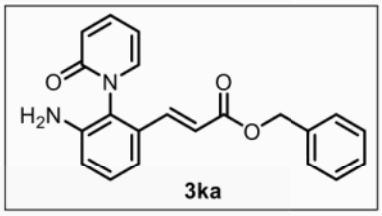

3ka

The residue was submitted for HRMS giving the product in trace amount. HRMS (ESI) m/z: $[M + Na]^+$ calcd for $C_{21}H_{18}N_2O_3Na$, 369.1210; found 369.1199.

Benzyl (*E*)-3-(3-methyl-2-(2-oxopyridin-1(2*H*)-yl)phenyl)acrylate (3la):

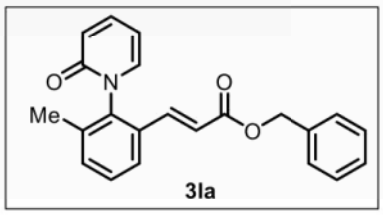

3la

The residue was submitted for HRMS giving the product in trace amount. HRMS (ESI) m/z: $[M + Na]^+$ calcd for $C_{22}H_{19}NO_3Na$, 368.1257; found 368.1280.

Benzyl (*E*)-3-(3-methoxy-2-(2-oxopyridin-1(2*H*)-yl)phenyl)acrylate (3ma):

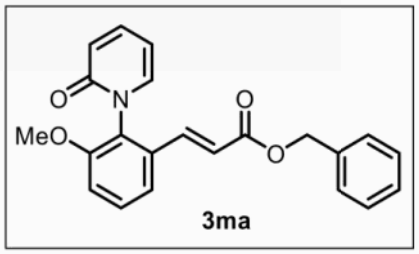

3ma

Physical state: colorless liquid (34 mg, 47% yield). R_f: 0.8 (50% EtOAc/DCM). ^{1}H NMR ($CDCl_3$, 400 MHz): δ 7.47–7.39 (m, 3H), 7.36–7.31 (m, 6H), 7.09–7.05 (m, 2H), 6.69 (d, J = 9.2 Hz, 1H), 6.44 (d, J = 15.6 Hz, 1H), 6.25 (t, J = 6.4 Hz, 1H), 5.17 (s, 2H), 3.81 (s, 3H). ^{13}C{^{1}H} NMR ($CDCl_3$, 175 MHz): δ 166.4, 162.7, 155.3, 140.7, 139.4, 139.0, 136.2, 133.4, 130.5, 128.9, 128.5, 128.4, 122.4, 121.8, 119.2, 113.8, 106.4, 66.7, 56.5. IR (KBr, cm^{-1}): 3028, 2942, 1714, 1663, 1285. HRMS (ESI) m/z: [M + H]$^+$ calcd for $C_{22}H_{20}NO_4$, 362.1387; found, 362.1411.

Benzyl (*E*)-3-(2-(4-methyl-2-oxopyridin-1(2*H*)-yl)phenyl)acrylate (3na):

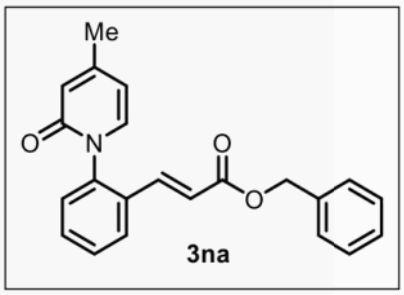

3na

Physical state: colorless liquid (43 mg, 63% yield). R_f: 0.6 (50% EtOAc/DCM). ^{1}H NMR ($CDCl_3$, 400 MHz): δ 7.76 (d, J = 7.6 Hz, 1H), 7.53–7.45 (m, 3H), 7.36–7.33 (m, 5H), 7.29 (d, J = 7.6 Hz, 1H), 7.07 (d, J = 7.2 Hz, 1H), 6.47 (d, J = 16.0 Hz, 2H), 6.12 (d, J = 7.2 Hz, 1H), 5.19 (s, 2H), 2.26 (s, 3H). ^{13}C{^{1}H} NMR ($CDCl_3$, 175 MHz): δ 166.5, 162.7, 152.5, 140.6, 139.7, 137.1, 136.2, 132.1, 131.5, 129.7, 128.9, 128.8, 128.6, 128.5, 127.8, 121.2, 120.5, 109.2, 66.8, 21.8. IR (KBr, cm^{-1}): 3065, 1713, 1661, 1583, 1280. HRMS (ESI) m/z: [M + H]$^+$ calcd for $C_{22}H_{20}NO_3$, 346.1438; found, 346.1456.

Benzyl (*E*)-3-(2-(5-methyl-2-oxopyridin-1(2*H*)-yl)phenyl)acrylate (3oa):

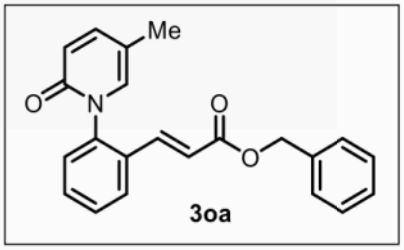

3oa

Physical state: colorless liquid (46 mg, 67% yield). R_f: 0.5 (50% EtOAc/DCM). ^{1}H NMR ($CDCl_3$, 700 MHz): δ 7.75 (d, J = 7.7 Hz, 1H), 7.51 (t, J = 7.7 Hz, 1H), 7.48–7.45 (m, 2H), 7.37–7.30 (m, 6H), 7.28 (d, J = 7.7 Hz, 1H), 6.95 (s, 1H), 6.63 (d, J = 9.1 Hz, 1H), 6.46 (d, J = 16.1 Hz, 1H), 5.19 (s, 2H), 2.09 (s,

3H). $^{13}C\{^1H\}$ NMR ($CDCl_3$, 175 MHz): δ 166.5, 162.1, 143.5, 140.8, 139.6, 136.2, 135.4, 132.0, 131.6, 129.7, 128.9, 128.7, 128.5, 128.4, 127.8, 121.9, 121.2, 115.5, 66.7, 17.3. IR (KBr, cm^{-1}): 3063, 2926, 1713, 1674, 1532, 1281. HRMS (ESI) m/z: $[M + H]^+$ calcd for $C_{22}H_{20}NO_3$, 346.1438; found, 346.1417.

Methyl (*E*)-3-(2-(2-oxopyridin-1(2*H*)-yl)phenyl)acrylate (3ab):

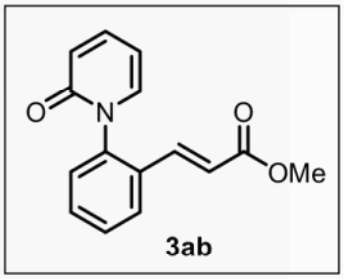

3ab

Physical state: brown solid (46 mg, 90% yield). mp: 87–89 °C. R_f: 0.2 (50% EtOAc/DCM). ^1H NMR (400 MHz, $CDCl_3$): δ 7.76 (dd, J = 7.2, 1.6 Hz, 1H), 7.55–7.44 (m, 3H), 7.41 (d, J = 16.0 Hz, 1H), 7.30 (dd, J = 8.0, 2.0 Hz, 1H), 7.18 (dd, J = 6.8, 1.2 Hz, 1H), 6.69 (d, J = 9.2 Hz, 1H), 6.40 (d, J = 16.0 Hz, 1H), 6.28 (td, J = 6.4, 1.2 Hz, 1H), 3.74 (s, 3H). $^{13}C\{^1H\}$ NMR (100 MHz, $CDCl_3$): δ 167.0, 162.7, 140.8, 140.5, 139.2, 138.3, 132.1, 131.5, 129.8, 128.7, 128.0, 122.5, 121.4, 106.5, 52.1. IR (KBr, cm^{-1}): 3022, 1698, 1536, 1240. HRMS (ESI) m/z: $[M + Na]^+$ calcd for $C_{15}H_{13}NO_3Na$, 278.0788; found, 278.0776.

Ethyl (*E*)-3-(2-(2-oxopyridin-1(2*H*)-yl)phenyl)acrylate (3ac):

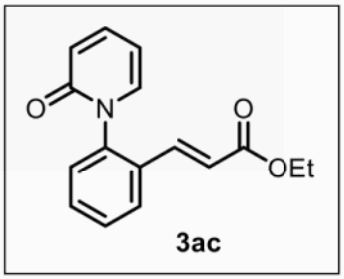

3ac

Physical state: brown solid (49 mg, 92% yield). mp: 91–93 °C. R_f: 0.5 (5% MeOH/DCM). ^1H NMR (700 MHz, $CDCl_3$): δ 7.76 (d, J = 7.7 Hz, 1H), 7.53–7.45 (m, 3H), 7.40 (d, J = 16.1 Hz, 1H), 7.30 (d, J = 7.7 Hz, 1H), 7.19 (dd, J = 7.0, 2.1 Hz, 1H), 6.69 (d, J = 9.8 Hz, 1H), 6.40 (d, J = 16.1 Hz, 1H), 6.28 (t, J = 6.3 Hz, 1H), 4.20 (q, J = 7.7 Hz, 2H), 1.10 (t, J = 7.7 Hz, 3H). $^{13}C\{^1H\}$ NMR (175 MHz, $CDCl_3$): δ 166.6, 162.7, 140.8, 140.5, 138.8, 138.3, 132.1, 131.4, 129.8, 128.6, 127.9, 122.4, 121.8, 106.5, 61.0, 14.5. IR (KBr, cm^{-1}): 3071, 2983, 1712, 1661, 1186. HRMS (ESI) m/z: $[M + Na]^+$ calcd for $C_{16}H_{15}NO_3Na$, 292.0944; found, 292.0951.

Butyl (*E*)-3-(2-(2-oxopyridin-1(2*H*)-yl)phenyl)acrylate (3ad):

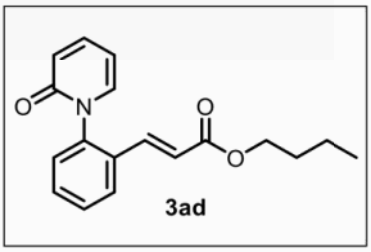

Physical state: colorless solid (43 mg, 72% yield). mp: 90–92 °C. *Rf*: 0.5 (50% EtOAc/DCM). ^{1}H NMR (400 MHz, $CDCl_3$): δ 7.77 (dd, J = 7.2, 2.0 Hz, 1H), 7.55–7.44 (m, 3H), 7.39 (d, J = 16.0 Hz, 1H), 7.31 (dd, J = 8.0, 2.0 Hz, 1H), 7.19 (dd, J = 6.8, 1.6 Hz, 1H), 6.70 (d, J = 9.2 Hz, 1H), 6.41 (d, J = 15.6 Hz, 1H), 6.28 (td, J = 6.8, 1.2 Hz, 1H), 4.14 (t, J = 6.8 Hz, 2H), 1.66–1.62 (m, 2H), 1.42–1.33 (m, 2H), 0.93 (t, J = 7.6 Hz, 3H). ^{13}C{^{1}H} NMR (100 MHz, $CDCl_3$): δ 166.7, 162.8, 140.7, 140.5, 138.8, 138.3, 132.1, 131.5, 129.8, 128.6, 127.9, 122.4, 121.8, 106.5, 64.9, 31.0, 19.5, 14.1. IR (KBr, cm^{-1}): 3065, 2959, 1709, 1661, 1279. HRMS (ESI) m/z: $[M + Na]^+$ calcd for $C_{18}H_{19}NO_3Na$, 320.1257; found, 320.1225.

Tert-butyl (*E*)-3-(2-(2-oxopyridin-1(2*H*)-yl)phenyl)acrylate (3ae):

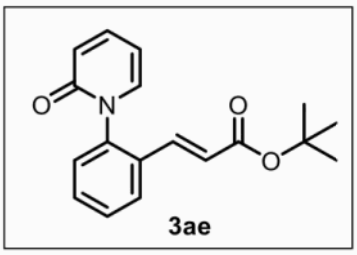

Physical state: colorless solid (37 mg, 63% yield). mp: 172–175 °C. *Rf*: 0.6 (50% EtOAc/DCM). ^{1}H NMR (400 MHz, $CDCl_3$): δ 7.77 (dd, J = 7.6, 2.0 Hz, 1H), 7.53–7.44 (m, 3H), 7.32–7.28 (m, 2H), 7.20–7.17 (m, 1H), 6.69 (d, J = 9.2 Hz, 1H), 6.36 (d, J = 16.0 Hz, 1H), 6.28 (td, J = 6.8, 1.6 Hz, 1H), 1.47 (s, 9H). ^{13}C{^{1}H} NMR (100 MHz, $CDCl_3$): δ 165.9, 162.8, 140.7, 140.5, 138.3, 137.6, 132.1, 131.2, 129.8, 128.6, 127.7, 123.6, 122.4, 106.4, 81.1, 28.4. IR (KBr, cm^{-1}): 3077, 2977, 1704, 1667, 1151. HRMS (ESI) m/z: $[M + Na]^+$ calcd for $C_{18}H_{19}NO_3Na$, 320.1257; found, 320.1284.

Isobutyl (*E*)-3-(2-(2-oxopyridin-1(2*H*)-yl)phenyl)acrylate (3af):

Physical state: colorless solid (46 mg, 77% yield). mp: 102–104 °C. *Rf*: 0.75 (50% EtOAc/DCM). ^{1}H NMR (400 MHz, $CDCl_3$): δ 7.78–7.75 (m, 1H), 7.52–7.46 (m, 2H), 7.44–7.38 (m, 2H), 7.32–7.29 (m, 1H), 7.17 (dd, J = 6.8, 2.0 Hz, 1H), 6.68 (d, J = 9.2 Hz, 1H), 6.40 (d, J = 15.6 Hz, 1H), 6.25 (t, J = 6.8 Hz, 1H), 3.92 (d, J = 6.4 Hz, 2H), 1.97–1.89 (m,

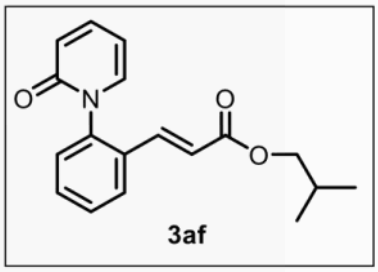

1H), 0.93 (s, 3H), 0.91 (s, 3H). $^{13}C\{^{1}H\}$ NMR (100 MHz, $CDCl_3$): δ 166.6, 162.7, 140.6, 138.9, 138.3, 132.2, 131.4, 129.8, 128.7, 127.9, 126.9, 122.5, 121.9, 106.3, 71.1, 28.1, 19.4. IR (KBr, cm^{-1}): 3068, 2962, 1662, 1532, 1279. HRMS (ESI) m/z: $[M + H]^+$ calcd for $C_{18}H_{20}NO_3$, 298.1438; found, 298.1444.

2-Ethylhexyl (*E*)-3-(2-(2-oxopyridin-1(2*H*)-yl)phenyl)acrylate (3ag):

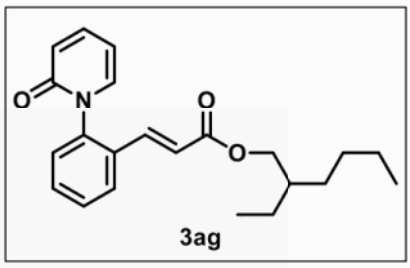

Physical state: colorless liquid (37 mg, 52% yield). R_f: 0.8 (50% EtOAc/DCM). ^{1}H NMR (400 MHz, $CDCl_3$): δ 7.78–7.76 (m, 1H), 7.53–7.41 (m, 3H), 7.38 (d, J = 16.0 Hz, 1H), 7.32–7.29 (m, 1H), 7.17 (dd, J = 6.8, 1.6 Hz, 1H), 6.68 (d, J = 9.2 Hz, 1H), 6.39 (d, J = 16.0 Hz, 1H), 6.25 (t, J = 6.8 Hz, 1H), 4.11–4.00 (m, 2H), 1.59–1.53 (m, 2H), 1.38–1.28 (m, 8H), 0.91–0.86 (m, 5H). $^{13}C\{^{1}H\}$ NMR (100 MHz, $CDCl_3$): δ 166.7, 162.7, 140.6, 138.7, 138.3, 132.2, 131.4, 129.8, 128.7, 127.9, 122.5, 122.0, 106.3, 67.4, 39.2, 30.9, 29.3, 24.3, 24.3, 23.3, 14.4, 11.4. IR (KBr, cm^{-1}): 2959, 2930, 1714, 1668, 1277. HRMS (ESI) m/z: $[M + H]^+$ calcd for $C_{22}H_{28}NO_3$, 354.2064; found, 354.2079.

4-Hydroxybutyl (*E*)-3-(2-(2-oxopyridin-1(2*H*)-yl)phenyl)acrylate (3ah):

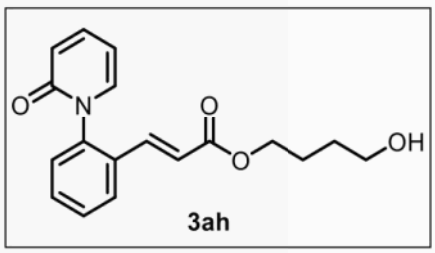

Physical state: yellow liquid (44 mg, 71% yield). R_f: 0.2 (50% EtOAc/DCM). ^{1}H NMR (700 MHz, $CDCl_3$): δ 7.77 (d, J = 7.7 Hz, 1H), 7.54–7.47 (m, 3H), 7.40 (d, J = 16.1 Hz, 1H), 7.31 (d, J = 7.7 Hz, 1H), 7.20 (d, J = 6.3 Hz, 1H), 6.70 (d, J = 9.1 Hz, 1H), 6.41 (d, J = 16.1 Hz, 1H), 6.30 (t, J = 7.0 Hz, 1H), 4.20–4.16 (m, 2H), 3.66 (t, J = 6.3 Hz, 2H), 1.76–1.72 (m, 2H), 1.64–1.60 (m, 2H). $^{13}C\{^{1}H\}$ NMR (175 MHz, $CDCl_3$): δ 166.6, 162.8, 140.9, 140.5, 139.0, 138.3, 132.0, 131.5, 129.9,

128.6, 127.8, 122.3, 121.6, 106.7, 64.8, 62.6, 29.5, 25.3. IR (KBr, cm^{-1}): 3073, 2947, 1708, 1660, 1282. HRMS (ESI) m/z: $[M + Na]^+$ calcd for $C_{18}H_{19}NO_4Na$, 336.1206; found, 336.1201.

Phenyl (*E*)-3-(2-(2-oxopyridin-1(2)-yl)phenyl)acrylate (3ai):

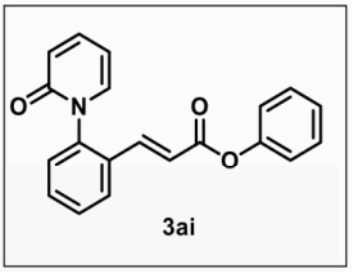

3ai

Physical state: colorless solid (54 mg, 85% yield). mp: 117–119 °C. *Rf*: 0.65 (50% EtOAc/DCM). ^1H NMR (400 MHz, $CDCl_3$): δ 7.85 (dd, J = 7.6, 1.6 Hz, 1H), 7.60–7.51 (m, 3H), 7.47–7.43 (m, 1H), 7.40–7.32 (m, 3H), 7.25–7.21 (m, 2H), 7.13–7.10 (m, 2H), 6.69 (d, J = 9.2 Hz, 1H), 6.60 (d, J = 15.6 Hz, 1H), 6.29 (td, J = 6.8, 1.2 Hz, 1H). $^{13}C\{^1H\}$ NMR (175 MHz, $CDCl_3$): δ 165.1, 162.8, 150.9, 140.9, 140.8, 140.7, 138.2, 131.9, 131.8, 129.9, 129.7, 128.7, 128.1, 126.2, 122.4, 121.9, 120.8, 106.6. IR (KBr, cm^{-1}): 3065, 1734, 1663, 1531, 1145. HRMS (ESI) m/z: $[M + Na]^+$ calcd for $C_{20}H_{15}NO_3Na$, 340.0944; found, 340.0948.

(*E*)/(*Z*)-3-(2-(2-Oxopyridin-1(2*H*)-yl)phenyl)acrylonitrile (3aj):

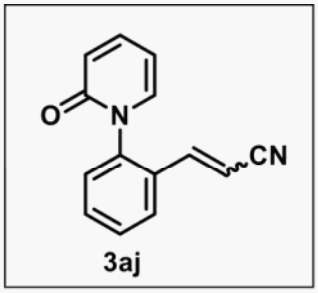

3aj

Physical state: colorless liquid (39 mg, 88% yield). *Rf*: 0.25 (50% EtOAc/Hexane). ^1H NMR (700 MHz, $CDCl_3$): δ 7.68 (d, J = 7.7 Hz, 1H), 7.58 (d, J = 7.0 Hz, 1H), 7.52 (t, J = 7.0 Hz, 1H), 7.49–7.48 (m, 1H), 7.31 (d, J = 7.7 Hz, 1H), 7.17 (d, J = 7.0 Hz, 1H), 7.15 (d, J = 16.1 Hz, 1H), 6.70 (d, J = 9.1 Hz, 1H), 6.31 (t, J = 6.3 Hz, 1H), 5.88 (d, J = 16.8 Hz, 1H). $^{13}C\{^1H\}$ NMR (175 MHz, $CDCl_3$): δ 162.5, 145.4, 141.0, 140.2, 138.0, 132.6, 131.3, 130.1, 128.8, 127.0, 122.5, 117.9, 106.9, 99.9. IR (KBr, cm^{-1}): 3064, 2219, 1661, 1532, 1280. HRMS (ESI) m/z: $[M + H]^+$ calcd for $C_{14}H_{11}N_2O$, 223.0866; found, 223.0862.

4-((2-(4-Isobutylphenyl)propanoyl)oxy)butyl(*E*)-3-(2-(2-oxopyridin-1(2*H*)-yl)phenyl)acrylate (3ak):

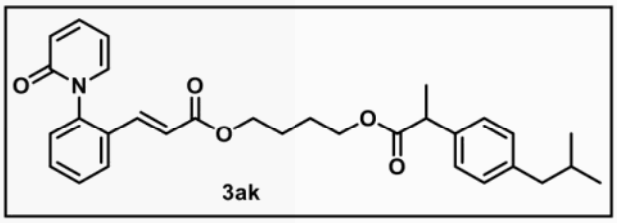

Physical state: yellow liquid (84 mg, 84% yield). R_f: 0.8 (50% EtOAc/DCM). ^{1}H NMR ($CDCl_3$, 700 MHz): δ 7.76 (d, J = 7.7 Hz, 1H), 7.51 (dt, J = 25.2, 7.7 Hz, 2H), 7.42 (t, J = 7.7 Hz, 1H), 7.38 (d, J = 16.1 Hz, 1H), 7.30 (d, J = 7.7 Hz, 1H), 7.19 (d, J = 7.7 Hz, 2H), 7.16 (t, J = 6.3 Hz, 1H), 7.08 (d, J = 7.7 Hz, 2H), 6.67 (d, J = 9.1 Hz, 1H), 6.38 (d, J = 16.1 Hz, 1H), 6.24 (t, J = 6.3 Hz, 1H), 4.11–4.06 (m, 4H), 3.69 (q, J = 7.0 Hz, 1H), 2.43 (d, J = 7.0 Hz, 2H), 1.85–1.81 (m, 1H), 1.65–1.59 (m, 4H), 1.48 (s, 3H), 0.89 (s, 3H), 0.88 (s, 3H). ^{13}C{^{1}H} NMR ($CDCl_3$, 175 MHz): δ 175.1, 166.5, 162.7, 140.9, 140.7, 140.5, 139.0, 138.3, 138.1, 132.0, 131.5, 129.8, 129.6, 128.6, 127.9, 127.5, 122.4, 121.5, 106.4, 64.4, 64.4, 45.5, 45.5, 45.3, 30.5, 25.6, 25.4, 22.7, 18.7. IR (KBr, cm^{-1}): 3073, 2950, 1732, 1716, 1172. HRMS (ESI) m/z: $[M + H]^+$ calcd for $C_{31}H_{36}NO_5$, 502.2588; found, 502.2592.

(*E*)-3,7-Dimethylocta-2,6-dien-1-yl(*E*)-3-(2-(2-oxopyridin-1(2*H*)-yl)phenyl)acrylate (3al):

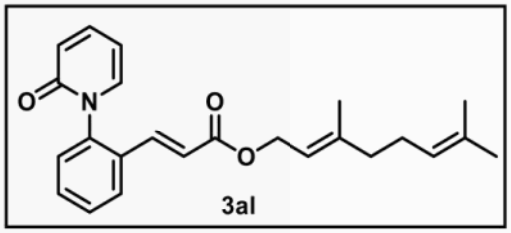

Physical state: yellow liquid (40 mg, 53% yield). R_f: 0.75 (50% EtOAc/DCM). ^{1}H NMR ($CDCl_3$, 700 MHz): δ 7.76 (d, J = 7.0 Hz, 1H), 7.53–7.44 (m, 3H), 7.41 (d, J = 16.1 Hz, 1H), 7.30 (d, J = 7.7 Hz, 1H), 7.18 (dd, J = 7.0, 2.1 Hz, 1H), 6.69 (d, J = 9.8 Hz, 1H), 6.42 (d, J = 16.1 Hz, 1H), 6.27 (t, J = 6.3 Hz, 1H), 5.35 (t, J = 7.0 Hz, 1H), 5.08 (t, J = 6.3 Hz, 1H), 4.66 (d, J = 7.0 Hz, 2H), 2.12-2.09 (m, 2H), 2.05–2.03 (m,

2H), 1.71 (s, 3H), 1.68 (s, 3H), 1.60 (s, 3H). $^{13}C\{^1H\}$ NMR ($CDCl_3$, 175 MHz): δ 166.6, 162.8, 142.9, 140.7, 140.5, 138.9, 138.3, 132.2, 132.1, 131.4, 129.8, 128.7, 127.9, 124.1, 122.5, 121.8, 118.5, 106.5, 61.9, 39.9, 26.7, 26.0, 18.0, 16.9. IR (KBr, cm^{-1}): 3077, 2972, 1713, 1668, 1282. HRMS (ESI) m/z: $[M + Na]^+$ calcd for $C_{24}H_{27}NO_3Na$, 400.1883; found, 400.1884.

4-((2-(6-Methoxynaphthalen-2-yl)propanoyl)oxy)butyl(*E*)-3-(2-(2-oxopyridin-1(2*H*)-yl)phenyl)acrylate (3am):

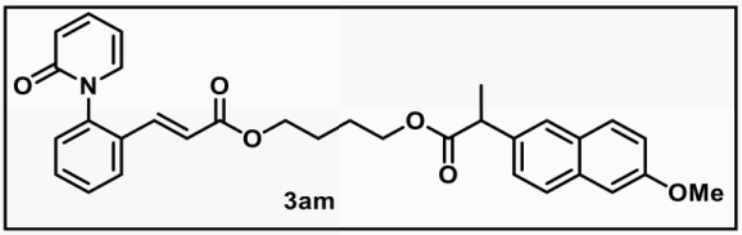

3am

Physical state: colorless liquid (81 mg, 77% yield). R_f: 0.6 (50% EtOAc/Hexane). ^1H NMR ($CDCl_3$, 400 MHz): δ 7.74 (d, J = 8.0 Hz, 1H), 7.70–7.66 (m, 3H), 7.54–7.46 (m, 2H), 7.43–7.34 (m, 3H), 7.29 (dd, J = 7.6, 1.6 Hz, 1H), 7.15–7.09 (m, 3H), 6.66 (d, J = 9.2 Hz, 1H), 6.35 (d, J = 16.0 Hz, 1H), 6.23–6.19 (m, 1H), 4.10–4.05 (m, 4H), 3.89 (s, 3H), 3.85 (q, J = 7.2 Hz, 1H), 1.64 (s, 3H), 1.57 (d, J = 7.2 Hz, 4H). $^{13}C\{^1H\}$ NMR ($CDCl_3$, 175 MHz): δ 175.0, 166.5, 162.7, 158.0, 140.7, 140.5, 139.0, 138.3, 136.0, 134.0, 132.0, 131.5, 129.8, 129.6, 129.2, 128.6, 127.9, 127.5, 126.5, 126.2, 122.4, 121.5, 119.3, 106.4, 105.9, 64.5, 64.4, 55.6, 45.8, 25.6, 25.5, 18.8. IR (KBr, cm^{-1}): 3064, 1718, 1664, 1532, 1278. HRMS (ESI) m/z: $[M + Na]^+$ calcd for $C_{32}H_{31}NO_6Na$, 548.2044; found, 548.2059.

4-Methyl-2-oxo-2*H*-chromen-7-yl(*E*)-3-(2-(2-oxopyridin-1(2*H*)-yl)phenyl)acrylate (3an):

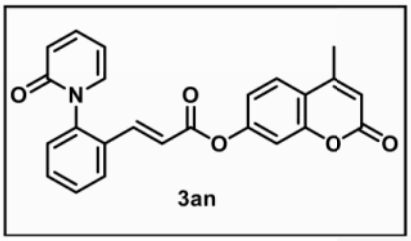

3an

Physical state: yellow solid (46 mg, 58% yield). mp: 195–197 °C. R_f: 0.4 (50% EtOAc/DCM). ^1H NMR ($CDCl_3$, 700 MHz): δ 7.85 (d, J = 7.7 Hz, 1H), 7.62–7.58 (m, 3H), 7.55 (d, J = 7.0 Hz, 1H), 7.49–7.46 (m,

1H), 7.34 (d, J = 7.7 Hz, 1H), 7.24 (dd, J = 7.0, 2.1 Hz, 1H), 7.15–7.12 (m, 2H), 6.70 (d, J = 9.1 Hz, 1H), 6.60 (d, J = 15.4 Hz, 1H), 6.31 (t, J = 6.3 Hz, 1H), 6.27 (s, 1H), 2.44 (s, 3H). $^{13}C\{^1H\}$ NMR ($CDCl_3$, 175 MHz): δ 164.3, 162.8, 160.9, 154.5, 153.4, 152.3, 141.9, 140.9, 140.8, 138.2, 132.3, 131.6, 130.0, 128.8, 128.1, 125.7, 122.4, 120.0, 118.4, 118.2, 114.9, 110.7, 106.7, 19.1. IR (KBr, cm^{-1}): 2925, 1733, 1661, 1615, 1261. HRMS (ESI) m/z: $[M + Na]^+$ calcd for $C_{24}H_{17}NO_5Na$, 422.0999; found, 422.1015.

13-Methyl-17-oxo-7,8,9,11,12,13,14,15,16,17-decahydro-6*H*-cyclopenta[a]phenanthren-3-yl(*E*)-3-(2-(2-oxopyridin-1(2*H*)-yl)phenyl)acrylate (3ao):

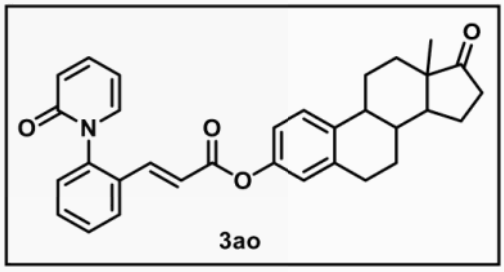

3ao

Physical state: colorless liquid (67 mg, 68% yield). R_f: 0.75 (50% EtOAc/DCM). ^1H NMR ($CDCl_3$, 700 MHz): δ 7.84 (d, J = 7.7 Hz, 1H), 7.58–7.52 (m, 2H), 7.46–7.44 (m, 1H), 7.33 (d, J = 7.7 Hz, 1H), 7.29 (d, J = 8.4 Hz, 2H), 7.22 (dd, J = 7.0, 2.1 Hz, 1H), 6.89–6.85 (m, 2H), 6.69 (d, J = 9.8 Hz, 1H), 6.59 (d, J = 16.1 Hz, 1H), 6.28 (t, J = 6.3 Hz, 1H), 2.91–2.90 (m, 2H), 2.53–2.49 (m, 1H), 2.41 (dd, J = 13.3, 4.2 Hz, 1H), 2.31–2.27 (m, 1H), 2.17–2.12 (m, 1H), 2.08–1.95 (m, 3H), 1.65–1.60 (m, 2H), 1.54–1.44 (m, 3H), 1.27–1.25 (m, 1H), 0.91 (s, 3H). $^{13}C\{^1H\}$ NMR ($CDCl_3$, 175 MHz): δ 221.2, 165.3, 162.8, 148.9, 140.8, 140.7, 140.7, 138.3, 138.2, 137.8, 131.9, 129.9, 128.8, 128.1, 126.7, 122.5, 121.9, 120.9, 119.1, 106.6, 50.8, 48.3, 44.5, 38.4, 36.2, 31.9, 29.7, 26.7, 26.1, 21.9, 14.2. IR (KBr, cm^{-1}): 3065, 2932, 1733, 1661, 1532, 1278. HRMS (ESI) m/z: $[M + Na]^+$ calcd for $C_{32}H_{31}NO_4Na$, 516.2145; found, 516.2144.

17-Acetyl-10,13-dimethyl-2,3,4,7,8,9,10,11,12,13,14,15,16,17-tetradecahydro-1*H*-cyclopenta[a]phenanthren-3-yl(*E*)-3-(2-(2-oxopyridin-1(2*H*)-yl)phenyl)acrylate (3ap):

Physical state: colorless liquid (84 mg, 78% yield). R_f: 0.75 (50% EtOAc/DCM). ^1H NMR ($CDCl_3$, 700 MHz): δ 7.77 (d, J = 7.7 Hz, 1H), 7.53–7.45 (m, 3H), 7.39 (d, J = 16.1 Hz,

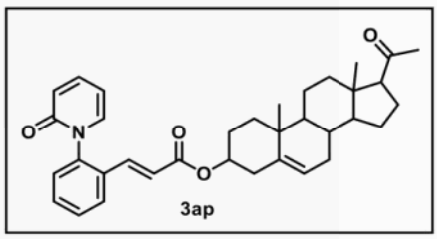

1H), 7.30 (d, J = 7.7 Hz, 1H), 7.18 (d, J = 7.0 Hz, 1H), 6.69 (d, J = 9.8 Hz, 1H), 6.39 (d, J = 16.1 Hz, 1H), 6.28 (t, J = 7.0 Hz, 1H), 5.38–5.37 (m, 1H), 4.69–4.64 (m, 1H), 2.54 (t, J = 9.1 Hz, 1H), 2.38–2.30 (m, 2H), 2.20–2.15 (m, 1H), 2.13 (s, 3H), 2.06–1.99 (m, 2H), 1.89–1.87 (m, 2H), 1.69–1.63 (m, 3H), 1.59–1.56 (m, 2H), 1.51–1.45 (m, 3H), 1.27–1.21 (m, 2H), 1.18–1.14 (m, 2H), 1.03 (s, 3H), 0.64 (s, 3H). $^{13}C\{^1H\}$ NMR ($CDCl_3$, 175 MHz): δ 209.9, 166.1, 162.8, 140.7, 140.5, 140.0, 138.8, 138.3, 132.1, 131.4, 129.8, 128.7, 127.9, 122.7, 122.4, 122.1, 106.5, 74.5, 64.0, 57.2, 50.2, 44.3, 39.1, 38.4, 37.3, 37.0, 32.2, 32.1, 31.9, 28.1, 24.8, 23.2, 21.4, 19.7, 13.6. IR (KBr, cm^{-1}): 3066, 2942, 1700, 1666, 1532, 1278. HRMS (ESI) m/z: $[M + Na]^+$ calcd for $C_{35}H_{41}NO_4Na$, 562.2928; found, 562.2941.

Phenyl (*E*)-3-(5-methyl-2-(2-oxopyridin-1(2*H*)-yl)phenyl)acrylate (3ci):

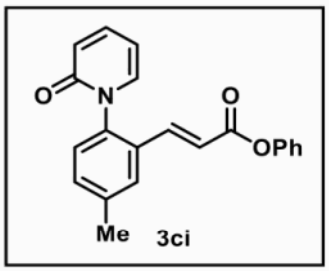

Physical state: colorless solid (52 mg, 78% yield). mp: 139–141 °C. R_f: 0.75 (50% EtOAc/DCM). ^1H NMR (700 MHz, $CDCl_3$): δ 7.65 (s, 1H), 7.54 (d, J = 16.1 Hz, 1H), 7.46–7.43 (m, 1H), 7.39–7.37 (m, 2H), 7.27–7.20 (m, 4H), 7.11 (d, J = 7.7 Hz, 2H), 6.69 (d, J = 9.8 Hz, 1H), 6.59 (d, J = 16.1 Hz, 1H), 6.28 (t, J = 6.3 Hz, 1H), 2.47 (s, 3H). $^{13}C\{^1H\}$ NMR (175 MHz, $CDCl_3$): δ 165.1, 163.0, 151.0, 141.0, 140.8, 140.0, 138.4, 138.3, 132.8, 131.4, 129.7, 128.6, 128.5, 126.2, 122.4, 121.9, 120.5, 106.6, 21.6. IR (KBr, cm^{-1}): 2930, 1737, 1637, 1196. HRMS (ESI) m/z: $[M + Na]^+$ calcd for $C_{21}H_{17}NO_3Na$, 354.1101; found, 354.1093.

4-Hydroxybutyl (*E*)-3-(5-methoxy-2-(2-oxopyridin-1(2*H*)-yl)phenyl)acrylate (3bh):

Physical state: colorless liquid (45 mg, 66% yield). R_f: 0.2 (50% EtOAc/DCM). ^1H NMR (700 MHz, $CDCl_3$): δ 7.47–7.45 (m, 1H), 7.35 (d, J = 16.1 Hz, 1H), 7.23–7.18 (m, 3H), 7.05 (dd, J = 8.4, 2.8 Hz, 1H), 6.69 (d, J = 9.1 Hz, 1H), 6.38 (d, J = 15.4 Hz, 1H), 6.27 (t, J

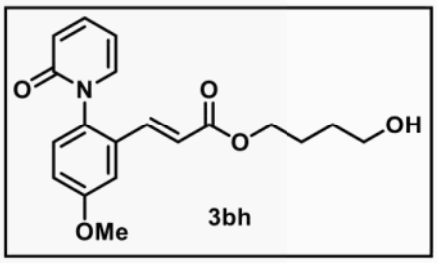

3bh

= 7.0 Hz, 1H), 4.21–4.15 (m, 2H), 3.88 (s, 3H), 3.67 (t, J = 7.0 Hz, 2H), 1.75–1.72 (m, 2H), 1.65–1.61 (m, 2H). $^{13}C\{^1H\}$ NMR (175 MHz, $CDCl_3$): δ 166.5, 160.2, 140.8, 139.1, 138.8, 133.5, 132.9, 129.6, 122.3, 121.7, 117.4, 112.3, 106.6, 64.8, 62.7, 56.0, 29.5, 25.3. IR (KBr, cm^{-1}): 3080, 2955, 1708, 1657, 1288. HRMS (ESI) m/z: $[M + Na]^+$ calcd for $C_{19}H_{21}NO_5Na$, 366.1312; found, 366.1283.

Methyl (*E*)-3-(5-fluoro-2-(2-oxopyridin-1(2*H*)-yl)phenyl)acrylate (3sb):

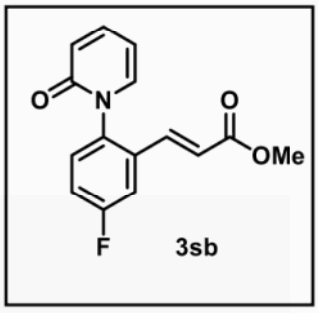

3sb

Physical state: colorless solid (51 mg, 93% yield). mp: 105–107 °C. R_f: 0.45 (50% EtOAc/DCM). ^1H NMR (700 MHz, $CDCl_3$): δ 7.49–7.46 (m, 1H), 7.44 (dd, J = 9.1, 2.8 Hz, 1H), 7.33 (d, J = 16.1 Hz, 1H), 7.30–7.28 (m, 1H), 7.23–7.21 (m, 1H), 7.16 (dd, J = 7.0, 2.1 Hz, 1H), 6.69 (d, J = 9.1 Hz, 1H), 6.40 (d, J = 15.4 Hz, 1H), 6.29 (t, J = 6.3 Hz, 1H), 3.75 (s, 3H). $^{13}C\{^1H\}$ NMR (175 MHz, $CDCl_3$): δ 166.7, 162.9 (d, $J_{C\text{-}F}$ = 249.7 Hz), 162.8, 140.9, 138.2, 138.1, 136.4, 134.2 (d, $J_{C\text{-}F}$ = 8.3 Hz), 130.6 (d, $J_{C\text{-}F}$ = 8.8 Hz), 122.6, 122.5, 118.6 (d, $J_{C\text{-}F}$ = 23.1 Hz), 114.4 (d, $J_{C\text{-}F}$ = 23.8 Hz), 106.7, 52.3. ^{19}F NMR (376 MHz, $CDCl_3$): δ -111.0. IR (KBr, cm^{-1}): 3073, 1718, 1664, 1278, 766. HRMS (ESI) m/z: $[M + Na]^+$ calcd for $C_{15}H_{12}FNO_3Na$, 296.0693; found, 296.0684.

Methyl (*E*)-3-(5-chloro-2-(2-oxopyridin-1(2*H*)-yl)phenyl)acrylate (3db):

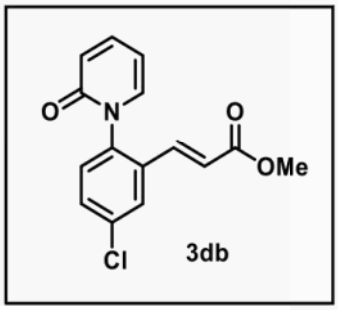

3db

Physical state: colorless solid (49 mg, 85% yield). mp: 138–140 °C. R_f: 0.47 (50% EtOAc/DCM). ^1H NMR ($CDCl_3$, 400 MHz): δ 7.72 (d, J = 2.4 Hz, 1H), 7.53–7.47 (m, 2H), 7.36–7.32 (m, 1H), 7.28 (d, J = 2.8 Hz, 1H), 7.17 (dd, J = 6.8, 1.6 Hz, 1H), 6.72 (d, J = 9.2 Hz, 1H), 6.40 (d, J = 15.6 Hz, 1H),

6.35 (t, J = 6.8 Hz, 1H), 3.75 (s, 3H). $^{13}C\{^{1}H\}$ NMR ($CDCl_3$, 100 MHz): δ 166.6, 162.7, 141.4, 138.1, 137.8, 136.0, 133.7, 131.4, 130.0, 128.2, 127.9, 122.8, 122.2, 107.4, 52.3. IR (KBr, cm^{-1}): 2960, 1718, 1669, 1534, 1286, 668. HRMS (ESI) m/z: $[M + Na]^+$ calcd for $C_{15}H_{12}ClNO_3Na$, 312.0398; found, 312.0371.

(*E*)-1-(2-(1,2-Diphenylvinyl)phenyl)pyridin-2(1*H*)-one (3as):

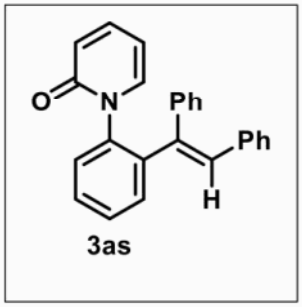

3as

Physical state: grey solid (13 mg, 19% yield). mp: 139–141 °C. R_f: 0.1 (20% EtOAc/Hexane). ^{1}H NMR ($CDCl_3$, 700 MHz): δ 7.52 (d, J = 7.0 Hz, 1H), 7.47–7.43 (m, 2H), 7.26–7.25 (m, 1H), 7.12–7.06 (m, 7H), 7.02 (d, J = 4.2 Hz, 2H), 6.97 (d, J = 7.0 Hz, 2H), 6.94 (d, J = 5.6 Hz, 1H), 6.72 (s, 1H), 6.33 (d, J = 9.1 Hz, 1H), 5.89 (t, J = 5.6 Hz, 1H). $^{13}C\{^{1}H\}$ NMR ($CDCl_3$, 175 MHz): δ 162.3, 142.1, 139.8, 139.8, 139.5, 139.3, 138.4, 137.2, 132.1, 131.9, 129.8, 129.7, 129.3, 129.1, 128.8, 128.5, 128.2, 127.6, 127.3, 121.8, 105.6. IR (KBr, cm^{-1}): 2962, 1687, 1558, 1366, 1225. HRMS (ESI) m/z: $[M + H]^+$ calcd for $C_{25}H_{20}NO$, 350.1545; found, 350.1540.

Benzyl (*E*)-3-(1-acetylindolin-7-yl)acrylate (3pa):

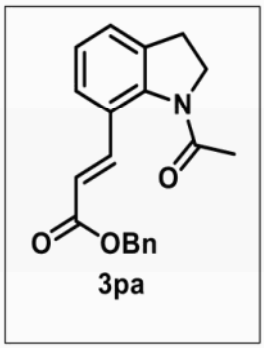

3pa

Physical state: colorless solid (37 mg, 57% yield). mp: 89–91 °C. R_f: 0.2 (30% EtOAc/Hexane). ^{1}H NMR ($CDCl_3$, 700 MHz): δ 7.74 (s, 1H), 7.42–7.40 (m, 3H), 7.37 (t, J = 7.0 Hz, 2H), 7.32 (t, J = 7.7 Hz, 1H), 7.23 (d, J = 7.7 Hz, 1H), 7.10 (t, J = 7.7 Hz, 1H), 6.39 (s, 1H), 5.24 (s, 2H), 4.15 (s, 2H), 3.04 (s, 2H), 2.25 (s, 3H). $^{13}C\{^{1}H\}$ NMR ($CDCl_3$, 175 MHz): δ 169.3, 167.2, 143.9, 142.5, 136.5, 128.9, 128.5, 128.4, 126.3, 125.9, 125.7, 116.7, 66.5, 51.3, 29.7, 24.0. IR (KBr, cm^{-1}): 2957, 1684, 1558, 1371, 1237. HRMS (ESI) m/z: $[M + Na]^+$ calcd for $C_{20}H_{19}NO_3Na$, 344.1257; found, 344.1240.

Benzyl (*E*)-3-(2-acetamidophenyl)acrylate (3qa):

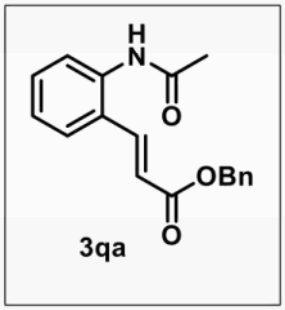

Physical state: colorless solid (36 mg, 61% yield). mp: 131–133 °C. R_f: 0.6 (30% EtOAc/DCM). ^{1}H NMR ($CDCl_3$, 700 MHz): δ 7.85 (d, J = 15.4 Hz, 1H), 7.72 (d, J = 8.4 Hz, 1H), 7.54 (d, J = 7.7 Hz, 1H), 7.40–7.33 (m, 7H), 7.18 (t, J = 7.7 Hz, 1H), 6.43 (d, J = 16.1 Hz, 1H), 5.24 (s, 2H), 2.20 (s, 3H). ^{13}C{^{1}H} NMR ($CDCl_3$, 175 MHz): δ 169.2, 166.9, 140.2, 136.2, 136.2, 131.2, 128.9, 128.7, 128.6, 127.9, 127.4, 126.3, 125.6, 120.5, 66.9, 24.5. IR (KBr, cm^{-1}): 2962, 1726, 1561, 1371, 1245. HRMS (ESI) m/z: [M + Na]$^+$ calcd for $C_{18}H_{17}NO_3Na$, 318.1106; found, 318.1104.

(*E*)-*N*-(2-Hydroxyethyl)-3-(2-(2-oxopyridin-1(2*H*)-yl)phenyl)acrylamide (4):

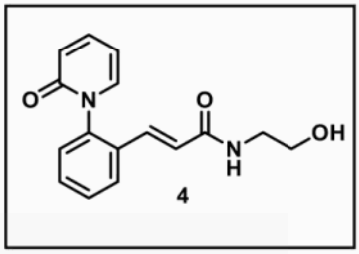

Physical state: colorless liquid (49 mg, 87% yield). R_f: 0.2 (5% MeOH/EtOAc). ^{1}H NMR ($CDCl_3$, 700 MHz): δ 7.71 (t, J = 4.9 Hz, 1H), 7.56–7.53 (m, 1H), 7.50 (t, J = 7.0 Hz, 1H), 7.46 (d, J = 7.7 Hz, 1H), 7.32 (t, J = 7.7 Hz, 1H), 7.28 (dd, J = 6.3, 1.4 Hz, 1H), 7.26 (d, J = 7.7 Hz, 1H), 7.16 (d, J = 15.4 Hz, 1H), 6.72 (d, J = 9.1 Hz, 1H), 6.42 (d, J = 15.4 Hz, 1H), 6.38 (t, J = 6.3 Hz, 1H), 3.71–3.68 (m, 1H), 3.58–3.55 (m, 1H), 3.51–3.47 (m, 1H), 3.21–3.17 (m, 1H). ^{13}C{^{1}H} NMR ($CDCl_3$, 175 MHz): δ 166.7, 163.5, 141.5, 140.2, 138.3, 133.4, 132.7, 130.7, 129.9, 127.9, 127.4, 125.4, 122.1, 107.6, 61.6, 43.3. IR (KBr, cm^{-1}): 3078, 2935, 1657, 1537, 1285. HRMS (ESI) m/z: [M + Na]$^+$ calcd for $C_{16}H_{16}N_2O_3Na$, 307.1053; found, 307.1047.

NMR spectra of Benzyl (*E*)-3-(2-(2-oxopyridin-1(2*H*)-yl)phenyl)acrylate (3aa):

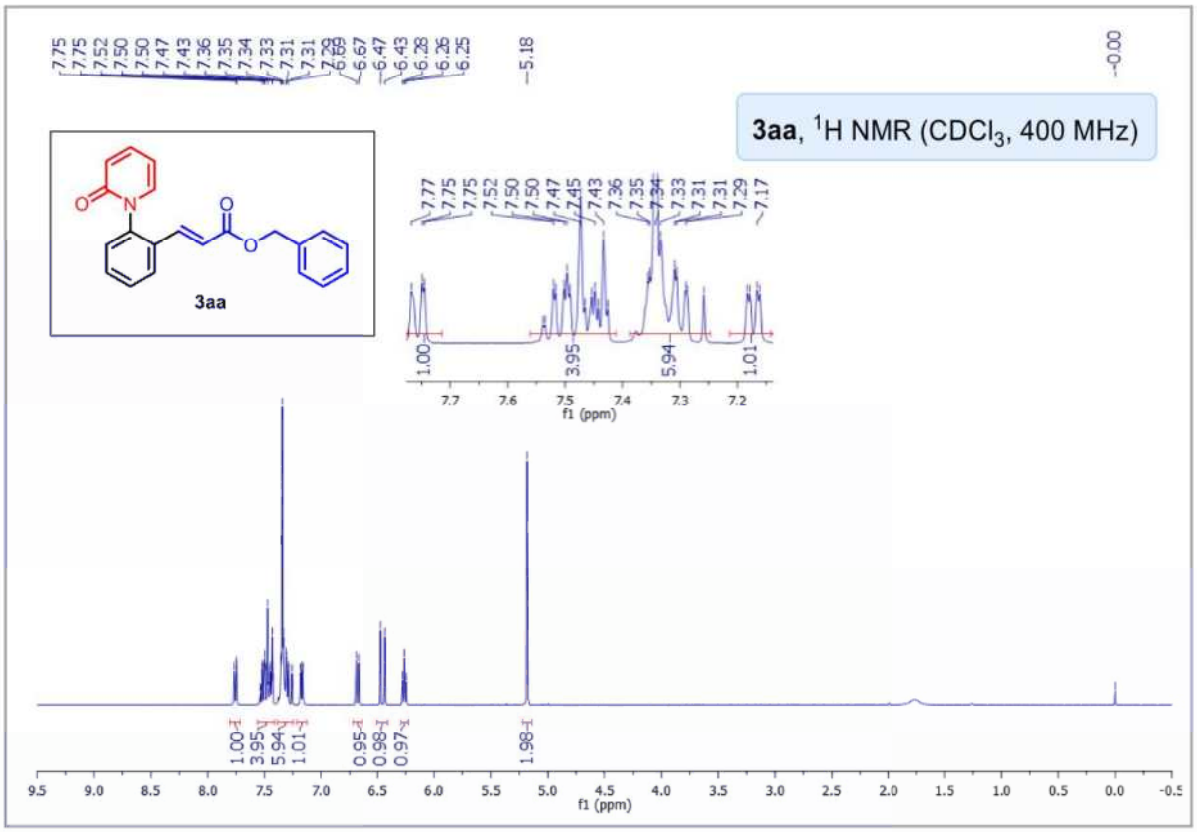

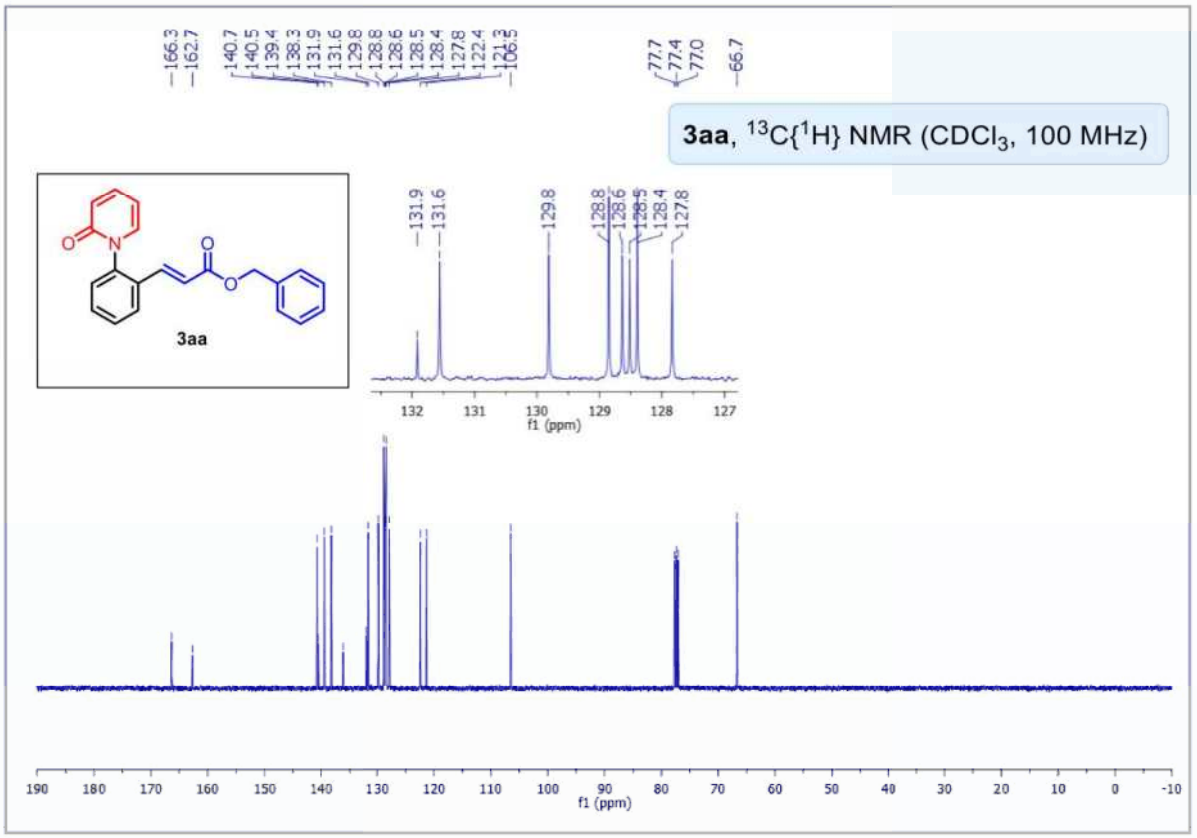

NMR spectra of (*E*)-*N*-(2-Hydroxyethyl)-3-(2-(2-oxopyridin-1(2*H*)-yl)phenyl)acrylamide (4):

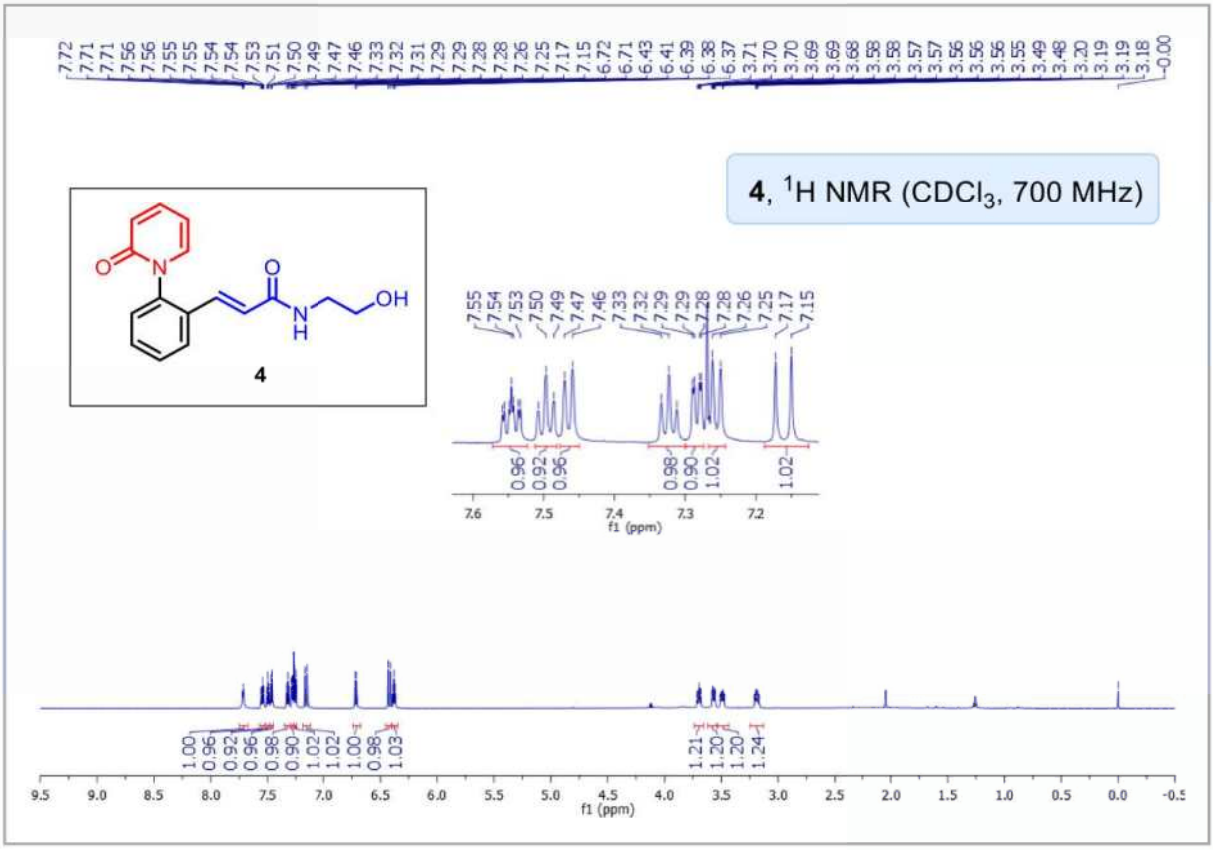

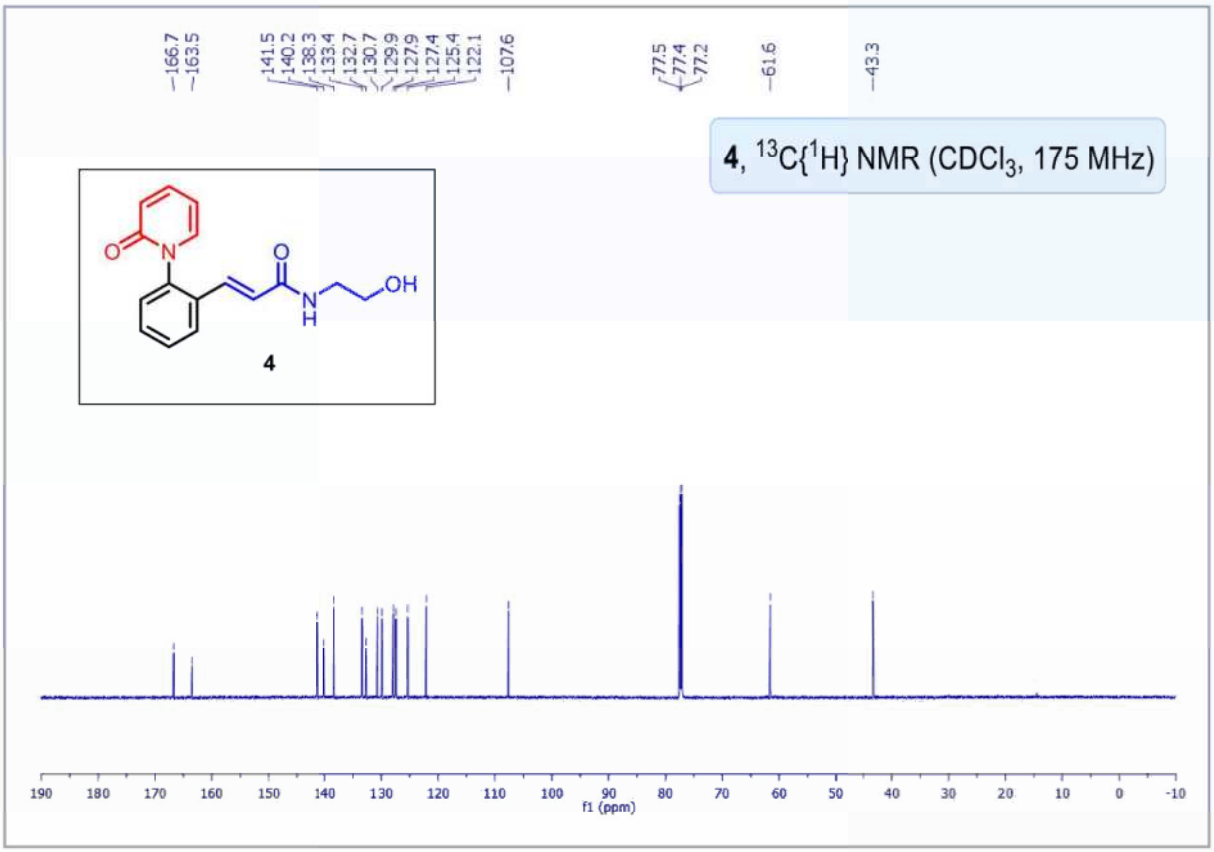

Detection of intermediate through HRMS:

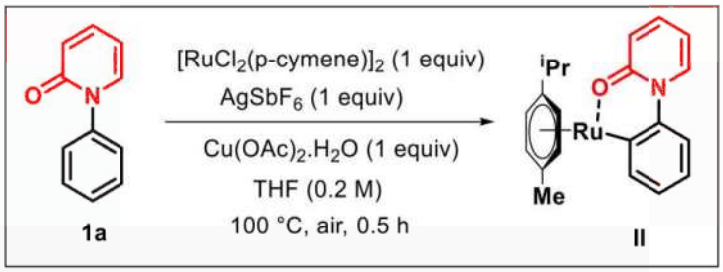

Intermediate II HRMS:

HRMS (ESI) m/z: $[M + H]^+$ calcd for $C_{21}H_{22}NORu$, 406.0745; found, 406.0726.

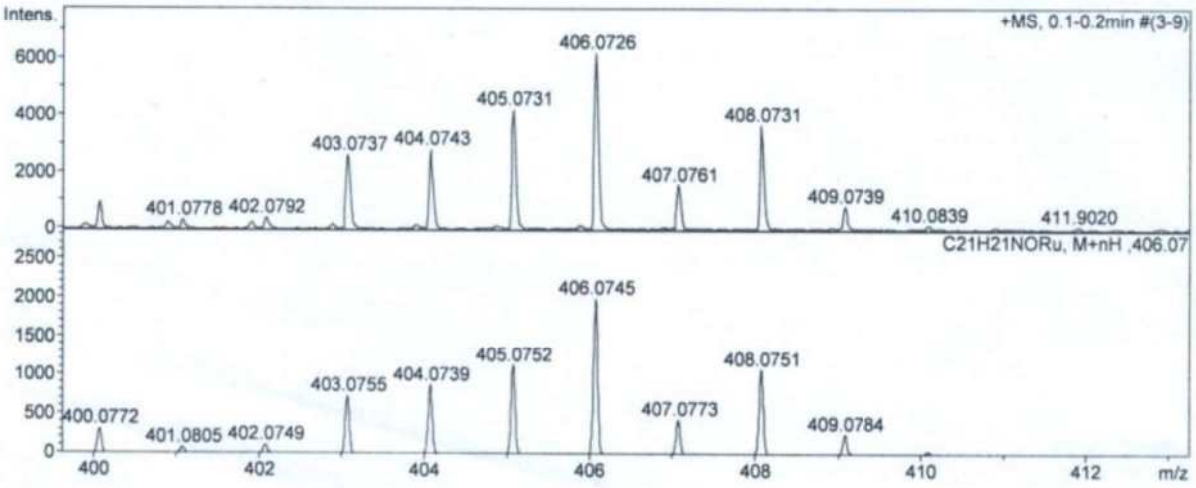

Crystal structure of 3af

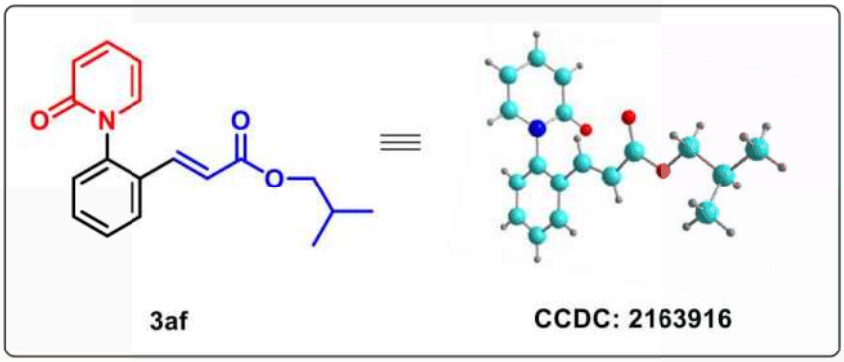

Datablock pcr-srm_1180 - ellipsoid plot

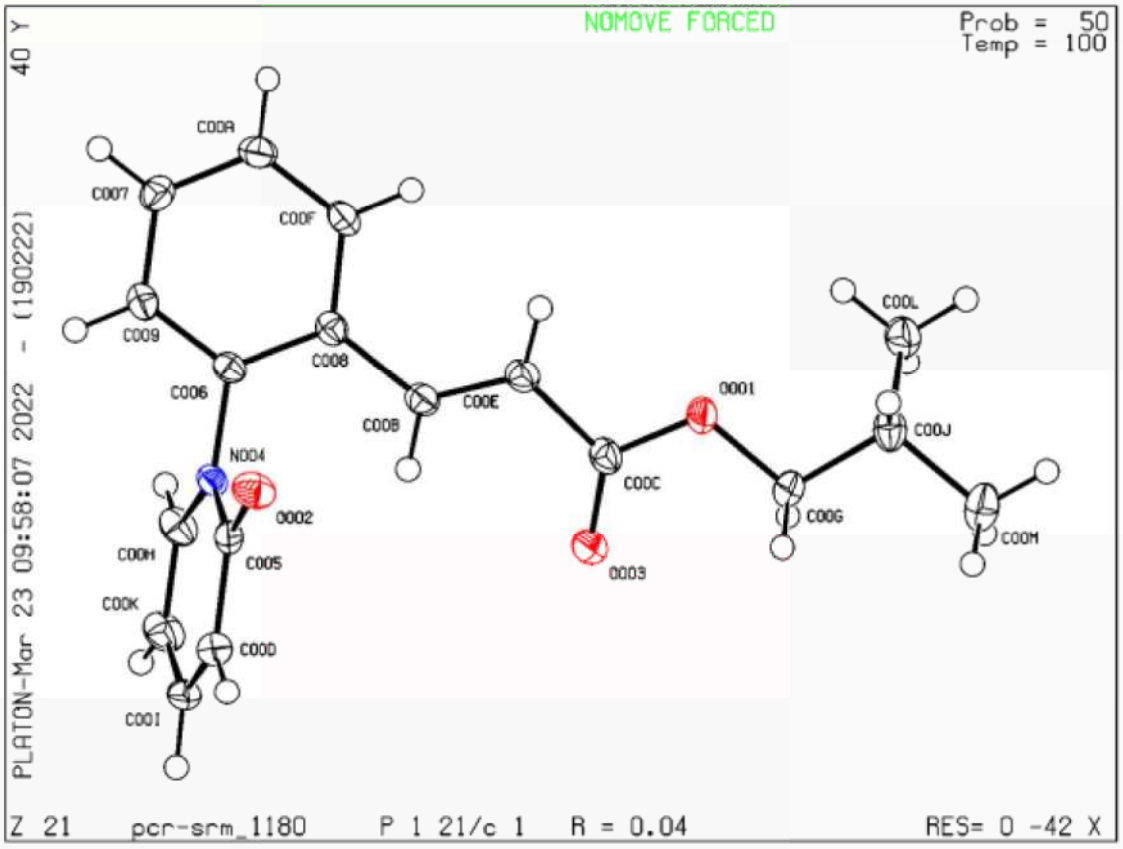

4.6 REFERENCES

1. (a) Murray, K. J.; Eden, R. J.; Dolan, J. S.; Grimsditch, D. C.; Stutchbury, C. A.; Patel, B.; Knowles, A.; Worby, A.; Lynham, J. A.; Coates, W. J. Citation for: The effect of SK&F 95654, a novel phosphodiesterase inhibitor, on cardiovascular, respiratory and platelet function. *Br. J. Pharmacol.* **1992**, *107*, 463−470. (b) Hanada, T.; Hashizume, Y.; Tokuhara, N.; Takenaka, O.; Kohmura, N.; Ogasawara, A.; Hatakeyama, S.; Ohgoh, M.; Ueno, M.; Nishizawa, Y. Perampanel: A novel, orally active, noncompetitive AMPA-receptor antagonist that reduces seizure activity in rodent models of epilepsy. *Epilepsia* **2011**, *52*, 1331−1340. (c) Hibi, S.; Ueno, K.; Nagato, S.; Kawano, K.; Ito, K.; Norimine, Y.; Takenaka, O.; Hanada, T.; Yonaga, M. Discovery of 2-(2-Oxo-1- phenyl-5-pyridin-2-yl-1,2-dihydropyridin-3-yl)benzonitrile (Perampanel): A Novel, Noncompetitive α-Amino-3-hydroxy-5-methyl-4- isoxazolepropanoic Acid (AMPA) Receptor Antagonist. *J. Med. Chem.* **2012**, *55*, 10584−10600. (d) Harrison, S. T.; Poslusney, M. S.; Mulhearn, J. J.; Zhao, Z.; Kett, N. R.; Schubert, J. W.; Melamed, J. Y.; Allison, T. J.; Patel, S. B.; Sanders, J. M.; Sharma, S.; Smith, R. F.; Hall, D. L.; Robinson, R. G.; Sachs, N. A.; Hutson, P. H.; Wolkenberg, S. E.; Barrow, J. C. Synthesis and Evaluation of Heterocyclic Catechol Mimics as Inhibitors of Catechol O-methyltransferase (COMT). *ACS Med. Chem. Lett.* **2015**, *6*, 318− 323.
2. (a) Raghu, G.; Johnson, W. C.; Lockhart, D.; Mageto, Y. Treatment of Idiopathic Pulmonary Fibrosis with a New Antifibrotic Agent, Pirfenidone. *Am. J. Respir. Crit. Care Med.* **1999**, *159*, 1061−1069. (b) Selness, S. R.; Devraj, R. V.; Devadas, B.; Walker, J. K.; Boehm, T. L.; Durley, R. C.; Shieh, H.; Xing, L.; Rucker, P. V.; Jerome, K. D.; Benson, A. G.; Marrufo, L. D.; Madsen, H. M.; Hitchcock, J.; Owen, T. J.; Christie, L.; Promo, M. A.; Hickory, B. S.; Alvira, E.; Naing, W.; Blevis-Bal, R.; Messing, D.; Yang,

J.; Mao, M. K.; Yalamanchili, G.; Vonder Embse, R.; Hirsch, J.; Saabye, M.; Bonar, S.; Webb, E.; Anderson, G.; Monahan, J. B. Discovery of PH-797804, a highly selective and potent inhibitor of p38 MAP kinase. *Bioorg. Med. Chem. Lett.* **2011**, *21*, 4066−4071. (c) Richeldi, L.; Yasothan, U.; Kirkpatrick, P. Pirfenidone. *Nat. Rev. Drug Discovery* **2011**, *10*, 489−490.

3. (a) Hillenbrand, J.; Ham, W. S.; Ritter, T. C−H Pyridonation of (Hetero-)Arenes by Pyridinium Radical Cations. *Org. Lett.* **2019**, *21*, 5363−5367. (b) Li, J.; Yang, Y.; Wang, Z.; Feng, B.; You, J. Rhodium(III)-Catalyzed Annulation of Pyridinones with Alkynes via Double C−H Activation: A Route to Functionalized Quinolizinones. *Org. Lett*. **2017**, *19*, 3083−3086. (c) Chen, Y.; Wang, F.; Jia, A.; Li, X. Palladium-catalyzed selective oxidative olefination and arylation of 2-pyridones. *Chem. Sci*. **2012**, *3*, 3231−3236.
4. For reviews on transition metal-catalyzed C−H functionalization, see: (a) Arockiam, P. B.; Bruneau, C.; Dixneuf, P. Ruthenium(II)-Catalyzed C–H Bond Activation and Functionalization. *Chem. Rev.* **2012**, *112*, 5879−5918. (b) Ackermann, L. Carboxylate-Assisted Transition-Metal-Catalyzed C−H Bond Functionalizations: Mechanism and Scope. *Chem. Rev*. **2011**, *111*, 1315−1345. (c) Engle, K. M.; Mei, T.-S.; Wasa, M.; Yu, J.-Q. Weak Coordination as a Powerful Means for Developing Broadly Useful C–H Functionalization Reactions. *Acc. Chem. Res.* **2012**, *45*, 788−802. (d) Chen, X.; Engle, K. M.; Wang, D.-H.; Yu, J.-Q. Palladium(II)-Catalyzed C–H Activation/C–C Cross-Coupling Reactions: Versatility and Practicality. *Angew. Chem., Int. Ed*. **2009**, *48*, 5094−5115. (e) Thirunavukkarasu, V. S.; Kozhushkov, S. I.; Ackermann, L. C–H nitrogenation and oxygenation by ruthenium catalysis. *Chem. Commun*. **2014**, *50*, 29−39. (f) Rao, Y.; Shan, G.; Yang, X.-L. Some recent advances in transition-metal-catalyzed ortho sp^2 C-H functionalization using Ru, Rh, and Pd. *Sci. China: Chem*. **2014**, *57*, 930−944.

5. (a) Grimster, N. P.; Gauntlett, C.; Godfrey, C. R. A.; Gaunt, M. J. Palladium-catalyzed intermolecular alkenylation of indoles by solvent controlled regioselective C-H functionalization. *Angew. Chem., Int. Ed.* **2005**, *44*, 3125−3129. (b) Beck, E. M.; Grimster, N. P.; Hatley, R.; Gaunt, M. J. Mild Aerobic Oxidative Palladium(II) Catalyzed C-H Bond Functionalization: Regioselective and Switchable C-H Alkenylation and Annulation of Pyrroles. *J. Am. Chem. Soc*. **2006**, *128*, 2528− 2529. (c) Lane, B. S.; Brown, M. A.; Sames, D. Direct palladium-catalyzed C-2 and C-3 arylation of indoles: a mechanistic rationale for regioselectivity. *J. Am. Chem. Soc*. **2005**, *127*, 8050−8057. (d) Phipps, R. J.; Grimster, N. P.; Gaunt, M. J. Cu(II)-Catalyzed Direct and Site-Selective Arylation of Indoles Under Mild Conditions. *J. Am. Chem. Soc*. **2008**, *130*, 8172−8174. (e) Bedford, R. B.; Durrant, S. J.; Montgomery, M. CatalystSwitchable Regiocontrol in the Direct Arylation of Remote C−H Groups in Pyrazolo[1,5-a]Pyrimidines. *Angew. Chem., Int. Ed*. **2015**, *54*, 8787−8790.
6. Kondrashov, M.; Provost, D. O.; Wendt, F. Regioselectivity in C–H activation: reagent control in cyclometallation of 2-(1-naphthyl)-pyridine. *Dalton Trans*. **2016**, *45*, 525−531.
7. Fabry, D. C.; Ronge, M. A.; Zoller, J.; Rueping, M. C–H Functionalization of Phenols Using Combined Ruthenium and Photoredox Catalysis: In Situ Generation of the Oxidant. *Angew. Chem., Int. Ed*. **2015**, *54*, 2801−2805.
8. Liu, W.; Ackermann, L. Versatile ruthenium(II)-catalyzed C–H cyanations of benzamides. *Chem. Commun*. **2014**, *50*, 1878−1881.
9. (a) Raju, S.; Annamalai, P.; Chen, P.-L.; Liu, Y.-H.; Chuang, S.-C. Palladium-Catalyzed C–H Bond Activation by Using Iminoquinone as a Directing Group and an Internal Oxidant or a Co-oxidant: Production of Dihydrophenanthridines, Phenanthridines, and Carbazoles. *Org. Lett.* **2017**, *19*, 4134−4137. (b) Zhao, J.; Huang, L.; Cheng, K.; Zhang,

Y. Zhao, J.; Huang, L.; Cheng, K.; Zhang, Y. *Tetrahedron Lett*. **2009**, *50*, 2758−2761. (c) Fujiwara, Y.; Maruyama, O.; Yoshidomi, M.; Taniguchi, H. Palladium-Catalyzed Alkenylation of Aromatic Heterocycles with Olefins. Synthesis of Functionalized Aromatic Heterocycles. *J. Org. Chem.* **1981**, *46*, 851−855.

10. Jadhav, P. P., Kahar, N. M., Dawande, S. G. Ruthenium(II)-Catalyzed Highly Chemo- and Regioselective Oxidative C6 Alkenylation of Indole-7-carboxamides. *Org. Lett.* **2021**, *23*, 8673−8677.
11. Bechtoldt, A.; Tirler, C.; Raghuvanshi, K.; Warratz, S.; Kornhaaß, C.; Ackermann, L. Ruthenium Oxidase Catalysis for Site-Selective C–H Alkenylations with Ambient O_2 as the Sole Oxidant. *Angew. Chem., Int. Ed*. **2016**, *55*, 264−267.
12. Mohanty, S. R.; Pati, B. V.; Banjare, S. K.; Adhikari, G. K. D.; Ravikumar, P. C. Redox-Neutral Cobalt(III)-Catalyzed C−H Activation/Annulation of *α,β*-Unsaturated Oxime Ether with Alkyne: One-Step Access to Multisubstituted Pyridine. *J. Org. Chem.* **2021**, *86*, 1074−1083.
13. Gottlieb, H. E.; Kotlyar, V.; Nudelman, A. NMR chemical shifts of common laboratory solvents as trace impurities. *J. Org. Chem*. **1997**, *62*, 7512−7515.
14. Li, J.; Yang, Y.; Wang, Z.; Feng, B.; You, J. Rhodium(III)-Catalyzed Annulation of Pyridinones with Alkynes via Double C−H Activation: A Route to Functionalized Quinolizinones. *Org. Lett*. **2017**, *19*, 3083−3086.
15. Xiao, Q.; He, Q.; Li, J.; Wang, J. 1,4-Diazabicyclo[2.2.2]octanePromoted Aminotrifluoromethyl thiolation of *α,β*-Unsaturated Carbonyl Compounds: *N*-Trifluoromethylthio-4-nitrophthalimide Acts as Both the Nitrogen and SCF_3 Sources. *Org. Lett*. **2015**, *17*, 6090−6093.

Chapter 5

Overcoming the challenges towards selective C(6)-H functionalisation of 2-pyridone with maleimide through Mn(I)-catalyst: Easy access to all-carbon quaternary center

Chapter 5

Overcoming the challenges towards selective C(6)-H functionalisation of 2-pyridone with maleimide through Mn(I)-catalyst: Easy access to all-carbon quaternary center

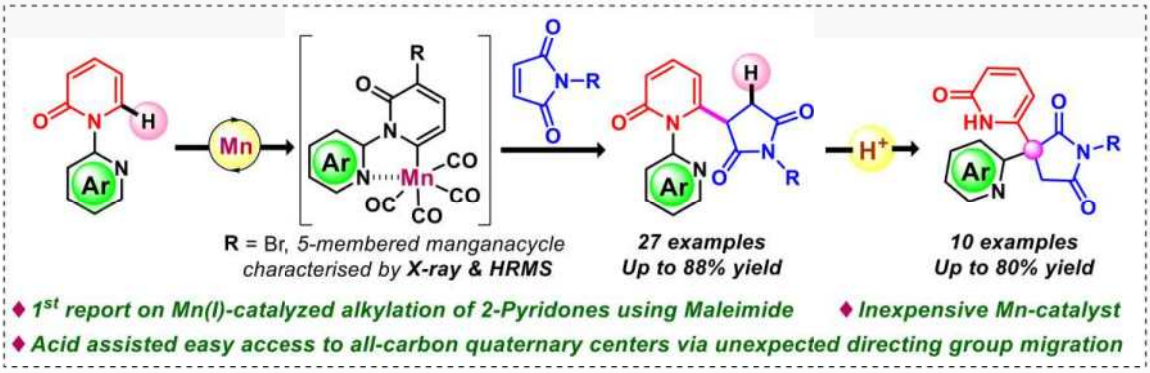

5.1 ABSTRACT: Generally, 2-pyridone reacts with maleimide to give Diels-Alder product. For the first time we have demonstrated Mn(I) catalyzed C-6 alkylation of 2-pyridone using maleimide as alkyl source. Notably, in the presence of acetic acid an unexpected rearrangement has been observed forming a unique class of compounds bearing three distinct *N*-heterocycles with an all-carbon quaternary carbon centre. Furthermore, a five-membered manganacycle intermediate was isolated and characterized by single crystal X-ray and HRMS. This methodology tolerates a wide range of functional groups delivering the alkylated products in moderate to excellent yields.

5.2 INTRODUCTION

Many pharmaceutically active molecules and natural products contain succinimide derivatives.[1] The succinimide moiety can be easily reduced to γ-lactams and pyrrolidines.[2] Moreover, it can also be converted into useful functional groups.[3] Substituted succinimide at 3-position is a key structural unit present in many pharmaceuticals and natural

products.[2b,4] In this regard, synthesis of succinimide derivatives are considered as one of the valuable organic transformation. During the last two decades significant progress has been achieved for the formation of C-C bonds through C-H activation reactions using second and third row transition metal (Rh, Pd, Ir, and Ru) catalysts.[5,6] However, the development of C-H bond activation reactions using first-row transition metals, such as manganese is advantageous on account of its higher abundance in the earth's crust,[7] low cost and low toxicity. So far, only a handful of examples of Mn-catalyzed C-C bond forming reactions via C-H bond activation have been reported.[8]

Figure 5.1: Examples of C-6 alkyl substituted 2-pyridone core structure in bioactive molecules.

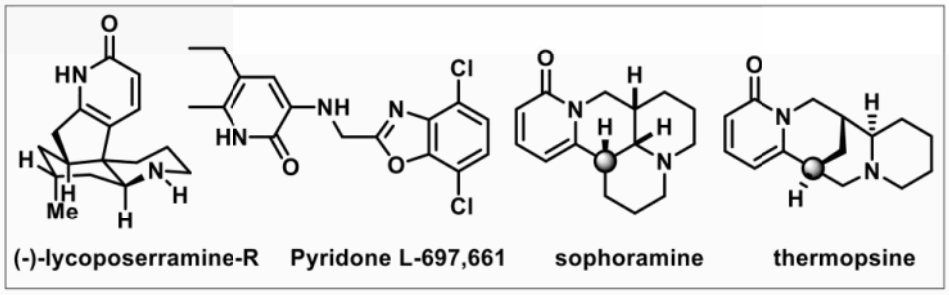

2-pyridone is an important heterocycle, which is widely present in numerous biologically active natural products.[9] As compared to C(3)-H,[10] C(4)-H,[11] C(5)-H[12] functionalization of 2-pyridone, selective functionalization at the electron-deficient C(6)-H position of 2-pyridone has gained huge attention from the synthetic community in recent years (Figure 5.1). Though there are few reports on C(6)-alkylation of 2-pyridone,[13] it has been a long-standing challenge for alkylation at the C(6)-position of 2-pyridones with maleimide by using Mn(I) catalyst. There are some major challenges in selective alkylation at the C(6)-position of 2-pyridones with maleimides such as (i) the reaction of maleimides with 2-pyridones leads to the formation of the corresponding Diels-alder products (Scheme 5.1a),[14] (ii) under basic conditions, succinimide ring undergoes fast hydrolysis,[15]

Scheme 5.1: Previous work and our work

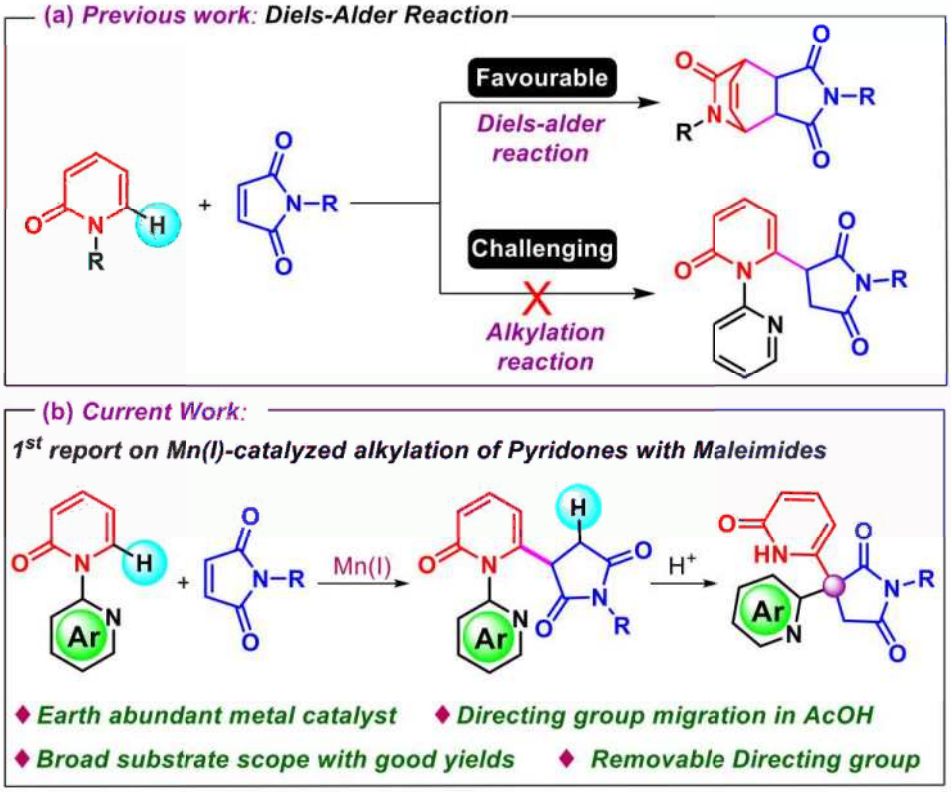

(iii) instead of protodemetalation for the alkylation,[16] facile β-hydride elimination can occur, which results in a Mizoroki-Heck type product.[17] Further, the reaction pathway depend on several factors, like reaction conditions, oxidation states of the metal,[18] and coordination ability of the heteroatom (strong/weak chelation to the metal).[19] Many studies have reported that the β-hydrogens of the alkyl group are not syn-periplanar to the metal, thereby obstructing the β-hydride elimination pathway and resulting in conjugate addition products.[20] Assuming that similar conditions will prevail in Mn(I) system, we were curious to check the alkylation of 2-pyridones with maleimides (Scheme 5.1b). Herein, we have reported the first Mn(I)-catalyzed alkylation at C(6) position of 2-pyridones with maleimide, leading to various biologically active succinimide derivatives.

5.3 RESULTS AND DISCUSSION

To get the optimized reaction condition for C-6 alkylation of 2-pyridones, we started the initial study by taking *2H*-[1,2'-bipyridin]-2-ones **1a** as the substrate and maleimide **2a** as the coupling partner with $MnBr(CO)_5$ (10 mol %) as the catalyst, Cy_2NH (20 mol %) as the base in THF at 120 °C for 12 h, but we failed to get any product (Table 5.1, entry 1). Then, we screened different solvents such as toluene, dioxane, hexane and acetone (Table 5.1, entries 2-5). To our delight, with hexane and acetone, the desired product was formed in 25% and 34% yields respectively. Enticed from the above results, we continued our optimization by changing different parameters sequentially. By keeping acetone as the solvent, we varied different bases such as NaOAc, Et_3N and diisopropylethylamine (DIPEA) all of them gave inferior results (Table 5.1, entries 6-8). Interestingly decreasing the solvent concentration improved the yield up to 55% (Table 5.1, entry 9). In addition, we modified the substrate to coupling partner ratio (2:1) which yielded the corresponding product up to 59% (Table 5.1, entry 10). Increasing the catalyst (20 mol %) and base (40 mol %) loadings lead to superior result with 77% yield (Table 5.1, entry 11) of the desired product. The yield of the product significantly reduced upon lowering or raising the reaction temperature and duration (Table 5.1, entries 12-15). We conducted two control experiments to understand, the effect of the catalyst and the base. Without catalyst, the required product was not obtained (Table 5.1, entry 16), but a trace amount of product was detected in absence of the base (Table 5.1, entry 17). These studies confirm that the catalyst and base is critical for this reaction.

After getting the optimized reaction conditions, we explored the scope of different substituted *2H*-[1,2'-bipyridin]-2-ones **1** (Scheme 5.2) under the same conditions. Neutral *2H*-[1,2'-bipyridin]-2-ones **1a** delivered the desired product **3aa** in 77% yield. Then, we

explored the variation of halogen substituent (-Cl, -Br) on 3-position of 2-pyridone giving 80% and 73% of the alkylated product **3ba**, **3ca** respectively. The structure of **3ca** was

Table 5.1. Optimization for C(6)-H functionalisation of 2-pyridone with maleimide[a]

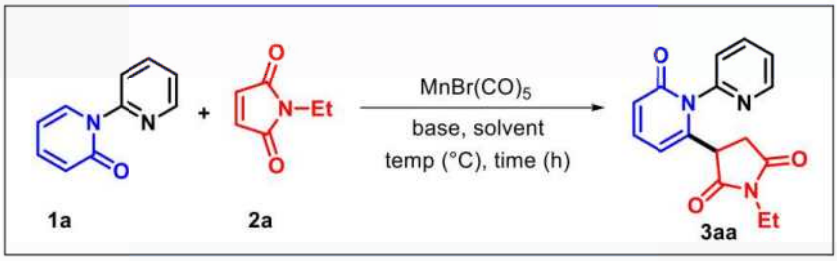

entry	additive	solvent	temperature	[b]yield of **3aa** (%)
1	Cy_2NH	THF	120 °C	nd
2	Cy_2NH	Toluene	120 °C	nd
3	Cy_2NH	Dioxane	120 °C	nd
4	Cy_2NH	Hexane	120 °C	25
5	Cy_2NH	Acetone	120 °C	34
6	NaOAc	Acetone	120 °C	8
7	Et_3N	Acetone	120 °C	15
8	DIPEA	Acetone	120 °C	18
9[c]	Cy_2NH	Acetone	120 °C	55
10[d]	Cy_2NH	Acetone	120 °C	59
11[e]	Cy_2NH	Acetone	120 °C	77
12[f]	Cy_2NH	Acetone	100 °C	54
13[g]	Cy_2NH	Acetone	140 °C	35
14[h]	Cy_2NH	Acetone	120 °C	48
15[i]	Cy_2NH	Acetone	120 °C	69
16[j]	Cy_2NH	Acetone	120 °C	nd
17[k]	-	Acetone	120 °C	trace

[a]Reaction conditions: **1a** (1 equiv, 0.16 mmol), **2a** (1.2 equiv, 0.19 mmol), [$MnBr(CO)_5$] (10 mol %), Cy_2NH (20 mol %), solvent (0.1 M), at 120 °C for 12 h. [b]isolated yield. [c]solvent (0.038 M). [d]1a (0.32 mmol), 2a (0.16 mmol). [e][$MnBr(CO)_5$] (20 mol %), Cy_2NH (40 mol %). [f]Reaction was carried out at 100 °C. [g]Reaction was carried out at 140 °C. [h]Reaction was carried out for 8 h. [i]Reaction was carried out for 16 h. [j]Reaction without Mn catalyst. [k]Reaction without base. nd = not detected.

unambiguously confirmed through single crystal X-ray analysis. Next, we examined the effect of electron donating group (3-OMe) at the C3-position which gave 88% yield of product **3da**. Moreover, we have also screened the effect of substituent on C4-position (4-Me) which gave the corresponding alkylated product **3ea** in good yield. Additionally, we also examined the effect of -Br and -Me group at the C5-position. Surprisingly, both the substituents produced trace amount of the products **3fa** and **3ga** respectively. The detrimental effect in the product formation may be due to the steric hindrance near to the reaction site. After exploring the various substrate's scope, we moved on to see the effect of different maleimide derivatives (Scheme 5.2). Treatment of *2H*-[1,2'-bipyridin]-2-one **1a** with different *N*-alkyl protected maleimides reacted well to furnish 67-74% of the desired product **3ab-3ae**. Under similar conditions, *N*-benzyl maleimides gave the corresponding product **3af** in 81% yield. Moreover, different electronically biased *N*-phenyl maleimide were also examined. *N*-phenyl maleimide reacted smoothly to give the product **3ag** in 84% yield. Both fluoro and chloro substituent at the *p*-position of *N*-phenyl maleimide has minimal effect on the yield of the reaction, resulting in 77% and 70% yield of the corresponding product **3ah**, **3ai** respectively. Additionally, we also screened the effect of electron donating and electron withdrawing substituent on phenyl ring of *N*-phenyl maleimide. It was found that electron donating group at the *p*-position (4-OMe, 4-Me) of *N*-phenyl maleimide showed higher reactivity **(3aj**, **3ak)** than electron withdrawing group at the *p*-position (4-COMe, 4-NO_2) of *N*-phenyl maleimides (**3al**, **3am**). Interestingly, substituent at the *m*-position of *N*-phenyl maleimide (*m*-Me, *m*-NO_2) underwent the reaction smoothly giving the product **3an** and **3ao** in 75% and 65% yield respectively. It is worthy to mention that the unprotected maleimide reacted well to give the alkylated product **3ap** in 55% yield. Further, we have explored the scope of the reaction with substitution on both 2-pyridone substrate as well as maleimide substrate. Pleasingly,

3-MeO and 4-Me substrate with *N*-methyl maleimide furnished the desired product **3db** and **3eb** in 70% and 76% yields respectively. In addition to that, 3-MeO pyridone **1d** with *N*-benzyl maleimide **2f** and *N*-cyclohexyl maleimide **2e** were found to be compatible under

Scheme 5.2: Scope of 2*H*-[1,2'-bipyridin]-2-ones and Maleimides for the Synthesis of alkylated products[a]

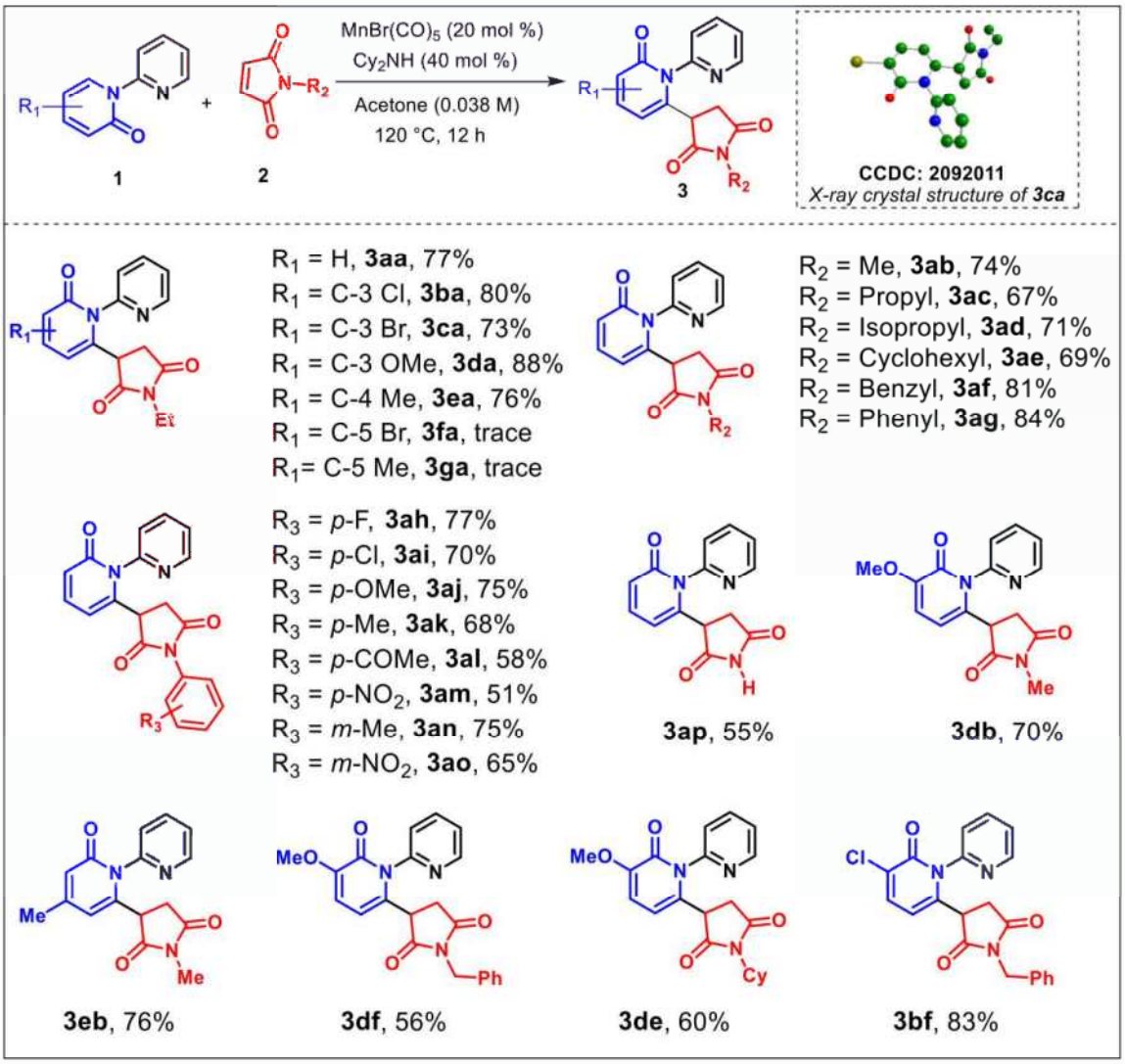

[a]Reaction conditions: **1a** (2.0 equiv), **2a** (1.0 equiv), [$MnBr(CO)_5$] (20 mol %), Cy_2NH (40 mol %), Acetone (0.038 M), 120 °C for 12 h.

the standard reaction conditions giving the product **3df** and **3de** in 56% and 60% yield respectively. Also, 3-Cl pyridone **1b** reacted well with *N*-benzyl maleimide **2f** to give desired alkylated product **3bf** with 83% yield.

To diversify the scope of the product, we attempted to reduce carbonyl group in the product **3aa** using Zinc and acetic acid condition. Interestingly, when the product **3aa** was treated with Zn/AcOH at 140 °C, we discovered an unusual rearrangement through C-N bond cleavage followed by the formation of a new C-C bond as well as an all-carbon quaternary

Scheme 5.3: Synthetic Application

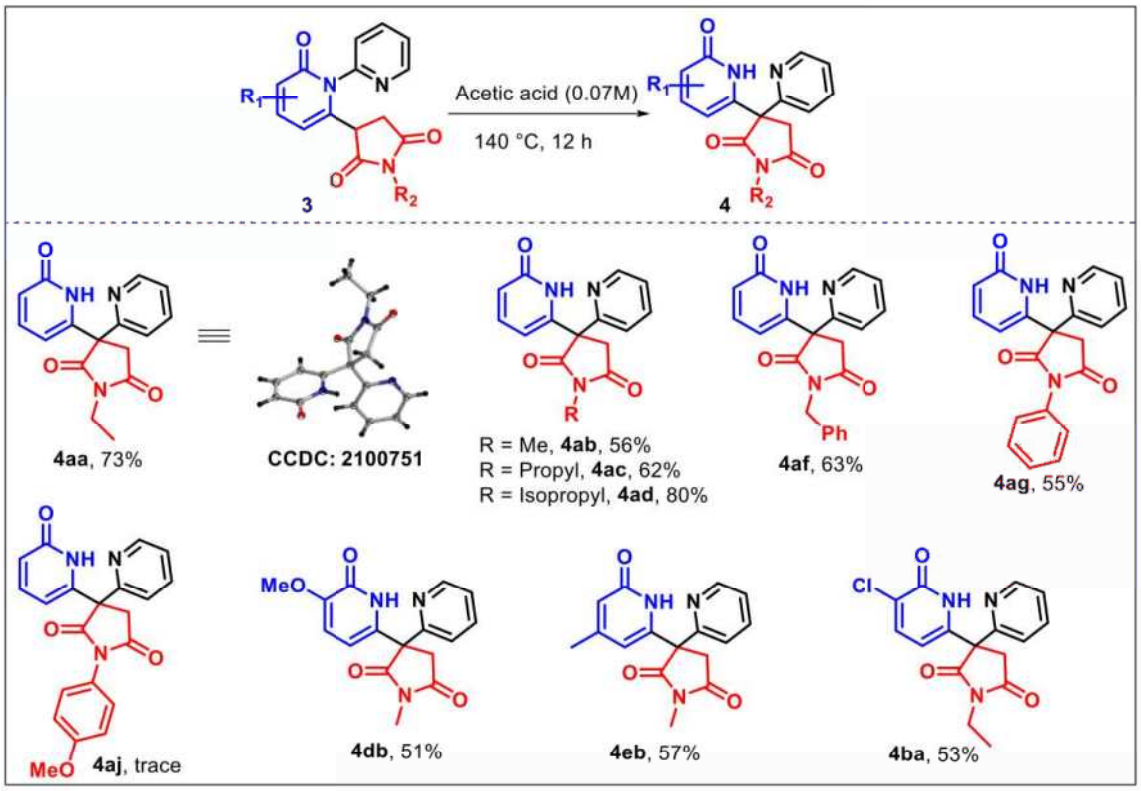

center **4aa** (Scheme 5.3). To ascertain the role of Zinc we performed a control experiment without Zn, we found that this reaction works well even without Zn. From single crystal X-ray analysis, we confirmed the structure of **4aa**. It is an interesting molecule with three different *N*-heterocycles with an all-carbon quaternary carbon center. Many bioactive compounds contain structural units with an all-carbon quaternary carbon center (Figure 5.1). However, synthesis of structural units with all carbon quaternary centers has been a challenging task for synthetic community due to the steric restriction imposed by all carbon quaternary centers. Intrigued by the structure of the product, we explored the scope with different alkylated products under the same condition. It was found that alkylated product

containing different *N*-alkyl group giving rearranged product in good to excellent yield(**4ab-4ad**). *N*-benzyl substrate **3af** also gave the desired rearranged product **4af** in 63%

Scheme 5.4: Mechanistic studies and synthetic applications

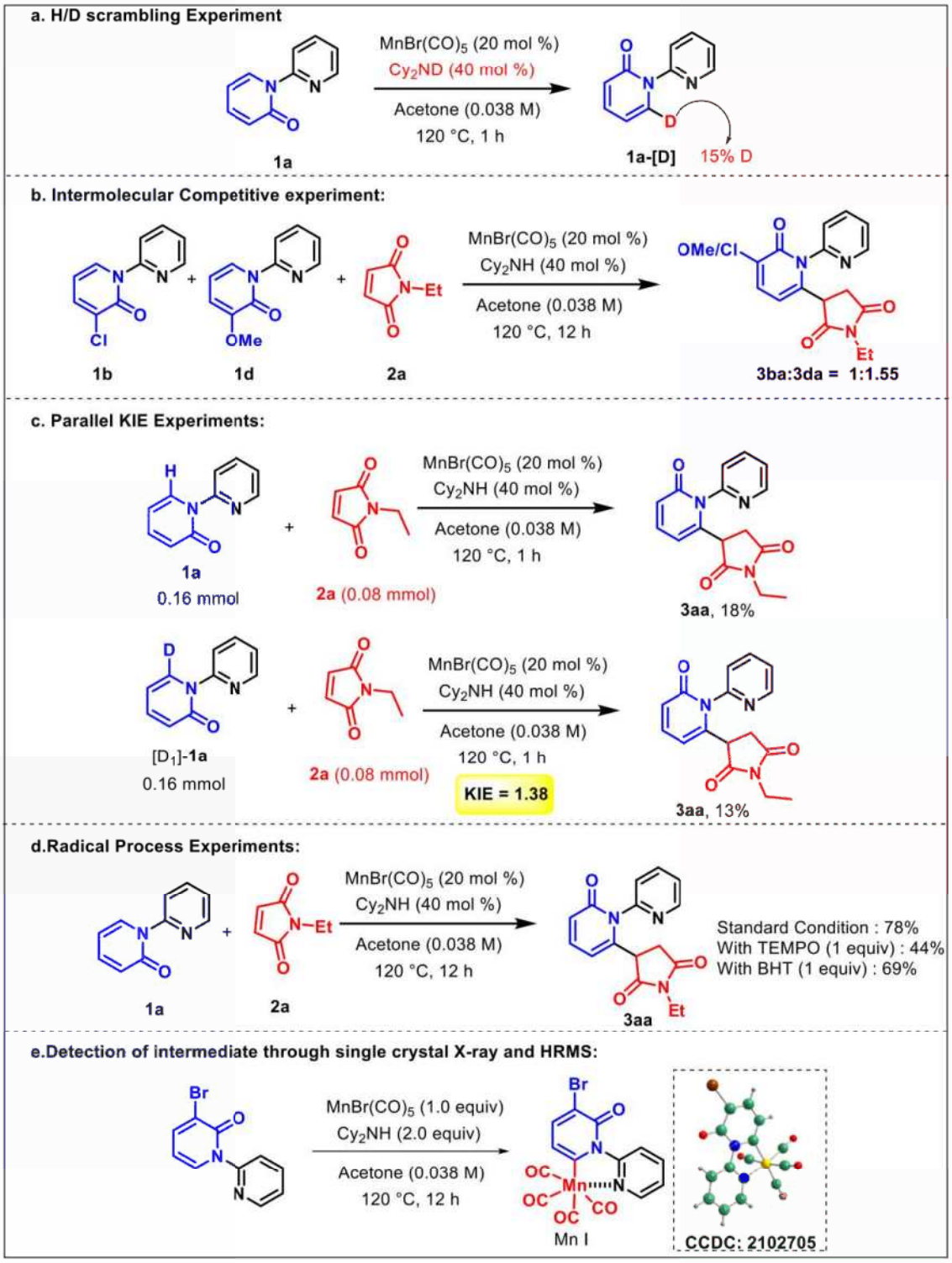

yield. *N*-phenyl group on succinimide ring underwent reaction smoothly giving **4ag** in decent yield. 3-OMe and 4-Me group on pyridone ring also gave rearranged product (**4db**, **4eb**) in good yields. Chloro group at the 3-position of pyridone gave the corresponding product (**4ba**). Overall, we have shown an efficient way to synthesize a new class of compound with an all carbon quaternary center involving three important heterocycles (succinimide, pyridine, pyridone) using our methodology.

To understand the reaction mechanism, we have done some mechanistic studies. We performed the H/D scrambling reaction with Cy_2ND. 2-pyridone was recovered with 15% D incorporation at C(6)-H position. It suggests that C-H activation step is reversible (Scheme-5.4a). Intermolecular competition experiment was performed between 3-chloro-*2H*-[1,2'-bipyridin]-2-one **1b** and 3-methoxy-*2H*-[1,2'-bipyridin]-2-one **1d** with maleimide **2a** giving the products **3ba**:**3da** in 1:1.55 ratio. This result suggests that the reaction goes through base-assisted intramolecular electrophilic substitution pathway (Scheme-5.4b).[21] We have performed parallel KIE experiment, we got low KIE value of 1.38. This value indicates that, C-H activation step might not be involved in the rate determining step (Scheme-5.4c).[21,22] From radical process experiment, it was found that reaction goes through ionic mechanism (Scheme-5.4d). A stoichiometric reaction was performed to isolate the manganacycle, we successfully isolated and characterized the manganacycle intermediate through HRMS and single crystal X-ray studies (Scheme-5.4e).

Scheme 5.5: 1 mmol scale reaction:

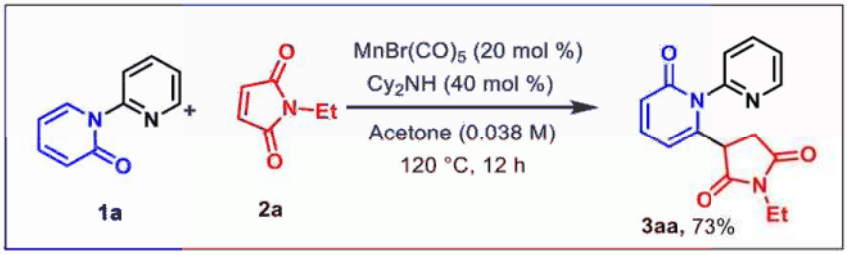

To demonstrate the application of this methodology in larger scales, a 1 mmol scale reaction was performed, we obtained the desired product **3aa** (217 mg) in 73% yield.

Scheme 5.6: Deprotection of 3aa:[23]

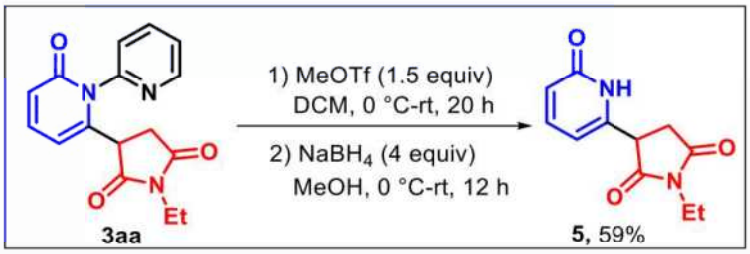

Finally, the directing group has been removed using a reaction sequence involving MeOTf and sodium borohydride. we obtained the directing group removal product **5** in 59% yield.

Scheme 5.7: Proposed catalytic cycle for the synthesis of alkylated product

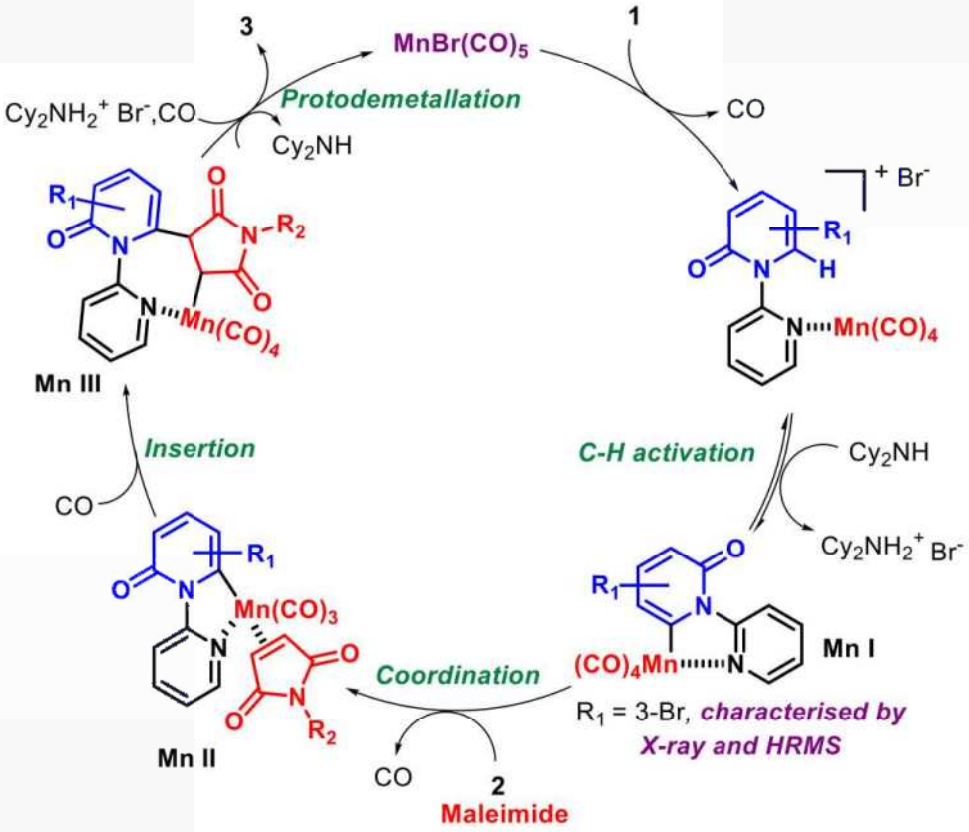

Based on mechanistic findings and previous literature reports,[24] herein we propose a plausible mechanism. The first step of the mechanism involves coordination of 2-pyridone **1** with $MnBr(CO)_5$ followed by C-H metalation forming a five membered manganacycle

(**Mn I**, characterized through single crystal X- ray and HRMS) (refer to see page no. 196-197). Coordination of maleimide **2** with **Mn I** gives **Mn II** intermediate. Subsequently, the maleimide gets inserted into the C-Mn bond of intermediate **Mn II** forming manganacycle **Mn III**. Protodemetallation of **Mn III** intermediate in presence of $Cy_2NH_2^+$ gives the product **3** and regenerates the catalyst for the next cycle**.**

Scheme 5.8: Proposed catalytic cycle for the synthesis of rearranged product

We propose a plausible mechanism for synthesis of the migratory product **4**. Alkylated product **3** under the influence of acetic acid undergoes enolization and also protonation at the pyridyl nitrogen **Int-1**. The enolized succinimide adds to the electrophilic carbon of pyridine to obtain **Int-2** through a transition state **TS-1**. Due to the loss of aromaticity and the formation of a four-membered strained ring, this intermediate (**Int-2)** is extremely unstable. Under acidic conditions, **Int-2** releases ring strain by gaining aromatisation leading to stable product **4**.

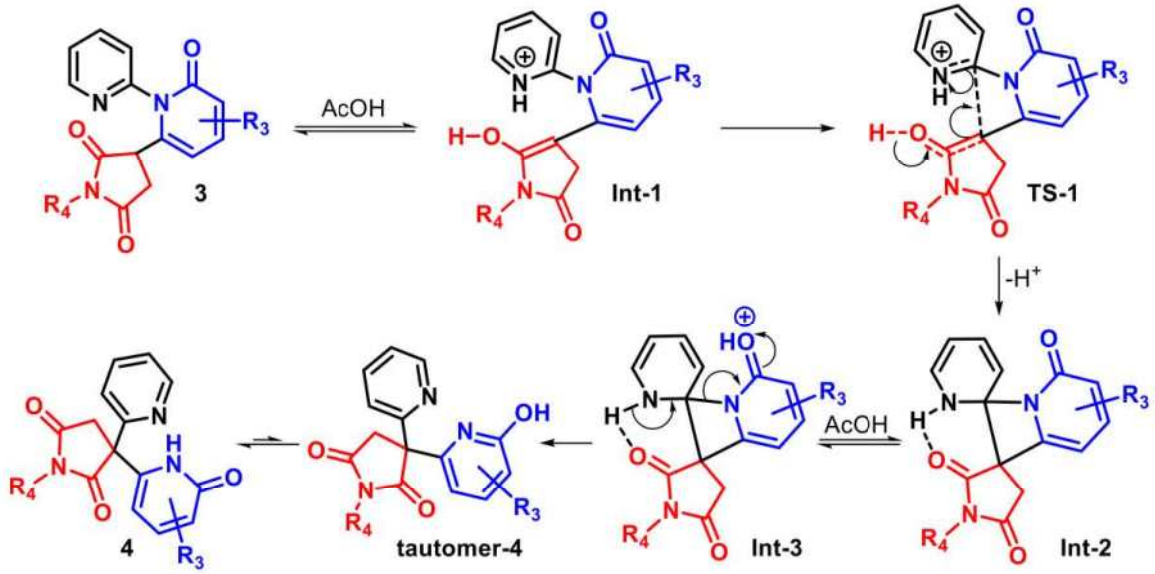

5.4 CONCLUSION

In conclusion, a Mn(I)-catalyzed C(6)-H alkylation of 2-pyridones using maleimides as coupling partner has been reported. The methodology highlights the specific formation of

alkylated product rather than the normal Diels-alder product. Also, an unexpected acid catalyzed rearrangement has been observed. Which is very interesting and leads to unique class of molecules containing three different *N*-heterocycles with an all-carbon quaternary carbon center. This methodology worked well with a variety of substrates.

5.5 EXPERIMENTAL SECTION

Reactions were performed using borosil sealed tube vial under N_2 atmosphere. Column chromatography was done by using 230-400 mesh silica gel of Acme synthetic chemicals company. A gradient elution was performed by using distilled petroleum ether and ethyl acetate. Merck TLC Silica gel 60 F_{254} aluminum plates were used. TLC plates detected under UV light at 254 nm and vanillin. ^{1}H NMR, $^{13}C\{^{1}H\}$ NMR and ^{19}F NMR were recorded on Bruker AV 400 and 700 MHz spectrometer using $CDCl_3$ as the deuterated solvent.[25] Multiplicity (s = singlet, d = doublet, t = triplet, q = quartet, quint = quintet, sept = septet, m = multiplet, dd = double of doublet, br = broad signal), integration, and coupling constants (*J*) in hertz (Hz). HRMS signal analysis was performed using micro TOF Q-II mass spectrometer. Reagents and starting materials were purchased from Sigma Aldrich, TCI, Avra, Spectrochem and other commercially available sources, used without further purification unless otherwise noted. All pyridones were prepared according to the reported literature procedure.[26]

5.5.1 Representative procedure for the synthesis of 1-Ethyl-3-(2-oxo-*2H*-[1,2'-bipyridin]-6-yl)pyrrolidine-2,5-dione:

To a flame-dried teflon-screw-capped tube was equipped with a magnetic stir bar, $MnBr(CO)_5$ (9 mg, 0.032 mmol, 20 mol %), acetone (4.2 ml, 0.038 M), *2H*-[1,2'-bipyridin]-2-one **1** (56 mg, 0.32 mmol, 2 equiv), maleimide **2** (20 mg, 0.16 mmol, 1 equiv) and Cy_2NH (12 mg, 0.064 mmol, 40 mol %) were added sequentially under nitrogen. The closed tube

was put into a pre-heated aluminum block at 120 ºC and stirred for 12 h. After completion of the reaction, the resulting mixture was cooled down to room temperature, diluted with DCM, filtered through a short pad of celite and washed with EtOAc. The filtrate was pre-absorbed on silica gel and concentrated by rotary evaporator. The crude product was purified by silica gel column chromatography (DCM:MeOH = 95:5) to afford the product **3**.

5.5.2 Representative procedure for the acid catalyzed rearrangement:

In a sealed tube solution of **3** (30 mg, 0.1 mmol, 1 equiv) was added in acetic acid (1.5 mL, 0.07 M), the reaction mixture was stirred for 12 h at 140 °C. The reaction mixture was quenched with saturated sodium bicarbonate and extracted with EtOAc. The solvent was removed under reduced pressure and the residue was purified by silica gel column chromatography using DCM/EtOAc to afford **4** in 51-80% yield.

5.5.3 Experimental characterization data of products:

1-Ethyl-3-(2-oxo-*2H*-[1,2'-bipyridin]-6-yl)pyrrolidine-2,5-dione (3aa):

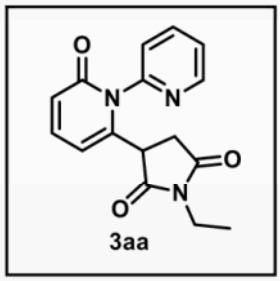

3aa

Physical state: yellow liquid (37 mg in 77% yield). R_f: 0.4 (5% MeOH/DCM). ^{1}H NMR (400 MHz, $CDCl_3$): δ 8.63 (dd, J = 4.8, 1.2 Hz, 1H), 7.92 (td, J = 7.6, 2.0 Hz, 1H), 7.49 (d, J = 8.0 Hz, 1H), 7.44–7.36 (m, 2H), 6.63 (d, J = 9.2 Hz, 1H), 6.07 (d, J = 6.8 Hz, 1H), 3.70–3.66 (m, 1H), 3.48 (q, J = 7.2 Hz, 2H), 2.90 (dd, J = 18.8, 5.6 Hz, 1H), 2.80–2.73 (m, 1H), 1.13 (t, J = 7.2 Hz, 3H). ^{13}C NMR (100 MHz, $CDCl_3$): δ 174.9, 174.8, 163.7, 151.3, 150.1, 145.3, 140.2, 139.1, 125.6, 124.9, 121.5, 105.6, 44.2, 37.3, 34.6, 13.3. IR (KBr, cm^{-1}): 1773, 1702, 1545, 1227. HRMS (ESI) m/z: $[M + Na]^+$ calcd for $C_{16}H_{15}N_3O_3Na$, 320.1006; found, 320.1000.

3-(3-Chloro-2-oxo-*2H*-[1,2'-bipyridin]-6-yl)-1-ethylpyrrolidine-2,5-dione (3ba):

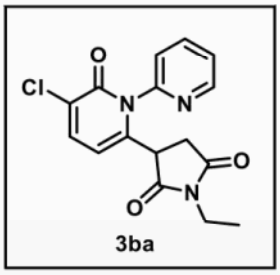

3ba

Physical state: light yellow solid (42 mg in 80% yield). mp: 190–192 °C. R_f: 0.4 (5% MeOH/DCM). ^{1}H NMR ($CDCl_3$, 400 MHz): δ 8.62 (dd, J = 4.8, 0.8 Hz, 1H), 7.94 (td, J = 7.6, 2.0 Hz, 1H), 7.58 (d, J = 7.6 Hz, 1H), 7.50–7.43 (m, 2H), 6.06 (d, J = 7.6 Hz, 1H), 3.70–3.67 (m, 1H), 3.47 (q, J = 6.8 Hz, 2H), 2.92–2.86 (m, 1H), 2.81–2.73 (m, 1H), 1.12 (t, J = 7.2 Hz, 3H). ^{13}C NMR ($CDCl_3$, 100 MHz): δ 174.5, 174.5, 159.9, 150.9, 150.1, 143.9, 139.2, 138.0, 126.8, 125.4, 125.2, 105.1, 44.0, 37.1, 34.6, 13.2. IR (KBr, cm^{-1}): 1775, 1700, 1665, 1404, 1226. HRMS (ESI) m/z: $[M + H]^+$ calcd for $C_{16}H_{15}ClN_3O_3$, 332.0796; found, 332.0812.

3-(3-Bromo-2-oxo-*2H*-[1,2'-bipyridin]-6-yl)-1-ethylpyrrolidine-2,5-dione (3ca):

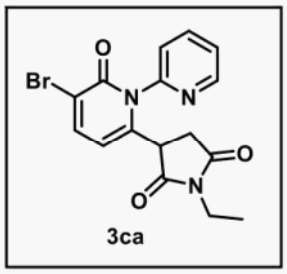

3ca

Physical state: yellow solid (44 mg in 73% yield). mp: 198–200 °C. R_f: 0.35 (5% MeOH/DCM). ^{1}H NMR ($CDCl_3$, 400 MHz): δ 8.61 (dd, J = 5.2, 1.2 Hz, 1H), 7.93 (td, J = 7.6, 2.0 Hz, 1H), 7.78 (d, J = 7.6 Hz, 1H), 7.50–7.42 (m, 2H), 6.01 (d, J = 7.6 Hz, 1H), 3.69–3.66 (m, 1H), 3.47 (q, J = 6.8 Hz, 2H), 2.89 (dd, J = 18.4, 5.6 Hz, 1H), 2.81–2.74 (m, 1H), 1.12 (t, J = 7.2 Hz, 3H). ^{13}C NMR ($CDCl_3$, 100 MHz): δ 174.5, 174.5, 159.9, 151.0, 150.0, 144.8, 141.9, 139.2, 125.3, 125.1, 116.9, 105.8, 44.1, 37.1, 34.6, 13.2. IR (KBr, cm^{-1}): 1775, 1699, 1662, 1599, 1349, 1225. HRMS (ESI) m/z: $[M + Na]^+$ calcd for $C_{16}H_{14}BrN_3O_3Na$, 398.0111; found, 398.0109.

1-Ethyl-3-(3-methoxy-2-oxo-*2H*-[1,2'-bipyridin]-6-yl)pyrrolidine-2,5-dione (3da):

Physical state: yellow liquid (46 mg in 88% yield). R_f: 0.3 (5% MeOH/DCM). ^{1}H NMR ($CDCl_3$, 400 MHz): δ 8.61 (dd, J = 4.8, 1.2 Hz, 1H), 7.91 (td, J = 7.6, 2.0 Hz, 1H), 7.49–7.40 (m, 2H), 6.63 (d, J = 7.6 Hz, 1H), 6.02 (d, J = 7.6 Hz, 1H), 3.86–3.84 (m, 3H), 3.68–3.64 (m, 1H), 3.46 (q, J = 6.8 Hz, 2H), 2.90–2.69 (m, 2H), 1.12 (t, J = 7.2 Hz, 3H). ^{13}C

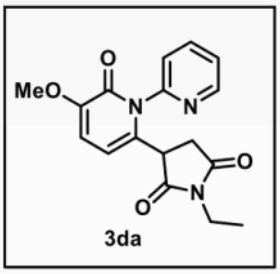

NMR ($CDCl_3$, 100 MHz): δ 175.4, 175.1, 159.2, 151.2, 150.2, 150.0, 139.0, 135.3, 125.7, 124.8, 112.4, 104.9, 56.4, 43.8, 37.4, 34.5, 13.3. IR (KBr, cm^{-1}): 1773, 1694, 1657, 1606, 1226. HRMS (ESI) m/z: $[M + H]^+$ calcd for $C_{17}H_{18}N_3O_4$, 328.1292; found, 328.1289.

1-Ethyl-3-(4-methyl-2-oxo-*2H*-[1,2'-bipyridin]-6-yl)pyrrolidine-2,5-dione (3ea):

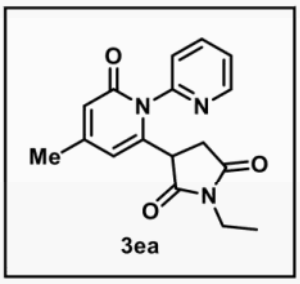

Physical state: brown liquid (38 mg in 76% yield). R_f: 0.2 (5% MeOH/DCM). ^1H NMR ($CDCl_3$, 400 MHz): δ 8.61 (dd, J = 5.2, 1.2 Hz, 1H), 7.90 (td, J = 7.6, 1.6 Hz, 1H), 7.48–7.39 (m, 2H), 6.43 (s, 1H), 5.90 (d, J = 1.2 Hz, 1H), 3.69–3.66 (m, 1H), 3.48 (q, J = 6.4 Hz, 2H), 2.93–2.87 (m, 1H), 2.79–2.72 (m, 1H), 2.21 (s, 3H), 1.13 (t, J = 7.2 Hz, 3H). ^{13}C NMR ($CDCl_3$, 100 MHz): δ 175.0, 174.9, 163.7, 151.8, 151.3, 150.0, 143.9, 139.0, 125.7, 124.7, 119.6, 108.4, 44.1, 37.3, 34.6, 21.9, 13.3. IR (KBr, cm^{-1}): 1773, 1699, 1590, 1546, 1351, 1227. HRMS (ESI) m/z: $[M + Na]^+$ calcd for $C_{17}H_{17}N_3O_3Na$, 334.1162; found, 334.1175.

1-Methyl-3-(2-oxo-*2H*-[1,2'-bipyridin]-6-yl)pyrrolidine-2,5-dione (3ab):

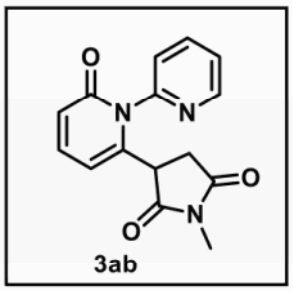

Physical state: light yellow liquid (34 mg in 74% yield). R_f: 0.35 (5% MeOH/DCM). ^1H NMR (400 MHz, $CDCl_3$): δ 8.62 (d, J = 2.8 Hz, 1H), 7.92 (t, J = 4.4 Hz, 1H), 7.49–7.37 (m, 3H), 6.64 (d, J = 5.2 Hz, 1H), 6.11 (d, J = 4.0 Hz, 1H), 3.73 (s, 1H), 2.98–2.94 (m, 1H), 2.89 (s, 3H), 2.82–2.78 (m, 1H). ^{13}C NMR (100 MHz, $CDCl_3$): δ 175.1, 175.0, 163.7, 151.2, 150.1, 144.8, 140.1, 139.0, 125.7, 124.9, 121.6, 106.1, 44.4, 37.1, 25.6. IR (KBr, cm^{-1}): 1781, 1702, 1544, 1438, 1286. HRMS (ESI) m/z: $[M + Na]^+$ calcd for $C_{15}H_{13}N_3O_3Na$, 306.0849; found, 306.0843.

3-(2-Oxo-*2H*-[1,2'-bipyridin]-6-yl)-1-propylpyrrolidine-2,5-dione (3ac):

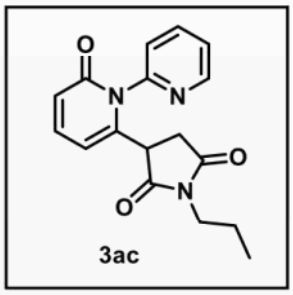

Physical state: brown liquid (33 mg in 67% yield). R_f: 0.2 (1% MeOH/DCM). ^{1}H NMR (700 MHz, $CDCl_3$): δ 8.63 (dd, J = 4.9, 1.4 Hz, 1H), 7.93 (td, J = 7.7, 1.4 Hz, 1H), 7.49 (d, J = 7.7 Hz, 1H), 7.44–7.42 (m, 1H), 7.39 (dd, J = 9.1, 7.0 Hz, 1H), 6.63 (d, J = 9.1 Hz, 1H), 6.07 (d, J = 7.0 Hz, 1H), 3.68 (s, 1H), 3.42–3.35 (m, 2H), 2.91–2.88 (m, 1H), 2.79–2.75 (m, 1H), 1.58–1.52 (m, 2H), 0.88 (t, J = 7.7 Hz, 3H). ^{13}C NMR (100 MHz, $CDCl_3$): δ 175.1, 175.0, 163.7, 151.3, 150.1, 145.3, 140.2, 139.1, 125.6, 124.9, 121.5, 105.5, 44.1, 41.2, 37.3, 21.3, 11.6. IR (KBr, cm^{-1}): 1774, 1699, 1663, 1545, 1402, 1206. HRMS (ESI) m/z: $[M + Na]^+$ calcd for $C_{17}H_{17}N_3O_3Na$, 334.1162; found, 334.1160.

1-Isopropyl-3-(2-oxo-*2H*-[1,2'-bipyridin]-6-yl)pyrrolidine-2,5-dione (3ad):

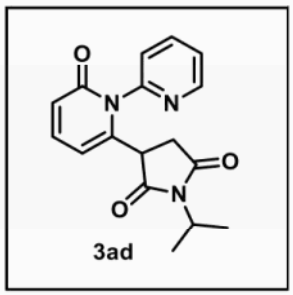

Physical state: light brown liquid (35 mg in 71% yield). R_f: 0.3 (1% MeOH/DCM). ^{1}H NMR (400 MHz, $CDCl_3$): δ 8.65 (dd, J = 4.0, 1.6 Hz, 1H), 7.93 (td, J = 7.6, 2.0 Hz, 1H), 7.50 (d, J = 8.0 Hz, 1H), 7.45–7.42 (m, 1H), 7.38 (dd, J = 9.6, 7.2 Hz, 1H), 6.62 (dd, J = 9.2, 0.8 Hz, 1H), 6.03 (d, J = 6.4 Hz, 1H), 4.40–4.30 (m, 1H), 3.58–3.57 (m, 1H), 2.84–2.68 (m, 2H), 1.35 (dd, J = 6.8, 3.6 Hz, 6H). ^{13}C NMR (100 MHz, $CDCl_3$): δ 175.0, 174.9, 163.6, 151.4, 150.2, 145.9, 140.2, 139.2, 125.4, 124.9, 121.4, 104.9, 44.7, 43.7, 37.4, 19.5, 19.4. IR (KBr, cm^{-1}): 1772, 1696, 1662, 1590, 1546, 1369. HRMS (ESI) m/z: $[M + H]^+$ calcd for $C_{17}H_{18}N_3O_3$, 312.1343; found, 312.1354.

1-Cyclohexyl-3-(2-oxo-*2H*-[1,2'-bipyridin]-6-yl)pyrrolidine-2,5-dione (3ae):

Physical state: yellow liquid (39 mg in 69% yield). R_f: 0.25 (5% MeOH/DCM). ^{1}H NMR (400 MHz, $CDCl_3$): δ 8.65 (dd, J = 4.8, 1.2 Hz, 1H), 7.93 (td, J = 8.0, 2.0 Hz, 1H), 7.51 (d, J = 8.0 Hz, 1H), 7.45–7.36 (m, 2H), 6.62 (dd, J = 9.2, 0.8 Hz, 1H), 6.02 (d, J = 6.4 Hz, 1H),

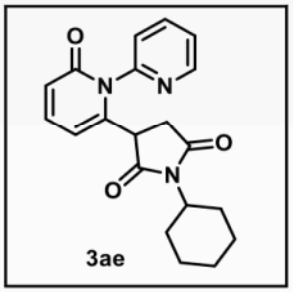

3.98–3.90 (m, 1H), 3.58 (s, 1H), 2.83–2.67 (m, 2H), 2.14–2.04 (m, 2H), 1.83–1.80 (m, 2H), 1.54–1.52 (m, 2H), 1.34–1.17 (m, 4H). ^{13}C NMR (100 MHz, $CDCl_3$): δ 175.1, 175.1, 163.6, 151.4, 150.2, 146.0, 140.2, 139.2, 125.4, 124.8, 121.4, 104.8, 52.6, 43.6, 37.3, 29.1, 29.0, 26.1, 25.2, 14.5. IR (KBr, cm^{-1}): 1772, 1699, 1667, 1592, 1545, 1374. HRMS (ESI) m/z: $[M + Na]^+$ calcd for $C_{20}H_{21}N_3O_3Na$, 374.1475; found, 374.1481.

1-Benzyl-3-(2-oxo-*2H*-[1,2'-bipyridin]-6-yl)pyrrolidine-2,5-dione (3af):

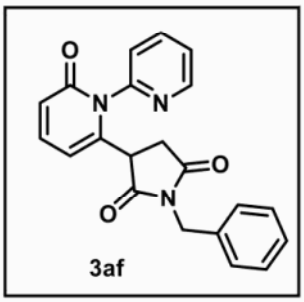

Physical state: light green liquid (47 mg in 81% yield). R_f: 0.5 (5% MeOH/DCM). ^{1}H NMR (400 MHz, $CDCl_3$): δ 8.57 (dd, J = 4.8, 1.2 Hz, 1H), 7.87 (td, J = 8.0, 2.0 Hz, 1H), 7.46 (d, J = 7.6 Hz, 1H), 7.39–7.29 (m, 7H), 6.61 (dd, J = 9.2, 0.8 Hz, 1H), 5.98 (d, J = 6.4 Hz, 1H), 4.60–4.52 (m, 2H), 3.70–3.66 (m, 1H), 2.92–2.86 (m, 1H), 2.80–2.73 (m, 1H). ^{13}C NMR (100 MHz, $CDCl_3$): δ 174.7, 174.6, 163.6, 151.2, 150.1, 145.1, 140.2, 139.1, 135.5, 129.4, 129.1, 128.6, 125.5, 124.8, 121.5, 105.7, 44.2, 43.2, 37.3. IR (KBr, cm^{-1}): 1776, 1706, 1669, 1589, 1545, 1398. HRMS (ESI) m/z: $[M + Na]^+$ calcd for $C_{21}H_{17}N_3O_3Na$, 382.1162; found, 382.1173.

3-(2-Oxo-*2H*-[1,2'-bipyridin]-6-yl)-1-phenylpyrrolidine-2,5-dione (3ag):

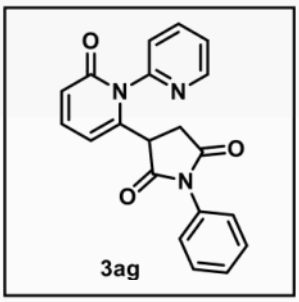

Physical state: yellow solid (46 mg in 84% yield). mp: 206–209 °C. R_f: 0.3 (5% MeOH/DCM). ^{1}H NMR (400 MHz, $CDCl_3$): δ 8.64 (d, J = 4.8 Hz, 1H), 7.90 (td, J = 7.6, 1.6 Hz, 1H), 7.50–7.37 (m, 6H), 7.18 (d, J = 7.2 Hz, 2H), 6.63 (d, J = 9.2 Hz, 1H), 6.20 (d, J = 6.8 Hz, 1H), 3.92–3.88 (m, 1H), 3.10–2.90 (m, 2H). ^{13}C NMR (100 MHz, $CDCl_3$): δ 174.0, 173.9, 163.6, 151.2, 150.0, 144.8, 140.1, 139.1, 131.6, 129.5, 129.2, 126.4, 125.6, 124.9, 121.6, 105.9, 44.2, 37.1. IR (KBr, cm^{-1}): 1778, 1710,

1667, 1592, 1545, 1387. HRMS (ESI) m/z: $[M + Na]^+$ calcd for $C_{20}H_{15}N_3O_3Na$, 368.1006; found, 368.1013.

1-(4-Fluorophenyl)-3-(2-oxo-*2H*-[1,2'-bipyridin]-6-yl)pyrrolidine-2,5-dione (3ah):

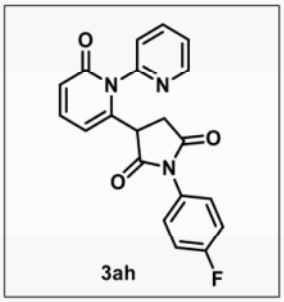

Physical state: light yellow liquid (45 mg in 77% yield). R_f: 0.4 (5% MeOH/DCM). ^{1}H NMR (400 MHz, $CDCl_3$): δ 8.66 (dd, J = 4.8, 1.2 Hz, 1H), 7.93 (td, J = 7.6, 1.6 Hz, 1H), 7.53 (d, J = 8.0 Hz, 1H), 7.46–7.39 (m, 2H), 7.22–7.12 (m, 4H), 6.67 (d, J = 9.2 Hz, 1H), 6.20 (d, J = 6.4 Hz, 1H), 3.94–3.90 (m, 1H), 3.14–3.08 (m, 1H), 3.01–2.94 (m, 1H). ^{13}C NMR (100 MHz, $CDCl_3$): δ 174.0, 173.8, 163.6, 162.6 (d, $J_{C\text{-}F}$ = 247.8 Hz), 151.3, 150.1, 140.1, 139.2, 128.3 (d, $J_{C\text{-}F}$ = 8.7 Hz), 127.6, 125.7, 125.0, 121.8, 116.6 (d, $J_{C\text{-}F}$ = 22.9 Hz), 105.9, 44.3, 37.1. ^{19}F NMR (376 MHz, $CDCl_3$): δ -111.5. IR (KBr, cm^{-1}): 1780, 1713, 1666, 1592, 1390, 752. HRMS (ESI) m/z: $[M + H]^+$ calcd for $C_{20}H_{15}FN_3O_3$, 364.1092; found, 364.1061.

1-(4-Chlorophenyl)-3-(2-oxo-*2H*-[1,2'-bipyridin]-6-yl)pyrrolidine-2,5-dione (3ai):

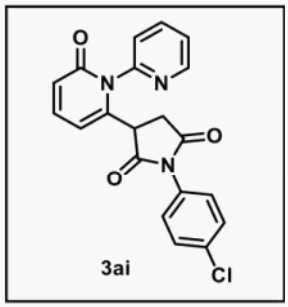

Physical state: colorless liquid (42 mg in 70% yield). R_f: 0.3 (5% MeOH/DCM). ^{1}H NMR (400 MHz, $CDCl_3$): δ 8.65 (d, J = 3.6 Hz, 1H), 7.92 (td, J = 7.6, 1.6 Hz, 1H), 7.53 (d, J = 8.0 Hz, 1H), 7.46–7.39 (m, 4H), 7.17 (d, J = 8.8 Hz, 2H), 6.67 (d, J = 9.2 Hz, 1H), 6.20 (d, J = 6.8 Hz, 1H), 3.94–3.90 (m, 1H), 3.15–3.09 (m, 1H), 3.02–2.95 (m, 1H). ^{13}C NMR (100 MHz, $CDCl_3$): δ 173.8, 173.6, 163.6, 151.3, 150.1, 140.1, 139.2, 135.1, 131.0, 130.1, 129.8, 127.6, 125.8, 125.0, 121.9, 106.1, 44.4, 37.1. IR (KBr, cm^{-1}): 1781, 1716, 1543, 1493, 1184. HRMS (ESI) m/z: $[M + H]^+$ calcd for $C_{20}H_{15}ClN_3O_3$, 380.0796; found, 380.0795.

1-(4-Methoxyphenyl)-3-(2-oxo-*2H*-[1,2'-bipyridin]-6-yl)pyrrolidine-2,5-dione (3aj):

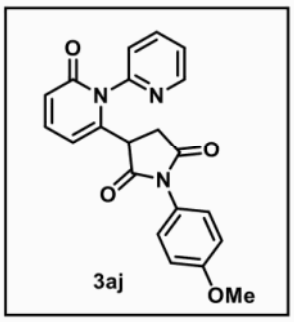

Physical state: yellow liquid (45 mg in 75% yield). R_f: 0.35 (5% MeOH/DCM). ^{1}H NMR (400 MHz, $CDCl_3$): δ 8.66 (dd, J = 4.4, 1.2 Hz, 1H), 7.93 (td, J = 7.6, 1.6 Hz, 1H), 7.53 (d, J = 8.0 Hz, 1H), 7.46–7.39 (m, 2H), 7.12–7.09 (m, 2H), 6.98–6.94 (m, 2H), 6.66 (d, J = 9.6 Hz, 1H), 6.21 (d, J = 6.8 Hz, 1H), 3.91–3.87 (m, 1H), 3.82 (s, 3H), 3.12–3.06 (m, 1H), 2.99–2.92 (m, 1H). ^{13}C NMR (100 MHz, $CDCl_3$): δ 174.3, 174.2, 163.7, 160.1, 151.3, 150.1, 145.0, 140.2, 139.2, 127.7, 125.7, 125.0, 124.2, 121.7, 114.9, 105.9, 55.9, 44.3, 37.2. IR (KBr, cm^{-1}): 1779, 1711, 1667, 1591, 1513, 1392, 1251. HRMS (ESI) m/z: $[M + H]^+$ calcd for $C_{21}H_{18}N_3O_4$, 376.1292; found, 376.1274.

3-(2-Oxo-*2H*-[1,2'-bipyridin]-6-yl)-1-(*p*-tolyl)pyrrolidine-2,5-dione (3ak):

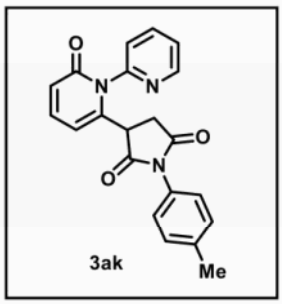

Physical state: yellow solid (39 mg in 68% yield). mp: 122–124 °C. R_f: 0.3 (5% MeOH/DCM). ^{1}H NMR (400 MHz, $CDCl_3$): δ 8.66 (dd, J = 4.8, 1.2 Hz, 1H), 7.92 (td, J = 7.6, 1.6 Hz, 1H), 7.52 (d, J = 8.0 Hz, 1H), 7.46–7.39 (m, 2H), 7.27–7.25 (m, 2H), 7.07 (d, J = 8.4 Hz, 2H), 6.66 (d, J = 9.2 Hz, 1H), 6.21 (d, J = 6.8 Hz, 1H), 3.91–3.87 (m, 1H), 3.13–3.06 (m, 1H), 2.99–2.92 (m, 1H), 2.37 (s, 3H). ^{13}C NMR (100 MHz, $CDCl_3$): δ 174.2, 174.1, 163.7, 151.4, 150.1, 145.0, 140.2, 139.5, 139.2, 130.2, 129.0, 126.3, 125.7, 125.0, 121.7, 105.9, 44.3, 37.2, 21.5. IR (KBr, cm^{-1}): 1775, 1705, 1654, 1542, 1515, 1392. HRMS (ESI) m/z: $[M + Na]^+$ calcd for $C_{21}H_{17}N_3O_3Na$, 382.1162; found, 382.1187.

1-(4-Acetylphenyl)-3-(2-oxo-*2H*-[1,2'-bipyridin]-6-yl)pyrrolidine-2,5-dione (3al):

Physical state: yellow liquid (36 mg in 58% yield). R_f: 0.2 (5% MeOH/DCM). ^{1}H NMR (400 MHz, $CDCl_3$): δ 8.65 (dd, J = 4.8, 2.4 Hz, 1H), 8.06–8.02 (m, 2H), 7.92 (td, J = 7.6,

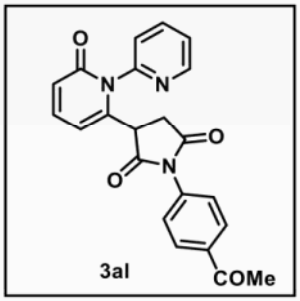

1.6 Hz, 1H), 7.53 (d, J = 8.0 Hz, 1H), 7.46–7.40 (m, 2H), 7.38–7.35 (m, 2H), 6.67 (dd, J = 9.2, 0.8 Hz, 1H), 6.22 (dd, J = 6.8, 0.8 Hz, 1H), 3.98–3.94 (m, 1H), 3.18–3.12 (m, 1H), 3.05–2.98 (m, 1H), 2.62 (s, 3H). ^{13}C NMR (100 MHz, $CDCl_3$): δ 197.1, 173.6, 173.4, 163.6, 151.3, 150.1, 144.5, 140.1, 139.2, 137.2, 135.6, 129.5, 126.4, 125.8, 125.0, 121.9, 106.2, 44.5, 37.1, 27.0. IR (KBr, cm^{-1}): 1715, 1542, 1466, 1386, 1266. HRMS (ESI) m/z: $[M + H]^+$ calcd for $C_{22}H_{18}N_3O_4$, 388.1292; found, 388.1277.

1-(4-Nitrophenyl)-3-(2-oxo-*2H*-[1,2'-bipyridin]-6-yl)pyrrolidine-2,5-dione (3am):

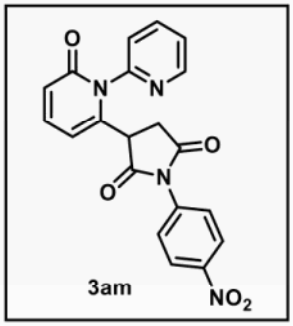

Physical state: light brown liquid (32 mg in 51% yield). R_f: 0.4 (5% MeOH/DCM). ^{1}H NMR (400 MHz, $CDCl_3$): δ 8.64 (dd, J = 4.8, 1.6 Hz, 1H), 8.32 (d, J = 9.2 Hz, 2H), 7.92 (td, J = 8.0, 2.0 Hz, 1H), 7.55–7.40 (m, 5H), 6.68 (d, J = 9.2 Hz, 1H), 6.21 (d, J = 6.8 Hz, 1H), 4.01–3.98 (m, 1H), 3.21–3.15 (m, 1H), 3.08–3.01 (m, 1H). ^{13}C NMR (100 MHz, $CDCl_3$): δ 173.3, 173.0, 163.6, 151.2, 150.1, 147.5, 144.0, 140.1, 139.2, 137.1, 126.9, 125.8, 125.1, 124.8, 122.1, 106.5, 44.5, 37.0. IR (KBr, cm^{-1}): 1718, 1663, 1593, 1528, 1343. HRMS (ESI) m/z: $[M + Na]^+$ calcd for $C_{20}H_{14}N_4O_5Na$, 413.0856; found, 413.0877.

3-(2-Oxo-*2H*-[1,2'-bipyridin]-6-yl)-1-(*m*-tolyl)pyrrolidine-2,5-dione (3an):

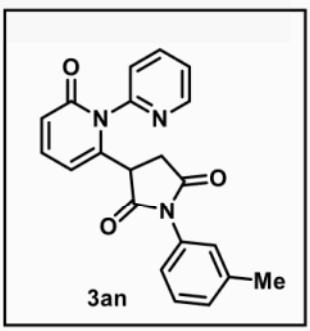

Physical state: light yellow solid (43 mg in 75% yield). mp: 124–127 °C. R_f: 0.2 (1% MeOH/DCM). ^{1}H NMR (400 MHz, $CDCl_3$): δ 8.66 (dd, J = 4.8, 1.2 Hz, 1H), 7.92 (td, J = 7.6, 2.0 Hz, 1H), 7.52 (d, J = 7.6 Hz, 1H), 7.46–7.39 (m, 2H), 7.34 (t, J = 7.6 Hz, 1H), 7.21 (d, J = 7.6 Hz, 1H), 6.97 (d, J = 8.0 Hz, 2H), 6.65 (d, J = 8.8 Hz, 1H), 6.21 (d, J = 6.8 Hz, 1H), 3.91–3.87 (m, 1H), 3.11–3.05 (m, 1H),

2.99–2.92 (m, 1H), 2.37 (s, 3H). ^{13}C NMR (100 MHz, $CDCl_3$): δ 174.1, 174.0, 163.6, 151.3, 150.1, 145.0, 140.2, 139.7, 139.2, 131.5, 130.1, 129.4, 127.1, 125.7, 124.9, 123.6, 121.6, 105.8, 44.3, 37.2, 21.6. IR (KBr, cm^{-1}): 1779, 1711, 1662, 1595, 1383. HRMS (ESI) m/z: $[M + Na]^+$ calcd for $C_{21}H_{17}N_3O_3Na$, 382.1162; found, 382.1160.

1-(3-Nitrophenyl)-3-(2-oxo-*2H*-[1,2'-bipyridin]-6-yl)pyrrolidine-2,5-dione (3ao):

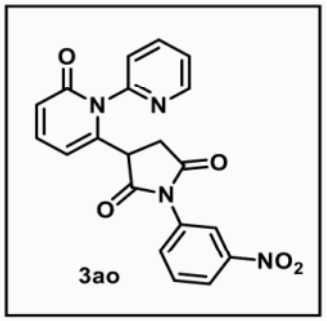

3ao

Physical state: brown liquid (41 mg in 65% yield). R*f*: 0.3 (1% MeOH/DCM). ^{1}H NMR (400 MHz, $CDCl_3$): δ 8.65 (dd, J = 4.4, 0.8 Hz, 1H), 8.28–8.25 (m, 1H), 8.11 (d, J = 2.0 Hz, 1H), 7.94 (td, J = 7.6, 1.6 Hz, 1H), 7.68–7.60 (m, 2H), 7.54 (d, J = 7.6 Hz, 1H), 7.47–7.41 (m, 2H), 6.69 (d, J = 9.2 Hz, 1H), 6.23 (d, J = 6.8 Hz, 1H), 4.04–4.00 (m, 1H), 3.28–3.22 (m, 1H), 3.10–3.03 (m, 1H). ^{13}C NMR (100 MHz, $CDCl_3$): δ 173.4, 173.2, 163.6, 151.2, 150.1, 148.8, 140.1, 139.3, 132.7, 132.2, 130.4, 125.9, 125.1, 123.9, 122.1, 121.8, 114.4, 106.7, 44.6, 37.0. IR (KBr, cm^{-1}): 1719, 1661, 1592, 1534, 1351. HRMS (ESI) m/z: $[M + K]^+$ calcd for $C_{20}H_{14}N_4O_5K$, 429.0601; found, 429.0602.

3-(2-Oxo-*2H*-[1,2'-bipyridin]-6-yl)pyrrolidine-2,5-dione (3ap):

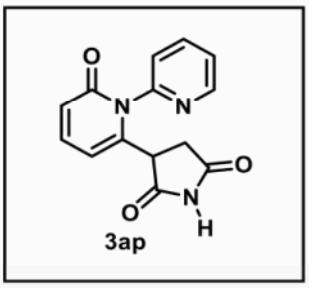

3ap

Physical state: colorless solid (24 mg in 55% yield). mp: 138–140 °C. R*f*: 0.35 (5% MeOH/DCM). ^{1}H NMR (400 MHz, $CDCl_3$): δ 8.64 (dd, J = 4.8, 1.2 Hz, 1H), 8.03 (s, 1H), 7.93 (td, J = 8.0, 2.0 Hz, 1H), 7.50–7.38 (m, 3H), 6.65 (dd, J = 9.6, 1.2 Hz, 1H), 6.18 (dd, J = 6.8, 0.8 Hz, 1H), 3.79–3.75 (m, 1H), 3.00–2.94 (m, 1H), 2.87–2.80 (m, 1H). ^{13}C NMR (100 MHz, $CDCl_3$): δ 174.9, 174.7, 163.7, 151.2, 150.1, 144.7, 140.3, 139.2, 125.6, 125.0, 121.7, 105.9, 45.5, 38.4. IR (KBr, cm^{-1}): 1776, 1716, 1657, 1546, 1194. HRMS (ESI) m/z: $[M + Na]^+$ calcd for $C_{14}H_{11}N_3O_3Na$, 292.0693; found, 292.0691.

3-(3-Methoxy-2-oxo-*2H*-[1,2'-bipyridin]-6-yl)-1-methylpyrrolidine-2,5-dione (3db):

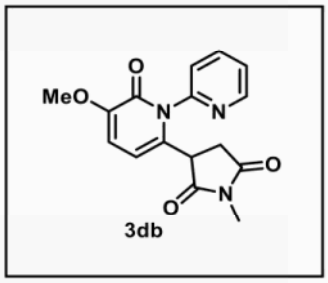

Physical state: colorless solid (35 mg in 70% yield). mp: 178–180 °C. R_f: 0.3 (1% MeOH/DCM). ^{1}H NMR ($CDCl_3$, 400 MHz): δ 8.59 (dd, J = 4.8, 1.2 Hz, 1H), 7.90 (td, J = 7.6, 1.6 Hz, 1H), 7.46 (d, J = 8.0 Hz, 1H), 7.42–7.39 (m, 1H), 6.63 (d, J = 7.6 Hz, 1H), 6.06 (d, J = 7.6 Hz, 1H), 3.84 (s, 3H), 3.72–3.69 (m, 1H), 2.95–2.89 (m, 1H), 2.86 (s, 3H), 2.78–2.71 (m, 1H). ^{13}C NMR ($CDCl_3$, 100 MHz): δ 175.6, 175.2, 159.2, 151.1, 150.2, 149.9, 138.9, 134.8, 125.8, 124.8, 112.3, 105.5, 56.3, 44.0, 37.1, 25.4. IR (KBr, cm^{-1}): 1775, 1697, 1658, 1602, 1440, 1286. HRMS (ESI) m/z: $[M + H]^+$ calcd for $C_{16}H_{16}N_3O_4$, 314.1135; found, 314.1152.

1-Methyl-3-(4-methyl-2-oxo-*2H*-[1,2'-bipyridin]-6-yl)pyrrolidine-2,5-dione (3eb):

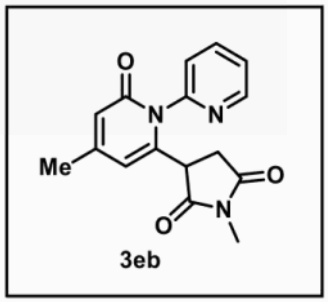

Physical state: colorless liquid (36 mg in 76% yield). R_f: 0.2 (1% MeOH/DCM). ^{1}H NMR ($CDCl_3$, 400 MHz): δ 8.59 (d, J = 4.4 Hz, 1H), 7.90 (t, J = 8.0 Hz, 1H), 7.46–7.38 (m, 2H), 6.43 (s, 1H), 5.95 (s, 1H), 3.73-3.70 (m, 1H), 2.97–2.91 (m, 1H), 2.88 (s, 3H), 2.81–2.74 (m, 1H), 2.21 (s, 3H). ^{13}C NMR ($CDCl_3$, 100 MHz): δ 175.2, 175.0, 163.6, 151.8, 151.2, 149.9, 143.5, 138.9, 125.8, 124.7, 119.6, 108.8, 44.3, 37.1, 25.5, 21.8. IR (KBr, cm^{-1}): 1774, 1697, 1659, 1546, 1441, 1289. HRMS (ESI) m/z: $[M + H]^+$ calcd for $C_{16}H_{16}N_3O_3$, 298.1186; found, 298.1159.

1-Benzyl-3-(3-methoxy-2-oxo-*2H*-[1,2'-bipyridin]-6-yl)pyrrolidine-2,5-dione (3df):

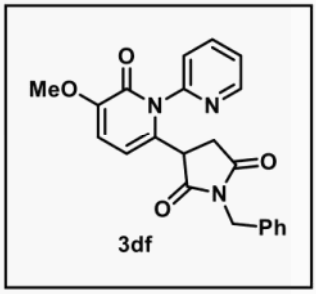

Physical state: colorless liquid (35 mg in 56% yield). R_f: 0.18 (2% MeOH/EtOAC). ^{1}H NMR ($CDCl_3$, 400 MHz): δ 8.54 (d, J = 4.0 Hz, 1H), 7.85 (td, J = 8.0, 1.6 Hz, 1H), 7.45 (d, J = 8.0 Hz, 1H), 7.37–7.29 (m, 6H), 6.58 (d, J = 8.0 Hz, 1H), 5.94 (d, J = 7.6 Hz, 1H), 4.58–4.50 (m, 2H), 3.83 (s, 3H), 3.67–3.64 (m,

1H), 2.88–2.82 (m, 1H), 2.76–2.69 (m, 1H). ^{13}C NMR ($CDCl_3$, 100 MHz): δ 175.2, 174.8, 159.2, 151.1, 150.2, 149.9, 139.0, 135.6, 135.1, 129.3, 129.1, 128.5, 125.6, 124.8, 112.4, 105.1, 56.4, 43.8, 43.1, 37.3. IR (KBr, cm^{-1}): 1774, 1702, 1657, 1611, 1398, 1168. HRMS (ESI) m/z: $[M + Na]^+$ calcd for $C_{22}H_{19}N_3O_4Na$, 412.1268; found, 412.1278.

1-Cyclohexyl-3-(3-methoxy-2-oxo-*2H*-[1,2'-bipyridin]-6-yl)pyrrolidine-2,5-dione (3de):

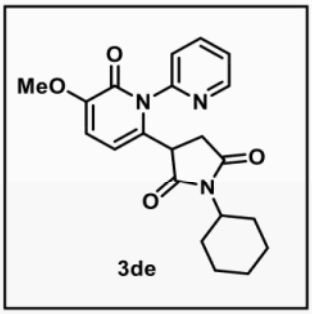

Physical state: colorless liquid (37 mg in 60% yield). R_f: 0.2 (2% MeOH/EtOAc). ^{1}H NMR ($CDCl_3$, 400 MHz): δ 8.63 (d, J = 4.4 Hz, 1H), 7.92 (t, J = 7.6 Hz, 1H), 7.50 (d, J = 7.6 Hz, 1H), 7.44–7.41 (m, 1H), 6.63 (d, J = 7.6 Hz, 1H), 5.97 (d, J = 8.0 Hz, 1H), 3.96–3.90 (m, 1H), 3.84 (s, 3H), 3.56 (s, 1H), 2.80–2.65 (m, 2H), 2.13–2.04 (m, 2H), 1.83–1.80 (m, 2H), 1.53–1.51 (m, 2H), 1.34–1.17 (m, 4H). ^{13}C NMR ($CDCl_3$, 100 MHz): δ 175.6, 175.4, 159.2, 151.3, 150.1, 150.0, 139.1, 136.1, 125.6, 124.8, 112.5, 104.1, 56.4, 52.5, 43.1, 37.4, 29.1, 29.0, 26.1, 25.2. IR (KBr, cm^{-1}): 1771, 1698, 1662, 1609, 1374, 1194. HRMS (ESI) m/z: $[M + Na]^+$ calcd for $C_{21}H_{23}N_3O_4Na$, 404.1581; found, 404.1550.

1-Benzyl-3-(3-chloro-2-oxo-*2H*-[1,2'-bipyridin]-6-yl)pyrrolidine-2,5-dione (3bf):

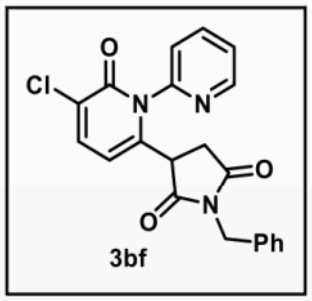

Physical state: yellow liquid (52 mg in 83% yield). R_f: 0.7 (2% MeOH/EtOAc). ^{1}H NMR ($CDCl_3$, 400 MHz): δ 8.56 (d, J = 4.4 Hz, 1H), 7.88 (t, J = 8.0 Hz, 1H), 7.53–7.30 (m, 8H), 5.96 (d, J = 7.6 Hz, 1H), 4.59–4.51 (m, 2H), 3.69–3.66 (m, 1H), 2.91–2.73 (m, 2H). ^{13}C NMR ($CDCl_3$, 100 MHz): δ 174.4, 174.3, 159.9, 150.8, 150.1, 143.7, 139.2, 137.9, 135.4, 129.4, 129.1, 128.7, 127.0, 125.3, 125.2, 105.2, 44.1, 43.3, 37.2. IR (KBr, cm^{-1}): 1776, 1705, 1666, 1603, 1397, 1170. HRMS (ESI) m/z: $[M + H]^+$ calcd for $C_{21}H_{17}ClN_3O_3$, 394.0953; found, 394.0939.

1-Ethyl-3-(6-oxo-1,6-dihydropyridin-2-yl)-3-(pyridin-2-yl)pyrrolidine-2,5-dione (4aa):

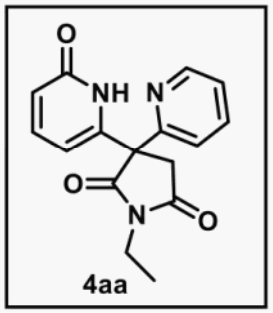

Physical state: light yellow solid (22 mg in 73% yield). mp: 181–183 °C. R_f: 0.2 (50% EtOAc/DCM). ^{1}H NMR ($CDCl_3$, 400 MHz): δ 10.77 (s, 1H), 8.57 (d, J = 4.0 Hz, 1H), 7.67 (td, J = 8.0, 1.6 Hz, 1H), 7.39 (dd, J = 9.2, 7.2 Hz, 1H), 7.28–7.25 (m, 2H), 6.49 (d, J = 9.2 Hz, 1H), 6.25 (d, J = 6.8 Hz, 1H), 3.91 (d, J = 17.6 Hz, 1H), 3.65 (q, J = 6.8 Hz, 2H), 3.23 (d, J = 18.0 Hz, 1H), 1.20 (t, J = 7.2 Hz, 3H). ^{13}C NMR ($CDCl_3$, 100 MHz): δ 176.4, 174.5, 163.8, 157.3, 150.1, 145.8, 141.0, 137.9, 123.8, 122.2, 120.5, 105.7, 57.2, 42.0, 34.9, 13.1. IR (KBr, cm^{-1}): 1775, 1701, 1654, 1612, 1228. HRMS (ESI) m/z: $[M + H]^+$ calcd for $C_{16}H_{16}N_3O_3$, 298.1186; found, 298.1182.

1-Methyl-3-(6-oxo-1,6-dihydropyridin-2-yl)-3-(pyridin-2-yl)pyrrolidine-2,5-dione (4ab):

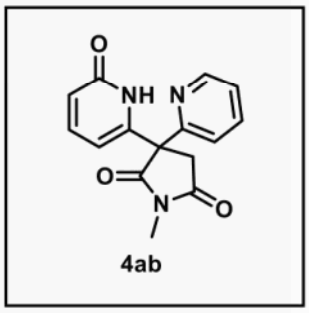

Physical state: yellow solid (16 mg in 56% yield). mp: 210–212 °C. R_f: 0.4 (2% MeOH/DCM). ^{1}H NMR ($CDCl_3$, 400 MHz): δ 10.40 (s, 1H), 8.57 (dd, J = 4.8, 1.2 Hz, 1H), 7.68 (td, J = 8.0, 2.0 Hz, 1H), 7.37 (dd, J = 9.6, 7.2 Hz, 1H), 7.32 (d, J = 8.0 Hz, 1H), 7.28–7.24 (m, 1H), 6.50 (dd, J = 9.2, 0.8 Hz, 1H), 6.23 (dd, J = 6.8, 0.4 Hz, 1H), 3.94 (d, J = 18.0 Hz, 1H), 3.25 (d, J = 18.0 Hz, 1H), 3.09 (s, 3H). ^{13}C NMR ($CDCl_3$, 100 MHz): δ 176.7, 174.8, 163.8, 157.0, 150.1, 145.8, 141.0, 137.9, 123.9, 122.4, 120.5, 105.8, 57.4, 41.9, 25.9. IR (KBr, cm^{-1}): 1778, 1703, 1654, 1612, 1289. HRMS (ESI) m/z: $[M + Na]^+$ calcd for $C_{15}H_{13}N_3O_3Na$, 306.0849; found, 306.0839.

3-(6-Oxo-1,6-dihydropyridin-2-yl)-1-propyl-3-(pyridin-2-yl)pyrrolidine-2,5-dione (4ac):

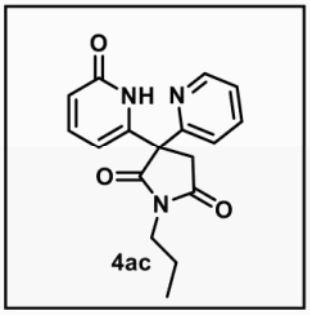

Physical state: colorless solid (19 mg in 62% yield). mp: 181–183 °C. R_f: 0.5 (50% EtOAc/Hexane). ^{1}H NMR ($CDCl_3$, 400 MHz): δ 10.64 (s, 1H), 8.57 (d, J = 4.8 Hz, 1H), 7.68 (t, J = 7.6 Hz, 1H), 7.40 (t, J = 7.6 Hz, 1H), 7.27–7.25 (m, 3H), 6.52 (d, J = 9.2 Hz, 1H), 6.26 (d, J = 6.8 Hz, 1H), 3.88 (d, J = 17.6 Hz, 1H), 3.57 (t, J = 7.2 Hz, 2H), 3.24 (d, J = 17.6 Hz, 1H), 1.68–1.61 (m, 2H), 0.89 (t, J = 7.2 Hz, 3H). ^{13}C NMR ($CDCl_3$, 175 MHz): δ 176.7, 174.7, 163.5, 157.5, 150.1, 145.7, 141.0, 138.0, 123.9, 122.1, 120.6, 105.5, 56.9, 42.0, 41.5, 21.1, 11.5. IR (KBr, cm^{-1}): 1775, 1702, 1654, 1613, 1399. HRMS (ESI) m/z: $[M + H]^+$ calcd for $C_{17}H_{18}N_3O_3$, 312.1343; found, 312.1328.

1-Isopropyl-3-(6-oxo-1,6-dihydropyridin-2-yl)-3-(pyridin-2-yl)pyrrolidine-2,5-dione (4ad):

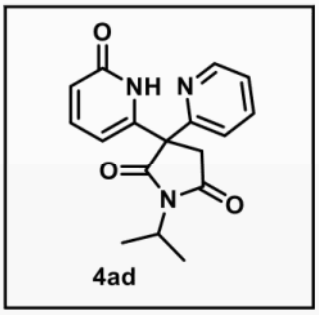

Physical state: colorless solid (25 mg in 80% yield). mp: 193–195 °C. R_f: 0.3 (2% MeOH/EtOAc). ^{1}H NMR ($CDCl_3$, 400 MHz): δ 10.51 (s, 1H), 8.57–8.55 (m, 1H), 7.66 (td, J = 7.6, 2.0 Hz, 1H), 7.38 (dd, J = 9.2, 6.8 Hz, 1H), 7.26–7.23 (m, 2H), 6.50 (dd, J = 9.2, 0.8 Hz, 1H), 6.22 (dd, J = 7.2, 0.8 Hz, 1H), 4.50–4.40 (m, 1H), 3.77 (d, J = 17.6 Hz, 1H), 3.20 (d, J = 17.6 Hz, 1H), 1.41 (dd, J = 12.0, 7.2 Hz, 6H). ^{13}C NMR ($CDCl_3$, 100 MHz): δ 176.6, 174.6, 163.6, 157.7, 150.1, 145.7, 141.0, 137.9, 123.8, 121.9, 120.7, 105.5, 56.4, 45.1, 42.0, 19.6, 19.1. IR (KBr, cm^{-1}): 1774, 1700, 1654, 1613, 1365. HRMS (ESI) m/z: $[M + Na]^+$ calcd for $C_{17}H_{17}N_3O_3Na$, 334.1162; found, 334.1155.

1-Benzyl-3-(6-oxo-1,6-dihydropyridin-2-yl)-3-(pyridin-2-yl)pyrrolidine-2,5-dione (4af):

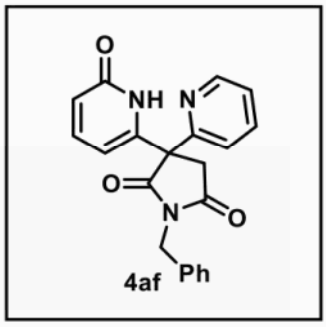

Physical state: light yellow liquid (23 mg in 63% yield). R_f: 0.2 (50% EtOAc/Hexane). ^{1}H NMR ($CDCl_3$, 400 MHz): δ 10.22 (s, 1H), 8.53 (d, J = 4.4 Hz, 1H), 7.66 (t, J = 8.0 Hz, 1H), 7.39–7.36 (m, 3H), 7.31–7.29 (m, 3H), 7.26–7.23 (m, 2H), 6.52 (d, J = 9.2 Hz, 1H), 6.19 (d, J = 6.8 Hz, 1H), 4.80–4.71 (m, 2H), 3.85 (d, J = 17.6 Hz, 1H), 3.26 (d, J = 17.6 Hz, 1H). ^{13}C NMR ($CDCl_3$, 100 MHz): δ 176.4, 174.1, 163.3, 157.3, 150.1, 145.7, 141.0, 138.0, 135.3, 129.0, 129.0, 128.5, 123.9, 122.0, 120.5, 105.5, 56.9, 43.5, 42.2. IR (KBr, cm^{-1}): 1776, 1705, 1653, 1614, 1395. HRMS (ESI) m/z: $[M + Na]^+$ calcd for $C_{21}H_{17}N_3O_3Na$, 382.1162; found, 382.1130.

3-(6-Oxo-1,6-dihydropyridin-2-yl)-1-phenyl-3-(pyridin-2-yl)pyrrolidine-2,5-dione (4ag):

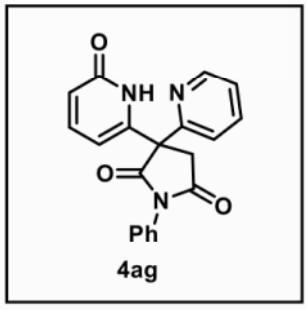

Physical state: light yellow solid (19 mg in 55% yield). mp: 212–214 °C. R_f: 0.2 (50% EtOAc/Hexane). ^{1}H NMR ($CDCl_3$, 400 MHz): δ 11.53 (s, 1H), 8.65–8.63 (m, 1H), 7.70 (td, J = 7.6, 2.0 Hz, 1H), 7.50–7.26 (m, 8H), 6.48 (d, J = 9.2 Hz, 1H), 6.25 (d, J = 6.8 Hz, 1H), 4.21–4.16 (m, 1H), 3.44 (d, J = 18.0 Hz, 1H). ^{13}C NMR ($CDCl_3$, 100 MHz): δ 175.8, 173.7, 164.1, 157.3, 150.1, 146.2, 141.0, 137.9, 132.1, 129.5, 129.3, 127.0, 124.0, 122.5, 120.2, 106.5, 57.8, 42.1. IR (KBr, cm^{-1}): 1781, 1714, 1655, 1613, 1382. HRMS (ESI) m/z: $[M + Na]^+$ calcd for $C_{20}H_{15}N_3O_3Na$, 368.1006; found, 368.1010.

3-(5-Methoxy-6-oxo-1,6-dihydropyridin-2-yl)-1-methyl-3-(pyridin-2-yl)pyrrolidine-2,5-dione (4db):

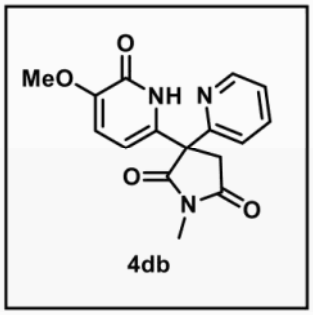

Physical state: brown solid (16 mg in 51% yield). mp: 228–230 °C. R_f: 0.1 (50% EtOAc/Hexane). ^{1}H NMR ($CDCl_3$, 400 MHz): δ 10.21 (s, 1H), 8.55 (dd, J = 4.4, 1.2 Hz, 1H), 7.68–7.64 (m, 1H), 7.26–7.23 (m, 2H), 6.63 (d, J = 7.6 Hz, 1H), 6.19 (d, J = 7.6 Hz, 1H), 3.84 (s, 3H), 3.77 (d, J = 17.6 Hz, 1H), 3.25 (d, J = 17.6 Hz, 1H), 3.11 (s, 3H). ^{13}C NMR ($CDCl_3$, 100 MHz): δ 177.1, 174.7, 158.4, 158.0, 150.3, 150.2, 138.0, 134.9, 123.8, 121.9, 113.0, 104.7, 56.4, 56.2, 42.1, 25.9. IR (KBr, cm^{-1}): 1775, 1700, 1651, 1577, 1436. HRMS (ESI) m/z: $[M + Na]^+$ calcd for $C_{16}H_{15}N_3O_4Na$, 336.0955; found, 336.0923.

3-(5-Chloro-6-oxo-1,6-dihydropyridin-2-yl)-1-ethyl-3-(pyridin-2-yl)pyrrolidine-2,5-dione (4ba):

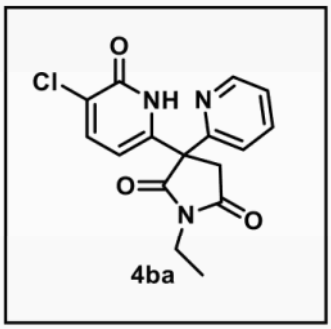

Physical state: colorless solid (18 mg in 53% yield). mp: 211–213 °C. R_f: 0.3 (50% EtOAc/Hexane). ^{1}H NMR ($CDCl_3$, 400 MHz): δ 11.08 (s, 1H), 8.58–8.57 (m, 1H), 7.71–7.66 (m, 1H), 7.55 (dd, J = 7.6, 1.2 Hz, 1H), 7.29–7.25 (m, 2H), 6.21 (dd, J = 7.6, 0.8 Hz, 1H), 3.90 (d, J = 17.6 Hz, 1H), 3.67 (q, J = 7.2 Hz, 2H), 3.22 (d, J = 18.0 Hz, 1H), 1.20 (t, J = 7.2 Hz, 3H). ^{13}C NMR ($CDCl_3$, 100 MHz): δ 176.2, 174.1, 159.6, 157.0, 150.2, 144.2, 138.8, 138.0, 126.5, 124.0, 121.9, 105.4, 56.8, 42.1, 35.0, 13.1. IR (KBr, cm^{-1}): 1774, 1702, 1649, 1460, 1400. HRMS (ESI) m/z: $[M + H]^+$ calcd for $C_{16}H_{15}ClN_3O_3$, 332.0796; found, 332.0772.

1-Methyl-3-(4-methyl-6-oxo-1,6-dihydropyridin-2-yl)-3-(pyridin-2-yl)pyrrolidine-2,5-dione (4eb):

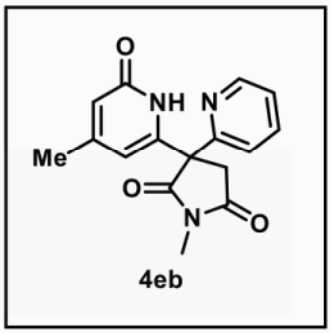

Physical state: yellow solid (17 mg in 57% yield). mp: 229–231 °C. R_f: 0.1 (50% EtOAc/Hexane). ^{1}H NMR ($CDCl_3$, 400 MHz): δ 10.52 (s, 1H), 8.57 (dd, J = 4.8, 0.8 Hz, 1H), 7.67 (td, J = 7.6, 1.6 Hz, 1H), 7.34 (d, J = 8.0 Hz, 1H), 7.27–7.24 (m, 1H), 6.27 (s, 1H), 6.06 (d, J = 1.2 Hz, 1H), 3.98 (d, J = 18.0 Hz, 1H), 3.22 (d, J = 18.0 Hz, 1H), 3.09 (s, 3H), 2.18 (s, 3H). ^{13}C NMR ($CDCl_3$, 100 MHz): δ 176.6, 174.7, 163.9, 157.1, 152.7, 150.0, 144.8, 137.9, 123.9, 122.5, 118.8, 108.3, 57.5, 41.9, 25.9, 22.1. IR (KBr, cm^{-1}): 1774, 1701, 1651, 1434, 1382. HRMS (ESI) m/z: $[M + H]^+$ calcd for $C_{16}H_{16}N_3O_3$, 298.1186; found, 298.1194.

1-Ethyl-3-(6-oxo-1,6-dihydropyridin-2-yl)pyrrolidine-2,5-dione (5):

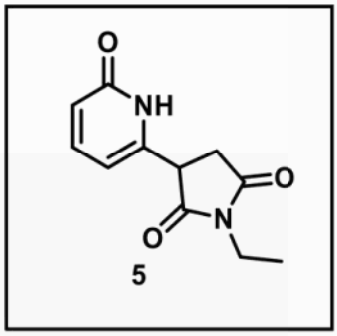

Physical state: colorless liquid (13 mg in 59% yield). R_f: 0.1 (50% EtOAc/DCM). ^{1}H NMR ($CDCl_3$, 400 MHz): δ 13.24 (s, 1H), 7.43–7.39 (m, 1H), 6.44 (d, J = 9.2 Hz, 1H), 6.18 (d, J = 6.8 Hz, 1H), 4.00–3.97 (m, 1H), 3.64 (q, J = 7.2 Hz, 2H), 3.23–3.16 (m, 1H), 2.96–2.90 (m, 1H), 1.22 (t, J = 7.2 Hz, 3H). ^{13}C NMR ($CDCl_3$, 100 MHz): δ 174.7, 174.6, 165.5, 143.7, 141.6, 119.2, 106.3, 43.8, 35.0, 34.5, 12.9. IR (KBr, cm^{-1}): 1779, 1695, 1648, 1450, 1410, 1228. HRMS (ESI) m/z: $[M + H]^+$ calcd for $C_{11}H_{13}N_2O_3$, 221.0921; found, 221.0933.

NMR spectra of 1-Ethyl-3-(2-oxo-*2H*-[1,2'-bipyridin]-6-yl)pyrrolidine-2,5-dione (3aa):

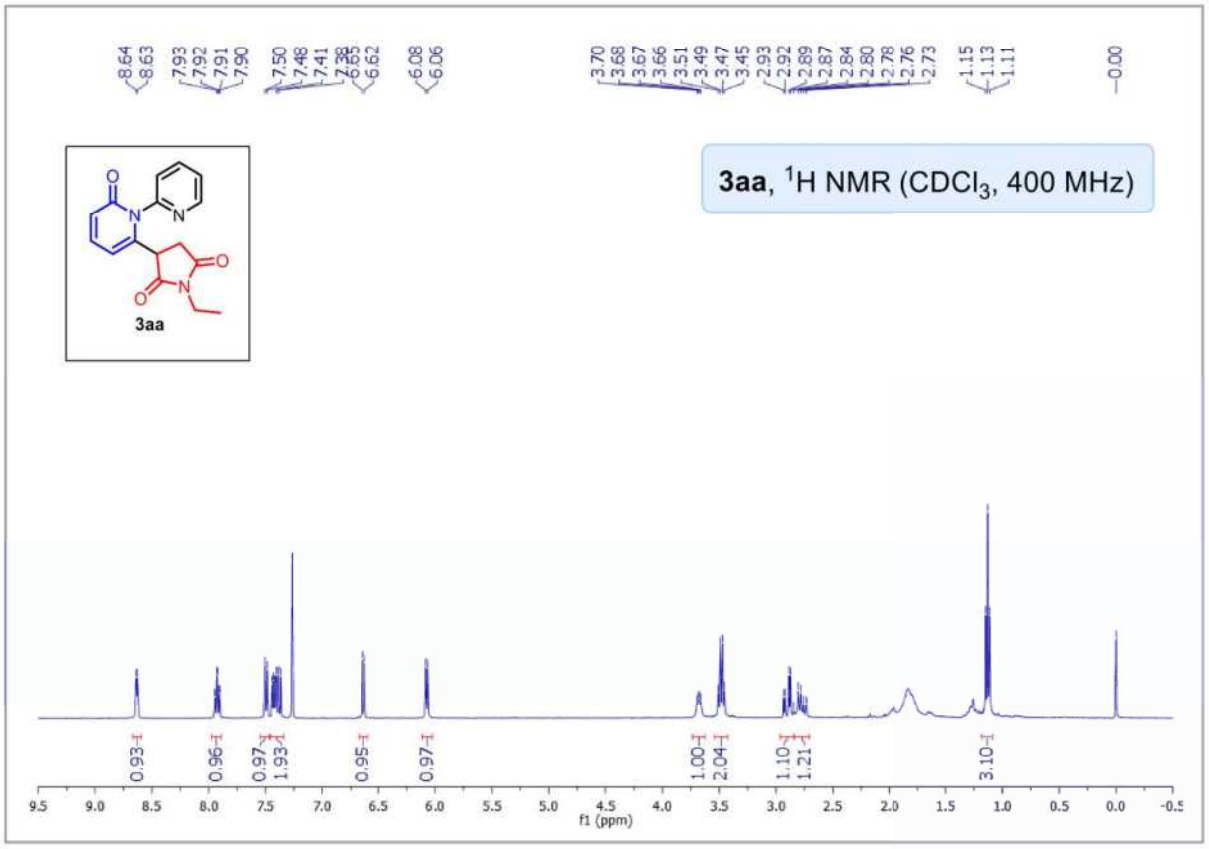

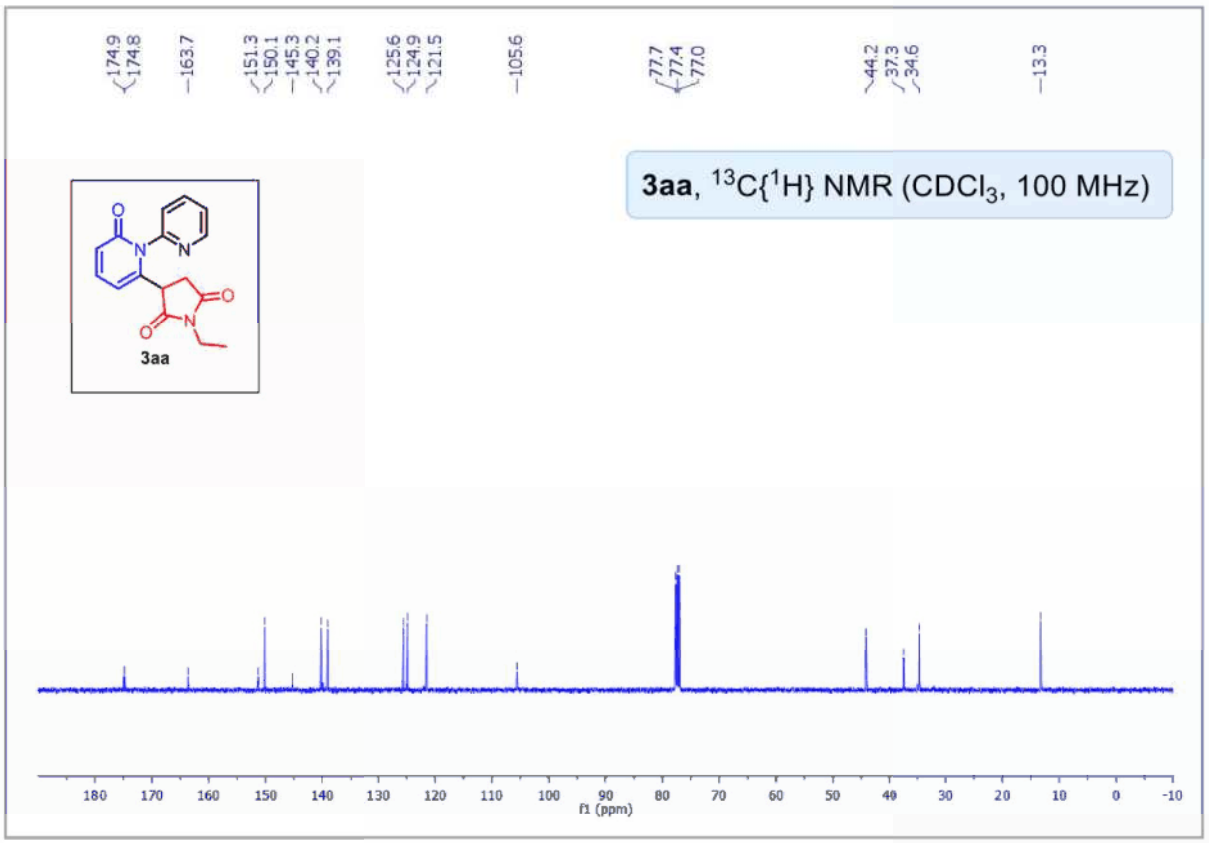

NMR spectra of 1-Ethyl-3-(6-oxo-1,6-dihydropyridin-2-yl)-3-(pyridin-2-yl)pyrrolidine-2,5-dione (4aa):

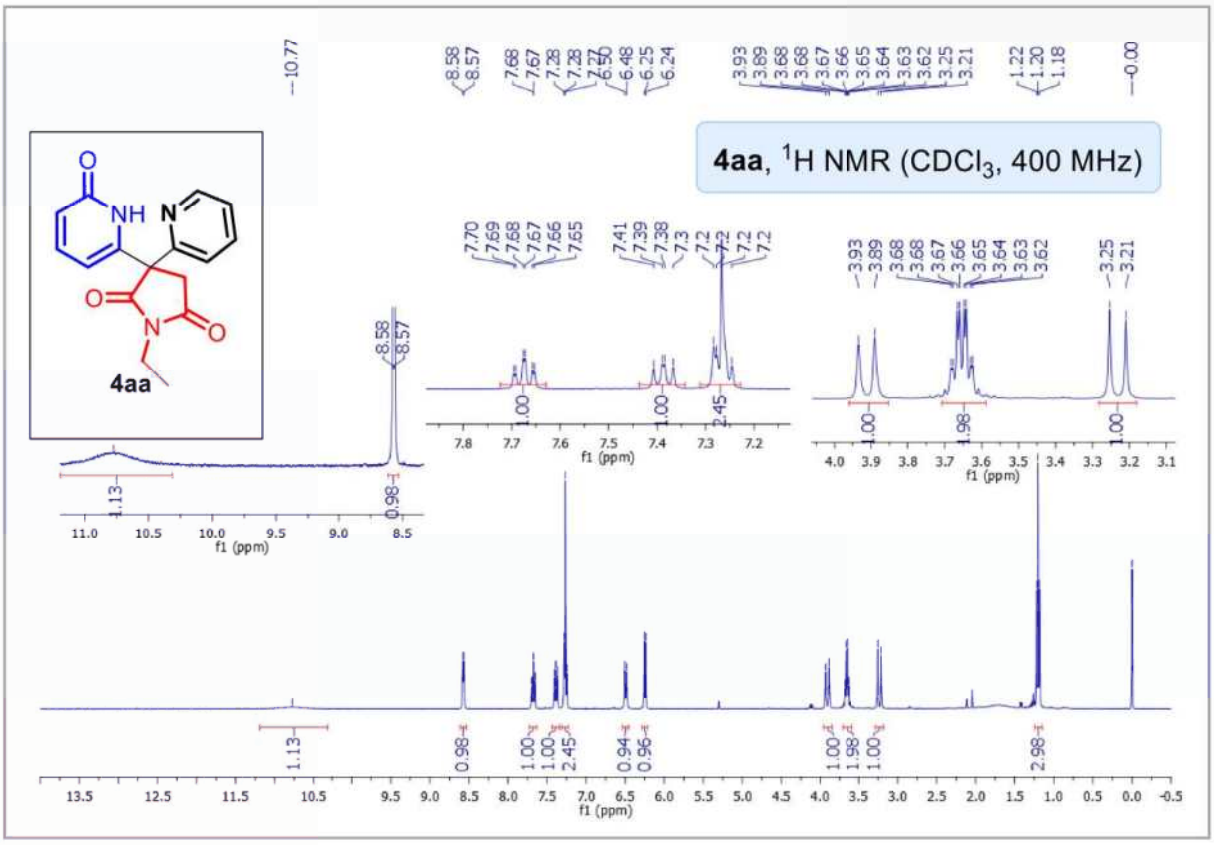

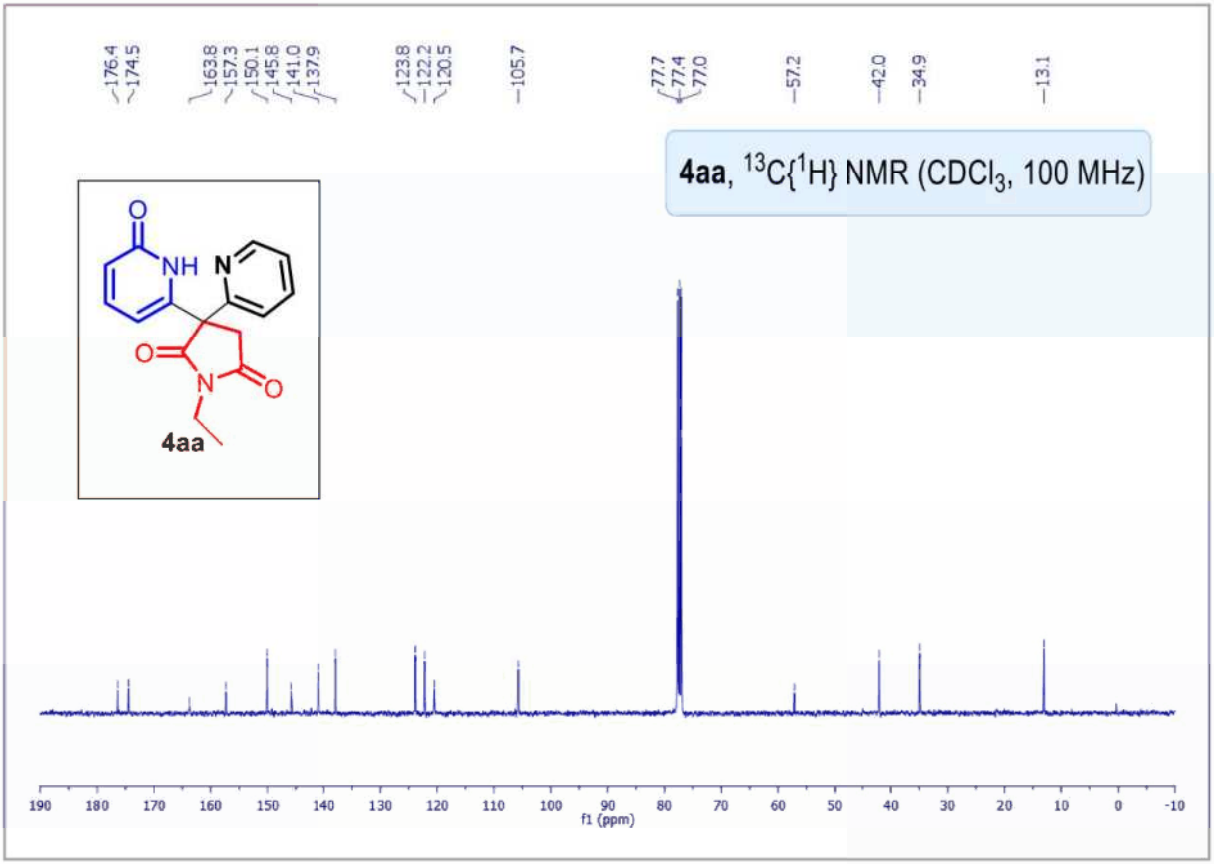

NMR spectra of 1-Ethyl-3-(6-oxo-1,6-dihydropyridin-2-yl)pyrrolidine-2,5-dione (5):

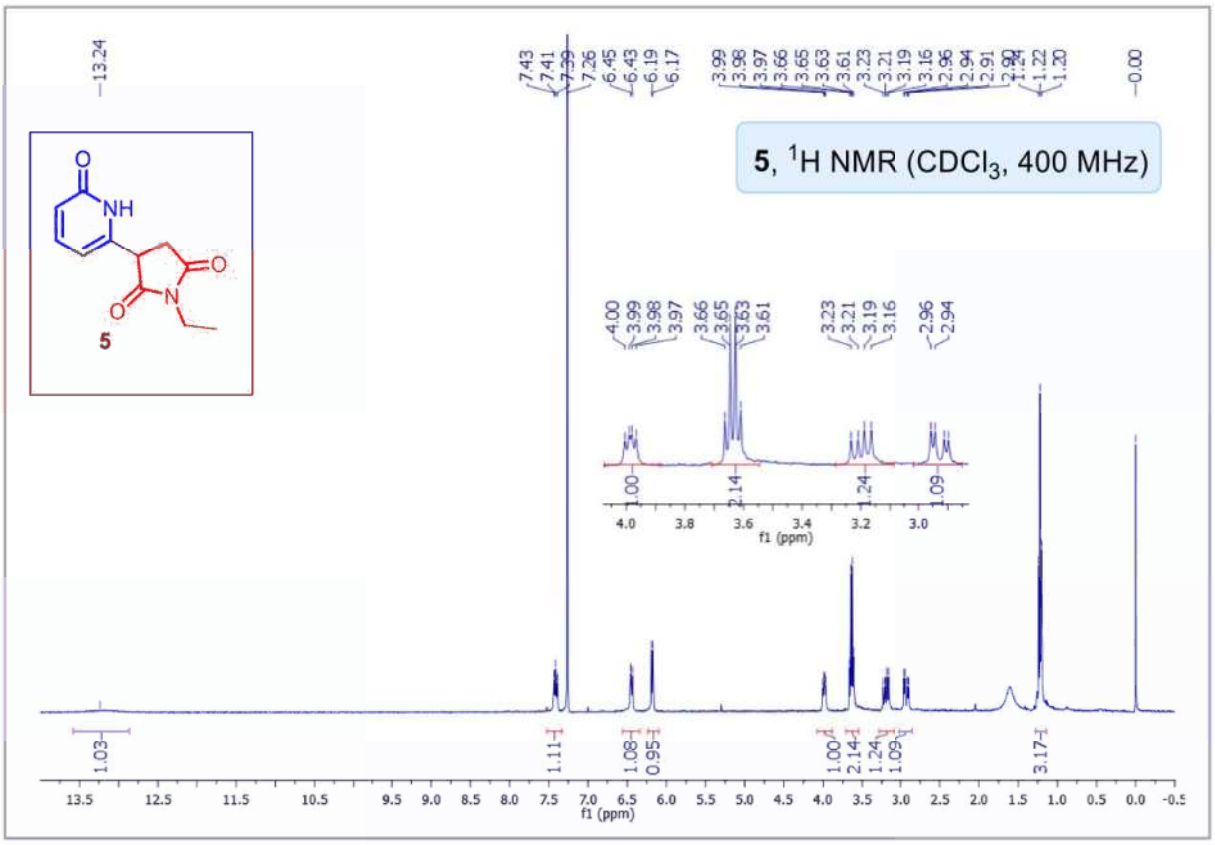

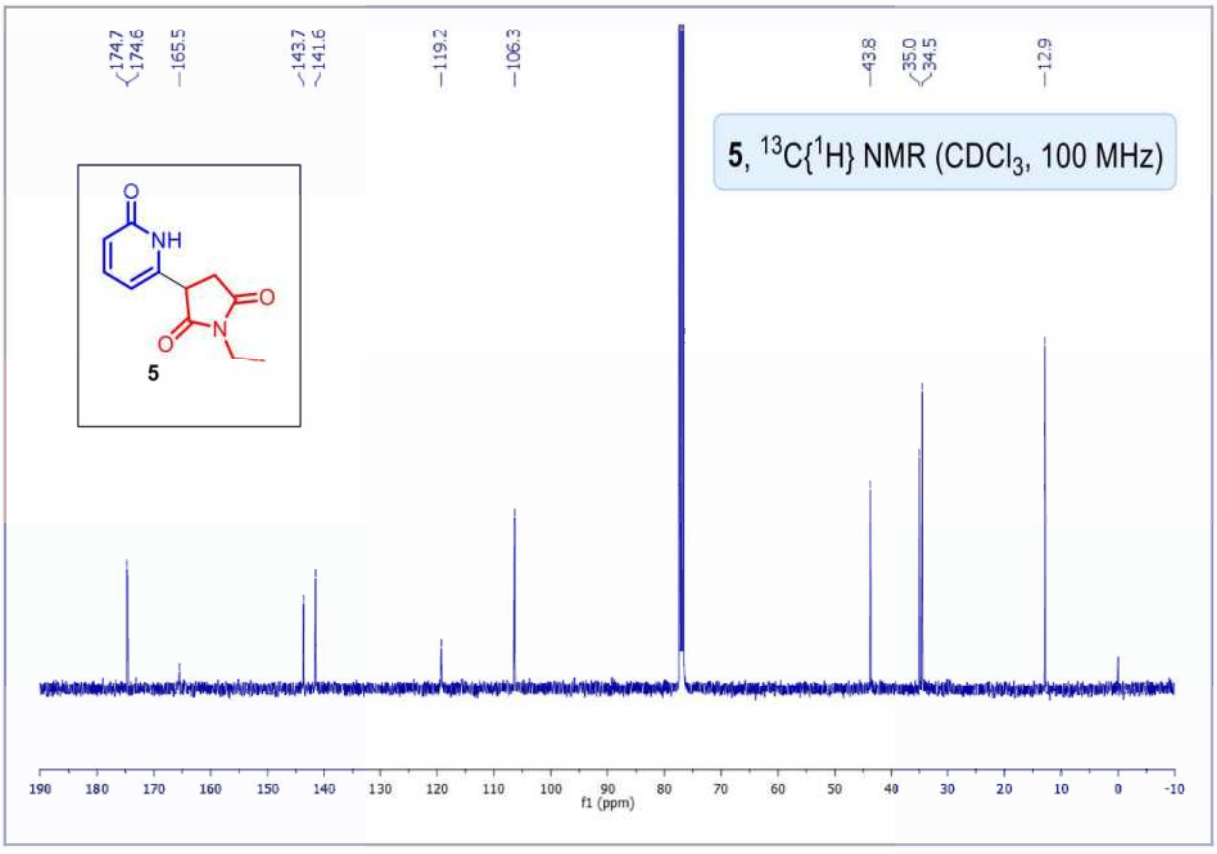

Detection of intermediate through single crystal X-ray and HRMS:

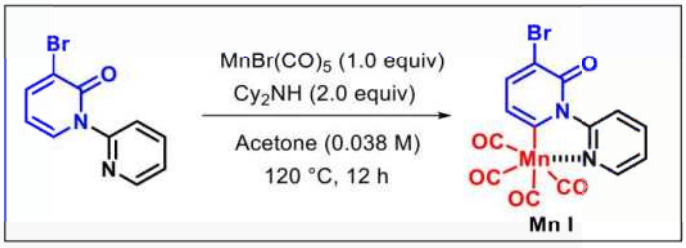

Intermediate Mn I HRMS:

HRMS (ESI) m/z: calcd for $C_{14}H_6BrMnN_2O_5Na$ $[M + Na]^+$: 438°C.8733; found: 438.8695.

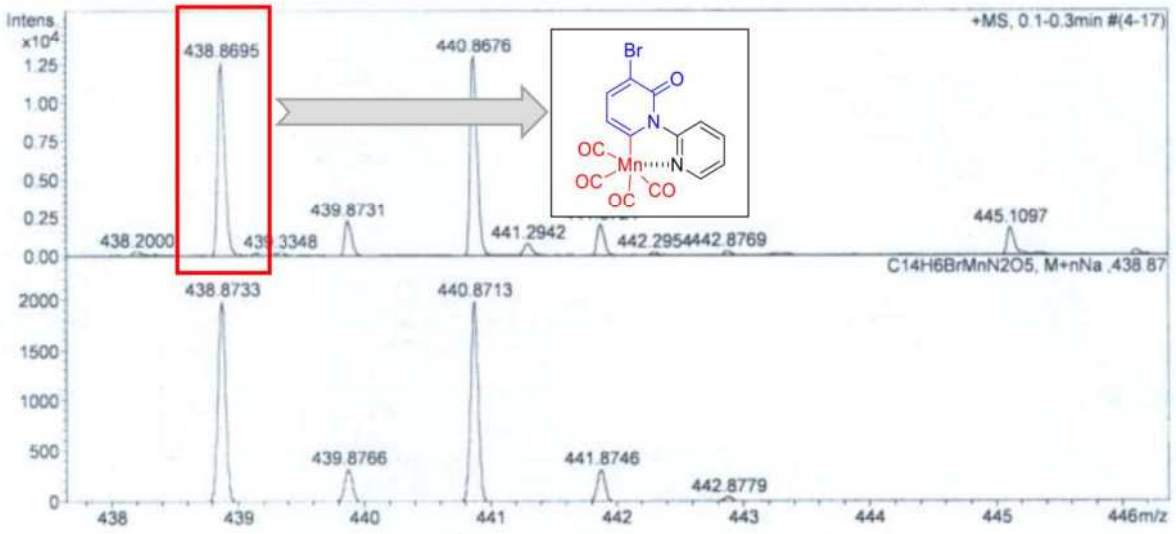

Crystal structure of Mn I

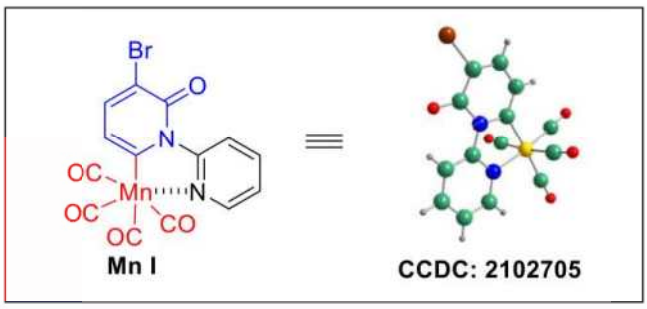

Datablock one_a - ellipsoid plot

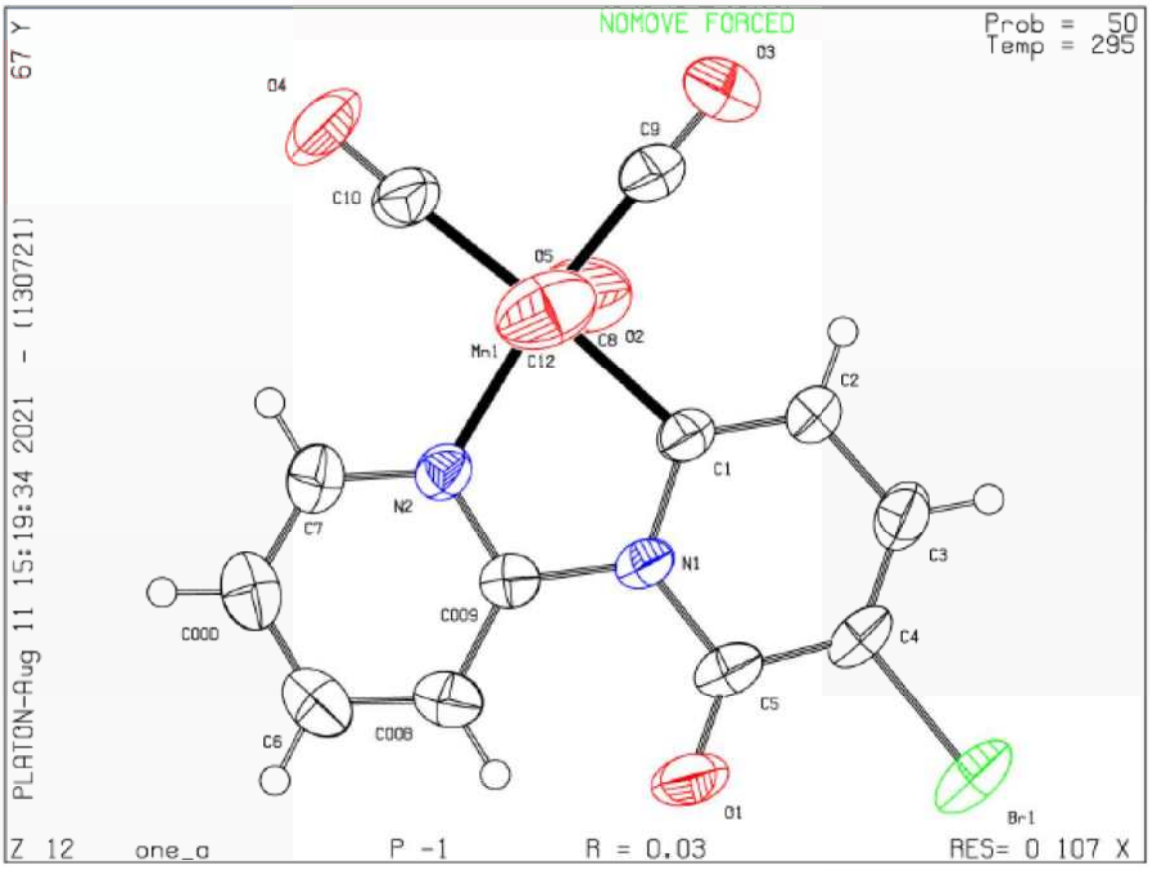

Crystal structure of 3ca

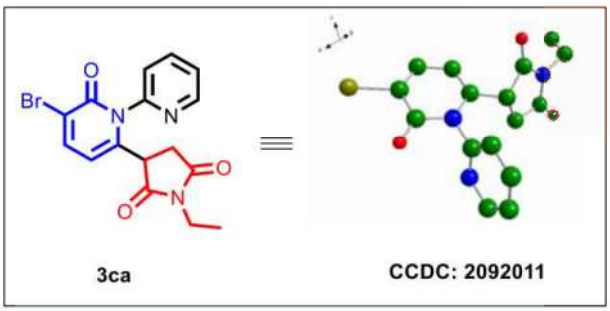

Datablock: pcr-srm-mld - ellipsoid plot

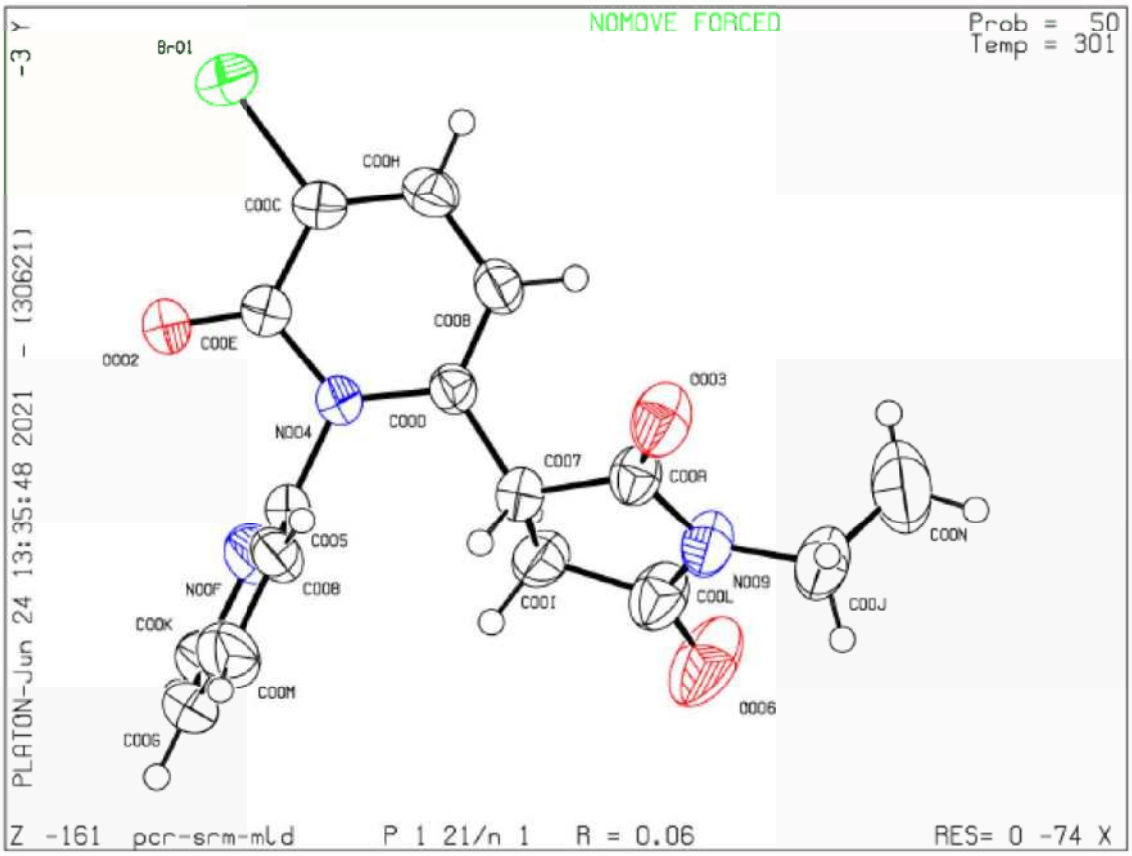

Crystal structure of 4aa

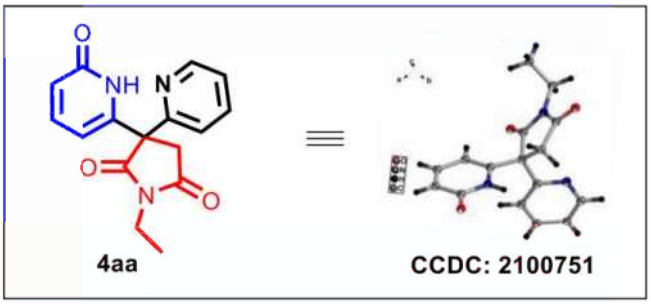

Datablock datam - ellipsoid plot

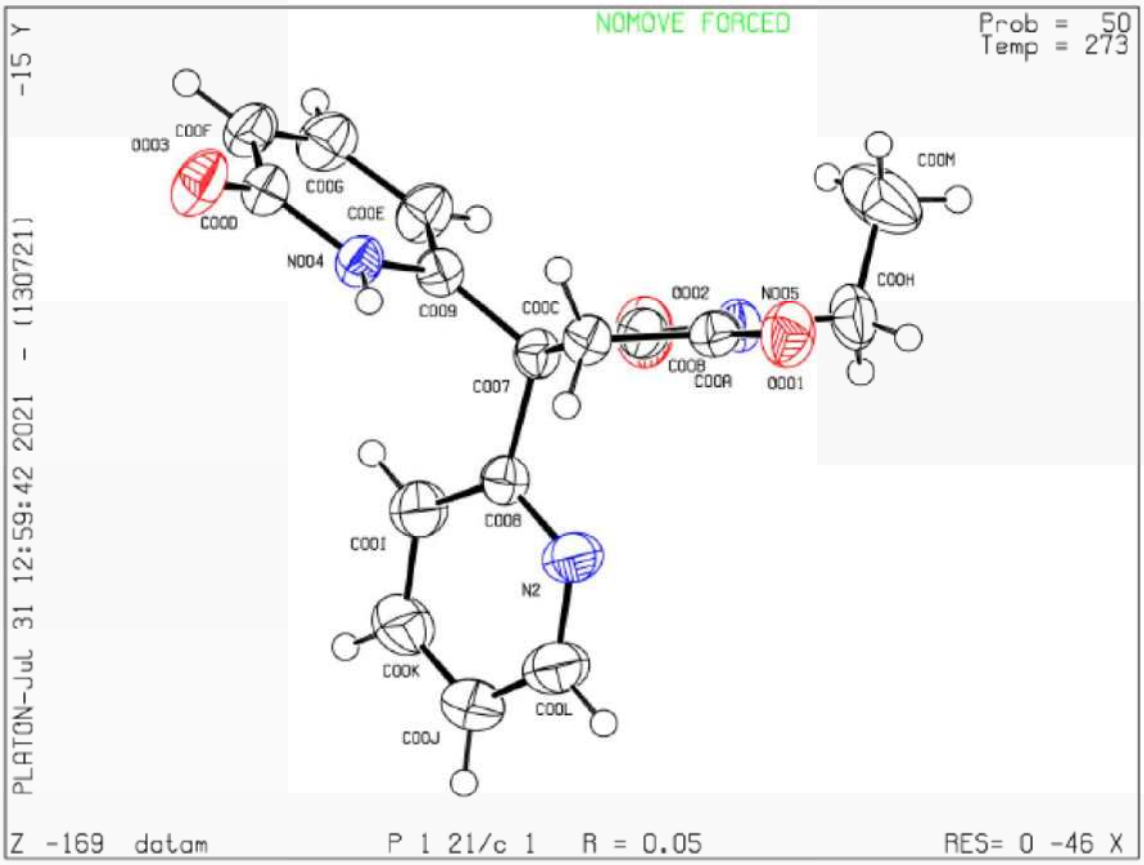

5.6 REFERENCES

1. Isaka, M.; Rugseree, N.; Maithip, P.; Kongsaeree, P.; Prabpai, S.; Thebtaranonth, Y. Hirsutellones A-E, Antimycobacterial Alkaloids from the Insect Pathogenic Fungus Hirsutella nivea BCC 2594. *Tetrahedron* **2005**, *61*, 5577−5583.
2. Zhang, L.; Tan, Y.; Wang, N. X.; Wu, Q. Y.; Xi, Z.; Yang, G. F. Design, syntheses and 3D-QSAR studies of novel *N*-phenyl pyrrolidin-2-ones and *N*-phenyl-*1H*-pyrrol-2-ones as protoporphyrinogen oxidase inhibitors. *Bioorg. Med. Chem*. **2010**, *18*, 7948−7956.
3. Katritzky, A. R.; Yao, J.; Qi, M.; Chou, Y.; Sikora, D. J.; Davis, S. Ring opening reactions of succinimides. *Hetrocycles*. **1998**, *48*, 2677−2691.
4. Shoji, A.; Kuwahara, M.; Ozaki, H.; Sawai, H. Modified DNA Aptamer That Binds the (*R*)-Isomer of a Thalidomide Derivative with High Enantioselectivity. *J. Am. Chem. Soc.* **2007**, *129*, 1456–1464.
5. Yu, J. Q. and Shi, Z. J. C–H Activation, *Springer, Berlin, Germany*, **2010**.
6. (a) Chen, Z.; Rong, M.-Y.; Nie, J.; Zhu, X.-F.; Shi, B.-F.; Ma, J.-A. Catalytic alkylation of unactivated C(sp3)−H bonds for C(sp3)−C(sp3) bond formation. *Chem. Soc. Rev*. **2019**, *48*, 4921−4942. (b) Mingo, M. M.; Rodriguez, N.; Arrayas, R. G.; Carretero, J. C. Remote C(sp3)–H functionalization via catalytic cyclometallation: beyond five-membered ring metallacycle intermediates. *Org. Chem. Front.*, **2021**, *8*, 4914-4946. (c) Shabani, S.; Wu, Y.; Ryan, H. G.; Hutton, C. A. Progress and perspectives on directing groupassisted palladium-catalysed C–H functionalisation of amino acids and peptides. *Chem. Soc. Rev.*, **2021**, *50*, 9278−9343. (d) Nishimura, T. Iridium-Catalyzed Hydroarylation via C-H Bond Activation. *Chem. Rec.* **2021**, *21*, 1–15. (e) Dalton, T.; Faber, T.; Glorius, F. C-H

Activation: Toward Sustainability and Applications. *ACS Cent. Sci.* **2021**, *7*, 245−261.

7. (a) Sun, C. L.; Li, B. J.; Shi, Z. J. Direct C−H Transformation via Iron Catalysis. *Chem. Rev*. **2011**, *111*, 1293−1314. (b) Wendlandt, A. E.; Suess, A. M.; Stahl, S. S. Copper-Catalyzed Aerobic Oxidative C-H Functionalizations: Recent Trends and Mechanistic Insights. *Angew. Chem., Int. Ed*. **2011**, *47*, 11062–11087. (c) Yoshikai, N. Cobalt Catalyzed, Chelation Assisted C−H Bond Functionalization. *Synlett* **2011**, *8*, 1047−1051. (d) Wang, C. Manganese Mediated C–C Bond Formation via C–H Activation: From Stoichiometry to Catalysis. *Synlett* **2013**, *24*, 1606−1613. (e) Khake, S. M.; Chatani, N. Chelation-Assisted Nickel Catalyzed C−H Functionalizations. *Trends Chem*. **2019**, *5*, 524−539. (f) Liu, Y.-H.; Xia, Y.-N.; Shi, B.-F. Ni-Catalyzed Chelation-Assisted Direct Functionalization of Inert C−H Bonds. *Chin. J. Chem*. **2020**, *38*, 635−662. (g) Rao, W.-H.; Shi, B.-F. Recent Advances in Copper-Mediated Chelation-Assisted Functionalization of Unactivated C-H Bonds. *Org. Chem. Front.* **2016**, *3*, 1028−1047. (h) Shang, M.; Sun, S.-Z.; Wang, H.-L.; Wang, M.-M.; Dai, H.-X. *Synthesis* **2016**, *48*, 4381-4399.
8. (a) Kuninobu, Y.; Nishina, Y.; Takeuchi, T.; Takai, K. Manganese Catalyzed Insertion of Aldehydes into a C-H Bond. *Angew. Chem., Int. Ed*. **2007**, *46*, 6518−6520. (b) Zhou, B.; Chen, H.; Wang, C. Mn Catalyzed Aromatic C−H Alkenylation with Terminal Alkynes. *J. Am. Chem. Soc.* **2013**, *135*, 1264−1267. (c) Hu, Y.; Zhou, B.; Wang, C. Inert C−H Bond Transformations Enabled by Organometallic Manganese Catalysis. *Acc. Chem. Res*. **2018**, *51*, 816−827.
9. Jessen, H. J.; Gademann, K. 4-Hydroxy-2-pyridone alkaloids: structures and synthetic approaches. *Nat. Prod. Rep*. **2010**, *27*, 1168–1185.

10. Nakatani, A.; Hirano, K.; Satoh, T.; Miura, M. Manganese-mediated C3-selective direct alkylation and arylation of 2-pyridones with diethyl malonates and arylboronic acids. *J. Org. Chem.* **2014**, *79*, 1377−1385.

11. Miura, W.; Hirano, K.; Miura, M. Iridium-Catalyzed Site-Selective C–H Borylation of 2-pyridones. *Synthesis* **2017**, *49*, 4745−4752.

12. Chen, Y.; Wang, F.; Jia, A.; Li, X. Palladium-catalyzed selective oxidative olefination and arylation of 2-pyridones. *Chem. Sci.* **2012** , *3*, 3231−3236.

13. (a) Tamura, R.; Yamada, Y.; Nakao, Y.; Hiyama, T. Alkylation of pyridone Derivatives By Nickel/Lewis Acid Catalysis. *Angew. Chem. Int. Ed*. **2012**, *51*, 5679−5682. (b) Das, D.; Biswas, A.; Karmakar, U.; Chand, S.; Samanta, R. C6-Selective Direct Alkylation of pyridones with Diazo Compounds under Rh(III)-Catalyzed Mild Conditions. *J. Org. Chem*. **2016**, *81*, 842−848. (c) Miura, W.; Hirano, K.; Miura, M. Nickel-Catalyzed Directed C6-Selective C−H Alkylation of 2-pyridones with Dienes and Activated Alkenes. *J. Org. Chem.* **2017**, *82*, 5337−5344. (d) Zhao, H.; Xu, X.; Yu, H.; Li, B.; Xu, X.; Li, H.; Xu, L.; Fan, Q.; Walsh, P. J. Rh(I)-Catalyzed C6-Selective Decarbonylative Alkylation of 2-pyridones with Alkyl Carboxylic Acids and Anhydrides. *Org. Lett*. **2020**, *22*, 4228−4234. (e) Zhu, C.; Kuniyil, R.; Jei, B. B.; Ackermann, L. Domino C−H Activation/Directing Group Migration/Alkyne Annulation: Unique Selectivity by d^6 -Cobalt(III) Catalysts. *ACS Catal*. **2020**, *10*, 4444−4450. (f) Ni, J.; Zhao, H.; Zhang, A. Manganese(I)- Catalyzed C-H 3,3-Difluoroallylation of pyridones and Indoles. *Org. Lett*. **2017**, *19*, 3159−3162.

14. (a) Tsypysheva, I. P.; Lobov, A. N.; Kovalskaya, A. V.; Petrova, P. R.; Ivanov, S. P.; Rameev, S. A.; Borisevich, S. S.; Safiullin, R. L.; Yunusov, M. S. Aza-Michael reaction of 12-N-carboxamide of (–)- cytisine under high pressure conditions. *Nat.*

Prod. Res. **2015**, *29*, 141–148. (b) Tsypysheva, I. P.; Borisevich, S. S.; Lobov, A. N.; Kovalskaya, A. V.; Shamukaev, V. V.; Safiullin, R. L.; Khursan, S. L. Inversion of diastereoselectivity under high pressure conditions: Diels−Alder reactions of 12-N-substituted derivatives of (−)-cytisine with Nphenylmaleimide. *Tetrahedron: Asymmetry* **2015**, *26*, 732−737.

15. Lim, L. H.; Zhou, J. A challenging Heck reaction of maleimides. *Org. Chem. Front*. **2015**, *2*, 775−777.
16. (a) Dong, Z.; Ren, Z.; Thompson, S. J.; Xu, Y.; Dong, G. Transition Metal Catalyzed C−H Alkylation Using Alkenes. *Chem. Rev*. **2017**, *117*, 9333−9403. (b) Yang, L.; Huang, H. M. Transition Metal Catalyzed Direct Addition of Unactivated C−H Bonds to Polar Unsaturated Bonds. *Chem. Rev*. **2015**, *115*, 3468−3517.
17. (a) Nicolaou, K. C.; Bulger, P. G.; Sarlah, D. Palladium Catalyzed Cross-Coupling Reactions in Total Synthesis. *Angew. Chem., Int. Ed*. **2005**, *44*, 4442−4489. (b) Nicolaou, K. C.; Bulger, P. G.; Sarlah, D. Palladiumkatalysierte Kreuzkupplungen in der Totalsynthese. *Angew. Chem*. **2005**, *117*, 4516−4563. (c) Manoharan, R.; Jeganmohan, M. Alkylation, Annulation and Alkenylation of Organic Molecules with Maleimides by Transition-Metal-Catalyzed C-H Bond Activation. *Asian J. Org. Chem*. **2019**, *8*, 1949−1969.
18. Kommagalla, Y.; Mullapudi, V. B.; Francis, F.; Ramana, C. V. Rutheniu(II)-catalyzed switchable C3-alkylation versus alkenylation with acrylates of 2-pyridylbenzofurans via C–H bond activation. *Catal. Sci. Technol*. **2015**, *5*, 114−117.
19. Kim, J.; Park, S.-W.; Baik, M.-H.; Chang, S. Complete Switch of Selectivity in the C-H Alkenylation and Hydroarylation Catalyzed by Iridium: The Role of Directing Groups. *J. Am. Chem. Soc*. **2015**, *137*, 13448−13451.

20. Banjare, S. K.; Chebolu, R.; Ravikumar, P. C. Cobalt Catalyzed Hydroarylation of Michael Acceptors with Indolines Directed by a Weakly Coordinating Functional Group. *Org. Lett*. **2019**, *21*, 4049−4053.

21. (a) Liu, W.; Richter, S. C.; Zhang, Y.; Ackermann, L. Manganese(I) Catalyzed Substitutive C-H Allylation. *Angew. Chem., Int. Ed*. **2016**, *55*, 7747−7750. (b) Ma, W.; Mei, R.; Tenti, G.; Ackermann, L. Ruthenium(II) Catalyzed Oxidative C-H Alkenylations of Sulfonic Acids, Sulfonyl Chlorides and Sulfonamides. *Chem. Eur. J*. **2014**, *20*, 15248−15251. (c) Mei, R.; Zhang, S.-K.; Ackermann, L. Ruthenium(II)-Catalyzed C−H Alkynylation of Weakly Coordinating Benzoic Acids. *Org. Lett*. **2017**, *19*, 3171−3174. (d) Liu, W.; Richter, S. C.; Mei, R.; Feldt, M.; Ackermann, L. Synergistic Heterobimetallic Manifold for Expedient Manganese(I)-Catalyzed C-H Cyanation. *Chem. Eur. J*. **2016**, *22*, 17958−17961. (e) Liu, W.; Bang, J.; Zhang, Y.; Ackermann, L. Manganese(I)-Catalyzed C–H Aminocarbonylation of Heteroarenes. *Angew. Chem*. **2015**, *127*, 14343−14346.

22. Simmons, E. M.; Hartwig, J. F. On the Interpretation of Deuterium Kinetic Isotope Effects in C-H Bond Functionalizations by Transition Metal Complexes. *Angew. Chem., Int. Ed.* **2012**, *51*, 3066−3072.

23. Das, D.; Samanta, R. Iridium(III)-Catalyzed Regiocontrolled Direct Amidation of Isoquinolones and pyridones. *Adv. Synth. Catal.* **2018**, *360*, 379−384.

24. Zhou, B.; Chen, H.; Wang, C. Mn Catalyzed Aromatic C−H Alkenylation with Terminal Alkynes. *J. Am. Chem. Soc.* **2013**, *135*, 1264−1267.

25. Gottlieb, H. E.; Kotlyar, V.; Nudelman, A. NMR chemical shifts of common laboratory solvents as trace impurities. *J. Org. Chem*. **1997**, *62*, 7512−7515.

26. Mohanty, S. R.; Prusty, N.; Gupta, L.; Biswal, P.; Ravikumar, P. C. Cobalt(III)-Catalyzed C-6 Alkenylation of 2-pyridones by Using Terminal Alkyne with High Regioselectivity. *J. Org. Chem.* **2021**, *86*, 9444−9454.

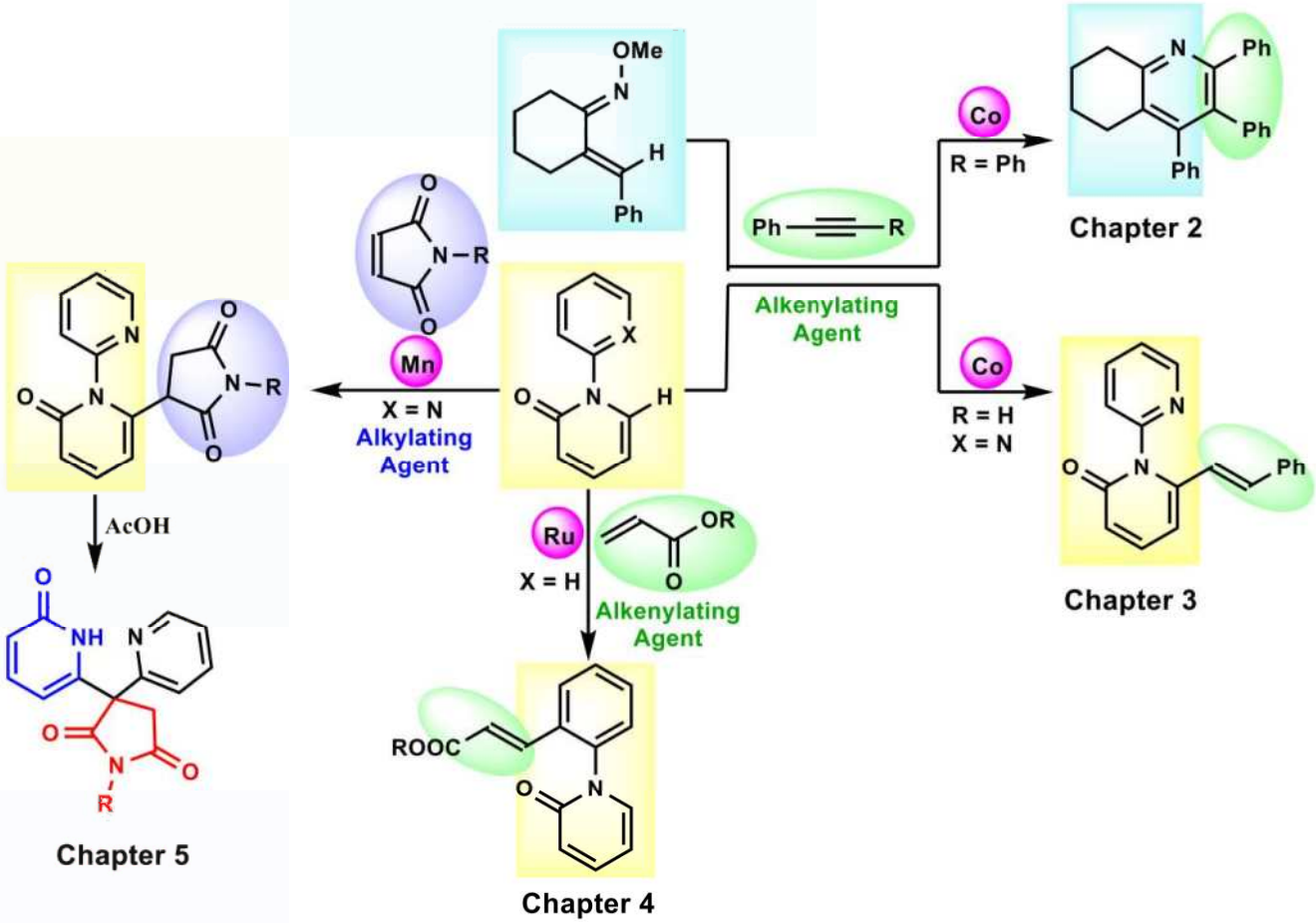
OMe
N
H
Ph
Co
R = Ph
Ph
N
Ph
Ph
Ph
Chapter 2
Ph
R
Alkenylating
Agent
O
N
R
O
Mn
X = N
Alkylating
Agent
X
O
N
H
Co
R = H
X = N
N
O
N
Ph
Chapter 3
N
O
N
R
O
AcOH
NH
N
O
N
O
R
Chapter 5
Ru
X = H
OR
O
Alkenylating
Agent
ROOC
O
N
Chapter 4

The author, Mr. Smruti Ranjan Mohanty was born on June26, 1992 at Jajpur, Odisha. After his initial schooling; he obtained his B.Sc. and M.Sc. degree from Ravenshaw University, Cuttack, Odisha. He joined the School of Chemical Sciences, National Institute of Science Education and Research, in the Ph.D. degree programme in July 2016. He passed the Comprehensive examination in September 2017. He completed his thesis defence on August 2022.